Dual-user Haptic Training System

Fei Liu

N° d'ordre NNT : 2016LYSEI082

THÈSE DE DOCTORAT DE L'UNIVERSITÉ DE LYON
opérée au sein de
l'Institut National des Sciences Appliquées de Lyon

École Doctorale N° 160
Electronique, Electrotechnique, Automatique (EEA)

Spécialité de doctorat : Automatique

Soutenue publiquement le 22/09/2016, par :
Fei LIU

Dual-user Haptic Training System

Devant le jury composé de :

BAYLE Bernard	Professeur des Universités Télécom Physique Strasbourg	Rapporteur
TAVAKOLI Mahdi	Associate Professor, University of Alberta	Rapporteur
FRAISSE Philippe	Professeur des Universités Université Montpellier II	Examinateur
NOVALES Cyril	Maître de Conférences Université d'Orléans	Examinateur
REDARCE Tanneguy	Professeur des Universités, INSA Lyon	Directeur de thèse
LELEVE Arnaud	Maître de Conférences, INSA Lyon	Co-directeur de thèse
EBERARD Damien	Maître de Conférences, INSA Lyon	Co-directeur de thèse

Département FEDORA – INSA Lyon - Ecoles Doctorales – Quinquennal 2016-2020

SIGLE	ECOLE DOCTORALE	NOM ET COORDONNEES DU RESPONSABLE
CHIMIE	**CHIMIE DE LYON** **http://www.edchimie-lyon.fr** Sec : Renée EL MELHEM Bat Blaise Pascal 3e etage secretariat@edchimie-lyon.fr Insa : R. GOURDON	M. Stéphane DANIELE Institut de Recherches sur la Catalyse et l'Environnement de Lyon IRCELYON-UMR 5256 Équipe CDFA 2 avenue Albert Einstein 69626 Villeurbanne cedex directeur@edchimie-lyon.fr
E.E.A.	**ELECTRONIQUE, ELECTROTECHNIQUE, AUTOMATIQUE** **http://edeea.ec-lyon.fr** Sec : M.C. HAVGOUDOUKIAN Ecole-Doctorale.eea@ec-lyon.fr	M. Gérard SCORLETTI Ecole Centrale de Lyon 36 avenue Guy de Collongue 69134 ECULLY Tél : 04.72.18 60.97 Fax : 04 78 43 37 17 Gerard.scorletti@ec-lyon.fr
E2M2	**EVOLUTION, ECOSYSTEME, MICROBIOLOGIE, MODELISATION** **http://e2m2.universite-lyon.fr** Sec : Safia AIT CHALAL Bat Darwin - UCB Lyon 1 04.72.43.28.91 Insa : H. CHARLES Safia.ait-chalal@univ-lyon1.fr	Mme Gudrun BORNETTE CNRS UMR 5023 LEHNA Université Claude Bernard Lyon 1 Bât Forel 43 bd du 11 novembre 1918 69622 VILLEURBANNE Cédex Tél : 06.07.53.89.13 e2m2@ univ-lyon1.fr
EDISS	**INTERDISCIPLINAIRE SCIENCES-SANTE** **http://www.ediss-lyon.fr** Sec : Safia AIT CHALAL Hôpital Louis Pradel - Bron 04 72 68 49 09 Insa : M. LAGARDE Safia.ait-chalal@univ-lyon1.fr	Mme Emmanuelle CANET-SOULAS INSERM U1060, CarMeN lab, Univ. Lyon 1 Bâtiment IMBL 11 avenue Jean Capelle INSA de Lyon 696621 Villeurbanne Tél : 04.72.68.49.09 Fax :04 72 68 49 16 Emmanuelle.canet@univ-lyon1.fr
INFOMATHS	**INFORMATIQUE ET MATHEMATIQUES** **http://infomaths.univ-lyon1.fr** Sec :Renée EL MELHEM Bat Blaise Pascal 3e etage infomaths@univ-lyon1.fr	Mme Sylvie CALABRETTO LIRIS – INSA de Lyon Bat Blaise Pascal 7 avenue Jean Capelle 69622 VILLEURBANNE Cedex Tél : 04.72. 43. 80. 46 Fax 04 72 43 16 87 Sylvie.calabretto@insa-lyon.fr
Matériaux	**MATERIAUX DE LYON** **http://ed34.universite-lyon.fr** Sec : M. LABOUNE PM : 71.70 –Fax : 87.12 Bat. Saint Exupéry Ed.materiaux@insa-lyon.fr	M. Jean-Yves BUFFIERE INSA de Lyon MATEIS Bâtiment Saint Exupéry 7 avenue Jean Capelle 69621 VILLEURBANNE Cedex Tél : 04.72.43 71.70 Fax 04 72 43 85 28 Ed.materiaux@insa-lyon.fr
MEGA	**MECANIQUE, ENERGETIQUE, GENIE CIVIL, ACOUSTIQUE** **http://mega.universite-lyon.fr** Sec : M. LABOUNE PM : 71.70 –Fax : 87.12 Bat. Saint Exupéry mega@insa-lyon.fr	M. Philippe BOISSE INSA de Lyon Laboratoire LAMCOS Bâtiment Jacquard 25 bis avenue Jean Capelle 69621 VILLEURBANNE Cedex Tél : 04.72 .43.71.70 Fax : 04 72 43 72 37 Philippe.boisse@insa-lyon.fr
ScSo	**ScSo*** **http://recherche.univ-lyon2.fr/scso/** Sec : Viviane POLSINELLI Brigitte DUBOIS Insa : J.Y. TOUSSAINT viviane.polsinelli@univ-lyon2.fr	Mme Isabelle VON BUELTZINGLOEWEN Université Lyon 2 86 rue Pasteur 69365 LYON Cedex 07 Tél : 04.78.77.23.86 Fax : 04.37.28.04.48

*ScSo : Histoire, Géographie, Aménagement, Urbanisme, Archéologie, Science politique, Sociologie, Anthropologie

To my family.

Acknowledgement

It was a long journey since I started this thesis four years ago at Laboratory Ampère, INSA de Lyon, Université de Lyon. The first year was my master study, with the following three years of Ph.D. study. I've found an exciting and fruitful experience through these time.

I want to express my great gratitude to my supervisors Prof. Tanneguy Redarce, Dr. Arnaud Lelevé and Dr. Damien Eberard. They always acted as the lights giving me right directions. Their ideas and advices along with the freedom of research are invaluable for me, which made the Ph.D. study a pleasure.

My heartfelt gratitude goes to all my colleagues at Ampère. They created a harmonious atmosphere and a supportive environment in the lab. I could got timely assistance and constant inspiration throughout my works. Furthermore, my research significantly benefited from the collaboration and resource sharing inside the lab. In particularly, I would like to give my special thanks to Dr. Minh Tu Pham, Dr. Richard Moreau, Dr. Paolo Massioni, Dr. Michael Di Loreto, Nemanja Babic, Mahya Rahimi, Setareh Javanmardi, etc.

I would like to thank my friends who accompanied me through the life in France. I appreciated the difficulties, the laughs shared with Dr. Hao Lu, Dr. Yaozhong Xu, Dr. Jinjiang Guo, Xiaoyu Wang, Teng Zhang, Chengsi Zhou, Meng Zhou, Changyi Xu, Xiaoshan Lu etc.

Special gratitude goes to China Scholarship Council (CSC), for providing the scholarship to my Ph.D. study in France.

Finally, I would give my deepest gratitude to my parents Zhaoli Liu and Xiuyu Yang, my fiancée Jie Fan, for their continuously love, support, encouragement and understanding all the way long.

Résumé

Dans le secteur médical tout particulièrement, la qualité du geste est primordiale et les professionnels doivent être formés par la pratique pour acquérir un niveau de compétences compatible avec l'exercice de leur métier. Depuis une dizaine d'année, les simulateurs informatiques aident les apprenants dans de nombreux apprentissages mais ils doivent encore être associés à des travaux pratiques sur mannequins, animaux ou cadavres, qui pourtant n'offrent pas toujours suffisamment de réalisme par rapport aux vrais patients, et sont coûteux à l'usage. Aussi, leur formation s'achève généralement sur de vrais patients, ce qui présente des risques. Les simulateurs haptiques (fournissant une sensation d'effort) deviennent aujourd'hui une solution plus appropriée car ils peuvent reproduire des efforts résistant réalistes et proposer une infinité de cas d'étude pré-enregistrés. Cependant, apprendre seul sur un simulateur n'est pas toujours aussi efficace qu'un apprentissage "à quatre mains" (celles de l'instructeur et de l'apprenant manipulant les mêmes outils en coopération).

Cette étude propose donc un système haptique de formation pratique à deux utilisateurs : l'instructeur et l'apprenant, interagissant chacun à travers leur propre interface haptique. Ils collaborent ainsi, avec des outils et un environnement de travail soit réels (l'outil est manipulé par un robot) soit virtuels. Une approche énergétique, faisant appel notamment à la modélisation par port-Hamiltonien, a été utilisée pour garantir la stabilité et la robustesse du système. Une étude comparative (en simulation) avec deux autres systèmes haptiques multi utilisateurs a montré l'intérêt de ce nouveau système pour la formation pratique. Il a été développé et validé expérimentalement sur des interfaces à un seul degré de liberté. Son extension à six degrés de liberté est facilitée par les choix de modélisation. Afin de pouvoir utiliser le système quand les deux protagonistes sont éloignés, cette étude propose des pistes d'amélioration qui ne sont pas encore optimisées.

Mots clefs : Haptique, Simulateur, Apprentissage supervisé, Dual-user, Passivité, Étude comparative, Retards de transmission, Système à ports hamiltoniens

Abstract

More particularly in the medical field, gesture quality is primordial. Professionals have to follow hands-on trainings to acquire a sufficient level of skills in the call of duty. For a decade, computer based simulators have helped the learners in numerous learnings, but these simulations still have to be associated with hands-on trainings on manikins, animals or cadavers, even if they do not always provide a sufficient level of realism and they are costly in the long term. Therefore, their training period has to finish on real patients, which is risky. Haptic simulators (furnishing an effort feeling) are becoming a more appropriated solution as they can reproduce realist efforts applied by organs onto the tools and they can provide countless prerecorded use cases. However, learning alone on a simulator is not always efficient compared to a fellowship training (or supervised training) where the instructor and the trainee manipulate together the same tools.

Thus, this study introduces an haptic system for supervised hands-on training: the instructor and the trainee interoperate through their own haptic interface. They collaborate either with a real tool dived into a real environment (the tool is handled by a robotic arm), or with a virtual tool/environment. An energetic approach, using in particular the port-Hamiltonian modeling, has been used to ensure the stability and the robustness of the system. This system has been designed and validated experimentally on a one degree of freedom haptic interface. A comparative study with two other dual-user haptic systems (in simulation) showed the interest of this new architecture for hands-on training. In order to use this system when both users are away from each other, this study proposes some enhancements to cope with constant communication time delays, but they are not optimized yet.

Keywords : Haptics, Simulation, Fellowship training, Hands-on training, Dual-User system, Passivity, Comparative study, Communication delay, port-Hamiltonian modeling

Acronyms

LTI	Linear Time-invariant
MSN	Master Slave Network
HSI	Human System Interaction
ESI	Environment System Interaction
IPC	Intrinsically Passive Controller
ESC	Energy Shared Control
CLC	Complementary Linear Combination
MCET	Masters Correspondence with Environment Transfer
MFS	Modulated Flow Sources
AAA	Adaptive Authority Adjustment
CWVT	Conventional Wave Variable Transformation
AWVT	Augmented Wave Variable Transformation
FVF	Forbidden-Region Virtual Fixture
GVF	Guidance Virtual Fixture
DOF	Degree of Freedom

Symbols

F_i	Force signal
V_i, X_i	Velocity/position signal
T_i	Torque signal
$\dot{\theta}_i, \theta_i$	Joint velocity/joint position signal
Z_i	Impedance
α, β_1, β_2	Dominance factors
$\mathcal{D}_i$	Dirac structure
H_i	Hamiltonian function
M_i	Inertial element
B_i, D_i	Damping element
K_i	Elastic element
m_{c_i}	Virtual mass m_c in IPC i
k_{c_i}	Stiffness of spring k_c in IPC i
k_{i_j}	Stiffness of spring k_i in IPC j
p_{c_i}	Moment of virtual mass m_c in IPC i
q_{c_i}	Displacement of spring k_c in IPC i
q_{i_i}	Displacement of spring k_i in IPC i
x_i	State vector of closed-loop/subsystem model
u_i, y_i	Input/output vector of closed-loop/subsystem model
E_p	Passivity controller energy function
B	Adaptive virtual boundary
T_v,	Virtual boundary torque
α_a	Adaptive dominance factor
α_o	Overrule dominance factor
k_b, k_v, T_0, B_0	Tuning parameter of AAA
V	Closed-loop energy function

P_i	Dissipated power
k_e	Stiffness of virtual wall
Φ_i	Position tracking preciseness
Δ_i	Standard deviation of position tracking error
u_i, v_i	Wave variable
$\Delta u_i, \Delta v_i$	Compensation terms of wave variable
γ_i	Passivity tuning parameter
Γ_i	Passivity tuning parameter according to α
E_i	Energy transfered into shared control structure
P_i	Power flow transfered into shared control structure
ΔE_i	Energy before passivity tuning
$\bar{\Pi}_i$	Energy to be tuned for passivity

Contents

List of Figures

List of Tables

Résumé

Introduction

Contexte global

La chirurgie minimale invasive (*Minimal Invasive Surgery* MIS) est une technique opératoire qui est apparue il y a environ vingt ans et qui est de plus en plus présente en chirurgie car moins traumatique que la chirurgie ouverte, ce qui accélère la guérison du patient [Park and Lee, 2011]. Cependant, du point de vue des praticiens, elle requiert des équipements complexes et coûteux et surtout des équipes longuement formées. En effet, les procédures MIS impliquent de manipuler les instruments chirurgicaux à travers des trocarts (induisant des mouvements inversés entre les poignées et les outils terminaux) et de les visualiser par le biais d'endoscopes. Cette manipulation indirecte des outils est de fait plus complexe pour le chirurgien qu'en chirurgie ouverte car son espace opératoire et son champ de vision sont limités. De plus, la position de l'endoscope par rapport aux outils induit une difficulté de coordination vision-main et une distorsion de l'effort ressenti induit par les contacts entre l'outil manipulé et son environnement [Tavakoli, 2008].

Pour s'entraîner à la pratique du geste opératoire dans le domaine médical, les apprenants ont traditionnellement recours à deux types distincts de simulation. La simulation synthétique, avec mannequins, pour rejouer des situations procédurales complexes; on la nomme aussi simulation relationnelle (*Medical Team Training - MTT*) dont l'objet recouvre le procédural et le décisionnel au sens communication du groupe soignant. Le second type de simulation consiste à s'entraîner par la pratique au geste médical sur des mannequins (maquettes reproduisant une partie de l'anatomie humaine), mais plus fréquemment sur des corps entiers ou préparés en pièces anatomiques de cadavres ou d'animaux. Cependant, d'une part, les cadavres et les animaux sont coûteux et ne sont pas disponibles en permanence, et, d'autre part, le pilotage par l'éthique tend vers l'usage des simulateurs. Notons que les simulateurs anthropomorphes synthétiques demeurent peu efficients et génèrent des coûts de maintenance élevés (il faut remplacer régulièrement leurs pièces d'usure), et, *in fine*, manquent encore de réalisme (carnation, toucher, ...) en basse comme en haute

définition.

La simulation informatique à but pédagogique (*Computer Based Simulation for Training*) est apparue au début du XXI^{e} siècle siècle (voir par exemple [Kaufmann and Liu, 2001] concernant la traumatologie). En 2011, Fairhust et al ont publié une synthèse [Fairhurst and Strickland, 2011] des progrès réalisés dans la simulation pour l'apprentissage en chirurgie. Y apparaissent notamment des simulateurs haptiques (à retour d'effort sur l'interface apprenant). La dernière synthèse connue sur ce sujet date de 2014 [Yiannakopoulou et al, 2014].

Les simulateurs forment des chirurgiens et améliorent leurs compétences: ces derniers peuvent faire des erreurs sans risque aucun. Ils informent les apprenants sur leurs progrès (cf. *Learning Analytics* [Dietz-Uhler and Hurn, 2013]), ce qui les situe sur leur courbe d'apprentissage [Lewis et al, 2011]. Ils sont conçus pour compenser les inconvénients des solutions classiques précédemment évoquées. Ils proposent ainsi aux apprenants un environnement de simulation plus réaliste, restitué en deux voire trois dimensions (cf. [Delorme et al, 2012]). Ce qui caractérise leur qualité est leur capacité à immerger l'utilisateur et estomper la sensation de situation artificielle, phénomène dit de suspension d'incroyance (*suspension of disbelief*) [Slater et al, 2001]. Ils sont une solution répondant aux recommandations de la Haute Autorité de Santé (HAS) qui préconise, depuis 2012, le développement de la simulation, avec comme leitmotiv: *"Jamais la première fois sur un patient"*.

Toutefois, les premières générations de simulateurs pédagogiques ne fournissaient pas de retour d'effort, ce qui les empêchait de reproduire fidèlement les forces exercées par les organes sur leurs outils (virtuels), ce qui peut être critique dans certaines procédures chirurgicales. Apparu avec la génération suivante des simulateurs haptiques, ce retour d'effort fournit un comportement réaliste de l'outil manipulé, tout particulièrement lorsqu'il est en contact avec des tissus ou des os, ce qui rend plus efficace la formation pour des tâches complexes [Coles et al, 2011]. On parlera alors plutôt de simulateurs robotiques du fait de l'introduction de cette dimension mécatronique supplémentaire.

Par exemple, le *LapSim*® (visible figure R-1[1]) commercialisé par *Surgical Science*© [SurgicalScience, 2016b] propose un entraînement à des procédures de chirurgie laparoscopique qui peuvent être reproduites à volonté avec un niveau de difficulté croissant. Ce type de système a pour objectif d'aider les chirurgiens à s'entraîner et se tenir prêt à intervenir dans des situations complexes et rares. Des simulateurs existent dans le commerce, comme par exemple, le *Minimally Invasive Surgery Trainer* (MIST™) développé par *Mentice Corporation*, ou encore le *Virtual Endoscopic Surgery Trainer* (VEST), par *Select-IT VEST Systems AG*.

Figure R-1: Simulateurs *LapSim* haptique (à gauche) et non-haptique (à droite)

Aujourd'hui, cette dernière génération de simulateurs est devenue suffisamment performante et réaliste pour être utilisée en formation dans les universités et hôpitaux. Une formation basique sur pièce anatomique est pratiquée (*Basic Skill Surgery BSS*). Concernant le LapSim, les modules d'apprentissage sont assez spécialisés et familiarisent l'étudiant qui peut rejouer un grand nombre de fois des situations.

Pour des gestes chirurgicaux, plus difficiles à acquérir, la méthode d'apprentissage classique, sur le terrain (autrement dit, en salle d'opération), consiste, pour un apprenant, à opérer un patient, les mains guidées par celles d'un formateur (méthode

[1]Image extraite de `http://www.surgical-science.com/lapsim-the-proven-training-system/`, mai 2016.)

surnommée "à quatre mains"). Or celle-ci ne trouve actuellement pas son équivalent dans les simulateurs informatiques où l'apprenant est seul avec ses outils plongés dans leur environnement. Elle présente pourtant quelques inconvénients: notamment, il est difficile pour les deux personnes de doser, pour l'un et d'estimer pour l'autre, les efforts à fournir quand les quatre mains sont jointes deux à deux car l'effort est partagé de manière aléatoire entre les deux personnes. C'est un frein réel pour l'apprentissage du geste car cette dimension est faussée.

Dans la synthèse [Coles et al, 2011] concernant les simulateurs pédagogiques dans le domaine médical, il apparaît que les simulateurs actuels sont principalement fondés sur des environnements réels ou virtuels où l'apprenant est seul, ce qui rend difficile toute possibilité de le guider dans ses gestes. Pourtant, comme dans une formation pratique à quatre mains, surtout pour des gestes complexes, il est important que le formateur puisse intervenir; pour guider l'apprenant, pour l'évaluer en temps réel, ou encore pour corriger des trajectoires potentiellement dangereuses. Il est également nécessaire, pour plus de flexibilité dans la formation de garder la possibilité pour le formateur d'intervenir dans la simulation comme il intervient classiquement en formation pratique classique. Il n'est pas possible de programmer à l'avance tous les cas de figure dans le simulateur. A l'usage, les plus récurrents peuvent être intégrés au fur et à mesure dans le simulateur mais il y aura toujours des cas particuliers où l'intervention du formateur sera nécessaire: pour débloquer l'apprenant, pour le conseiller, ... D'où l'intérêt de proposer des simulateurs intégrant le formateur dans la simulation.

Le robot *da Vinci Si dual-console system* [SurgicalScience, 2016a] visible en figure R-2[2] propose un mode de formation à deux utilisateurs simultanés. Cependant, un seul utilisateur à la fois a accès aux instruments et aucun des deux utilisateurs n'a de retour haptique.

Pourtant, il serait utile de bénéficier d'un simulateur réunissant apprenant et formateur, qui fournisse un bon niveau de réalisme aux deux utilisateurs simultanément

[2]Image extraite de `http://www.intuitivesurgical.com/company/media/images/davinci_si_images.html`, Mai 2016.

Figure R-2: Le simulateur *da Vinci Si dual console system.*

(notamment par le biais d'un retour haptique individuel), et qui allie les avantages des simulateurs et de l'accompagnement, avec un niveau décroissant d'intervention de la part du formateur. C'est donc l'objet de ce travail de thèse.

Exigences et principal cas d'utilisation

Pour cette application spécifique à la formation chirurgicale, nous avions besoin d'un système haptique intégrant deux interfaces haptiques (une pour l'apprenant et une autre pour le formateur) leur offrant la possibilité de manipuler et de se suivre l'un l'autre, autrement dit, proposant un fonctionnement de type "chef de file - suiveur" sachant que les deux utilisateurs peuvent changer de rôle à tout moment. Supposons, en premier lieu, que le formateur (un chirurgien expérimenté) veut montrer des trajectoires à reproduire avec son outil chirurgical dans le contexte d'une tâche chirurgicale dans laquelle son outil peut ou doit rentrer en contact avec l'environnement. Ceci implique qu'il soit équipé d'un retour d'effort réaliste pour pouvoir doser son effort à l'instar d'une vraie opération chirurgicale (éventuellement réalisée à distance dans le cadre d'un dispositif de téléopération). À cet effet, il place le simulateur en mode "chef de file" (l'apprenant est donc en mode suiveur) puis guide l'outil (qui peut être un outil réel dans un environnement réel placé par exemple dans une boite noire

proche du simulateur, ou un outil et un environnement complètement virtuels). Le formateur récupère alors un retour d'effort réaliste, comme s'il manipulait directement ses outils.

Simultanément, l'interface haptique de l'apprenant suit le mouvement de celle du formateur. Si l'apprenant dévie la trajectoire "modèle" quand l'outil n'est pas en contact avec un élément de l'environnement, la compliance de l'interface la ramène "sur le bon chemin", celui imposé par le formateur. Quand l'outil est en contact avec son environnement, avec un effort exercé par le formateur pour maintenir ce contact, le simulateur doit faire ressentir à l'apprenant ce même effort afin qu'il apprenne à le doser. L'apprenant n'étant pas à l'origine de cette interaction, le niveau d'effort qu'il doit fournir devra lui être affiché comme cible sur son écran accompagné de l'effort qu'il applique actuellement.

Le simulateur doit pouvoir inverser facilement les rôles afin que, ensuite, l'apprenant manipule les outils et le formateur l'évalue tant sur les trajectoires générées que sur les efforts appliqués.

Dans la pratique, les chirurgiens expérimentés ne sont pas très disponibles; un usage à distance où chaque interface est localisée dans des lieux différents (service de l'hôpital pour le formateur et université pour l'apprenant) et connectée, pourrait éviter des déplacements humains et donc résulter en des gains de temps appréciables.

Objectifs

Afin de répondre au besoin explicité précédemment, offrant au formateur et à l'apprenant un moyen de s'entraîner ensemble sur une même tâche, avec les mêmes outils, sans aucun risque pour un patient, nous proposons de concevoir et développer un simulateur haptique leur offrant chacun une interface haptique couplée à l'environnement et à l'autre protagoniste. A terme, à travers ce simulateur, les utilisateurs pourront réaliser différents types de gestes (suivi de trajectoire, maintien en position, insertion d'aiguille, évitement d'obstacles, sutures, ...).

Pour respecter les contraintes des situations d'apprentissage réelles dans lesquelles les chirurgiens chevronnés sont souvent localisés loin des étudiants en médecine,

un usage à distance doit être envisagé. D'autre part, les étudiants nécessitant ce type d'apprentissage du geste étant nombreux, l'extension future de ce simulateur à plusieurs apprenants simultanés est à prendre en compte (*"scalabilité"*).

En termes plus techniques, ces objectifs impliquent de:

- concevoir un système à deux (ou plus) utilisateurs (*dual-user system*) pour un usage de formation au geste ;
- proposer un contrôleur assurant la stabilité robuste des trois sous-systèmes interconnectés (interfaces apprenant, formateur et outil/environnement évoluant dans le temps) ;
- évaluer expérimentalement les performances de ce système, notamment par rapport à l'existant.

Contributions

Pour atteindre ces objectifs, nous avons réalisé une étude bibliographique (présentée au chapitre 2 et traduite dans la suite de ce résumé) qui nous a amené à conclure qu'il existe plusieurs architectures de systèmes *dual-user*, proposant un contrôle partagé d'un même outil, avec un partage de l'autorité entre les deux utilisateurs réglable. Se fondant sur des approches de modélisation variées, certaines contributions de la communauté se concentrent sur la gestion du partage d'autorité, d'autres sur la qualité du retour d'effort et la minimisation de l'impact des retards de transmission. Partant de ce constat, nous avons affiné nos exigences[3] en terme d'approche de modélisation, de scénarios pédagogiques et de prise en compte des retards de transmission. Les contributions de ce travail sont donc les suivantes.

Premièrement, nous avons conçu un nouveau simulateur pédagogique, de formation au geste, utilisable à deux utilisateurs (formateur et apprenant) fondé sur un contrôleur inédit, gérant les échanges d'énergie entre sous-systèmes (*Energy Shared Control - ESC*). Ce simulateur ne possède actuellement qu'un seul degré de liberté

[3]Dans le contexte de l'Ingénierie Système, les exigences d'un système regroupent les besoins et les contraintes exprimées en partie dans le cahier des charges initial.

(une rotation) mais, du fait des choix de modélisation évoqués ultérieurement, une extension du nombre de degrés de liberté ne remet pas en cause sa structure. Il est présenté au chapitre 3. Cette architecture autorise explicitement de répartir de manière continue le contrôle entre les deux utilisateurs sans remettre en cause la passivité du système. Une amélioration a été apportée afin que cette répartition se réalise automatiquement (cf. chapitre 4) pour que le formateur se concentre principalement sur sa tâche et non sur le réglage du niveau de partage de l'autorité, ce qui facilite notamment la reprise urgente d'autorité de sa part en situation critique. Quel que soit le niveau d'autorité accordé à un utilisateur, celui-ci perçoit un retour d'effort conforme aux efforts d'interaction outil-environnement, même si ce n'est pas l'utilisateur à l'origine de cette interaction; ainsi la personne qui observe le mouvement ressent les mêmes efforts que la personne qui manipule effectivement l'outil. Une modélisation par ports hamiltoniens (approche énergétique garantissant explicitement la passivité d'un système) a été réalisée. La passivité du simulateur est garantie par un contrôleur temporel de passivité, quelle que soit la nature des utilisateurs et de l'environnement. Les performances du simulateur ont été évaluées expérimentalement: il affiche de bonnes performances en terme de suivi de position et de reproduction d'effort, ainsi que dans la gestion automatique de l'autorité accordée à chaque utilisateur.

Afin d'évaluer les performances de notre système par rapport à l'existant, nous avons réalisé une étude comparative. Les performances des systèmes étudiés sont évaluées en simulation en terme de suivi de position (cf. chapitre 5) en fonction des niveaux d'autorité pour différentes trajectoires types. Une réflexion est menée quant aux performances de ces architectures concernant le retour d'effort offert aux utilisateurs. Cette étude conclut que notre simulateur apporte une plus-value sur cet aspect en comparaison avec les deux autres architectures.

La troisième contribution est une étude préliminaire de la prise en compte des retards de transmission dans l'architecture ESC (développée au chapitre 6). Nous avons intégré la transformation AWVT (*Augmented Wave Variable Transformation*) dans l'ESC pour assurer le maintien de la passivité du système en cas de retards de transmission. Des exemples de paramètres garantissant la passivité du système sont

proposés.

Organisation de ce mémoire

L'ensemble de ce mémoire est organisé en six chapitres comme suit:

Le chapitre 2 présente un état de l'art concernant les systèmes haptiques des systèmes bilatéraux (téléopération classique) aux systèmes multilatéraux. Les mécanismes nécessaires pour réaliser des fonctions de téléopération sont étudiés, notamment les interfaces haptiques, la modélisation maître-esclave, les stratégies de stabilité, la problématique de la transparence. Une attention est portée sur les systèmes *dual-user*. Ce chapitre conclut sur les exigences à satisfaire pour répondre au cahier des charges évoqué précédemment.

Le chapitre 3 présente le contrôleur ESC. Il détaille le mécanisme de partage d'autorité et construit étape par étape l'ensemble de l'architecture. Une modélisation par ports hamiltoniens est développée et une étude de la passivité nous a amené à intégrer un contrôleur de passivité.

Le chapitre 4 se concentre sur l'amélioration de l'attribution de l'autorité. Un mécanisme adaptatif (*Adaptive Authority Adjustment*, AAA) est proposé pour faciliter l'usage du simulateur en donnant le moyen au formateur de reprendre la main rapidement en cas de gestes inappropriés de la part de l'apprenant. Le maintien de la passivité est étudié et confirmé. Des expérimentations valident le bon fonctionnement du mécanisme.

Le chapitre 5 détaille l'étude comparative de l'ESC avec deux autres systèmes *dual-user*. L'étude s'attache à comparer les performances des trois architectures en terme de suivi de position. Du fait de stratégies différentes en terme de partage d'effort, pour les trois architecture, une étude de suivi d'effort n'avait pas lieu d'être. Par contre, une réflexion est menée quant à l'intérêt de l'ESC pour une application pédagogique comparativement au comportement des deux autres architectures.

Le chapitre 6 dessine une étude préliminaire de prise en compte des retards de transmission pour le contrôleur ESC. L'intégration de la transformation AWVT (*Augmented Wave Variable Transformation*) dans l'ESC pour assurer le maintien de la

passivité du système est étudiée.

Nous concluons ensuite sur les contributions apportées par ce travail et proposons des perspectives pour les prochaines recherches.

État de l'art: systèmes haptiques et dual-user

Systèmes haptiques

Le terme *haptique* provient du grec *haptomai* qui signifie toucher. Les systèmes haptiques fournissent aux humains le moyen d'interagir avec un système logiciel ou mécatronique à l'aide de leurs sens (tactile) et/ou kinesthésique. Le sens du toucher (ou tactile) nous informe, par contact de la peau sur un objet, de sa température, la pression appliquée, sa texture, sa dureté, tandis que la perception kinesthésique nous fait sentir la position de nos membres et les efforts impliqués lors d'une interaction avec un objet, à travers nos muscles, tendons et articulations.

Les systèmes haptiques se composent d'une interface haptique et d'un logiciel. L'interface haptique offre à l'utilisateur la possibilité de transmettre un mouvement ou un effort au logiciel et, simultanément, au logiciel de retourner une information sous forme de force ou de mouvement. Dans les applications de téléopération, le logiciel est juste un maillon intermédiaire de la chaîne liant l'interface haptique de l'opérateur au robot téléopéré. Dans les systèmes *dual user*, plusieurs interfaces haptiques sont connectées à un robot (réel ou virtuel) grâce à un logiciel.

Les systèmes haptiques sont utilisés dans de nombreuses applications, dont les jeux vidéo (via un joystick à retour d'effort), des téléphones portables (par le biais de vibrations), en robotique, pour la formation pratique, ... (voir [Hayward et al, 2004, Varalakshmi et al, 2012]). Les joysticks à retour d'effort utilisés par les joueurs de jeux vidéo jouant sur des simulateurs de vol, par exemple, fournissent des sensations réalistes [Deng et al, 2014]. Concernant le domaine de la robotique, les systèmes haptiques sont principalement utilisés pour la commande à distance (téléopération) de robots situés sous la surface de la mer ou dans l'espace, comme dans [Hokayem

and Spong, 2006]. L'usage médical pour la formation pratique, l'assistance au geste chirurgical, ou en réhabilitation, s'est beaucoup développé [Coles et al, 2011].

Ce travail s'est concentré sur la formation pratique dans le domaine médical mais d'autres secteurs d'application ne sont pas exclus.

Les interfaces haptiques

Les interfaces haptiques sont des dispositifs créant un échange d'information entre un humain et une machine, impliquant la perception haptique. La plupart du temps, elles fournissent une information sous une forme kinesthésique. Cependant, des chercheurs étudient également des interfaces haptiques faisant appel au sens du toucher (voir [Ware et al, 2014] par exemple). Par exemple, le Phantom Omni (qui fournit une information sous une forme kinesthésique) possède une cinématique à trois degrés de liberté motorisés. L'interface haptique BioTac® est, quant à elle, tactile (elle est développée par l'équipe du SIRSLab, à l'Université de Sienne en Italie). Elles sont toutes deux visibles en figure R-3[4].

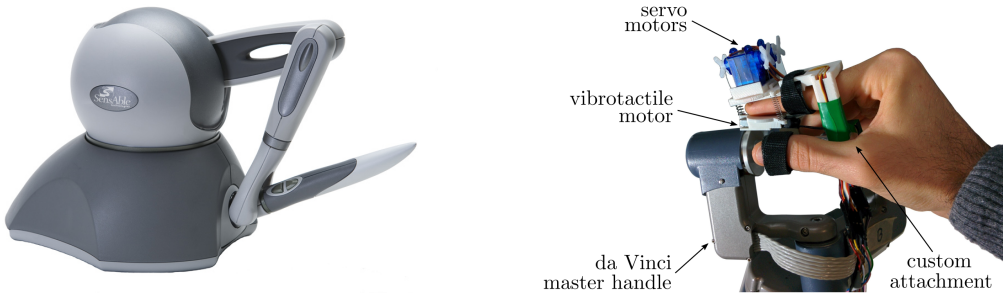

Figure R-3: Dispositifs haptiques à 3 degrés de liberté: le Phantom Omni de SensAble® (à gauche) et l'interface tactile BioTac® (à droite).

Idéalement, quand une interface haptique, actionnée par un utilisateur est en régime libre, c'est à dire, dans un mode où elle est sensée ne pas reproduire d'interaction avec un environnement éloigné ou virtuel, aucune force ne doit être transmise à l'utilisateur. Les actionneurs et éléments de transmission qui composent l'interface

[4]Images extraite de `http://www.dentsable.com/haptic-phantom-omni.htm` et `https://prattichizzoblog.files.wordpress.com`, mai 2016.

doivent donc présenter le minimum de frottements et une compensation de gravité pour rendre l'interface la plus transparente possible pour l'utilisateur.

Quand l'interface doit informer l'utilisateur d'une collision, d'un suivi de surface, ... d'une interaction avec l'environnement distant/virtuel, ce sont ses actionneurs qui créent des efforts transmis à l'utilisateur.

En téléopération, cette situation arrive quand le robot esclave entre en interaction avec son environnement. L'interface haptique maître tente alors de reproduire ces efforts d'interaction (cf. par exemple [Sun et al, 2016]). Dans certaines applications, ces actionnements sont utilisé pour guider l'utilisateur dans ses mouvements (on parle alors de *virtual fixtures*, cf. [Liu et al, 2015])

Aujourd'hui de nombreuses architectures d'interfaces haptiques existent, dont certaines sont solidaires du poste de travail de l'utilisateur, et d'autres sont détachées du poste pour être solidaires de l'opérateur (voir la classification de [Hayward and Astley, 1996]). Les moteurs électriques sont, le plus souvent, les actionneurs utilisés, mais les actionneurs pneumatiques (cf. [Herzig et al, 2015]) ou hydrauliques ([Buerger and Hogan, 2010]) peuvent être utilisés avantageusement pour produire des efforts importants avec une grande bande passante et une compliance maîtrisée.

Des actionneurs plus récents, comme les moteurs piezo-électriques, les alliages à mémoire de forme ou magnétiques, étendent le champ des possibles pour des dispositifs de petite taille et légers [Mazzone et al, 2003].

Les interfaces haptiques du commerce sont généralement actionnées électriquement. On en trouve avec des caractéristiques variées (nombre de degrés de liberté, volume de travail, amplitude des efforts et couples transmis à l'utilisateur, ou encore la forme de l'effecteur). Pour plus de précisions, lire [Coles et al, 2011]. Une classification fondée sur l'espace de travail et les capacités de rendu en effort des dispositifs les plus répandus dans le commerce est visible en figure R-4 [5].

D'autres types novateurs d'interfaces haptiques ont été développés, comme par exemple, l'interface magnétique de [Berkelman and Hollis, 2000], mais elles n'ont pas

[5]Image extraite de `http://kb.eurovr-association.org/index.php/Haptic_Hardware`, mai 2016.

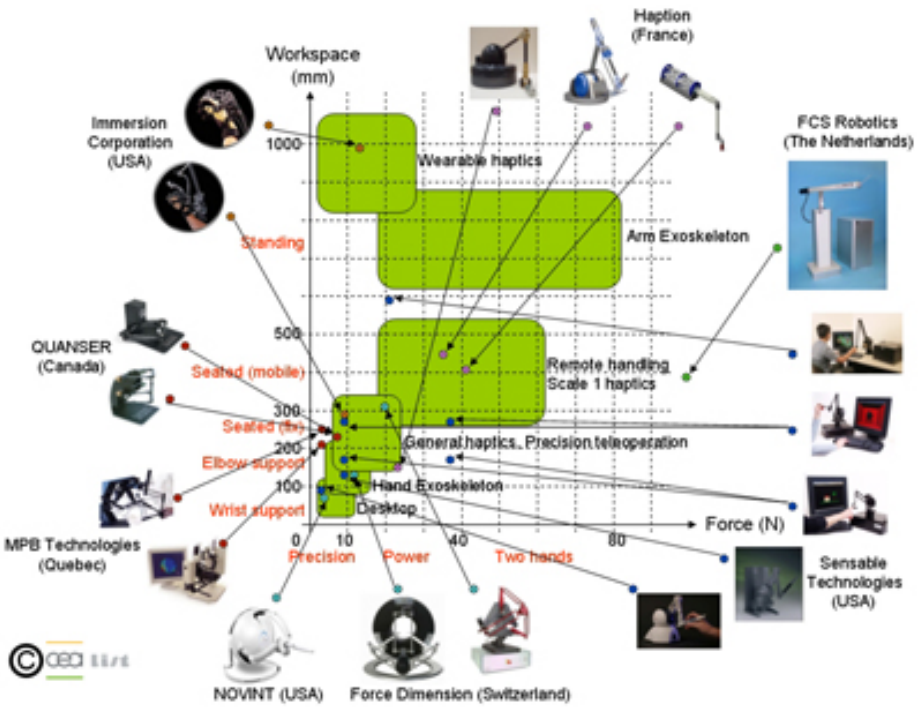

Figure R-4: Classification des interfaces haptiques disponibles dans le commerce

encore été intégrées dans des solutions de formation au geste médical.

Systèmes maître esclave

Les systèmes haptiques sont communément utilisé dans une architecture maître-esclave, en présence d'un humain et plongée dans un environnement (voir figure R-5).

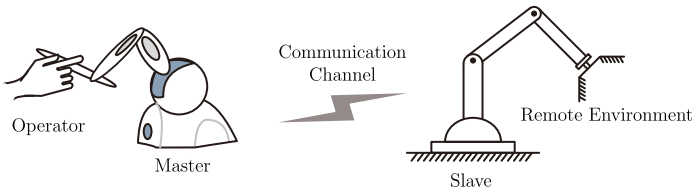

Figure R-5: Système maître-esclave

L'utilisateur manipule une interface haptique, le maître et lui transmet des efforts qui résultent en mouvements. Le robot distant (ou virtuel dans le cas de simulateur informatiques), dispositif esclave, réceptionne des informations traduisant ces interactions et reproduit le geste de l'opérateur pour réaliser des tâches dans l'environnement distant (ou virtuel). Simultanément, l'interaction entre l'effecteur du robot et son environnement est retransmise à l'utilisateur. Selon la distance entre le maître et

l'esclave, un délai de transmission peut apparaître dans le canal de communication. Il est primordial de tenir compte de ce délai car il est fortement destabilisant pour la boucle de contrôle incluant le maître et l'esclave. Des retours visuels et parfois audio apportent des informations complémentaires et améliorent l'ergonomie pour l'utilisateur.

Téléopération

Les systèmes maître-esclave sont classiquement utilisés pour réaliser de la téléopération haptique où l'esclave est un robot distant réel. Quand le comportement de l'esclave n'affecte pas celui du maître, on parlera de *téléopération unilatérale*. A l'inverse, quand les positions et/ou efforts du maître et de l'esclave sont transmis dans les deux sens, on utilise le terme de *téléopération bilatérale*. Les systèmes de téléopération bilatérale sont les plus développés dans la littérature scientifique car plus performants que les unilatéraux. Le premier téléopérateur a été conçu et réalisé par Goertz [Sheridan, 1989] dans les années 1940 pour l'industrie nucléaire. Le maître et l'esclave étaient liés par des câbles mécaniques. Notons qu, à notre connaissance, le système de téléopération chirurgicale da Vinci ne propose qu'une téléopération unilatérale: le chirurgien n'a pas de retour d'effort.

La téléopération bilatérale

Les systèmes de téléopération bilatérale ont fait l'objet de nombreuses recherches depuis 70 ans. Cet effort est motivé par les progrès technologiques (en robotique mais aussi en réseaux de télécommunication) et des applications concrètes.

Ils trouve leur utilité notamment dans le domaine spatial [Penin, 2000], dans l'exploration sous-marine [Saltaren et al, 2007], dans les milieux nucléaires ou plus généralement dans des applications avec des ambiances toxiques pour l'homme, voire explosives [Kron et al, 2004], mais aussi dans des applications médicales de téléchirurgie [Guthart and Salisbury, 2000]. Un historique des recherches en téléopération a été publié en 2006 dans [Hokayem and Spong, 2006].

Les qualités recherchées d'un système de téléopération sont un bon suivi en position et en effort entre le maître et l'esclave (transparence) tout en assurant la stabilité de l'ensemble. Ces deux objectifs ont été étudiés sous l'angle de la passivité par Lawrence et al dans [Lawrence, 1993]. Une étude précise et comparée des premières approches est lisible dans [Arcara and Melchiorri, 2002]. Plus récemment, [Aliaga et al, 2004, Kim et al, 2007, Muradore and Fiorini, 2016] ont proposé des études comparatives des différentes contrôleurs publiés dans la littérature scientifique. Il existe aussi une étude des systèmes de téléopération faisant spécifiquement appel au principe de passivité [Nuno et al, 2011].

Modélisation

Traditionnellement, un système de téléopération bilatérale est modélisé sous la forme d'un réseau intégrant un canal de communication (*Master Slave Network* - *MSN*) liant le maître et l'esclave, ceux-ci étant liés respectivement à un opérateur (via une *Human System Interaction* - HSI) et à l'environnement distant (via une *Environment System Interaction* - ESI) (cf. Fig. R-6).

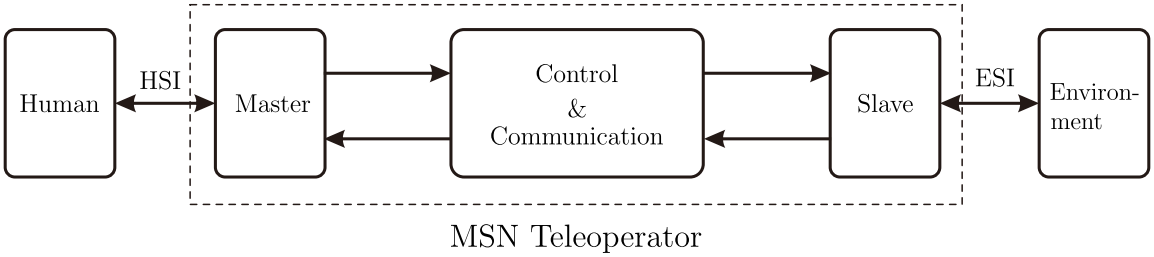

Figure R-6: Système de téléopération bilatérale

Modélisations linéaires Plusieurs architectures de contrôle fondées sur des modèles linéaires existent, par exemple: les schémas à deux canaux [Anderson and Spong, 1989b] dont l'architecture position-position (*Position Error Based* - PEB), force-position (*Direct Force Reflection* - DFR) [Tavakoli, 2008], mais aussi des schémas à trois ou quatre canaux [Lawrence, 1993, Tavakoli, 2008]. En l'absence de délai de transmission, ces systèmes sont généralement modélisés en tant que systèmes linéaires invariant dans le temps (*Linear time-invariant*, LTI).

Modélisations non linéaires Des propositions de modélisation non linéaire des téléopérateurs ont été développées dans [Liu and Tavakoli, 2011, Malysz and Sirouspour, 2009, Mohammadi et al, 2011, Nuno and Basanez, 2009, Nuno et al, 2010]. De manière générale, ces modélisations se fondent sur un modèle de Lagrange de la mécanique des interfaces maître et esclave. Leur stabilité est assurée par la recherche de fonctions de Lyapunov [Daly and Wang, 2014, Kawada and Namerikawa, 2008, Nuno et al, 2009].

Modélisations énergétiques D'un point de vue énergétique, un téléopérateur peut être vu comme un réseau à deux ports qui transmet de l'énergie entre l'opérateur et l'environnement. L'opérateur et l'environnement sont alors modélisés en éléments de réseau à un port, possédant chacun une source d'énergie.

Les informations échangées dans le système sont représentées par des variables de puissance (vitesse et force), cf. figure R-7 dans laquelle F_i, F_i^* $(i \in \{h, e\})$ représentent des efforts et V_i, V_i^* des vitesses. Z_t est l'impédance de l'environnement vue par l'opérateur et les impédances Z_h et Z_e sont resp. celles de l'opérateur et de l'environnement.

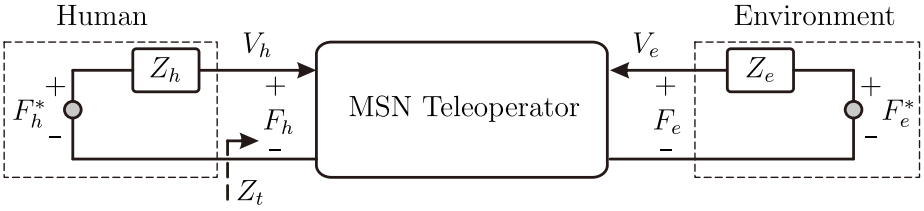

Figure R-7: Modèle énergétique d'un téléopérateur bilatéral.

A ce sujet, il a été démontré dans [Secchi et al, 2007] que la théorie de la passivité associée au formalisme par ports hamiltoniens présente des avantages en terme de simplification des conditions de stabilité pour les systèmes automatisés.

Stabilité

La problématique intrinsèque aux systèmes de téléopération est qu'il s'agit de systèmes multi entrées et sorties (*Multiple Inputs, Multiple Outputs* - MIMO) d'une part

et qu'ils forment une boucle interne entre le maître et l'esclave, boucle intégrant éventuellement des retards (de communication). Aujourd'hui le canal de communication est numérique: réseau local, réseau de grande dimension, Internet, communications sans fil, par satellite, ... Ils présentent donc naturellement des retards de transmission souvent variables mais également des pertes de paquets de données. Dans le meilleur des cas, avec un canal de transmission dédié, on ne peut éviter le délai de propagation (communications terre - satellite géostationnaire, par exemple).

Plusieurs approches ont été proposées pour garantir la stabilité des téléopérateurs. Elles peuvent se classer en trois catégories:

- pour les modèles linéaires :
  des approches traditionnelles applicables aux systèmes LTI:
  critère de Nyquist [Hannaford, 1989b], à celles plus évoluées comme H_∞ [Leung et al, 1995, Yan and Salcudean, 1996], en passant par le critère de Llewellyn [Tavakoli, 2008] ;

- pour les modèles non linéaires, qui incluent par exemple des frottements secs, des interfaces à plusieurs degrés de liberté, des retards de transmission, des incertitudes sur les modèles, ... :
  plusieurs techniques ont été appliquées : contrôle adaptatif [Lee and Chung, 1998, Ryu and Kwon, 2001], contrôle par mode glissant [Buttolo et al, 1994, Park and Cho, 1999], contrôle prédictif [Bemporad, 1998] , etc.

- pour les modèles énergétiques :
  la théorie des réseaux est typiquement utilisée. Le critère de Llewellyn vérifie la stabilité absolue d'un système modélisé sous la forme d'un réseau LTI à deux ports [Hashtrudi-Zaad and Salcudean, 2001]. Pour les systèmes modélisé en non-linéaire, d'autres approches basées sur la passivité sont proposées dans [Anderson and Spong, 1989b, Hannaford, 1989a, Lawrence, 1993].

Transparence

La transparence est le second objectif à atteindre pour un téléopérateur. Il s'agit d'un indicateur traduisant la qualité du suivi en position du système et surtout de la qualité du retour d'effort. En d'autres termes, un téléopérateur est transparent quand l'opérateur a l'impression de manipuler directement son outil en interaction avec l'environnement, malgré la présence du système de téléopération [Hannaford, 1989b, Lawrence, 1993]. Il est admis qu'un système de téléopération ne peut être complètement stable et transparent simultanément. Il s'agit alors de trouver un compromis entre ces deux objectifs (voir [Niemeyer and Slotine, 1991, Nuno et al, 2011] par exemple). Plusieurs approches ont été proposées pour améliorer la transparence de téléopérateurs.

Une première approche se base sur le concept d'impédance. Un système de téléopération idéal est transparent si l'impédance de l'environnement est parfaitement reproduite par l'interface haptique de l'opérateur [Hashtrudi-Zaad and Salcudean, 2002, Kim et al, 2013, Lawrence, 1993].

Une approche plus fine consiste à évaluer la variété d'impédances de l'environnement ("minimale", "maximale" et "amplitude") que le téléopérateur est susceptible de reproduire à l'opérateur, qui doit naturellement être la plus large possible [Baser et al, 2012, Cavusoglu et al, 2001, Khademian and Hashtrudi-Zaad, 2012].

Une dernière approche consiste à évaluer le niveau de transparence en comparant directement les variables de puissance échangées entre l'opérateur et son interface d'une part et l'outil et son environnement d'autre part [Moreau et al, 2012, Yokokohji and Yoshikawa, 1994]. Elles sont comparées à une trajectoire (en position et effort) idéale souhaitée pour déterminer la qualité de la téléopération.

Pour conclure, la première et deuxième famille d'approches nécessite de formaliser explicitement, sous forme de fonctions de transfert, les différentes impédances, ce qui n'est possible qu'avec des modélisations linéaires. La dernière famille est plus générique mais la qualité du système étant évaluée en fonction de modèles de trajectoires, ceux-ci sont difficiles à générer de manière anticipée et générique.

Conclusion

Les systèmes de téléopération ont fait beaucoup de progrès depuis l'invention de Raymond C. Goertz. Les distances admissibles ont énormément augmenté, accompagnées de nouvelles difficultés à contourner. Aussi, l'usage des canaux de communication numérique a facilité l'interconnexion entre maître et esclave mais a introduit des retards variables et des pertes de données. Des travaux de recherche récents proposent des lois de commande offrant un bon compromis stabilité-transparence avec des systèmes dont les délais de communication sont asymétriques et variables, qui ne nécessitent pas de modéliser l'opérateur (ce qui est intrinsèquement ardu) ou l'environnement (qui évolue souvent de manière imprévisible), et sans capteurs d'effort coûteux.

Cependant, ces systèmes ne fonctionnent qu'avec un seul utilisateur (l'apprenant, dans un contexte pédagogique), ce qui fait qu'ils ne sont pas utilisables tels quels pour notre application de simulateur pédagogique "à quatre mains". Toutefois, cette étude des systèmes de téléopération était nécessaire car ils sont le fondement des systèmes multilatéraux décrits dans la section suivante.

Systèmes haptiques multilatéraux

Quand le nombre d'utilisateurs, de maîtres et/ou d'esclaves n'est plus unique dans un téléopérateur avec retour d'effort, il s'agit de *téléopérateurs multilatéraux*.

Dans ce contexte, trois cas se présentent: les téléopérateurs à

- maître unique et esclaves multiples,
- multiples maîtres et esclave unique, et
- multiples maîtres et multiples esclaves.

Ces systèmes ont été conçus notamment pour des usages de formation dans le domaine médical [Nudehi et al, 2005] et de manipulation collaborative [Buss et al, 2009, Lee et al, 2005, Lee and Spong, 2005].

Plusieurs stratégies ont été développées pour assurer et stabilité et transparence pour ces systèmes. Par exemple, Sirouspour et al [Sirouspour, 2005] ont développé

par μ-synthèse une architecture de contrôle multilateral (multiples maîtres et esclaves) robuste pour une téléopération collaborative en sa basant sur l'hypothèse que l'opérateur et l'environ-nement sont passifs (ce qui n'est pas toujours le cas et a été explicité dans [Islam et al, 2015]). Le contrôleur de téléopération non-linéaire adaptatif développé dans [Zhu and Salcudean, 2000] a été étendu à la coopération par [Sirouspour and Setoodeh, 2005] mais sans système d'autorité réglable entre utilisateurs. Polushin et al [Polushin et al, 2013], quant à eux, font appel à l'approche petit gain pour concevoir son contrôleur, ce qui leur garantit la stabilité en présence de multiples contraintes de communication. Ces travaux se limitent cependant aussi à un usage coopératif.

Du point de la recherche de la passivité, les auteurs de [Mendez and Tavakoli, 2010] ont explicité un critère à un réseau de systèmes à n ports, qui peut être appliqué à un système multilatéral dont les systèmes connectés sont inconnus. Ce critère s'applique sur la matrice d'impédance du système, ce qui impose de pouvoir modéliser ces impédances sous forme linéaire sous peine d'obtenir difficilement des conditions applicables en cas de non linéarité dans les modèles des interfaces haptiques typiquement.

Systèmes haptiques dual-user

Les systèmes haptiques trilatéraux à deux utilisateurs *dual-user* sont un cas particulier des systèmes multilatéraux où deux utilisateurs travaillent ensemble avec un seul esclave. Ils ont été présentés une première fois pour un usage de formation médicale en 2005 dans [Nudehi et al, 2005] et pour de la télé-réhabilitation plus récemment dans [Shahbazi et al, 2014].

Les systèmes *dual-user* sont composés d'une interface haptique par utilisateur et d'une architecture logicielle qui connecte ces interfaces pour réaliser un contrôle combiné de l'esclave (cf. fig. R-8). L'esclave peut être un robot réel équipé d'un outil ou une simulation informatique reproduisant un outil virtuel en interaction avec un environnement virtuel. Ainsi les utilisateurs interagissent sur l'environnement simultanément à travers leurs interfaces haptiques dans un objectif de comanipulation ou de formation typiquement.

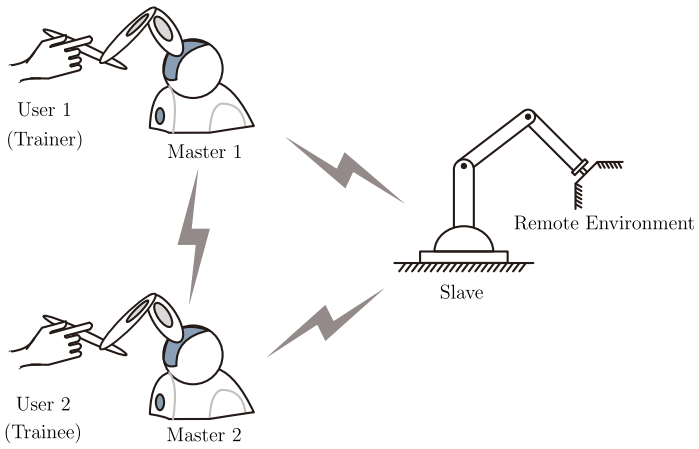

Figure R-8: Système *dual-user*

Concept principal

Le concept commun aux différentes architectures étudiées est que chaque inteface haptique fournit un retour d'effort à chaque utilisateur, fonction d'un *facteur de domination* ($\alpha \in [0, 1]$). Quand $\alpha = 1$ (resp. 0), l'utilisateur 1 (resp. l'utilisateur 2) a toute autorité sur l'interface de l'utilisateur 2 (resp. 1) et sur l'esclave. Quand $0 < \alpha < 1$, les deux utilisateurs partagent le contrôle de l'esclave avec un niveau de domination (sur l'autre utilisateur) qui est fonction de α. En pratique, ce niveau d'autorité partagée est déterminé par les compétences relatives et de l'expérience de chaque utilisateur.

Un exemple d'évolution de l'autorité dans la formation d'un apprenant utilisant un système dual-user est présenté en figure R-9 où les lignes solides représentent les échanges prenant part au contrôle de l'esclave, tandis que les pointillés ne représentent que les signaux de retour d'information. On peut constater que cette évolution fait passer par des scénarios de formation ($\alpha = 0$), guidage ($0 < \alpha < 1$) et évaluation ($\alpha = 1$).

Architectures existantes

Plusieurs architectures ont été proposées pour le contrôle des systèmes *dual-user*. Le concept du contrôle partagé (*shared control*) a été amené par Nudehi et al. dans [Nudehi et al, 2005]. Dans un contexte de formation, α peut être réglé à 1 (100%)

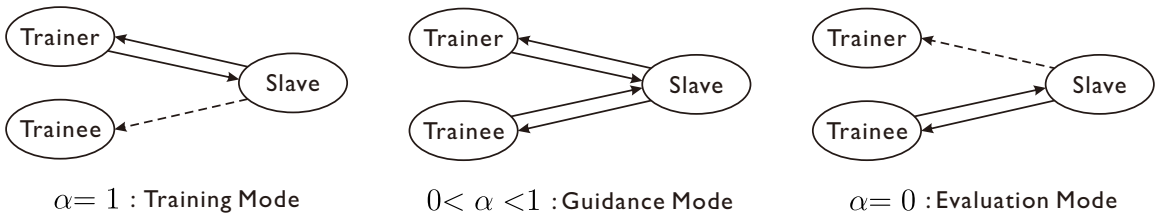

Figure R-9: Structure de scénarios de formation avec un système *dual-user*.

pour le formateur dans un premier lieu puis, au fur et à mesure que l'apprenant progresse, α peut être diminué jusqu'à 0 [Ghorbanian et al, 2013].

Dans l'architecture proposée par Nudehi, les dispositifs maîtres fournissent un retour d'effort aux deux utilisateurs, proportionnel à la distance entre les positions indiquées par leurs interfaces haptiques et inversement proportionnel à leur niveau d'autorité. Cette architecture peut être utilisée en présence de délais de communication. Cependant l'utilisateur qui a le contrôle absolu sur l'esclave ne reçoit pas de retour d'effort de l'environnement, ce qui limite intrinsèquement la transparence de la manipulation.

Chez [Khademian and Hashtrudi-Zaad, 2011], cette limitation de la transparence est surmontée en créant un contrôle multilatéral à trois ports. Deux architectures différentes sont proposées. La première, *Complementary Linear Combination* (CLC), qui fournit un retour d'effort combinant les efforts appliquées par l'environnement sur l'outil et les efforts appliqués par l'autre utilisateur (resp. F_e et F_{h_2}, pour l'utilisateur 1). Les signaux de commande pour obtenir la position désirée et le retour d'effort pour chaque interface haptique sont une combinaison linéaire complémentaire des positions et des efforts captés des deux autres dispositifs (l'autre interface et l'esclave). Quand $\alpha = 1$, le maître 1 et l'esclave forment un système de téléopération quatre canaux, et la position du maître 1 agit comme une position désirée pour le maître 2 (le comportement est symétrique quand $\alpha = 0$). Quand $0 < \alpha < 1$, les deux utilisateurs peuvent collaborer sur une même tâche dans un environnement partagé.

La seconde architecture proposée par [Khademian and Hashtrudi-Zaad, 2011] s'appelle *Masters Correspondence with Environment Transfer* (MCET). Ici, les deux interfaces haptiques suivent mutuellement la position de l'autre et chaque utilisateur

reçoit en retour d'effort, la moité de l'effort appliqué par l'environnement sur l'outil de l'esclave, soit $F_e/2$. Le signal de commande transmis à l'esclave est pondéré par α. Une analyse de la transparence (à travers le retour d'effort) et des études expérimentales de perception ont montré que l'architecture MCET possède la meilleure transparence avec le moins de sensibilité à la valeur de α. Dans notre contexte, malgré ces résultats intéressants, la modélisation linéaire utilisée dans cette étude (limitant le réalisme de la modélisation des utilisateurs et de l'environnement), combinée au fait que les auteurs ne tiennent pas compte des retards de transmsission, rend incompatible ces deux architectures avec nos exigences et le fait que le deuxième utilisateur soit isolé en situations de formation/évaluation.

Dans [Ghorbanian et al, 2013], les auteurs définissent deux facteurs de domination: α (resp. $(1-\alpha)$) qui détermine l'autorité du formateur (resp. apprenant) sur l'apprenant (resp. formateur), tandis que β et $(1-\beta)$ indiquent la suprématie des deux utilisateurs respectifs sur le robot esclave. Une relation non linéaire entre α et β est proposée pour ajuster l'autorité du *leader* (l'utilisateur pour qui le facteur de dominance $\alpha > 0.5$) sur l'esclave par rapport à l'autorité sur le suiveur. Les performances de cette architecture n'étant pas comparées à d'autres, il n'est pas possible de déterminer si cette architecture est plus transparente que d'autres. Son intérêt dans le contexte de notre étude réside dans l'approche de modélisation non linéaire et la prise en compte des délais de communication incertains, de pertes et d'inversion de données. Nous n'avons pas développé cette piste car nous en avons pris connaissance après avoir développé la stratégie énergétique présentée dans ce mémoire. Toutefois, il serait intéressant par la suite de comparer ultérieurement les performances entre cette approche et la notre.

Partage d'autorité

L'ensemble des architectures de systèmes *dual user* font appel au concept du contrôle partagé où il est possible de donner à l'un ou l'autre des utilisateurs une autorité sur l'esclave: absolue, nulle ou partagée. Les mécanismes diffèrent cependant d'un auteur à l'autre. Par exemple, Nudehi et al le mettent en place en suivant une analogie d'un

système mécanique "en forme de H" [Nudehi et al, 2005]. Razi et al proposent plutôt un modèle construit sur l'analogie avec une boite de vitesses à trois voies [Razi and Hashtrudi-Zaad, 2014]. Une autre architecture a été développée pour des systèmes multi utilisateurs avec un même esclave décrits dans [Shahbazi et al, 2015]. Ce qui différencie principalement ces différentes approches est le retour d'effort: F_e chez [Shahbazi et al, 2015], $F_e/2$ pour l'architecture MCET de [Khademian and Hashtrudi-Zaad, 2011] ou encore d'autres possibilités. Il est clair que pour notre application de formation pratique, un retour d'effort complet (F_e) pour chaque utilisateur, quel que soit son niveau d'autorité est une fonction essentielle.

Stabilité

En ce qui concerne la stabilité de ces architectures, plusieurs approches ont été abordées dans la littérature scientifique. Les systèmes *dual user* sont souvent modélisés en systèmes LTI. Nudehi et al. [Nudehi et al, 2005] font appel à la méthode H_∞ pour garantir la stabilité même en présence de délais de communication (jusqu'à 25ms au cours de leurs expérimentations).

La stabilité est analysée en appliquant le critère de stabilité inconditionnelle de Llewellyn dans [Khademian and Hashtrudi-Zaad, 2011]. Ainsi, l'architecture CLC est inconditionnellement stable alors que l'architecture MCET demeure potentiellement instable.

Une extension du critère de Zeheb-Walach concernant la stabilité absolue d'un réseau à n ports est proposée dans [Razi and Hashtrudi-Zaad, 2014]. Elle est appliquée à des architectures de téléopération à deux canaux et a montré que lorsque les deux utilisateurs ont la même autorité sur l'esclave, il est possible d'appliquer des gains plus élevés dans les contrôleurs, et donc d'obtenir une meilleure transparence. Mendez et al font appel à la modélisation de systèmes LTI en réseau à n ports dans [Mendez and Tavakoli, 2010], pour modéliser des systèmes multilatéraux. Un critère nécessaire et suffisant pour obtenir la passivité du système est proposé. Il est démontré que lorsque $n = 2$, les conditions résultant de l'application de ce critère convergent vers celles du critère de passivité de Raisbeck défini pour les systèmes à deux ports. De plus, une

comparaison entre le critère de passivité de Raisbeck et le critère de stabilité absolue de Llewellyn est détaillée dans [Li et al, 2014], concluant que, pour des systèmes à 3 ports, le critère de stabilité absolue est moins conservatif que le critère de passivité.

Dans [Ghorbanian et al, 2013], une fonction de Lyapunov-Krasovski est proposée pour assurer la stabilité. Cette approche est la plus générique mais cette étude ne tient pas compte de la transparence, ce qui rend difficile la comparaison avec d'autres travaux.

La conception et l'évaluation des performances d'un système de formation trilatéral sont décrites dans [Shamaei et al, 2015]. Le critère de Llewellyn est utilisé pour vérifier la stabilité. Les résultats montrent que le système demeure stable pour différentes valeurs de α.

En conclusion, à part pour [Ghorbanian et al, 2013], toutes ces architectures ont été étudiées à partir de modèles LTI. Aussi, leur applicabilité est limitée pour représenter fidèlement des systèmes complexes ou au comportement non linéaire ou inconnu. Seul [Ghorbanian et al, 2013] tient compte des retards de transmission, inhérents à toute communication sur réseau informatique de moyenne ou grande envergure. Par ailleurs, aucune d'entre elles ne considère explicitement la stabilité quand α varie en temps réel.

Transparence

A notre connaissance, très peu d'articles scientifiques étudient la transparence des systèmes *dual user* : [Khademian and Hashtrudi-Zaad, 2011, 2012, Shamaei et al, 2015]. Les contributions se fondent sur une extension des méthodes appliquées en téléopération (impédance sous forme de fonction de transfert, amplitude d'impédance reproductible) présentée en section 2.2.3. La difficulté d'évaluer la transparence est de la lier au partage d'autorité. De nouvelles définitions devraient être proposées pour s'adapter à ces systèmes et pouvoir comparer les performances.

Le problème se pose précisément du fait du partage d'autorité. En effet, ce concept fonctionne bien pour une manipulation collaborative mais n'est pas conçu initialement pour une formation pratique: quand le formateur fait une démonstration incluant des

interactions outil-environnement, il doit recevoir le bon niveau de retour d'effort pour pouvoir doser son geste certes, mais l'apprenant également pour apprendre lui aussi à doser ses gestes. Or, ce n'est le cas d'aucune des architectures étudiées.

Conclusion

En reprenant les exigences de notre simulateur pédagogique (à usage dans un contexte médical) exposées en section "Exigences et principal cas d'utilisation", les systèmes *dual-user* sont les plus à même d'y répondre. Cependant cet état de l'art a montré qu'ils ne répondent pas exactement à toutes nos exigences dans l'état actuel. Il nous a donc fallu proposer une nouvelle architecture s'inspirant de l'existant et répondant parfaitement au cahier des charges.

Contributions

Le système à concevoir n'a pas pour objectif d'aider deux personnes à co-manipuler efficacement un robot distant (objectif général des systèmes *dual-user*) mais de faciliter la formation pratique d'un apprenant en présence d'un formateur et ainsi combiner les avantages des simulateurs haptiques avec ceux des méthodes de formation à quatre mains, ou plus généralement de **formation pratique supervisée**.

Néanmoins, l'intérêt de ces architectures est leur mécanisme de modification de l'autorité entre les deux utilisateurs. Celle-ci peut ainsi être appliquée au formateur pour qu'il puisse réaliser une démonstration d'un mouvement à réaliser, par exemple, puis progressivement déplacée vers l'apprenant jusqu'à ce que celui-ci soit suffisamment autonome pour que le formateur puisse l'évaluer.

Suite à l'étude des architectures précédentes [Ghorbanian et al, 2013, Khademian and Hashtrudi-Zaad, 2011, Nudehi et al, 2005, Razi and Hashtrudi-Zaad, 2014, Shahbazi et al, 2015], nous avons donc retenu et adapté le concept du contrôle partagé. La stabilité a également été un objectif indispensable à atteindre, sachant que les utilisateurs ne seront jamais les mêmes et l'environnement peut être réel comme virtuel et dynamique, ce qui n'autorise pas de modélisation a priori. Partant du constat

de [Secchi et al, 2007] stipulant que la théorie de la passivité associée au formalisme par ports hamiltoniens présente des avantages en terme de simplification des conditions de stabilité pour les systèmes automatisés, nous avons pris le parti d'étendre cette modélisation aux systèmes *dual-user*. Ce formalisme vérifie la passivité relativement simplement pour des systèmes non linéaires et présente l'intérêt de pouvoir être étendu à de nouveaux utilisateurs sans complexifier outre mesure l'étude.

Nous avons donc conçu une nouvelle architecture intrinsèquement passive (développée au chapitre 3.2), fondée sur des contrôleurs IPC (cf. section 3.3) qui sont eux-même intrinsèquement passifs. Cette architecture intègre un mécanisme de partage d'autorité inspiré de celui utilisé dans l'architecture CLC [Khademian and Hashtrudi-Zaad, 2011]. Cette architecture est conçue sur un seul degré de liberté mais nous avons pris soin de choisir un outil de modélisation offrant la possibilité d'augmenter ce nombre sans remettre en cause l'édifice.

Cependant, celle-ci n'était pas en mesure de fournir un retour d'effort à l'utilisateur qui n'est pas dominant. Nous avons donc amélioré cette architecture pour remplir cette fonction indispensable (voir section 3.4). Cette nouvelle fonction pouvant potentiellement rendre le système non passif, la condition de passivité a été établie et un contrôleur de passivité intégré à cette architecture veille à ce que cette condition ne soit pas violée. En mode formation ($\alpha = 1$), le formateur a le contrôle total de l'esclave. L'apprenant suit ses mouvements à travers sa propre interface haptique et est capable de ressentir l'effort à appliquer (le même que celui du formateur), lors de palpations par exemple. En régime libre (pas d'interaction outil environnement), si l'apprenant change volontairement la trajectoire de son interface, celle-ci va fournir un effort de rappel proportionnel à la distance entre la trajectoire réalisée par le formateur et celle imposée par l'apprenant. Ainsi l'apprenant s'aperçoit rapidement s'il s'éloigne de la trajectoire modèle. Cette architecture a été validée expérimentalement; ces expérimentations sont détaillées en section 3.8.1.

Suite aux diverses expérimentations, nous avons constaté qu'il n'était pas toujours facile pour le formateur d'avoir à modifier le niveau d'autorité manuellement, notamment dans les situations d'urgence où il est en mode suiveur ($\alpha = 0$) et qu'il se rend

compte qu'il faut très rapidement empêcher l'apprenant de continuer un geste potentiellement dangereux s'il s'agissait d'un vrai patient. Il doit en effet prendre la main instantanément mais pour cela modifier manuellement α. Nous avons donc étudié un **mécanisme de gestion adaptative du niveau d'autorité** afin que dans ce genre de situation le formateur n'ait qu'à éloigner l'outil de sa trajectoire actuelle à travers l'interface haptique qu'il tient en permanence en main pour qu'il reprenne le contrôle de l'esclave. Cette fonctionnalité a été développée et testée expérimentalement au chapitre 4.

Afin de situer notre nouvelle architecture par rapport à celles existantes, nous avons sélectionné les deux architectures les plus proches de la notre en terme de fonctions et de modèle de partage de l'autorité: CLC et MCET [Khademian and Hashtrudi-Zaad, 2011]. Nous avons comparé (au chapitre 5) ces trois architectures en terme de suivi de position sur des trajectoires prédéfinies et selon différentes valeurs de α, sur un degré de liberté. Nous avons du définir un critère de performance adapté à un système *dual-user* et avons utilisé Matlab Simulink ® pour comparer les trois architectures de manière systématique. Par soucis de neutralité, nous avons paramétré chaque architecture en choisissant les réglages qui donnent indépendamment l'une de l'autre, les meilleures performances (selon le critère défini) pour les tâches définies. L'étude conclut que les performances en suivi de trajectoire des trois architectures sont semblables. Nous n'avons pas pu réaliser d'étude comparative sur la qualité des retours d'effort car les trois architectures ont des politiques de retour (en fonction de α) totalement différentes et donc incomparables. Comme CLC et MCET ne proposent pas (contrairement à la notre) de retourner l'effort de l'environnement sur l'esclave aux deux utilisateurs simultanément, quelle que soit leur autorité, nous avons donc pu conclure que notre architecture apporte globalement une plus value.

Étant donné que ce système sera amené à être utilisé avec des utilisateurs distants, nous avons abordé au chapitre 6 la problématique de la présence de retards de transmission. Une approche basée sur la transformation en variables d'ondes a été étudiée (*Augmented Wave Variable Transformation - AWVT*) [Li and Kawashima, 2014]. Elle a été complétée par une amélioration du contrôleur de passivité présenté

précédemment pour tenir compte des retards de transmission. Des expérimentations valident ce concept mais font apparaître une dérive des positions entre les maîtres et l'esclave, qui reste à ce jour un problème ouvert. Un guide pour le paramétrage du système est également proposé.

Conclusion et perspectives

La simulation informatique pour l'apprentissage pratique est apparue il y a environ deux décennies mais elle commence seulement aujourd'hui à se démocratiser. Elle répond à des contraintes de temps de formation toujours plus réduits qui engendrent des situations dangereuses notamment dans le cadre médical où les internes finissent leur formation pratique sur de réels patients. Elle répond également à un besoin de réalisme qui n'est plus toujours satisfaisant avec les moyens traditionnels (toujours en médecine, sur des cadavres, des cochons, des mannequins en matière plastique, ... qualifiés de simulateurs basse fidélité) étant donné les progrès technologiques. Si elle aide les apprenants à acquérir des compétences gestuelles en autonomie, actuellement elle n'offre pas de moyen satisfaisant de transposer un apprentissage à quatre mains réalisé en collaboration formateur-apprenant. En effet, si le formateur a généralement accès via un écran à des informations concernant la simulation de son apprenant, il n'a pas accès à une interface haptique pour montrer, corriger, accompagner l'apprenant dans ses gestes dans des situations complexes ou imprévues dans le simulateur initialement.

Nous nous sommes donc penchés sur cette problématique en établissant un cahier des charges précis du fonctionnement attendu de ce type de simulateur où doser l'effort est primordial. Nous avons étudié la littérature scientifique concernant les systèmes de téléopération ainsi que les systèmes *dual user* afin de cartographier les différentes approches déjà explorées, leurs avantages, leurs faiblesses. Nous sommes arrivés à la conclusion qu'aucune ne répondait complètement à notre cahier des charges. Nous avons donc développé une nouvelle architecture se fondant sur le concept de partage d'autorité, commun aux architectures existantes. Cette architecture n'a été étudiée

que sur un seul degré de liberté mais nous avons pris soin de choisir un outil de modélisation (approche énergétique, systèmes à port hamiltoniens) qui nous facilite son extensibilité à plusieurs degrés de liberté mais également à plusieurs apprenants le cas échéant. La passivité du système est garantie par un contrôleur de passivité. Nous avons testé expérimentalement ce système, qui a démontré des performances conformes à notre cahier des charges. Suite à des constatations lors des expérimentations, nous avons doté cette architecture d'un mécanisme adaptatif de gestion de l'autorité afin de faciliter les gestes d'urgence de la part du formateur en cas de situation critique. Nous avons prouvé que ce mécanisme ne remettait pas en cause la passivité du système et nous avons validé son fonctionnement expérimentalement.

Afin de situer notre architecture par rapport à l'existant, nous avons réalisé une étude comparative avec deux autres architectures *dual user*. Cette étude a démontré des performances équivalentes en terme de suivi de trajectoires et un gain indéniable en terme de retour d'effort aux deux utilisateurs quel que soit leur niveau d'autorité.

Pour ouvrir l'usage du simulateur à des utilisateurs distants, nous avons débuté une étude visant à préserver la passivité du système tout en limitant la dégradation de la transparence, en présence de retards de communication. Nous avons validé expérimentalement un nouveau contrôleur de passivité, avec cependant un phénomène de dérive qu'il faudra compenser dans les prochains travaux.

Ce travail ouvre le champ à de nombreuses améliorations et extensions déjà évoquées:

- passage à des modèles à plusieurs degrés de liberté: soit en intégrant des modèles non linéaires des interfaces haptiques et de l'esclave soit en faisant appel à des contrôleurs bas niveau découplant et linéarisant afin de dupliquer l'architecture actuelle en fonction du nombre de nouveaux degrés de liberté ;

- amélioration des solutions de passivation proposées en présence de retards de transmission, notamment élimination du problème de dérive en position. Il existe d'autres solutions à base de contrôleurs de passivité dans des applications de téléopération. Il serait intéressant d'étudier dans quelle mesure elles peuvent

s'appliquer à notre architecture ;

- extension à plusieurs apprenants: en mode démonstration, cela éviterait au formateur de répéter n fois ses gestes; les étudiants pourraient aussi comparer leurs trajectoires entre eux ;

- une étude d'usage devra être réalisée pour évaluer l'intérêt réel en terme d'apprentissage par rapport à des apprenants n'utilisant pas de simulateur haptique ou un simulateur haptique sans supervision ;

- une application de ce simulateur dans des domaines différents du médical. Cette étude s'est placée dans un contexte médical mais rien dans la solution ne la cantonne à ce contexte. Il est donc tout à fait envisageable d'appliquer ce simulateur pour former des pilotes d'avion, par exemple, et toute personne dont les compétences font appel à une gestuelle précise et à un dosage des efforts à appliquer.

Part I

Background

Chapter 1

Introduction

1.1 Main context

Minimally Invasive Surgery (MIS) is only about 20 years old, but it is becoming more and more important in medical surgeries [Park and Lee, 2011]. MIS is less traumatic than classical surgery as it allows the patient to recover from diseases faster. On the other hand, it requires complex and costly equipments, trained staffs and skilled surgeons. Indeed, MIS procedures imply manipulating instruments through trocars and visualizing them by way of a 2D (or 3D) endoscopic camera. It requires more skills from the surgeon than in open surgery, because of the limited operation and view field, disorienting hand-eye coordination, distortion of kinesthetic feedback from the instruments and difficult manipulations [Tavakoli, 2008]. To overcome these problems, the da Vinci® Surgical System introduced by Intuitive Surgical [Surgical, 2016] is used for multi-domain MIS operations, such as urology, gynecology, cardiac surgery etc, in order to help the surgeon in his surgical tasks.

To perform practical training, medical trainees traditionally make use of two types of simulations. The first one is the synthetic simulations, with manikins, in order to replay complex procedural situations (*Medical Team Training - MTT*); it is also called *relational simulation* which aims at covering procedural and decisional aspects in the communication in the medical group. The second type consists in training to practice to medical gesture on phantoms (synthetic parts reproducing a part of

human anatomy) but more regularly on real anatomical parts or entire cadavers and animals. Nevertheless, on the one hand, cadavers and animals are costly and not available anytime and, on the other hand, ethics recommendations foster phantoms and computer based simulators. Notice that anthropomorphic simulators remain inefficient as they still lack realism (carnation, touch, ...) in low and even in high definition. Moreover they generate high maintenance costs (one has to regularly renew some parts that wear out).

All these solutions often lack realism (with biomechanical behaviors different than human tissues, for instance). Computer based simulation for training has appeared in early 2000 (see for instance [Kaufmann and Liu, 2001] for trauma training). In 2011, Fairhust et al provide a comprehensive overview [Fairhurst and Strickland, 2011] of the progress of simulation in surgical training, featuring the appearance of haptic simulators (with force feedback on hand-held interface). The latest review on this topic has been written in [Yiannakopoulou et al, 2014].

Simulators permit to train and improve the skills of the surgeons without any risk. They provide training feedback which allows trainees to make mistakes [Lewis et al, 2011]. As a sample, the LapSim ® system (shown in Fig. 1-1[1]) from Surgical Science© [SurgicalScience, 2016b] provides laparoscopic training procedures that can be practiced again and again with different levels of difficulty. They are designed to overcome the drawbacks of aforementioned traditional models, and aim at improving the skills of a surgeon during education program or through long life training. They provide to trainees a realistic environment rendered in 2D and more recently in 3D (such as in [Delorme et al, 2012]).

These simulators have competitive advantages compared to animals and cadavers, in terms of logistics (they can be available 24h a day), they do not pose any problem of ethics, they enable to repeat the same operation as many times as necessary. What characterizes particularly a simulator is its ability to immerse the user and to blur the feeling of artificial situation; in other words, to achieve a *suspension of*

[1]Image extracted from `http://www.surgical-science.com/lapsim-the-proven-training-system/`, May 2016.

Figure 1-1: LapSim Haptic & LapSim Non-Haptic Systems

disbelief [Slater et al, 2001]. In France, they are a solution recommended by the *"Haute Autorité de Santé" (HAS)* which advocates, since 2012, the development of simulation in medical training, with the leitmotiv: *"Never the first time on the patient"*. The first generation of simulators did not feature any force feedback, so they could not reproduce exactly the forces exerted by the organs on the virtual tools, which can be critical in the success of some medical operations. With haptic training simulators, the force feedback provides (at least, should provide) a realistic tool behavior. The trainee is aware when his (virtual) tools are, for instance, in contact with the (simulated) tissues. It leads to a more efficient training for advanced tasks (see [Coles et al, 2011]).

Nowadays, a basic training on anatomical parts is practiced (Basic Skill Surgery, BSS). Indeed, concerning the LapSim simulator, training modules are sufficiently specialized to enable trainees to familiarize themselves with medical issues and situations and to replay a high number of times over some critical situations. These simulation based trainings can be seen as a complementary way of training with four hand fellowship training (also known as supervised training) where the trainer takes the hands of the trainee in his own hands in order to follow or guide him in his task. The main drawback of this manual training method is that it is difficult for both

users to dose their own efforts, so that the trainer cannot learn efficiently the right level of force to produce. Its advantage is the flexibility offered to the trainer to explain, demonstrate, supervise the trainee. Therefore, combining the advantages of single user haptic simulators and fellowship training would permit to get the best of both approaches. Indeed, simulators are programmed to handle a given number of situations which have been anticipated at design. Even if, with the experience, it is possible to foresee and integrate into the simulator the most recurrent cases, it is not feasible to program every situation. It is more efficient to provide some flexibility to allow the trainer to intervene during the simulation as he traditionally does during classical hands-on training sessions: to unfreeze a delicate situation, to advise and accompany the trainee, etc.

Figure 1-2: The da Vinci Si dual console system.

Considering the survey [Coles et al, 2011] covering medical training simulators, it can be seen that current devices are mainly based on physical setups or virtual environments where the trainee is alone and for which the guidance for his/her gesture is difficult. As far as we know, the da Vinci Si dual-console system [SurgicalScience, 2016a] shown in Fig 1-2[2] is the only one which enables training for two users simultaneously. However, the drawback of this system is that only one user can control the

[2]Image extracted from `http://www.intuitivesurgical.com/company/media/images/davinci_si_images.html`, May 2016.

instruments during training (while the other user has no control input), even if users can freely and quickly exchange their roles. Moreover, no haptic feedback is provided on this system.

Still, it would be useful to benefit from a simulator gathering trainee and trainer and furnishing a good level of realism simultaneously to both users (by way of two individual haptic interfaces), and combining the advantages of simulators and fellowship, with an adjustable and decreasing level of intervention from the trainer.

Thus, this motivates the use of dual-user training simulators.

1.2 Requirements and Main Use Case

For this specific application of surgical training, we needed an haptic system featuring two haptic interfaces (one for the trainee and the other one for the trainer) enabling leader-follower and collaborative modes. As a matter of fact, suppose at first that the trainer (an experienced surgeon) aims at showing the right trajectories of his surgical tool to a trainer by way of a simulator, in order to perform a task featuring some tool-environment contact. This implies that he requires a realistic force feedback to dose the efforts he applies on the tool, as in a traditional bilateral teleoperation context. He would then set his device in **leader** mode (and so, the trainee's one in **follower** mode). Thus the trainer guides the slave (which can be either a real surgical robot handling a surgical tool dived into a real environment located in a near black box for instance, or a virtual tool-environment). He should get full force feedback in order to perform his task as if he was handling the real instruments. In practice, mentor surgeons work in hospitals while trainees study in their universities. A remote usage would be appreciated to gain transport time delays.

Meanwhile, the trainee's device would follow the trajectory of the leader one. If the trainee deviates from this reference trajectory in free motion stage, the compliance of the device should bring him back on the right position. He should also feel in his hand the right level of effort to provide to the tool in case of interaction between the tool and its environment, by means, for instance, of a display which guides him

towards a target effort. The system should be able to be freely inverted so that the trainee manipulates and the trainer follows and evaluates trainee's motions and applied efforts.

1.3 Objectives

To overcome the absence of such simulation solution providing a full force feedback to both users, we propose to design a haptic simulator where both the trainee and trainer interact on the same task, each one with his own haptic interface. This simulator should permit to perform different types of medical tasks (such as trajectory tracking, position holding, needle insertion, obstacle avoiding etc.) with a sufficient transparency to be efficient for gesture training.

To comply with real life situations, as skilled surgeons cannot always be presented in universities for training, a remote usage of this simulator should also be available. Moreover, as many trainees may require the same training at the same time, this simulator should be easily scalable to more than one trainee.

In more technical terms, these objectives will imply to:

- Design a dual-user (and likely a multi-user) system for haptic training.
- Propose a controller ensuring robust stability of the whole system, knowing that the two (or more) users and the environment may not be modeled because of their complexity and evolution in time.
- Evaluate experimentally the performance of this system, in terms of transparency.
- Evaluate experimentally the interest of this system, in terms of training.

1.4 Contributions

In order to achieve these objectives, we carried out a wide state-of-the-art survey (presented in Chapter 2) which led us to conclude that existing dual-user systems

make use of a shared control mechanism which enables them to share the control authority over the slave between each user. There exists various modeling and control approaches, including linear, non-linear and energetic models. Only a few of them consider all together the issues of authority management, full force feedback and time delays. Taking into account these observations, we refined our requirements (modeling approach, training scenarios, adaptive authority, delays). Our contributions are summarized as follows:

Firstly, we designed a novel dual-user haptic training system featuring an Energy Shared Controller (ESC), introduced in Chapter 3, with one degree of freedom. This has led to an architecture providing full feedback to both users independantly from their own level of authority over the slave. This contribution provides a method for setting the authority in real-time without stability issue. A port-Hamiltonian approach is applied to model this system and warrants the passivity of the system. We validated its performances through experiments. We could conclude that the proposed system provides good performance in terms of position and force tracking. Moreover, in order to help in emergency situations, we added an adaptive authority adjustment mechanism which helps the trainer to get back some authority over the tool, to correct a bad gesture, for instance. We address the authority management issue in Chapter 4.

The second contribution addresses the position of this new architecture with respect to the ones existing in the literature. We provide a comparative study based on the position tracking performance, in Chapter 5. From these results, it is possible to conclude that our ESC scheme is competitive in terms of position tracking. From the force tracking point of view, the ESC architecture is the only one which provides a full force feedback to both users whatever authority level they are assigned.

The last contribution concerns a preliminary study of the ESC architecture with time delays, in Chapter 6. The Augmented Wave Variable Transformation (AWVT) approach [Li and Kawashima, 2014] is integrated into the dual-user framework. In order to ensure its passivity, we investigate it both from the closed-loop global system and subsystems point of view. An example of configuration is also presented, which

could be used as a guideline for selecting suitable parameters to meet the passivity requirements. We manage to obtain a stable system with a reasonable decrease of transparency (inevitable with delays). Still, this solution has a defect: a position drift which we will try to avoid in future works.

1.5 Document Outline

The aforementioned contributions of this thesis are organized in six chapters as follows:

Chapter 2 details a state of the art survey on haptic systems, ranging from bilateral to multilateral teleoperation systems. The necessary tools to design and to assess a bilateral teleoperation are surveyed, such as haptic interfaces, master/slave modeling, stability, transparency etc. Specifically, the existing dual-user systems are investigated.

Chapter 3 introduces our ESC dual-user haptic system. Built upon an authority sharing mechanism, we construct it as a closed-loop system, step by step. The final global system enables not only shared control, but also it provides both users with full feedback. The modeling of this system using port-Hamiltonian approach is presented. Furthermore, a passivity study is performed and a time-domain passivity controller is embedded. The last contribution concerns a preliminary study of ESC architecture with time delays, in Chapter 6. The Augmented Wave Variable Transformation (AWVT) approach (from [Li and Kawashima, 2014]) is integrated into the dual-user framework. In order to ensure its passivity, we investigate it both from the closed-loop global system and subsystems point of view. Furthermore, an example of parameter configuration is also presented, which could be used as a guideline for selecting suitable parameters to meet the passivity requirements. Real-time experiments are conducted to validate the proposed methods. An analysis is fulfilled, both from the closed-loop global system and from the subsystems point of view.

Chapter 4 addresses the problem of authority management. An Adaptive Authority Adjustment (AAA) method is introduced, based on the Virtual Fixture concept.

Three parameters permit to obtain an adaptive authority. An overrule function is also indicated for the presence of emergency situations. In addition, the passivity of the AAA mechanism is demonstrated. At last, real-time experiments are conducted through a set of training scenarios.

Chapter 5 focuses on the comparative study with two other dual-user frameworks. Position tracking tasks are implemented, with an assessment criteria. The results are provided with different authority values and different desired trajectories.

Chapter 6 introduces a preliminary study of the ESC architecture with time delays. The Augmented Wave Variable Transformation (AWVT) is incorporated into our dual-user system. An improved ESC shared control is established, which leads to new passivity control parameters. Finally, the performance of this architecture is evaluated through real-time experiments.

This report ends with conclusions and a discussion about future directions.

Chapter 2

State of the Art: Haptic and Dual-user System

2.1 Haptic System

Haptic term derives from the Greek term *haptomai*, which means "I touch". Haptic systems enable the human to interact with a software or a mechatronic system trough the touch. Haptic senses incorporate the sense of touch and the kinesthetic one. The sense of touch (or *cutaneous* perception) enables us, by skin contact with an object, to feel its temperature, the applied pressure, its texture, its toughness, while the kinesthetic one enables us to feel the position and forces involved in an interaction with an object through the muscles, tendons and joints.

Haptic systems are composed of an haptic interface and a software part. The haptic interface enables the user to send position or/and force information to the software. At the same time, the software sends (force or/and position) information back to the user. In teleoperation applications, the software is just an intermediary block between this system and a robot located in a remote location. In dual-user systems, several haptic interfaces are connected together with a (real or virtual) robot through a software.

Haptic systems are widely used in gaming, mobile electronics, robotics, learning and medical applications, etc (see [Hayward et al, 2004, Varalakshmi et al, 2012]). For

instance, the force feedback joystick used by gamers on simulator softwares provides realistic feeling [Deng et al, 2014]. Regarding the aspect of robotics, haptic systems are mostly used for remote operation purpose, such as underwater and outer space exploration [Hokayem and Spong, 2006]. Medical usage, such as haptic training, robotic-assisted surgery, rehabilitation, is also widely developed [Coles et al, 2011].

In this thesis, we focus on the context of medical training.

2.1.1 Haptic Interfaces

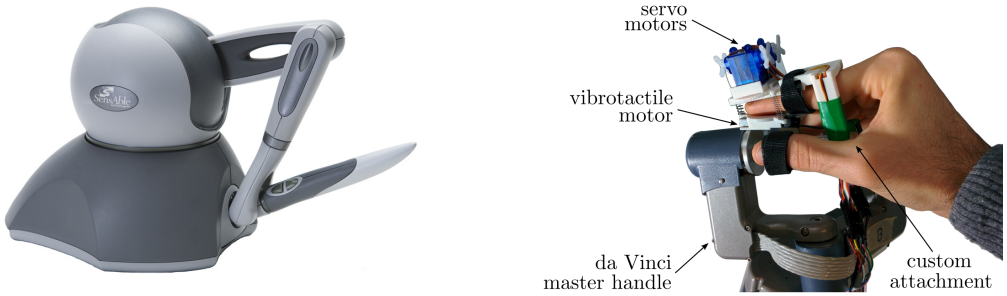

Figure 2-1: 3-DoFs kinematics haptic devices: the SensAble® PHANTOM Omni (Left) and the BioTac® tactile sensing based device (Right).

Haptic interfaces are the devices providing simultaneous information exchange between a human and a machine involving haptic perception. Most of the time, they provide kinesthetic information to the user. Yet, some researches are also held to design haptic interfaces exciting the sense of touch (see [Ware et al, 2014] for instance). As examples, the Phantom Omni (providing kinesthetic feedback) haptic device with 3-DoFs kinematics, and the BioTac® tactile sensing (providing cutaneous feedback) based haptic device (developed by the team of SIRSLab, University of Siena, Italy) are shown in Fig. 2-1 [1].

Ideally, when the haptic device is in free motion, no force is exerted on the user. The actuation and transmission incorporated in the interfaces should provide low friction and gravity compensation to achieve this "no force" rendering fidelity. When the device is under constrained motion, the actuators inside the haptic device play a

[1]Image extracted from `http://www.dentsable.com/haptic-phantom-omni.htm` and `https://prattichizzoblog.files.wordpress.com`, May 2016.

role as returning a force to the user. This is the case, for instance, when the simulator makes use of virtual fixtures to guide the motions of the user (e.g., [Liu et al, 2015]) or for teleoperation cases when the remote tool is in contact with its environment (e.g., [Sun et al, 2016]).

Electrical motors are mostly used for the force feedback function, but pneumatic (e.g., [Herzig et al, 2015]) and also hydraulic ([Buerger and Hogan, 2010]) actuators also start to appear as they provide a higher force/weight ratio, a wide bandwidth and a natural variable compliance (for the pneumatic ones). Some novel actuators, such as piezoelectric, shape memory metals, magnetic materials, also extend the possibilities for small size and lightweight portable haptic devices [Mazzone et al, 2003].

Nowadays, various types of haptic devices have been developed, which can be classified into two classes: the *grounded* class (with one locus interaction, see left picture[2] of Fig. 2-2 which depicts a Sigma.7 medical workstation presented at the Automatica industrial fair in Munich by DLR and Force Dimension) where interfaces are manipulated through an affordable end-effector, and the *non-grounded* class (attached to a part of human body, see right picture[3] of Fig. 2-2 which depicts the EXARM exoskeleton developed by ESA Telerobotics & Haptics Laboratory) where interfaces are mainly developed as hand or arm exoskeletons (see classification in [Hayward and Astley, 1996]).

Commercial haptic devices are mostly electrically actuated systems. They differ by the number of actuated degrees of freedom, their available workspace, the magnitude of the forces and torques applied on the user, or the shape of their end-effector. For more details, the reader can refer to [Coles et al, 2011]. A classification based on the workspace versus the force rendering capability of common devices is provided in Fig. 2-3[4].

Other kinds of novel haptic devices have been developed, such as the magnetic type

[2]Image extracted from `http://www.forcedimension.com/products/sigma-7/overview`, May 2016.

[3]Image extracted from `http://www.esa.int/Our_Activities/Space_Engineering_Technology/Telerobotics_Haptics_Laboratory`, May 2016.

[4]Image extracted from `http://kb.eurovr-association.org/index.php/Haptic_Hardware`, May 2016.

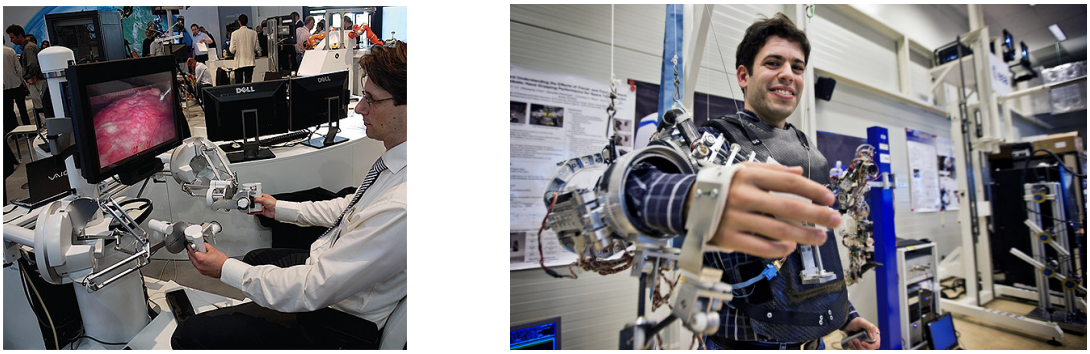

Figure 2-2: Examples of haptic interfaces (Left: grounded Sigma.7 medical workstation. Right: non-grounded EXARM exoskeleton.)

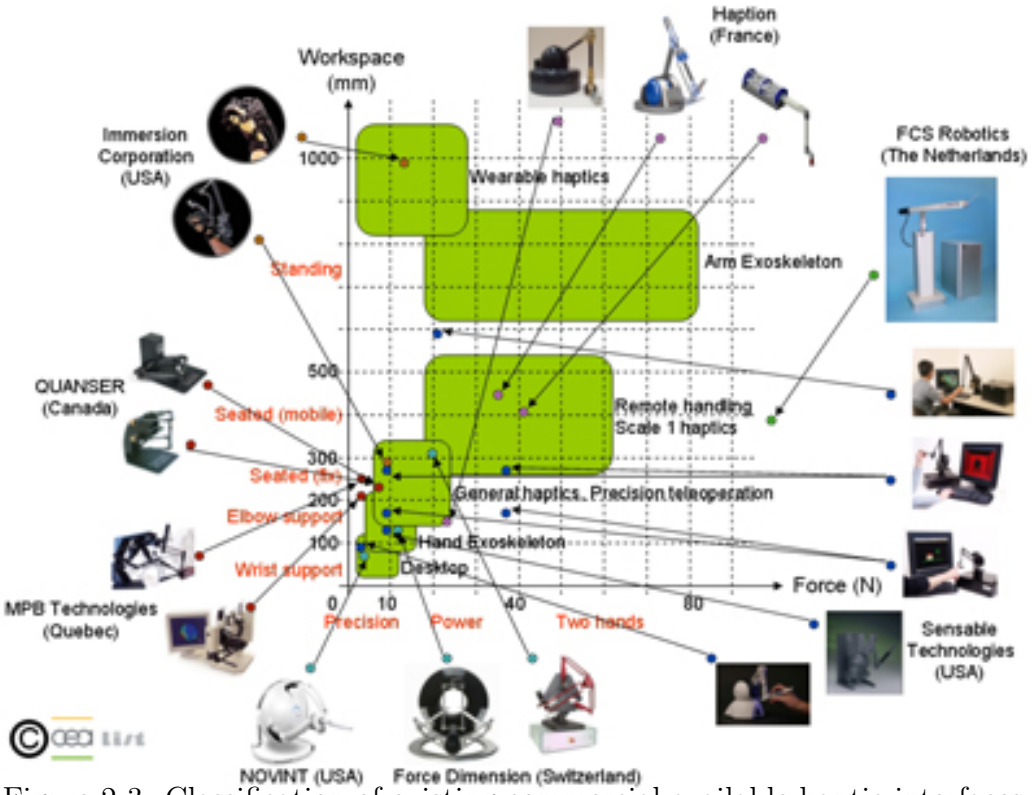

Figure 2-3: Classification of existing commercial available haptic interfaces.

[Berkelman and Hollis, 2000], but they have not been yet used for medical solutions.

Finally, the haptic interfaces can be classified into two categories of devices: either impedance type (sensed position, actuated force, which is widely used) or admittance type (sensed force, actuated position), based on the physical interaction causality [Peer, 2008].

2.1.2 Master-Slave System

Haptic systems commonly make use of master-slave systems with human and environment in the loop, as shown in Fig. 2-4.

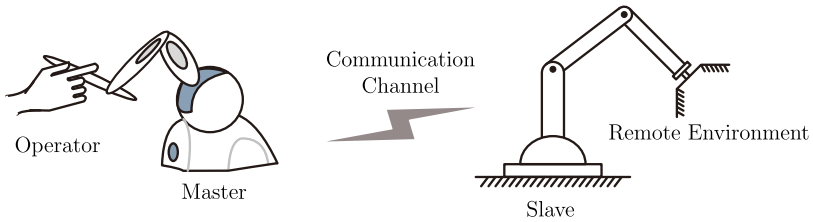

Figure 2-4: Master-Slave system with human and environment in the loop

The human user manipulates a local haptic interface, the *master device*, and applies some force and motion command to the system. The remote (or virtual, in the case of simulators) robot, the *slave device*, receives user interaction information and reproduces the user gesture to perform tasks in the remote (or virtual) environment. At the same time, the perceived interaction of the environment over the tool is fed back to the user through the communication channel. According to the distance between the master and the slave, a time delay may be present in the communication channel. Visual and audio feedbacks are supplementary pieces of information which are often transmitted besides for good ergonomics.

2.1.3 Teleoperation System

Typically, the aforementioned master-slave system is commonly referred as a *haptic teleoperation* system (when the slave is a real robot in a real environment). When force and position information are transmitted symmetrically, one uses the term of

bilateral teleoperation. When there is only feed-forward master actions but no force feedback from the slave, the system is named as **unilateral teleoperation**.

According to the usage, different types of teleoperation systems have been instantiated in practice. Bilateral teleoperation is the most developed haptic system in the literature as it provides better performances than unilateral one. The first master-slave teleoperator was built by Goertz [Sheridan, 1989] in mid 1940s which is cable driven aimed for the nuclear industry. It is worth to mention that the commercial teleoperators which have been introduced into medical therapy adopt only unilateral teleoperation (without haptic feedback), as for the da Vinci surgical robot.

2.2 Bilateral Teleoperation

Bilateral teleoperation systems have been studied from various aspects over the past 70 years. It is a key technology which extends the capabilities of the human to perform tasks in a remote environment by providing haptic feedback.

Bilateral teleoperation has been used into space operation [Penin, 2000], deep sea exploration [Saltaren et al, 2007], nuclear/toxic/explosive material handling and disposal [Kron et al, 2004], as well as medical application, for instance telesurgery [Guthart and Salisbury, 2000]. A survey about the first history of bilateral teleoperation was carried out in [Hokayem and Spong, 2006]. The goal of teleoperation systems is good motion tracking between the master and the slave with the following control properties: **stability** and **transparency**. These two problems have been studied from the passivity point of view at first in [Lawrence, 1993]. Inspired by it, many other studies improved the passivity approaches, such as [Chawda and O'Malley, 2015, Li and Kawashima, 2014, Ryu et al, 2010, Sun et al, 2016]. A review study based on the passivity can be found in [Nuno et al, 2011]. Further discussion on comparative study and evaluation of the main features over different control architectures could be found in [Aliaga et al, 2004, Arcara and Melchiorri, 2002, Kim et al, 2007]. More recently, a review of bilateral algorithms has been conducted and reported in [Muradore and Fiorini, 2016].

2.2.1 Model

Traditionally, bilateral teleoperation systems are modeled by way of a network representation, composed by **Master Slave Network** (**MSN**) parts linked together with the human and the environment, as shown in Fig. 2-5. Human and environment are connected to the system through Human System Interaction (HSI) and Environment System Interaction (ESI). Controllers and communication channel are located inside the MSN teleoperator.

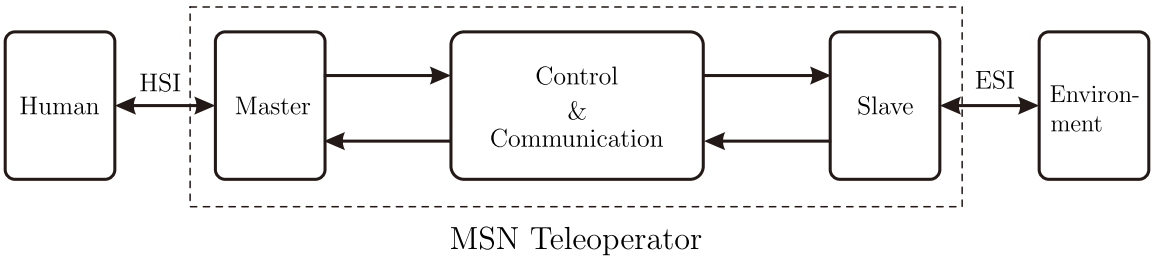

Figure 2-5: Bilateral teleoperation system

Linear Modeling

Different linear models of control architectures have been developed in the literature: two channel schemes (for instance, Position Error Based (PEB) and Direct Force Reflection (DFR) [Tavakoli, 2008]), three channel [Hashtrudi-Zaad and Salcudean, 2002] and four-channel architectures [Lawrence, 1993, Tavakoli, 2008]. For such frameworks, the stability analysis can be developed in frequency or time domains.

Non-linear Modeling

Some works make use of non-linear teleoperator models [Liu and Tavakoli, 2011, Malysz and Sirouspour, 2009, Mohammadi et al, 2011, Nuno and Basanez, 2009, Nuno et al, 2010], based on Lagrange equations. The stability of these approaches is supported by Lyapunov-like function candidates that apply in cases with or without communication time delays [Kawada and Namerikawa, 2008], with or without position tracking [Nuno et al, 2009], with or without force estimation [Daly and Wang, 2014].

Energetic Modeling

From an energetic point of view, the MSN teleoperator can be considered as a two-port network (as shown in Fig. 2-6 where F_i, F_i^*, $i \in \{h, e\}$ denote force signals and V_i, V_i^* denote position/velocity signals, Z_t is the transmitted environment impedance (seen by the human), and impedances Z_h Z_e denote dynamic characteristics of resp. the human and the remote environment) which transmits the energy received from the human to the environment side, and conveys the perception of the environment back to the operator. The human and the environment are modeled as one-port networks with active energy sources, that define the interactions with the system, i.e., HSI and ESI. In numerous works such as [Anderson and Spong, 1989a, Franken et al, 2011, Jazayeri and Tavakoli, 2011, Lawn and Hannaford, 1993, Lee and Spong, 2006], they are considered with passive behavior to ensure the stability of the closed-loop system. According to the studied cases, the communication channel inside a MSN is considered with/without constant or variant delays, with packet losses or disorders (see a survey on passivity-based controllers by [Nuno et al, 2011]).

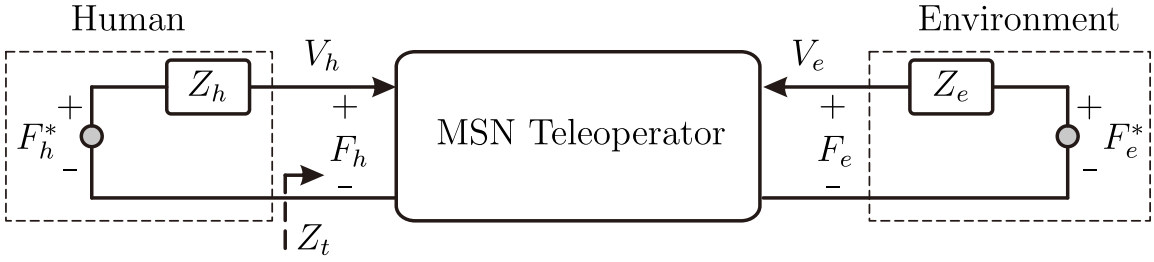

Figure 2-6: An impedance type of bilateral teleoperation system.

The information exchanged in the system are power variables, i.e., position/velocity and force signals. Depending on the choice of the network input and output variables (i.e., physical interaction causality), four types of MSN teleoperator (the immittance category, see [Hashtrudi-Zaad and Salcudean, 2001]) are formed:

- Impedance, as shown in Fig. 2-6, where the human and environment position signals are transmitted into the MSN, while the respective force signals are outgoing.

- Admittance, where the human and environment force signals are transmitted into the MSN, while the respective position signals are outgoing.
- Hybrid, where the human position and environment force signals are transmitted into the MSN, while the human force and environment position signals are outgoing.
- Inverse hybrid, where the human force and environment position signals are transmitted into the MSN, while the human position and environment force signals are outgoing.

On the environment side (see [Adams and Hannaford, 1999]), impedance type teleoperators receive a force command and apply a force to their environment in response to the measured position. On the other hand, admittance type teleoperators receive a position command and set a position to the slave tool in response to the measured contact forces. The choice of admittance/impedance type for master and slave side is performed in section 3.5.2.

2.2.2 Stability

Stability is the first objective to be achieved for any automated system. The intrinsic issue with teleoperation systems is the fact they are MIMO systems and the presence of an internal loop featuring delays. Indeed, the communication channel nowadays is a computer network, at least a LAN[5] but possibly a WAN[6], so variable delays and packet drops are to be considered. Even specific telecommunication channels will present transport delays, such as for geostationary satellite - earth communications.

Several approaches has been put forward to guarantee the stability. According to the survey of the literature, the stability approaches could be divided into three categories:

- for linear models, LTI models:

  Niquist criterion [Hannaford, 1989b], loop-shaping [Fite et al, 1999], frequency

[5]Local Area Network
[6]Wide Area Network

domain analysis [Niculescu et al, 2003], Llewelyn's criterion [Tavakoli, 2008] or H_∞ [Leung et al, 1995, Yan and Salcudean, 1996].

- for non-linear models, for instance including dry frictions, several degrees of freedom, time delays, model uncertainties etc.:
  the non-linear techniques provide a stable teleoperation, such as adaptive control [Lee and Chung, 1998, Ryu and Kwon, 2001], sliding-mode control [Buttolo et al, 1994, Park and Cho, 1999], predictive control [Bemporad, 1998], ...

- for energetic models:
  Network theory is employed. Time-domain passivity of systems has been explored in many studies [Anderson and Spong, 1989a, Hannaford and Ryu, 2002, Lee and Li, 2003, Lee and Spong, 2006]. The Llewellyn's criteria helps to check the absolute stability when the system is modeled as a LTI 2-port network [Hashtrudi-Zaad and Salcudean, 2001]. In case of non-linear systems, other approaches such as energy based ones are used to check **passivity** [Anderson and Spong, 1989a, Hannaford, 1989a, Lawrence, 1993]. Note that passivity of the MSN is a conservative condition. Thus, stability could be ensured as long as the passivity condition is satisfied. A survey has been conducted on passivity-based controllers for nonlinear bilateral teleoperation with guaranteed stability properties, providing energy interpretation, in [Nuno et al, 2011]. It presents a unified Lyapunov-like function V that can be used to analyze the stability of the studied schemes. It concluded that most schemes ensured stability, and showed robustness properties. However, position tracking performances vary in presence of communication delays.

2.2.3 Transparency

Transparency is another quality aspect needed to be considered during design of teleoperation system. Transparency, is the measure of kinesthetic performance. In other words, with a transparent teleoperator, the operator feels like he/she is touching the remote environment directly [Hannaford, 1989b, Lawrence, 1993]. It can be found

in the literature that there is always a trade-off between transparency and stability (see [Niemeyer and Slotine, 1991, Nuno et al, 2011], for instance). Several approaches have been developed, as follows.

A first type of transparency evaluation consists of directly comparing the power variables at the human-master and slave-environment ports of the MSN [Moreau et al, 2012, Yokokohji and Yoshikawa, 1994]. The ideal responses in terms of force and position tracking are predefined as reference signals at the HSI and ESI interactions. These responses have identical position rates or identical interaction forces or both.

A second type of methods is based on the impedance concepts. In the ideal bilateral teleoperation systems, a good transparency is achieved if the impedance transmitted to the user matches the environment impedance [Hashtrudi-Zaad and Salcudean, 2002, Kim et al, 2013, Lawrence, 1993]. The impedances are calculated by way of transfer functions which represent the force and position rate at each interaction port (i.e., HSI and ESI).

A last type of approaches, picked up from the haptic system literature, studies the minimum, maximum, and range of achievable impedances (defined in frequency domain as well). The range of achievable impedances should be as wide as possible to faithfully reproduce haptic sensations to the users (see [Baser et al, 2012, Cavusoglu et al, 2001, Khademian and Hashtrudi-Zaad, 2012]).

As a conclusion, the second and last methods require the knowledge of explicit impedance transfer function which could be easily obtained in frequency domain. Therefore, there is a limitation in using them. In our case, the first solution is well suited, but it is difficult to predefine ideal responses.

2.2.4 Conclusion about Bilateral Teleoperation

Teleoperation systems have progressively enhanced since the first one designed by Raymond C. Goertz. Distances have increased but some difficulties appeared accordingly. The use of numerical communication media introduced variable transport delays besides packet loss and disordered. Recent researches provide powerful controllers enabling to guarantee a good trade-off between stability and transparency

for systems with non symmetric variable delays, unknown operator and environment properties and even without costly force sensors. Even if, as they only feature one user, they do not directly comply with our requirements they are an interesting basis for dual-user system design. Note that some modeling approaches (energetic ones, for instance) used for teleoperation systems can be easily extended with a second master, but not everyone (more complex with LTI modeling). This section was necessary to lay the foundations for the following theoretical discussion.

2.3 Multilateral Haptic System

When the number of users, masters or slaves is greater than one in a teleoperation system, in presence of a *kinesthetic* feedback coupling them, then the system is named as **multilateral teleoperation**, as shown in Fig. 2-7.

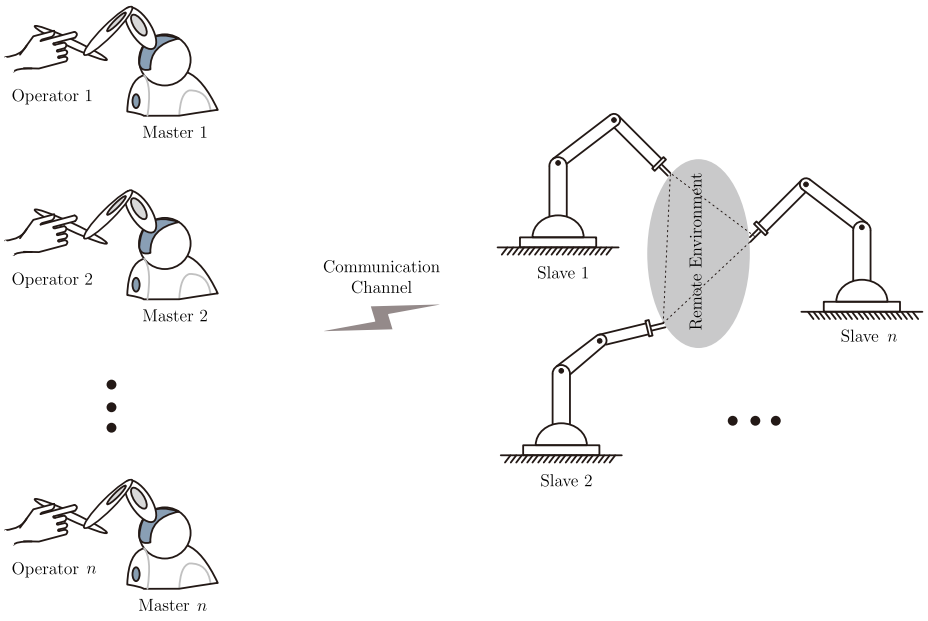

Figure 2-7: Multilateral system architecture

In this category, according to the number of users and slave robots, three cases exist:

- single-master/multi-slave,
- multi-master/single-slave, and

- multi-master/multi-slave systems

These kinds of systems have been designed for different domain usage, such as medical training [Nudehi et al, 2005], cooperative manipulation [Buss et al, 2009], grasping [Lee et al, 2005, Lee and Spong, 2005] etc. The control protocols are different from the ones used in bilateral teleoperation, since the system is coupled not only between the masters and the slaves, but also among each other (i.e., master and master, slave and slave).

Several strategies have been envisaged to ensure stability and transparency. For instance, Sirouspour [Sirouspour, 2005] proposed a multilateral robust control architecture for cooperative teleoperation (multiple masters, multiple slaves) by way of μ-synthesis method. However, it assumes that the operator and the environment are both unknown but passive. This strong assumption limits the application field to slaves not linked together and more generally to potentially non passive operators and environments as listed in [Islam et al, 2015, Jazayeri and Tavakoli, 2015]. Also, an adaptive nonlinear control architecture introduced in [Zhu and Salcudean, 2000] for bilateral teleoperation has been extended to the multilateral cooperative teleoperation by [Sirouspour and Setoodeh, 2005] but without any variable authority mechanism. A framework for stability analysis of cooperative network-based force reflecting teleoperation systems has been developed in [Polushin et al, 2013] using small gain framework. It guarantees the stability in the presence of multiple network-induced communication constraints and provides less conservative results than passivity approaches but its use is limited to cooperation between several users.

From the passivity point of view, authors of [Mendez and Tavakoli, 2010] introduced a criterion to check the passivity of n-port networks connected to unknown terminations. This criterion can be used to check the passitivity of multilateral teleoperation systems and was applied to a dual-user system. This criterion is applied on the internal impedance matrix of the system, which requires an internal linear model; if not, the criterion computations might be difficult to handle.

2.4 Dual-user Haptic System

Dual-user haptic systems are a special case affiliated to the type of multi-master/single slave systems. They have been introduced for haptic-based surgical training in [Nudehi et al, 2005] and tele-rehabilitation in [Shahbazi et al, 2014], for instance. In this thesis, we focus on this design for training purpose.

Dual-user systems provide an haptic master interface per user and a software architecture which connects these devices to perform a combined control over a slave (see Fig. 2-8). This slave can be a real robot handling a real tool or a simulation providing a virtual tool inside a virtual environment. It enables the users to interact with the environment simultaneously by providing haptic feedback to both user.

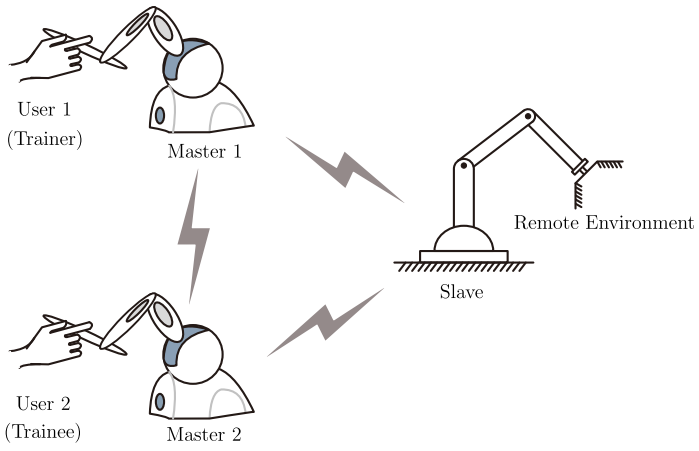

Figure 2-8: Scheme of a dual-user system

2.4.1 Design Concept

The common design concept for the dual-user haptic systems is that the interfaces provide force feedback to both master users (trainer and trainee) according to a dominance factor ($\alpha \in [0, 1]$). When $\alpha = 1$ (resp. 0), user 1 (resp. user 2) has full authority on user 2's (resp. user 1's) device and on the slave. When $0 < \alpha < 1$, both users share the slave control with a dominance (over the other user and the slave) which is function of α. In practice, this control authority, shared between the surgeons, is manually chosen based on their relative level of surgical skills and experience. It determines the extent to which the motion of the slave tool depends

on their individual commands. An example of dual-user training progress by setting different α, is shown in Fig. 2-9. Notice that, in this figure, the solid lines represent both feedback and feed-forward control signals, while the dashed line is only feedback signals. As it can be seen, it is divided into the training ($\alpha = 0$), guidance ($0 < \alpha < 1$) and evaluation ($\alpha = 1$) scenarios.

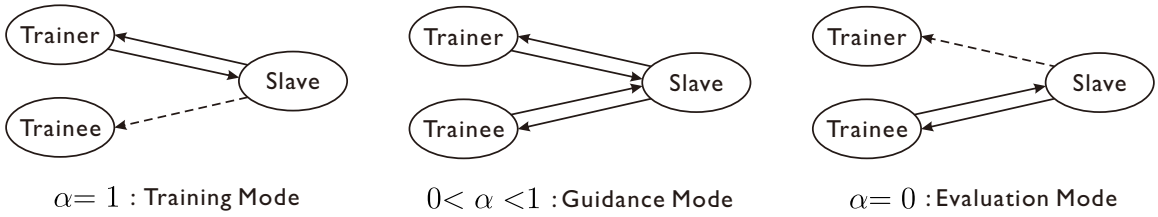

Figure 2-9: Structure of dual-user training scenarios by setting α.

2.4.2 Existing Architectures

Various architectures have been proposed for the control of dual-user haptic systems. The **shared control** concept has been introduced by Nudehi et al. in [Nudehi et al, 2005]. The control authority is set by way of a dominance factor α; it can be set at 1 (100%) for the trainer at first and then, as long as the trainee acquires more skills, it can be shifted towards 0 as depicted in [Ghorbanian et al, 2013].

In Nudehi's architecture, the master devices provide force feedback to both users, proportional to the difference of their actions and reversely proportional to the control authority shared between them. The system can be used in presence of communication delays. However, the user who has full control on the slave is not provided with a kinesthetic feedback from the slave, which means a limited transparency.

In [Khademian and Hashtrudi-Zaad, 2011], this transparency limit is overcome by creating a three-port multilateral control architecture. Two different architectures are proposed (shown in Fig. 2-10). The first one is the *Complementary Linear Combination* (CLC) architecture which provides feedback forces combining the environment and the other user forces (resp. F_e and F_{h_2} for user 1). The desired position and force commands for each device are a complimentary weighted sum of positions and

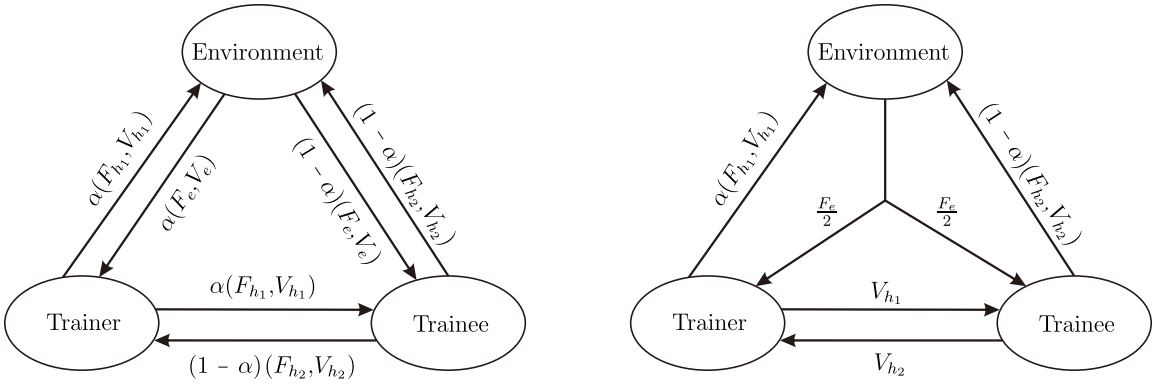

Figure 2-10: Signal flow of CLC (left) and MCET (right) architectures [Ghorbanian et al, 2013].

forces of the other two devices. When $\alpha = 1$, master 1 and the slave compound a four-channel bilateral teleoperation system, and the position of master 1 acts as an exogenous input for the master 2 (the behavior is symmetric when $\alpha = 0$). When $0 < \alpha < 1$, both users can perform a task collaboratively in a shared environment.

In the second architecture proposed by [Khademian and Hashtrudi-Zaad, 2011], called *Masters Correspondence with Environment Transfer* (MCET), both user devices follow the motion of each other and the effort feedback to both users is $F_e/2$. The command to the slave is weighted by α. Kinesthetic performance analysis and experimental user perception studies showed that out of these two architectures, the MCET one provides the best kinesthetic feedback to both users with the least sensitivity to dominance factor. In our context, despite these interesting results, the linear modeling used in this work combined to a design neglecting delays did not fit with our specifications.

In addition, in [Ghorbanian et al, 2013], authors define two dominance factors: α (resp. $1-\alpha$) which determines the authority of the trainer (resp. trainee) over the trainee (resp. trainer), while β and $(1-\beta)$ indicates the supremacy of trainer and trainee over the slave robot respectively. A nonlinear relation between α and β is given, which adjusts the authority of the leader (the user for which $\alpha > 0.5$) over the slave with respect to his authority over the follower.

Similiarly, in [Shamaei et al, 2015], authors introduced both dominance (α) and

observation (β) factors. The dominance factor α indicates each user's control authority over the slave robot. The observation factor β (set as $\beta \geq 1-\alpha$) is used to ensure that the trainee obtains force and velocity feedback directly from the environment at least as much as the authority of him/her over the slave. For instance, if the trainee has 80% authority over the slave (i.e., $\alpha = 0.2$), $\beta \geq 0.8$ is given in order to feed back at least 80% of force and velocity directly from the environment.

Also, in [Shahbazi et al, 2015], a training application has been studied, based on the small gain criterion introduced in [Polushin et al, 2013]: a system able to host several simultaneous trainees with a shared authority on the slave and a common full force feedback from the slave, in presence of time-varying communication delays. The objectives are very close to ours but we could observe some important differences. As a matter of fact, if we assume that user #1 is the trainer, when he gets the whole authority to show some motions, other users are not guided: they are only provided with the slave force feedback. Also, when the authority is shared, the slave motion is the weighted sum of every user while the force feedback for each one is the same. Therefore users do not follow exactly the slave motion (except if every user provided the same motion, which is not the case with beginners) while getting the force feedback for a motion which is not theirs.

As this work is not compared with CLC or MCET, it cannot be determined whether the transparency of this architecture is better. Its interest in our context resides in the nonlinear teleoperator dynamics modeling and in the support of uncertain communication channels in presence of delays, packet loss, data duplication and packet swapping[7].

2.4.3 Authority Sharing

Every dual-user architecture use the shared control concept to allow each user to handle (totally, partially or not at all) the slave. In order to weight the level of control of each user over the slave tool, dominance factors compose the authority

[7]We became aware of this advanced work after having chosen the modeling strategy proposed in this paper; it should be interesting to compare both strategies when we have taken a step forward.

sharing mechanism. In practice, these factors are, in general, manually (sometimes automatically) tuned according to the skills of each user. In a training context, it depends on the targeted skill acquisition curve of the trainee and evolves towards the trainee dominance while the trainer supervises him.

The shared control concepts differ from author to author. For instance, Nudehi et al introduce their shared control idea as an equivalent H-shape mechanical system (see [Nudehi et al, 2005]). Razi et al rather propose a three-way gearbox [Razi and Hashtrudi-Zaad, 2014]. The same concept appears also in a more general way for multi-user/single-slave systems in [Shahbazi et al, 2015]. What mainly differentiates these approaches is the force feedback from the slave: F_e in [Shahbazi et al, 2015], $F_e/2$ for MCET architecture in [Khademian and Hashtrudi-Zaad, 2011], and many other ways.

These approaches have been validated for a collaborative use. For a training use, the requirements differ: in a leader-follower mode (the trainer showing the right gesture to a trainee, for instance), the follower must receive the same (position and force) information as the leader to train efficiently. If both users receive a differently weighted environment force (applied on the tool), the leader will not be able to reproduce the right gesture and the follower will not be able to learn how much force to provide.

2.4.4 Stability

Concerning the stability of these dual-user architectures, various results are provided in the literature. The difficulty resides in the structure of interconnected systems connected with varying and unknown environment and operator's dynamics,

Linear time-invariant (LTI) models are usually used to model dual-user systems. For instance, Nudehi et al. [Nudehi et al, 2005] use H_∞ method to guarantee stability even when there are communication delays (up to 25ms in his experiments). Some other stability criteria is often used for dual-user systems: the *unconditional stability*, checked through the Llewellyn's criterion (in [Khademian and Hashtrudi-Zaad, 2011], for instance). The CLC architecture was found to be virtually unconditionally stable

for very large sampling rate, whereas the MCET architecture remains potentially unstable. The result that robustness of stability will be increased when reducing sampling rate, is also presented. Another criterion applied on LTI models is the Zeheb-Walach absolute stability [Razi and Hashtrudi-Zaad, 2014], which is a set of frequency-domain, passivity based necessary and sufficient conditions for stability.

An extension of the Zeheb-Walach criteria for absolute stability of an n-port network is provided in [Razi and Hashtrudi-Zaad, 2014]. It is applied to 2-channel teleoperation architectures showing that when both operators have same authority over the task, a larger set of stabilizing gains is available.

Mendez et al make use a n-port network LTI model in [Mendez and Tavakoli, 2010], to model multilateral systems. A criterion which is necessary and sufficient for passivity of the n-port network is introduced. It is shown that when $n = 2$, the proposed conditions reduce to the well-known Raisbeck's passivity criterion for two-port networks.

Furthermore, a comparison between extended Raisbeck's passivity criterion and Llewellyn's absolute stability criterion is detailed in [Li et al, 2014]. It shows that, for three-port networks, the absolute stability criterion is less conservative than the passivity criterion.

In [Ghorbanian et al, 2013], a Lyapunov-Krasovski function is proposed to ensure stability. The results show that constraints over the PD controller gains should preserve the stability of the system. This approach is the more general case, but no transparency analysis is provided so it is difficult to compare this work with [Khademian and Hashtrudi-Zaad, 2011] in absence of time delays.

The design and performance evaluation of a trilateral teleoperated training architecture is reported in [Shamaei et al, 2015]. Llewellyn's criterion is used for stability verification. Results show that the system remains stable regardless different values of the dominance factor α, the observation factor β, the trainee's hand impedance and the system transfer function frequency.

Except in [Ghorbanian et al, 2013], all these architectures have been studied using LTI models. Thus, their applicability would be limited in the cases of complex

nonlinear system dynamics. Besides, only [Ghorbanian et al, 2013] considers time delays in communication channel. Furthermore, none of them explicitly consider the stability when switching dominance between users (by changing dominance factor in real-time).

It has been shown in [Secchi et al, 2007] that passivity theory and port-Hamiltonian formalism can be profitably used for bilateral teleoperation system. Within this framework the energetic properties of physical systems are highlighted, and it is possible to build energy based controllers. Secchi et al designed a passive teleoperation controller taking into account sampling energy creation issue and variable delay packet switching communication channels. They used it in a complex telegrasping system, which shows stable behaviors both in contact with the remote environment and in free motion. Transparency is also studied (in port behavioral control) which is suitable for the analysis of complex telemanipulators. These works, applied on bilateral teleoperation systems have provided interesting and promising results. This is why we adopted the port-Hamiltonian approach, as they enable to explicitly check the passivity even with nonlinear models. Furthermore, with this approach, the system could easily be analyzed for different training scenarios, with varying control authority values (since the passivity could always be checked and ensured in real-time, see Fig. 2-9). This is why we design our system based on this approach.

2.4.5 Transparency

To the best of our knowledge, only a few papers are concerned with transparency of dual-user systems: [Khademian and Hashtrudi-Zaad, 2011, 2012, Shamaei et al, 2015]. Their methods (e.g., impedance transfer function, range of achievable impedance) derive from the ones developed for bilateral systems, expounded in Section 2.2.3. The difference lies in the presence of a second user who should feel the environment response and/or the other user actions.

2.5 Conclusions

Considering the medical training requirements exposed in Section 1.2 and this survey about multilateral teleoperation/simulation systems, the dual-user architecture appears the best fitting one with its two users interacting each one through their own haptic interface and a single slave robot (either a real remote robot or a virtual one).

However this survey showed that existing dual-user systems do not exactly fit every aforementioned requirement. Therefore, we had to design a novel architecture, inspired from existing ones and fulfilling every requirement for a efficient haptic simulator for training purposes.

Part II

Contributions

Chapter 3

ESC Dual-user Haptic Systems

3.1 Introduction

Dual-user Haptic Systems extend the capabilities of two users to manipulate a remote environment collaboratively and simultaneously. They are affiliated to the category of **multilateral teleoperation** systems. As stated in Section 2.4, several architectures have been developed. They have been designed for remote collaborative tasks at first, but this kind of system can also apply for haptic training [Khademian and Hashtrudi-Zaad, 2011], and two-handed telerehabilitation therapy, where the patient makes use of his/her healthy arm to train the impaired arm [Shahbazi et al, 2014, 2016]. In this thesis, we focus on a hands-on training application.

Dual-user systems involve not only interactions between the users and the environment, but also the interactions between the two users. In this application, the objectives of users are not to achieve together a given cooperative task but, for the trainer, to help the trainee to learn complex gestures necessitating the control of hand motions but also efforts applied on the tool. It can be used, for instance, at first, to guide the trainee's hand, following trainer's motions, while the trainee doses his efforts to apply on the tool accordingly to those of the trainer. It can then be used for supervision of the trainee's motions by the trainer, as well as collaborations between them.

Besides this applicative objective, our dual-user system should also provide good

stability and **transparency**, as for traditional bilateral teleoperation.

Drawing inspiration from dual-user architectures in [Nudehi et al, 2005], [Khademian and Hashtrudi-Zaad, 2011], [Ghorbanian et al, 2013], [Razi and Hashtrudi-Zaad, 2014] and [Shahbazi et al, 2015], we reused and adapted the shared control concept, designed for cooperative teleoperation, in order to fit to our training requirements. The stability of the interconnected subsystems in a dual-user system has been the second problem to solve. It may be impacted by the evolution in time of the environment and operators' dynamics.

As evoked in Section 2.4.4, bilateral teleoperation works from Secchi et al, reported in [Secchi et al, 2007] provided interesting and promising results. We adopted them as a basis for the design of our system.

This chapter details the design of a passive dual-user architecture. Accordingly with the previous study, we chose to use an energy approach under port-Hamiltonian framework. This approach provides theoretical tools (the fundamental concepts and tools are given in Appendix B) which help in adding this second user in the loop without increasing excessively the complexity of the study. Moreover, the adding of new extra users is also conceivable. The design of this architecture started from a dual-user intrinsically passive system detailed in sections 3.2 and 3.3. Yet, this architecture was not able to provide full slave feedback to both users. This is why we enhanced it (see Sec. 3.4) to fulfill this purpose.

3.2 Authority Sharing Mechanism

Inspired by the CLC architecture stated in [Khademian and Hashtrudi-Zaad, 2011], we propose an authority sharing mechanism, as shown in Fig. 3-1, using parameter α.

It features three linear Multiple-Input-Multiple-Output (MIMO) subsystems (whose representation are $\mathcal{D}_{m_1}, \mathcal{D}_{m_2}$ and $\mathcal{D}_s$) which, all together, redirect the power flows (conveyed by power port variables $\dot{\theta}_i, T_i$ with $i \in \{r_1, r_2, s_1, s_2, r_s\}$, where $\dot{\theta}_i$ represents velocity signals and T_i torque signals (see definitions in Appendix A.1) exchanged be-

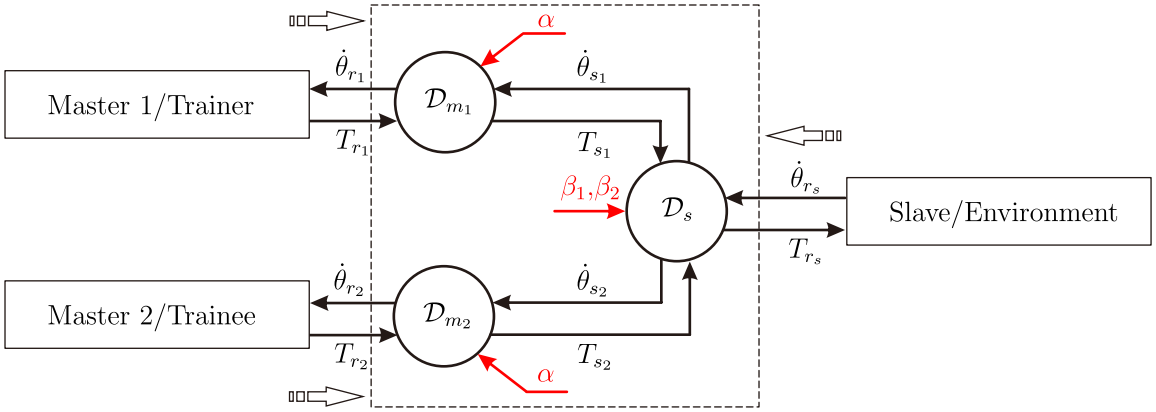

Figure 3-1: Authority Sharing Mechanism

tween both users and the slave tool. Three dominance factors $\alpha, \beta_1, \beta_2 \in [0, 1]$ are introduced to achieve the goal of shared control. The $\mathcal{D}_{m_1}, \mathcal{D}_{m_2}$ and $\mathcal{D}_s$ relations are provided in Eq. (3.1)[1].

$$
\begin{aligned}
\mathcal{D}_{m_1} &: \begin{pmatrix} \dot{\theta}_{r_1} \\ T_{s_1} \end{pmatrix} = \begin{pmatrix} 0 & \alpha \\ -\alpha & 0 \end{pmatrix} \begin{pmatrix} T_{r_1} \\ \dot{\theta}_{s_1} \end{pmatrix} \\
\mathcal{D}_{m_2} &: \begin{pmatrix} \dot{\theta}_{r_2} \\ T_{s_2} \end{pmatrix} = \begin{pmatrix} 0 & 1-\alpha \\ \alpha - 1 & 0 \end{pmatrix} \begin{pmatrix} T_{r_2} \\ \dot{\theta}_{s_2} \end{pmatrix} \\
\mathcal{D}_s &: \begin{pmatrix} \dot{\theta}_{s_1} \\ \dot{\theta}_{s_2} \\ T_{r_s} \end{pmatrix} = \begin{pmatrix} 0 & 0 & \beta_1 \\ 0 & 0 & 1-\beta_2 \\ \beta_1 & 1-\beta_2 & 0 \end{pmatrix} \begin{pmatrix} T_{s_1} \\ T_{s_2} \\ \dot{\theta}_{r_s} \end{pmatrix}
\end{aligned}
\tag{3.1}
$$

It can be seen that the energy exchanged between the authority sharing mechanism and the rest of the architecture (trainer/trainee/slave) goes through three power ports: $(T_i, \dot{\theta}_i), i = r_1, r_2, r_s$. By straightforward calculation, the relationship of the power flowing (the positive direction of power flows are indicated by white arrows [2]

[1]The notations of time-varying variables with $*(t)$ are abridged for simplification.

[2]Without specific notation, all the white arrows shown in Fig. 3-1 throughout this report indicate the positive direction of power flows.

in Fig. 3-1) into the authority sharing mechanism is:

$$T_{r_1}(t)\dot{\theta}_{r_1}(t) + T_{r_2}(t)\dot{\theta}_{r_2}(t) + T_{r_s}(t)\dot{\theta}_{r_s}(t) = 0 \tag{3.2}$$

Thus, the three structures ($\mathcal{D}_{m_1}, \mathcal{D}_{m_2}$ and $\mathcal{D}_s$) form each one a power-conserving interconnection whatever values of α. This means that this global authority sharing mechanism is passive and lossless. Moreover, α can vary as desired as long as it remains in its definition interval, as opposite to LTI models introduced in [Khademian and Hashtrudi-Zaad, 2011] where α was considered as a constant parameter for the stability study.

The relationship between α and β_1, β_2 are defined as,

$$\beta_1 = \begin{cases} \alpha, & \alpha = 1, 0 \\ 1, & 0 < \alpha < 1 \end{cases} \qquad \beta_2 = \begin{cases} \alpha, & \alpha = 1, 0 \\ 0, & 0 < \alpha < 1 \end{cases} \tag{3.3}$$

We had to introduce β_1, β_2 in order to avoid the duplication of the shared authority distribution in $\mathcal{D}_s$, since the shared power flow is already formed in $\mathcal{D}_{m_1}$ and $\mathcal{D}_{m_2}$. The role of $\mathcal{D}_s$ is to sum up the forces sent towards the slave and to deliver the velocities $\dot{\theta}_{s_1}$ and $\dot{\theta}_{s_2}$ to both users. Keeping α inside $\mathcal{D}_s$ would provide some expressions of $\dot{\theta}_{r_1}$ and $\dot{\theta}_{r_2}$ function of α. It is worth noting that α and β_1, β_2 are one dimension values (not matrices) even in multiple degree of freedom cases, which means that each joint has the same authority configuration.

Regarding the different desired control authorities, we obtain three modes by changing the dominance factor α:

- training mode ($\alpha = 1$),
- guidance mode ($0 < \alpha < 1$), and
- evaluation mode ($\alpha = 0$).

3.3 Adding Compliance

The previous core architecture does only redirect signals between the three power ports, it does not permit to control efficiently the end interfaces (Master 1, Master 2 and Slave). For this purpose, we inserted three Intrinsically Passive Controllers (IPC) (resp. IPC M1, IPC M2 and IPC S) in between them.

The IPC controllers, expounded in Section A.3.3 have the property to ensure a passive interaction of the controlled system with an unknown environment (or user). Any robot model error may degrade the performances of the system but not its passivity. Thus, they provide a robust and powerful solution to control the associated devices (Master 1, 2 and Slave). Therefore, their linking through power-conserving interconnections, with the passive core dual-user architecture composes a new passive system, whatever controllers parameters and devices characteristics. This provides a natural robustness and leaves freedom to tune all IPC parameters for performance and global transparency. Moreover, IPC controllers provide a natural compliance which helps in training tasks. Thus, we obtain an intrinsically passive dual-user system, depicted in Fig. 3-2. The only defect of this architecture is visible when $\alpha = 1$

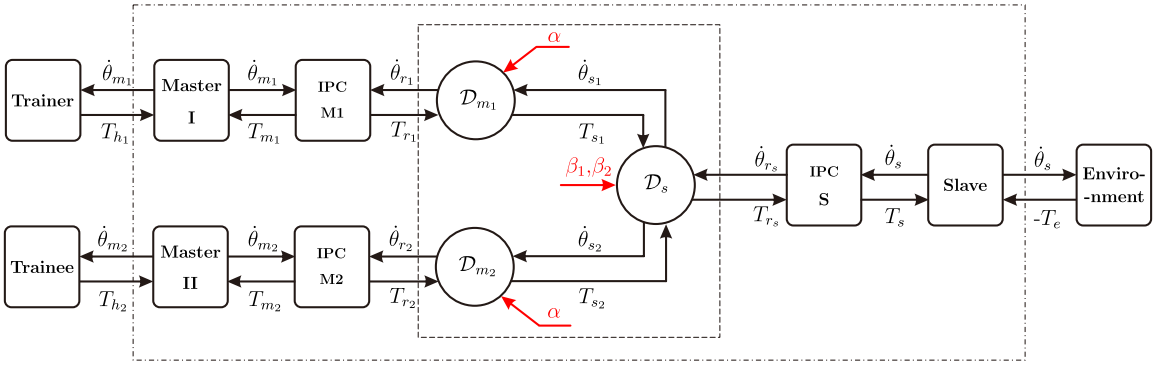

Figure 3-2: Dual-user haptic system with IPC controller

(resp. 0); in this case, the trainer (resp. trainee) exchanges all his energy exclusively with the slave. The system acts as a classical teleoperation system and completely isolates the trainee (resp. trainer) who can neither control the slave (this is wanted) nor get any feedback from it (this is not practicable). This is opposite to the training

requirements stipulating that the trainee (resp. trainer) should be able, at least, to observe the trainer (resp. trainee) motions.

3.4 Providing Full Feedback to Both User

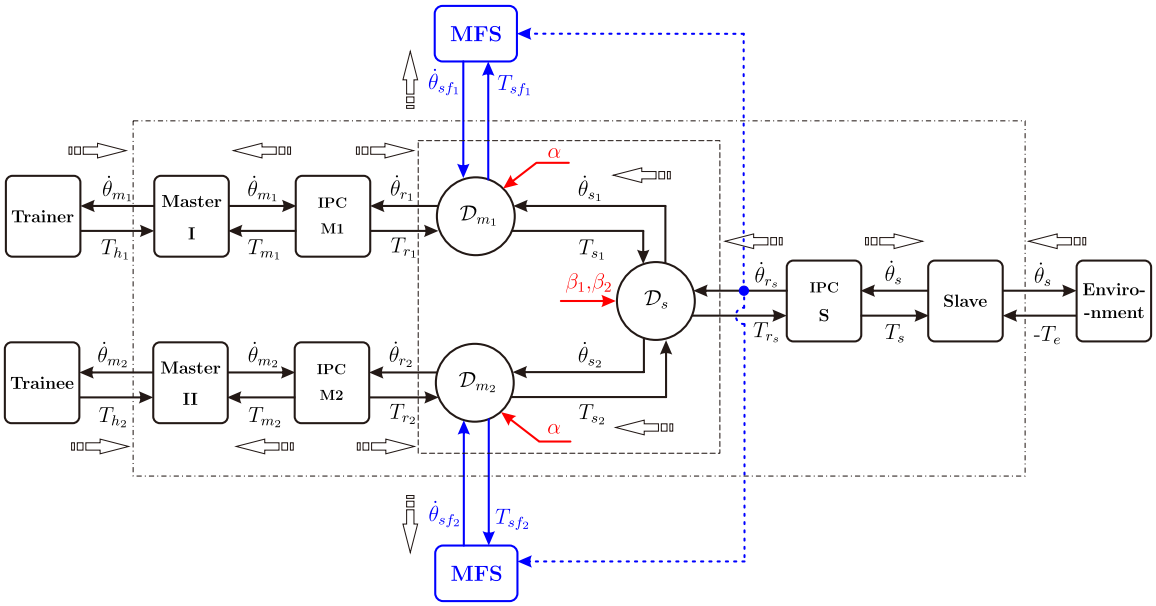

Figure 3-3: Energy Shared Control (ESC) dual-user training system.

In order to solve the aforementioned problem, we added two identical modulated flow sources (MFS), associated with the velocity signal $\dot{\theta}_{r_s}$, and visible as blue signals in Fig. 3-3 (where the authority sharing mechanism is located inside the inner dashed box).

The aim of the two flow sources is to feed back the complementary motion information of the slave which is missing in the core passive dual-user architecture. Then,

the authority sharing mechanism is redefined in Eq. 3.4.

$$
\begin{aligned}
\mathcal{D}_{m_1} : \begin{pmatrix} \dot{\theta}_{r_1} \\ T_{s_1} \\ T_{sf_1} \end{pmatrix} &= \begin{pmatrix} 0 & \alpha & 1-\alpha \\ -\alpha & 0 & 0 \\ \alpha - 1 & 0 & 0 \end{pmatrix} \begin{pmatrix} T_{r_1} \\ \dot{\theta}_{s_1} \\ \dot{\theta}_{sf_1} \end{pmatrix} \\
\mathcal{D}_{m_2} : \begin{pmatrix} \dot{\theta}_{r_2} \\ T_{s_2} \\ T_{sf_2} \end{pmatrix} &= \begin{pmatrix} 0 & 1-\alpha & \alpha \\ \alpha - 1 & 0 & 0 \\ -\alpha & 0 & 0 \end{pmatrix} \begin{pmatrix} T_{r_2} \\ \dot{\theta}_{s_2} \\ \dot{\theta}_{sf_2} \end{pmatrix} \\
\mathcal{D}_{s} \quad : \begin{pmatrix} \dot{\theta}_{s_1} \\ \dot{\theta}_{s_2} \\ T_{r_s} \end{pmatrix} &= \begin{pmatrix} 0 & 0 & \beta_1 \\ 0 & 0 & 1-\beta_2 \\ \beta_1 & 1-\beta_2 & 0 \end{pmatrix} \begin{pmatrix} T_{s_1} \\ T_{s_2} \\ \dot{\theta}_{r_s} \end{pmatrix}
\end{aligned}
\tag{3.4}
$$

As it can be seen in the figure, the modulated flow sources are taken from the slave controller side, given as $\dot{\theta}_{sf_i} = \dot{\theta}_{r_s}$ ($i \in \{1; 2\}$). Consequently, both users experience a full motion feedback regardless of the control authority (i.e. the value of α)[3], and a shared force is feed-forward to the slave (notice that a negative sign is present indicating the force direction).

$$
\begin{aligned}
&\dot{\theta}_{r_1}(t) = \alpha\dot{\theta}_{s_1}(t) + (1-\alpha)\dot{\theta}_{sf_1}(t) = \alpha\beta_1\dot{\theta}_{r_s}(t) + (1-\alpha)\dot{\theta}_{r_s}(t) = \dot{\theta}_{r_s}(t) \\
&\dot{\theta}_{r_2}(t) = (1-\alpha)\dot{\theta}_{s_2}(t) + \alpha\dot{\theta}_{sf_2}(t) = (1-\alpha)(1-\beta_2)\dot{\theta}_{r_s}(t) + \alpha\dot{\theta}_{r_s}(t) = \dot{\theta}_{r_s}(t) \\
&T_{r_s}(t) = -\beta_1\alpha T_{r_1}(t) - (1-\beta_2)(1-\alpha)T_{r_2}(t) = -\alpha T_{r_1}(t) - (1-\alpha)T_{r_2}(t)
\end{aligned}
\tag{3.5}
$$

It is worth to mention that additional energy may be injected into the system by the modulated flow sources. This could violate the passivity of the whole architecture which may cause unstable behaviors. Thus, we propose a passivity controller to ensure stability in the following sections.

[3]According to Eq. 3.3, $\alpha\beta_1 = \alpha$ and $(1-\alpha)(1-\beta_2) = (1-\alpha)$ are always satisfied regardless of α.

3.5 Modelling the ESC Dual-User System

In this section, the port-Hamiltonian approach (see mathematical foundations in Section A.3) is applied to model our dual-user haptic training system. The bond-graphs (see Section A.4) are used for the representation of close-loop systems..

3.5.1 Modelling the Master/Slave Robots

In dual-user system, the corresponding dynamics of the n-dof master/slave robots can be modeled in port-Hamiltonian form as follows:

$$J_i = \begin{bmatrix} 0 & I_n \\ -I_n & 0 \end{bmatrix} \quad R_i = \begin{bmatrix} 0 & 0 \\ 0 & B_i(\theta_i, p_i) \end{bmatrix} \quad G_i = \begin{bmatrix} g_i & h_i \end{bmatrix} = \begin{bmatrix} 0 & 0 \\ I_n & I_n \end{bmatrix} \tag{3.6}$$

where the state variable are defined by $x_i := [\theta_i^T \quad p_i^T]^T,\ i \in \{m_1, m_2, s\}$. $\theta_i \in \mathbb{R}^n$, $p_i \in \mathbb{R}^n$ represent respectively the joint position and the joint momentum. $B_i(p_i, \theta_i) \in \mathbb{R}^{n\times n}$ is a symmetric positive-definite matrix, indicating the dissipation elements.

The input and output matrices are provided by

$$u_i = \begin{bmatrix} T_{ext,i} \\ T_i \end{bmatrix} \quad y_i = \begin{bmatrix} \dot{\theta}_i \\ \dot{\theta}_i \end{bmatrix} \tag{3.7}$$

where $T_i \in \mathbb{R}^n$ is the control torque, while $T_{ext,i} \in \mathbb{R}^n$ represents the external torque exerted by the trainer/trainee and the environment, as shown in Fig. 3-3, namely T_{h_1}, T_{h_2} and $-T_e$.

The total energy H_i (Hamiltonian) is the sum of a kinetic energy due to the inertial elements $M_i(\theta_i) \in \mathbb{R}^{n\times n}$ and of a potential energy $V_i(\theta_i)$ due to the gravity, which is given by

$$H_i(x_i) = \frac{1}{2} p_i^T M_i^{-1}(\theta_i) p_i + V_i(\theta_i) \tag{3.8}$$

3.5.2 IPC Controller

The physical representation of masters/slave's IPC controllers is illustrated in Fig. A-6 and A-8. Notice that in order to adapt ourselves to the force(torque)-position causality interconnection (i.e., the torque is transmitted from the master to the slave, while the velocity is transmitted back), the controllers are designed in two different forms for the masters and the slave.

Considering the master's IPC controller, it consists a virtual mass, two springs and a damper [4]. The displacements of the two springs can be represented by $q_{r,i} \in \mathbb{R}^n$ and $q_{c,i} \in \mathbb{R}^n$, respectively. The momenta of the virtual mass is given by $p_{c,i} \in \mathbb{R}^n$. Denote the state variable by $x_{c,i} := [q_{r,i}^T \;\; p_{c,i}^T \;\; q_{c,i}^T]^T, i \in \{m_1, m_2\}$, and the Hamiltonian is given as

$$H_{c,i}(x_{c,i}) = \frac{1}{2} q_{r,i}^T K_{r,i} q_{r,i} + \frac{1}{2} q_{c,i}^T K_{c,i} q_{c,i} + \frac{1}{2} p_{c,i}^T M_{c,i}^{-1} p_{c,i} \tag{3.9}$$

where $K_{r,i} \in \mathbb{R}^{n\times n}, K_{c,i} \in \mathbb{R}^{n\times n}$ are the elasticity matrices, and $M_i \in \mathbb{R}^{n\times n}$ are the inertial elements [5].

The master IPC controller can be modeled in port-Hamiltonian framework with input/output matrices as

$$\begin{aligned} J_{c,i} &= \begin{bmatrix} 0 & -I_n & 0 \\ I_n & 0 & -I_n \\ 0 & I_n & 0 \end{bmatrix} \quad R_{c,i} = \begin{bmatrix} 0 & 0 & 0 \\ 0 & B_{c,i} & 0 \\ 0 & 0 & 0 \end{bmatrix} \\ G_{c,i} &= \begin{bmatrix} g_{c,i} & h_{c,i} \end{bmatrix} = \begin{bmatrix} 0 & I_n \\ 0 & 0 \\ I_n & 0 \end{bmatrix} \quad u_{c,i} = \begin{bmatrix} -\dot{\theta}_i \\ \dot{\theta}_{r_j} \end{bmatrix} \quad y_{c,i} = \begin{bmatrix} T_i \\ -T_{r_j} \end{bmatrix} \end{aligned} \tag{3.10}$$

where $j = 1, 2$ represent the master 1 and master 2 and $B_{c,i} \in \mathbb{R}^{n\times n}$ are the dissipation

[4] In the case of n-dof case, these elements are duplicated in parallel for each dof, without any coupling, assuming that an input/output decoupling low level controller (such as in [Stramigioli, 1996] is potentially used).

[5] These matrices are composed of constant values, representing parallel elements. The following notations hold for the slave.

elements. Note that the minus sign in $-\dot{\theta}_i$ and $-T_{r_j}$ corresponds to the specified causality (positive force/position direction, see Fig. A-7).

Concerning the slave IPC controller, one of the springs which were present for the master IPC has been removed for causality interconnection stake. Defining $x_{c,s} := [p_{c,s}^T \;\; q_{c,s}^T]^T$, the Hamiltonian for the slave IPC is:

$$H_{c,s}(x_{c,s}) = \frac{1}{2} q_{c,s}^T K_{c,s} q_{c,s} + \frac{1}{2} p_{c,s}^T M_{c,s}^{-1} p_{c,s} \tag{3.11}$$

The slave IPC controller is given by

$$\begin{aligned} J_{c,s} &= \begin{bmatrix} 0 & -I_n \\ I_n & 0 \end{bmatrix} \quad R_{c,s} = \begin{bmatrix} B_{c,s} & 0 \\ 0 & 0 \end{bmatrix} \\ G_{c,s} &= \begin{bmatrix} g_{c,s} & h_{c,s} \end{bmatrix} = \begin{bmatrix} 0 & I_n \\ I_n & 0 \end{bmatrix} \quad u_{c,s} = \begin{bmatrix} -\dot{\theta}_s \\ -T_{r_s} \end{bmatrix} \quad y_{c,s} = \begin{bmatrix} T_s \\ \dot{\theta}_{r_s} \end{bmatrix} \end{aligned} \tag{3.12}$$

where $B_{c,s} \in \mathbb{R}^{n \times n}$ is the dissipation element. Note that the minus sign in $-\dot{\theta}_s$ and $-T_{r_s}$ means the specified causality (positive force/position direction, see Fig. A-9).

3.5.3 Coupled Robot-Controller Subsystems

The subsystems of the slave/master robots and the IPC controllers are coupled by interconnection of port-Hamiltonian systems (see Sect. A.3.2), that is,

$$\begin{aligned} u_i^2 &= T_i = y_{c,i}^1 \\ u_{c,i}^1 &= -\dot{\theta}_i = -y_i^2 \end{aligned} \tag{3.13}$$

where $i \in \{m_1, m_2, s\}$, and the superscripts 1 and 2 represent the number of input/output signal [6]. This forms a new port-Hamiltonian system defined by:

$$\begin{aligned} J_{rc,i} &= \begin{bmatrix} J_i & g_i g_{c,i}^T \\ -g_{c,i} g_i^T & J_{c,i} \end{bmatrix} \quad R_{rc,i} = \begin{bmatrix} R_i & 0 \\ 0 & R_{c,i} \end{bmatrix} \\ G_{rc,i} &= \begin{bmatrix} g_{rc,i} & h_{rc,i} \end{bmatrix} = \begin{bmatrix} g_i & 0 \\ 0 & h_{c,i} \end{bmatrix} \quad u_{rc,i} = \begin{bmatrix} u_i^1 \\ u_{c,i}^2 \end{bmatrix} \quad y_{rc,i} = \begin{bmatrix} y_i^1 \\ y_{c,i}^2 \end{bmatrix} \end{aligned} \tag{3.14}$$

where $x_{rc,i} := [x_i^T \quad x_{c,i}^T]^T$, and the Hamiltonian function is given by

$$H_{rc,i}(x_i) = H_i(x_i) + H_{c,i}(x_{c,i}) \tag{3.15}$$

Notice that the dimensions of the state variables are different for the masters and the slave, and the value of $u_{c,i}^2$ and $y_{c,i}^2$ are given as

$$\begin{aligned} u_{c,m_1}^2 &= \dot{\theta}_{r_1} \quad u_{c,m_2}^2 = \dot{\theta}_{r_2} \quad u_{c,s}^2 = -T_{r_s} \\ y_{c,m_1}^2 &= -T_{r_1} \quad y_{c,m_2}^2 = -T_{r_2} \quad y_{c,s}^2 = \dot{\theta}_{r_s} \end{aligned} \tag{3.16}$$

3.5.4 Closed-loop ESC Based Dual-user System

In this section, the model of closed-loop ESC dual-user system (see Fig. A-10) is exploited by composing with the authority sharing mechanism.

From the equations defined in Eq. (3.4), (3.16), we can conclude that:

$$\begin{aligned} u_{c,m_1}^2 &= \alpha y_{c,s}^2 + (1-\alpha)\dot{\theta}_{sf_1} \\ u_{c,m_2}^2 &= (1-\alpha) y_{c,s}^2 + \alpha \dot{\theta}_{sf_2} \\ u_{c,s}^2 &= -\alpha y_{c,m_1}^2 - (1-\alpha) y_{c,m_2}^2 \\ T_{sf_1} &= (1-\alpha) y_{c,m_1}^2 \\ T_{sf_s} &= \alpha y_{c,m_2}^2 \end{aligned} \tag{3.17}$$

By integrating this set of equations into the robot-controller subsystems given by

[6] The following notations, with respect to input u_i and output y_i, comply to the same convention.

Eq. (3.14), we obtain the global ESC based dual-user system model expressed in port-Hamiltonian framework:

$$
\begin{aligned}
J_g &= \begin{bmatrix} J_{rc,m_1} & 0 & \alpha h_{rc,m_1} h_{rc,s}^T \\ 0 & J_{rc,m_2} & (1-\alpha) h_{rc,m_2} h_{rc,s}^T \\ -\alpha h_{rc,s} h_{rc,m_1}^T & -(1-\alpha) h_{rc,s} h_{rc,m_2}^T & J_{rc,s} \end{bmatrix} \\
R_g &= \begin{bmatrix} R_{rc,m_1} & 0 & 0 \\ 0 & R_{rc,m_2} & 0 \\ 0 & 0 & R_{rc,s} \end{bmatrix} \quad G_g = \begin{bmatrix} g_{rc,m_1} & 0 & 0 \\ 0 & g_{rc,m_2} & 0 \\ 0 & 0 & g_{rc,s} \end{bmatrix} \\
Q_g &= \begin{bmatrix} (1-\alpha) h_{rc,m_1} & 0 \\ 0 & \alpha h_{rc,m_2} \\ 0 & 0 \end{bmatrix} \\
u_g &= \begin{bmatrix} T_{h_1} \\ T_{h_2} \\ -T_e \end{bmatrix} \quad v_g = \begin{bmatrix} \dot{\theta}_{sf_1} \\ \dot{\theta}_{sf_2} \end{bmatrix} \quad y_g = \begin{bmatrix} \dot{\theta}_{m_1} \\ \dot{\theta}_{m_2} \\ \dot{\theta}_s \end{bmatrix} \quad s_g = \begin{bmatrix} T_{sf_1} \\ T_{sf_s} \end{bmatrix}
\end{aligned}
\tag{3.18}
$$

which can be rewritten in the following form:

$$
\begin{cases}
\dot{x}_g = [J_g - R_g] \nabla_{x_g} H_g + G_g u_g + Q_g v_g \\
y_g = G_g^T \nabla_{x_g} H_g \\
s_g = Q_g^T \nabla_{x_g} H_g
\end{cases}
\tag{3.19}
$$

where the state variables are $x_g := [x_{rc,m_1}^T \;\; x_{rc,m_2}^T \;\; x_{rc,s}^T]^T$, and the Hamiltonian is given by

$$
H_g(x_g) = H_{rc,m_1} + H_{rc,m_s} + H_{rc,s} \tag{3.20}
$$

By modelling each subsystem (i.e., master/slave robot, IPC controller, interconnection), we managed to obtain a global system represented in port-Hamiltonian framework. There, it is possible for us to study the passivity by taking advantage of the port-Hamiltonian properties and methods (see Section A.3.1 for instance).

3.6 Passivity of ESC Dual-User System

The study of the passivity of the architecture is necessary to ensure its stability. In this section, we study it from both the closed-loop and the subsystem point of view. Consequently, these two approaches are eventually unified into a same passivity controller.

3.6.1 Passivity Analysis from Closed-loop System point of view

In the previous port-Hamiltonian model, the system is composed with both the human/environment power port (u_g, y_g) and modulated source power port (v_g, s_g). The energy balance can be given by

$$\frac{dH_g}{dt} = -\frac{\partial^T H_g}{\partial x_g} R_g \frac{\partial H_g}{\partial x_g} + y_g^T u_g + s_g^T v_g \tag{3.21}$$

or, equivalently:

$$\begin{aligned} &H_g(x_g(t)) - H_g(x_g(0)) \\ &= \int_0^t y_g^T(\tau) u_g(\tau) \mathrm{d}\tau + \int_0^t s_g^T(\tau) v_g(\tau) \mathrm{d}\tau - D(t) \end{aligned} \tag{3.22}$$

where $D(t)$ is a non-negative function representing the dissipated energy.

Only the human/environment global power port (u_g, y_g) is associated with the external world. With respect to the supplied power through it, the passivity condition is defined as,

$$H_g(x_g(t)) - H_g(x_g(0)) \leq \int_0^t y_g^T(\tau) u_g(\tau) \mathrm{d}\tau \tag{3.23}$$

Since the modulated source power port (v_g, s_g) may violate this passivity condition, the following equation must always be satisfied:

$$\int_0^t s_g^T(\tau) v_g(\tau) \mathrm{d}\tau - D(t) \leq 0 \tag{3.24}$$

As the dynamics of the robots may be sometimes unknown, which makes it hard to get the precise knowledge of $D(t) > 0$, we deduce a less conservative condition:

$$\int_0^t s_g^T(\tau) v_g(\tau) \mathrm{d}\tau \leq 0 \tag{3.25}$$

Otherwise, the two MFS could inject extra energy into the system and potentially destabilize it. By integrating Eq. (3.4), (3.18) and knowing that $\dot{\theta}_{sf_1}(t) = \dot{\theta}_{sf_2}(t) = \dot{\theta}_{r_s}(t)$, the above passivity condition can be rewritten as

$$E_p = \int_0^t \left[(1-\alpha) T_{r_1}(\tau) + \alpha T_{r_2}(\tau)\right]^T \dot{\theta}_{r_s}(\tau)\ \mathrm{d}\tau \geq 0,\ \forall t \geq 0 \tag{3.26}$$

3.6.2 Passivity Analysis from Subsystems point of view

Every part of the dual-chain (masters and slave robots controlled by the IPC controllers and energy shared control based architecture) being passive as stated in previous subsection, as long as both modulated flow sources hold passive behaviors, the passivity of the close-loop dual-user teleoperation system will be preserved.

According to the definition of passivity in [Schaft, 2000], both MFS should only be able to extract energy from the dual-user chain (by the way, from the masters and the slave), which is translated by:

$$\int_0^t \left(-T_{sf_1}^T(\tau)\dot{\theta}_{sf_1}(\tau) - T_{sf_2}^T(\tau)\dot{\theta}_{sf_2}(\tau)\right) \mathrm{d}\tau \geq 0,\ \forall t \geq 0 \tag{3.27}$$

Otherwise, the two MFS could inject extra energy into the system and potentially destabilize it. By integrating Eq. (3.1) and knowing that $\dot{\theta}_{sf_1}(t) = \dot{\theta}_{sf_2}(t) = \dot{\theta}_{r_s}(t)$, the above passivity condition can be rewritten as,

$$E_p = \int_0^t \left[(1-\alpha) T_{r_1}(\tau) + \alpha T_{r_2}(\tau)\right]^T \dot{\theta}_{r_s}(\tau)\ \mathrm{d}\tau \geq 0,\ \forall t \geq 0 \tag{3.28}$$

It is worth to notice that the above passivity condition is eventually unified into the same form as Eq. (3.26), from the closed-loop point of view.

As a conclusion, we need to design a controller to ensure this condition in real-time, avoiding undesired behaviors, or even instability.

3.6.3 Passivity Controller

In practice, the passivity condition expressed in Eq. (3.26) or Eq. (3.28) must always be satisfied. So, we use the following control laws for the modulated flow sources:

$$\dot{\theta}_{sf_1} = \dot{\theta}_{sf_2} = \begin{cases} \dot{\theta}_{r_s}, & \text{if } E_p \geq 0 \\ 0, & \text{otherwise} \end{cases} \tag{3.29}$$

As long as the passivity condition is satisfied, both MFS will be activated providing full feedback to both users. Otherwise, both MFS are deactivated, forcing the modulated flows $\dot{\theta}_{sf_1}$ and $\dot{\theta}_{sf_2}$ to 0 until the condition becomes checked again. This controller always guarantees the global passivity and only deteriorates the additional feedback which means that in critical situations, the quality of feedback corresponds to the basic authority sharing mechanism.

It is worth to notice that, as α is computed in E_p, its evolution is not constrained. Its variations do not have any effect on the closed-loop passivity (which will be detailed in Section 4.4).

3.7 IPC Tuning for Compliance and Transparency

The IPC controllers parameters can be set arbitrarily without affecting the passivity (see Section A.3.3). Yet, the performance of the dual-user system, in terms of compliance and transparency, is highly effected by these parameters. Thus, proper parameters should be set.

The stiffness of the robots should be set so that it corresponds to the desired task. For instance, the slave robot should be stiff while the trainer's interface should be compliant. Also, their damping should be set in order to avoid overshooting and undesirable oscillatory effects.

In [Stramigioli, 1996], a basic guideline for the IPC controller is introduced. In order to have critical damping and compliance control for the system, we provide the following relationships using the parameters given in Section 3.5:

$$\begin{aligned}
&diag\,(B_{c,i},k) \approx 2\sqrt{diag\,(K_{r,i},k)\cdot M_i^{k,k}}\\
&diag\,(M_{c,i},k) \ll M_{min,i}^k\\
&diag\,(K_{c,i},k) \gg \max(diag\,(M_{c,i},k)\,M_{max,i}^k, diag\,(B_{c,i},k)\,M_{max,i}^k, K_{rmax,i})\\
&M_{min,i}^k = \min\left\{M_i^{k,k}(\theta_i)\right\}\\
&M_{max,i}^k = \max\left\{M_i^{k,k}(\theta_i)\right\}\\
&K_{rmax,i} = \max\left\{diag\,(K_{r,i})\right\}
\end{aligned} \tag{3.30}$$

where $i = m_1, m_2, s$, and k represents the k^{th} element (row and column) of corresponding signal. It is worth to notice that when $i = s$, the matrix $K_{r,i} = 0^{n\times n}$ for there is no spring setting in the slave IPC controller, and $K_{r,i}, K_{c,i}, M_{c,i}, B_{c,i}$ are diagonal matrices as indicated in Eq. 3.9, representing parallel elements for multiple DoF systems.

Furthermore, a good transparency should also be achieved. By making use of the transparency approaches detailed in Section 2.2.3, we could tune the IPC parameters so as to obtain the following position and force tracking:

$$\begin{aligned}
\theta_i &\rightarrow \theta_{r,i}\\
T_j &\rightarrow T_{r,i}\\
-T_e &\rightarrow T_{r,s}
\end{aligned} \tag{3.31}$$

where $i = m_1, m_2, s$ and $j = h_1, h_2$.

3.8 Real-time Experiments

3.8.1 Experiment Setup

In order to evaluate the performances of the ESC dual-user framework featuring the shared control structure and the passivity controller, we made several attempts to build an experiment bench.

Two Sensable® PHANTOM Omni act as our haptic devices, as shown in Fig. 3-4. To our best knowledge, the usage for two PHANTOM Omni devices on the same computer is not officially supported in QUARC® control software [QUARC, 2016] (compatible with MATLAB/Simulink®). From our experience, a solution consists of using the OpenHaptics® Toolkit [OpenHaptics, 2016].

Also, we needed to link them by way of the Robot Operating System (ROS) [ROS, 2016] framework, in order to achieve a simulation environment providing high-performance physics engines such as Gazebo [Gazebo, 2016]. We hence managed to drive and control two Omni devices at the same time on the same computer but the result architecture turned out to be very complex when integrating the discretized IPC controller, physical contact modeling in Gazebo, etc. Actually, we found another haptic interface block developed in [Aldana et al, 2014], which is compatible with two Omni devices. The following setup makes use of it.

The haptic training software part was built into MATLAB/Simulink® as shown in

Figure 3-4: Experimental bench

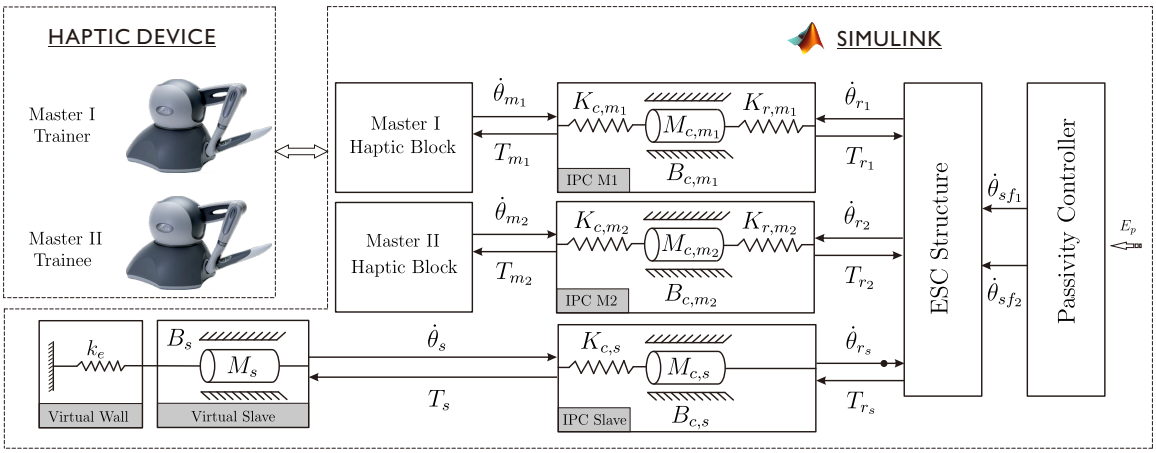

Figure 3-5: Experimental setup

Fig. 3-5. Two Sensable® PHANTOM Omni devices (only their first joint, in one dimensional case) were used as the two masters operated by the trainer and the trainee. The devices' kinematic and dynamic parameters could be found in [Sansanayuth et al, 2012]. The haptic blocks (see [Aldana et al, 2014]) are used as communication interface between Simulink and the Omni devices. A simulated one d.o.f. joint mass robot was set up for the virtual slave as shown in Fig. A-8. The IPC controllers were tuned for compliant motion. Note that the slave robot interconnects with a different form of IPC controller compared with the ones of masters, in order to fit reverse causality interaction with the masters. The IPC controller (see tuning approach in Section 3.7) were tuned with the values provided in Table 3.1. The passivity controller is realized in real-time through calculation of energy checking function, i.e., E_p (see Eq. 3.26 or Eq. 3.28).

Table 3.1: Real-time experiment parameters

Items	**Parameters**	**Unit**	**Value**
Slave Robot Dynamics	B_s	$\mathrm{N \cdot m \cdot s/rad}$	0.5
	M_s	$\mathrm{kg \cdot m^2}$	0.1
IPC Controller ($i = m_1, m_2, s$)	$K_{c,i}$	$\mathrm{N \cdot m/rad}$	10
	$K_{r,i}$	$\mathrm{N \cdot m/rad}$	10
	$M_{c,i}$	$\mathrm{kg \cdot m^2}$	0.01
	$B_{c,i}$	$\mathrm{N \cdot m \cdot s/rad}$	0.5

3.8.2 Experimental Results

The three different modes (training , guidance and evaluation) of the proposed ESC architecture have been experimented. A virtual wall (which may represent a human bone) was set at angle 0.5 rad. The wall model was:

$$-T_e = \begin{cases} 0, & \theta_s < 0.5 \text{ rad} \\ -k_e(\theta_s - 0.5), & \theta_s \geq 0.5 \text{ rad} \end{cases} \tag{3.32}$$

where $k_e = 10$ N $\cdot$ m/rad is the wall stiffness and θ_s is the slave robot's joint angle. The hand torques were estimated by a Nicosia observer described in [Nicosia and Tomei, 1990]. The tracking of positions and hand/environment torques are shown in Fig. 3-6. The experiment time is separated into six periods (from A to F), with corresponding parameter and properties given in Table 3.2.

Table 3.2: Experiment periods

Period	A	B	C	D	E	F
α	1	0	0.5	0	0	1
Mode	T	E	G	E	E	T
Wall Contact	N	N	N	N	Y	N

Mode: T=Training, G=Guidance, E=Evaluation
Wall Contact: Y=Yes, N=No

From the figure, the trainer has full control authority during period A when he leads his device to the target position. Meanwhile, the trainee and the slave follow him (training mode). In phase B, the control authority is switched to the trainee for evaluation purpose; the slave and the trainer follow him. However, the slave only gets to angle 0.2 rad, that the trainee fails to reach the target position. After then, in period C, both the trainer and the trainee experience a shared control over the slave where the trainer tries to guide the slave to the target position. The trainee notices his own incorrect motion and then he leads his device to the target position as well. The full control authority is switched back to the trainee again in phase D during which he leads the slave up to the virtual wall. The slave collides the wall in period E. The trainee feels the reaction torque from the environment. Note that, by default,

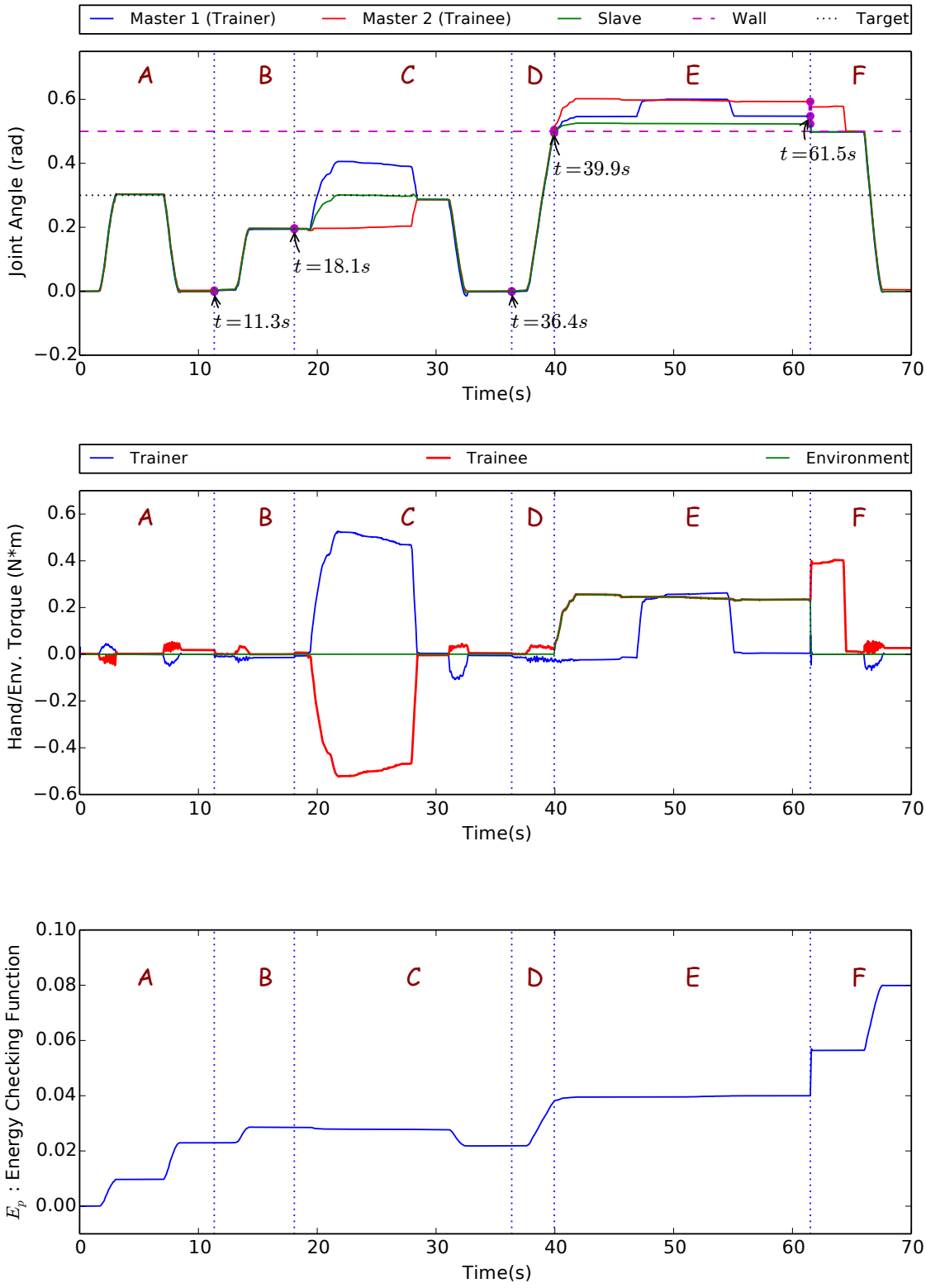

Figure 3-6: The positions, torques tracking and energy passivity checking

in this situation, the trainer has no environment force feedback as $\alpha = 0$. He needs to guide his device to the same position as the trainee's one to be able to feel the same reaction torque (visible during 47s to 55s time lapse). Note that, in contact period, as usual with many teleoperators, the masters' position is not exactly the same as the slave because of their own compliance. Stiffer masters would decrease this offset but could also introduce oscillations in free motion. On authority switching, in period F, the slave moves back from the wall as the new leader (the trainer) does not provide enough torque at this moment to counter the previous wall reaction torque. Finally, the slave and the trainee follow the trainer's motion towards the initial position.

Regarding passivity of the system during the whole training process, the energy checking function of Eq. 3.28 is shown in subfigure 3. It is always non-negative that ensures the passivity condition. Therefore, the MFS are always activated to providing full slave motion feedback.

To conclude, experiments demonstrate a shared control behavior and a good tracking performance in view of motion and forces. The three different modes (training, guidance and evaluation) could be implemented by changing the control authority. Passivity of the system could be ensured by the proposed controller.

3.9 Conclusion

In this chapter, we introduced the ESC based dual-user haptic system architecture. The authority sharing mechanism is put forward to manage the control permissions for the two users over the slave. Regarding the control authority, which is represented by a dominance factor α, three modes are obtained, i.e., training/guidance/evaluation modes. The IPC controllers are used to obtain compliant motions, and two modulated flow sources provided to both users with the slave's complementary feedback, in oder to obtain a good transparency. The global system is modeled within port-Hamiltonian framework, which simplifies the passivity study. We ensure stable behaviors of the system by making use of a passivity controller, derived from two different passivity condition checking approaches. Real-time experiments are conducted for validation.

Chapter 4

Adaptive Authority Adjusting

4.1 Introduction

By default, teleoperation systems do not provide any artificial or intelligent assistance to help the users to perform their task. So their accuracy is highly dependent on the human operators skills. For instance, a force feedback can be sent only after collision between the remote tool and its environment; in some case where collisions are dangerous (for the tissues in robotic surgery, for instance), this haptic information comes back too late to the users who may not have anticipated this collision.

Assisted teleoperation systems are a way to solve this problem. They are sometimes implemented using *Virtual Fixtures* (VF), firstly introduced in [Rosenberg, 1993]. It consists of software-based constraints applied to the user interface motions. They act as guidance rulers, that assist users to perform a task along a restricted region/or along a desired trajectory. Virtual fixtures help to obtain a better accuracy by locking some degrees of freedom in order for the user to focus on fewer important ones (guidance). They can also potentially ensure a safer operation by inhibiting dangerous motions. They have been introduced into teleoperation schemes using various approaches. One can distinguish *Forbidden-Region Virtual Fixtures* (FRVFs) from *Guidance Virtual Fixtures* (GVFs) [Abbott et al, 2007] (see Fig. 4-1). The FRVFs keep the slave out of predefined forbidden regions, while the GVFs lead the slave to desired paths or surfaces alternatively. The virtual fixtures can be arbitrarily de-

fined using different geometries according to the desired task and application. It has been shown that virtual fixtures improve the precision and the dexterity in minimally invasive surgery (MIS) [Guthart and Salisbury, 2000].

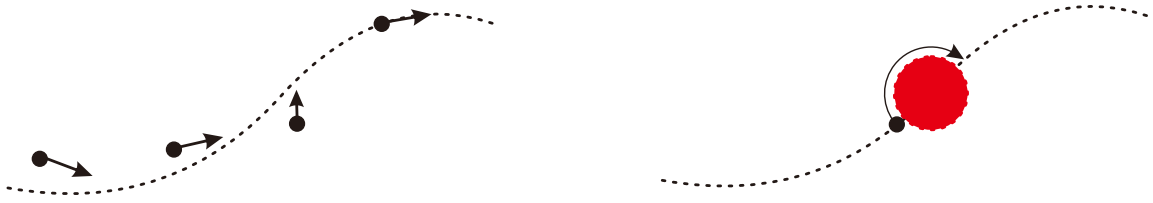

Figure 4-1: An example for GVFs (left) and FRVFs (right). The dashed line is the desired path, and the red filled circle is the forbidden region.

Many works have been carried out about virtual fixtures, using a mesh shape or a simple virtual wall. In [Abbott et al, 2007], both the FRVFs and GVFs have been studied through the aspects of passivity, human modelling and applications. Most of the virtual fixtures are based on an active impedance behavior, where the stored potential energy may generate unstable motions. Conversely, admittance-type virtual fixtures provide greater accuracy and the property of natural passivity. They bring some advantages in terms of transparency (i.e., position and force tracking). Some of them have been implemented on the Johns Hopkins University Steady-Hand Robot in [Li et al, 2005], and also in [Fichtinger et al, 2008, Pezzementi et al, 2007].

Concerning dual-user teleoperation systems, some virtual fixtures have been incorporated into the control authority mechanism by Shahbazi et al in [Shahbazi et al, 2013]. These VFs allow concurrent performance of a robotic surgical task by a trainer and a trainee. They prevent to have to manually switch between the two users. In fact, the involvement of the two users in the procedure is adjusted on-line. The control authority is a function of the force generated by the implemented virtual fixtures.

In this chapter, we describe how we adopted the principle of GVFs, to develop an Adaptive Authority Adjusting (AAA) mechanism. It allows changing the level of control of the users over the slave in accordance with the skill of the trainee. In addition, an overrule function is introduced for emergency situations so that the trainer can always set the control authority at a desired value anytime.

4.2 Adaptive Authority Adjustment (AAA)

Fig. 4-2 provides an illustration of the main principle of the Adaptive Authority Adjustment (AAA) mechanism introduced in this section. One can obtain a overall view over it, before diving into the details in each following subsection.

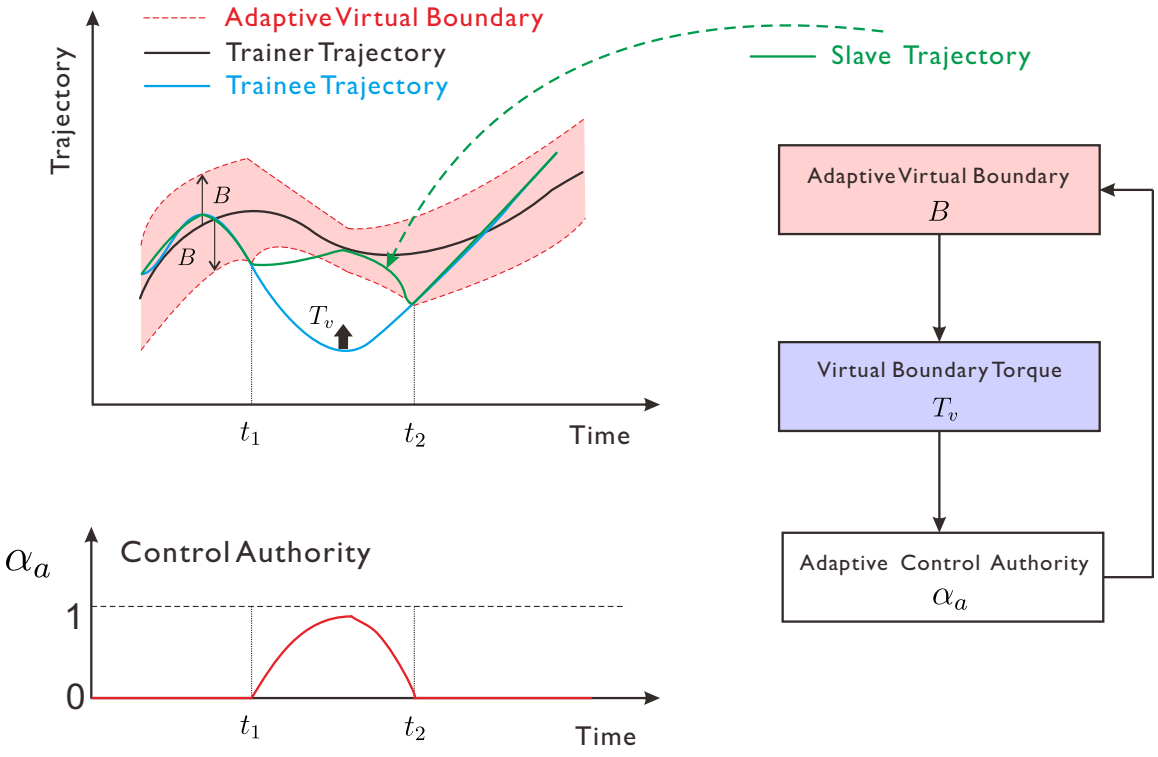

Figure 4-2: Flow chart of AAA

The mechanism is active in the supervision mode, when the trainee is leader and the trainer is follower, i.e. $\alpha = 0$. During the period from t_1 to t_2, the trajectory of the trainee goes beyond the adaptive virtual boundaries. Meanwhile, the authority is partly brought back to the trainer so that the slave is partly deviated towards the right motion, and a virtual torque is yielded as the authority is shifted towards the trainer. The value of α is computed on-line and is adapted according to the distance between the trainee interface and the closest boundaries. A reaction torque (indicating position differences between the trainer and trainee) is naturally generated by the dual-user system that delivering a notification to the trainee for his transboundary behavior. Finally, we could conclude the slave's trajectory as indicated by the green line.

4.2.1 Adaptive Virtual Boundary

Firstly, we introduce the concept of adaptive virtual boundary in order to guide the trainee in the right path. We define the virtual boundary as the maximum allowed distance between both master positions. The position of the trainer always generates a virtual area (a line segment in 1D, a circle in 2D, a sphere in 3D). The trainee can move his device freely inside this boundary. It is defined as:

$$d_{\theta_m} = (\theta_{m_1} - \theta_{m_2})^2 \leq B \tag{4.1}$$

where B defines the maximum allowed distance between the trainer and the trainee. We adopted the form of B specified in [Shahbazi et al, 2013], as a function of the adaptive dominance factor (see the following section), that is:

$$B = B_0 - k_b \cdot \ln(\alpha_a + \epsilon) \tag{4.2}$$

where B_0 is the maximum allowed distance when the trainer gets full control($\alpha_a = 1$). The $\ln(\cdot)$ function enables a non-linear behavior which results in the decreasing of the boundary as the trainee gets qualified (i.e. $\alpha = 0$). k_b is a tuning gain and ϵ is a very small value to avoid the zero argument case for $\ln(\cdot)$, i.e. when $\alpha_a = 0$.

4.2.2 Virtual Boundary Torque

As soon as the condition given in Eq. 4.1 is violated, i.e., the trainee tries to move beyond the authorized area, a virtual boundary torque is generated. This torque is modeled by a spring as follows:

$$T_v = \begin{cases} 0, & d_{\theta_m} \leq B \\ -k_v(\theta_{m_1} - \theta_{m_2}), & d_{\theta_m} > B \end{cases} \tag{4.3}$$

where k_v acts as a virtual stiffness. Notice that in our architecture, this torque will not be transmitted to the trainee, but this virtual torque is used as a criterion for evaluation of the expertise of the trainee in the following section.

4.2.3 Adaptive Dominance Factor

The adaptive dominance factor refers to α_a, which determines the shared control authority based on the expertise of the trainee. The worse the trainee performs, the higher virtual torque T_v is generated. Therefore, we can use this virtual torque as a quantitative measurement to evaluate the performance of the trainee. For an expert trainee, whose motion is always located inside the virtual boundary ($T_v = 0$), α_a should be equal to 0 (the trainee holds full control authority). For a complete novice, when the virtual torque exceeds a given threshold, α_a should be set to 1. Based on these requirements, we define α_a in a Gaussian function by making use of T_v as follows:

$$\alpha_a = 1 - e^{-\frac{T_v^2}{2\cdot(T_0)^2}} \tag{4.4}$$

where T_0 is a task based parameter. It is straightforward to conclude that α_a ranges from 0 to 1, as shown in Fig. 4.2.3, which represents expertise of the trainee ranges from inexperienced to professional.

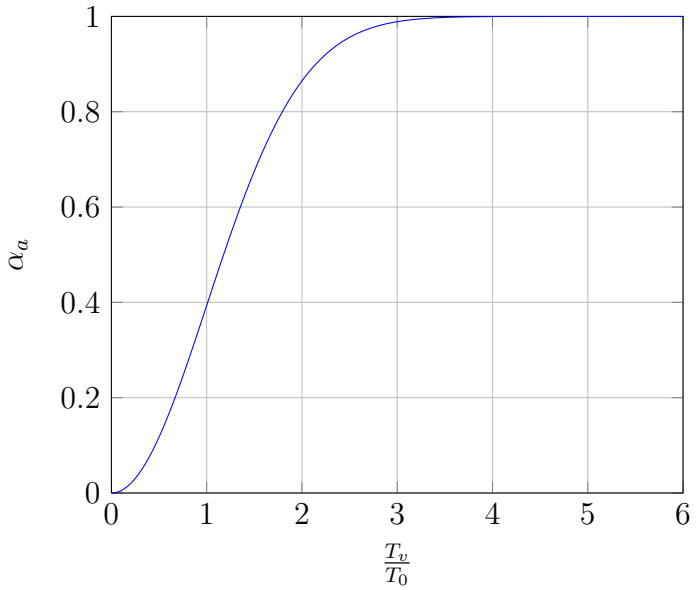

Figure 4-3: Adaptive dominance factor α_a.

4.2.4 Configuration

All the parameters introduced by the implementation of AAA are task dependant. For instance, when performing micro-operation or a task that requires high precision, the value B_0 should be set as small as possible in order to avoid the unskilled trainee to obtain undesired control authority. k_b is a tuning gain that determines the sensitivity over the virtual boundary in response to control authority variation. For a skilled trainee, k_b should be small in order to reduce the sensitivity.

k_v and T_0 are related to the virtual force, one possible configuration for these parameters is to match (or approximately equal) T_v with the trainee's reaction torque (T_{h_2}) which is naturally generated by the dual user system. The following steps could be carried out:

- **Step 1**: Give a series of α values, and set IPC controller parameters properly according Section 3.7.
- **Step 2**: The trainer holds his/her device at a constant position (for instance, $\theta_{m_2} = 0$), while the trainee moves his/her device to the maximum position (depends on the robot's workspace) continuously.
- **Step 3**: Obtain a correspondence sequence of trainee's torque (T_{h_2}) and position error ($\theta_{m_1} - \theta_{m_2}$) for each α. Combine all the sequences into a single array (i.e., $[T_{h_2}, \theta_{m_1} - \theta_{m_2}, \alpha]$) regarding α.
- **Step 4**: Based on a parameter identification approach (for instance, least squares method), use the first two columns of step-3 array (i.e.,$[T_{h_2}, \theta_{m_1} - \theta_{m_2}]$) concerning Eq. 4.3, to get the estimated $\widetilde{k}_v$. Substitute $\widetilde{k}_v$ into Eq. 4.4, then use first column and the third column of step-3 arrary (i.e.,$[T_{h_2}, \alpha]$. to obtain the estimated $\widetilde{T}_0$.
- **Step 4**: Set $k_v = \widetilde{k}_v$ and $T_0 = \widetilde{T}_0$.

It is worth to notice that all the parameters can vary in real-time, which will result in a time-varying control authority α.

4.3 Overrule Function

It is worth to notice that the control authority should be switched to any expected value on-line by the trainer manually, especially in emergency cases. For instance, the trainer may need to demonstrate the trajectories (in full control) even if the trainee acts well, or the trainer could need to avoid a collision before contact even if the trainee remains inside the virtual boundary. For this purpose, we introduce another dominance factor, denoted by α_o. We call it the **overrule** function. Then the final decision of control authority α is:

$$\alpha = \begin{cases} \alpha_a, & \text{overrule} = \text{False} \\ \alpha_o, & \text{overrule} = \text{True} \end{cases} \tag{4.5}$$

where *overrule* is a boolean input available to the trainer on his interface (typically, on a Phantom device, it is one of the buttons available on the tip).

4.4 Passivity of AAA

Our proposed adaptive authority adjustment (AAA) featuring the overrule function is based on an impedance-type implementation, that acts in an active way. Hence, it may violate the passivity of the close-loop system. In fact, there is no explicit position/force signals virtual fixture injected into the system. The AAA mechanism only affects the value of α, in contrary to other approaches in the literature. For instance, explicit virtual fixtures are created in [Ferraguti et al, 2015, Shahbazi et al, 2013]. The following proposition proves the non-violation of passivity regardless variations of α.

Proposition 1. *The closed-loop system shown in Fig. 3-3, with respect to AAA, is passive regardless variations of control authority* $\alpha \in [0, 1]$.

Proof. In order to analyze the close-loop system passivity, we separate the system into several subsystems: the masters/slave sides couping with IPC controllers and users/environment, the ESC structure, and the modulated flow sources.

Firstly, we consider the ESC structure. It forms a lossless architecture which is intrinsically passive as the energy stored inside it is always zero. Then, by denoting the Hamiltonian function of each subsystem at masters and slave sides (in Port-Hamiltonian framework) with H_{m_1}, H_{m_2}, H_s and considering the energy generated by **MFS** as internal stored part (assumed with a passive behavior), we write the close-loop energy function $V(t)$ as,

$$\begin{aligned}\frac{\mathrm{d}}{\mathrm{d}t}V(t) &= \frac{\mathrm{d}H_{m_1}}{\mathrm{d}t} + \frac{\mathrm{d}H_{m_2}}{\mathrm{d}t} + \frac{\mathrm{d}H_s}{\mathrm{d}t} + T_{sf_1}^T\dot{\theta}_{sf_1} + T_{sf_2}^T\dot{\theta}_{sf_2} + 0 \\ &= T_{h_1}^T\dot{\theta}_{m_1} + T_{h_2}^T\dot{\theta}_{m_2} - T_e^T\dot{\theta}_s - P_{m_1} - P_{m_2} - P_s\end{aligned} \tag{4.6}$$

where 0 represents the energy in the ESC structure and P_{m_1}, P_{m_2}, P_s are the dissipated power at each subsystem.

Since the closed-loop energy function has no relationship with the control authority α, and according to the condition of passivity of a switched system given by [Mahapatra and Zefran, 2003], we confirm the conclusion of Proposition 2. □

4.5 Real-time Experiments

4.5.1 Experiment Setup

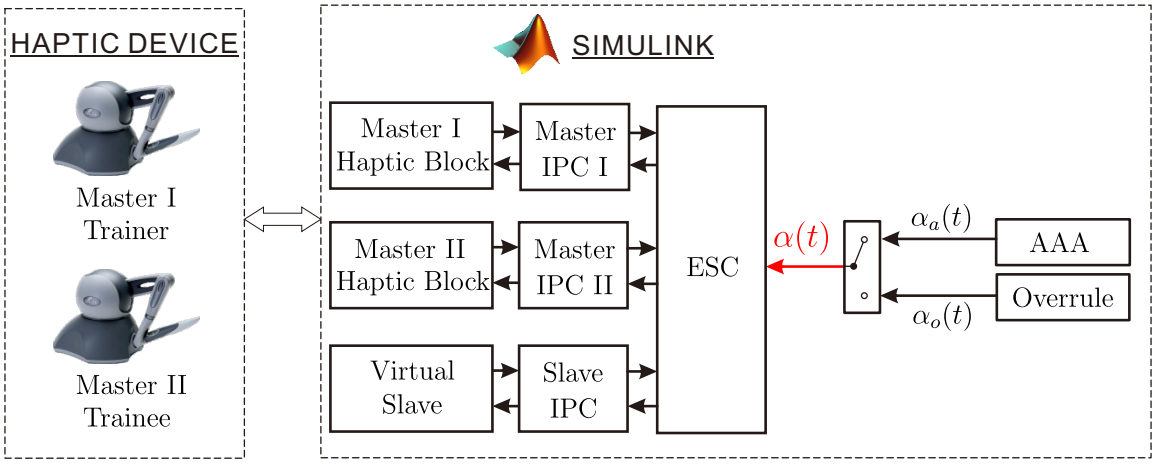

Figure 4-4: Experimental setup

Real-time experiments are carried out to validate the ESC dual-user framework

featuring the Adaptive Authority Adjustment (AAA) mechanism. The experimental setup is shown in Fig. 4-4. Two Sensable® PHANTOM Omni devices are the two masters robots. The other components, including the haptic blocks, the virtual slave, the IPC controllers and the ESC shared control structure, take the same configuration as given in Section 3.8.1. Parameters for these configurations can be found in Table 3.1.

Furthermore, the AAA mechanism and the overrule function are introduced into the system, to determine the control authority in real-time. The AAA parameters are provided in Table 4.1.

Table 4.1: Real-time experiments of AAA parameters

Items	**Parameters**	**Unit**	**Value**
AAA	B_0	rad	0.05
	k_b	rad	0.01
	k_v	$\mathrm{N \cdot m/rad}$	10
	T_0	$\mathrm{N \cdot m}$	0.707

4.5.2 AAA Mechanism Experimental Validation

To evaluate the performances of our proposed framework featuring the Adaptive Authority Adjustment (AAA) mechanism, following experiments have been conducted.

The training goal of this experiment was to move the slave device at target position located at angle 0.3 rad. A virtual wall was set at angle 0.5 rad using the same model indicated in Eq. 3.32. The hand torques were estimated with a Nicosia observer described in [Nicosia and Tomei, 1990]. The tracking of positions and hand/environment torques are shown in Fig. 4-5. The experiment time is separated into nine phases, i.e. A-I, given as Table 4.2.

In Figure 4-5, one can check that the phase A corresponds to the training mode: the authority is overruled by the trainer with $\alpha_o = 1$. The trainer guides the trainee and the slave to the target position. The authority is set to the trainee (manually, by the trainer) during phase B. But due to an unskilled behavior of the trainee, the

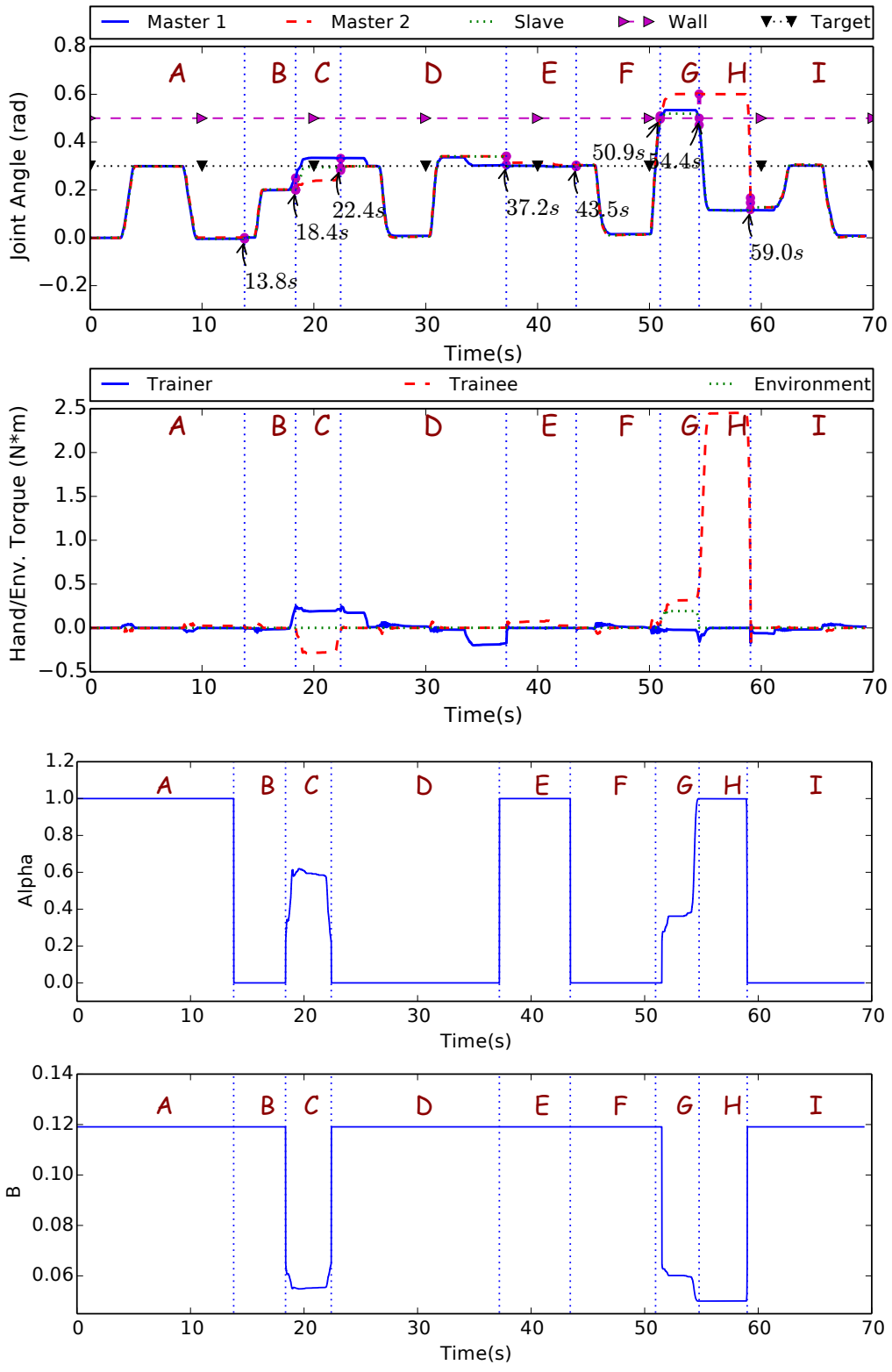

Figure 4-5: Positions and torques tracking with variations of authority and virtual boundary (the environment torque is plotted as the same direction of the human torque, that is $-T_e$).

Table 4.2: AAA Experiment phases

Phase	**A**	**B**	**C**	**D**	**E**	**F**	**G**	**H**	**I**
α	1	0	[0,1]	0	1	0	[0,1]	≈1	0
β_1	1	0	1	0	1	0	1	1	0
β_2	1	0	0	0	1	0	0	0	0
α_a	0	0	[0,1]	0	1	0	[0,1]	≈1	0
α_o	1	0	0	0	1	0	0	0	0
Mode	T	E	G	E	T	E	G	G	E
Wall Contact	N	N	N	N	N	N	**Y**	N	N
Overrule	**Y**	N	N	N	**Y**	N	N	N	N

Mode: T=Training, G=Guidance, E=Evaluation
Wall Contact: Y=Yes, N=No Overrule: Y=Yes, N=No

slave does not reach the target position. Then, the trainer tries to lead the slave to the right position in phase C. The virtual boundary narrows down. There is a variation of authority during this period where the authority of the trainee over the slave automatically decreased down to around 0.4 based on the adaptive distance evaluation method, according to Eq. 4.4. Both the trainer and the trainee felt a torque on their hands during this period, which acts as a signal sent to the trainee to tell him that his/her gestures are undesired. In phase D, the full authority is given back to the trainee again according to AAA. But this latter leads the slave beyond the target position. The trainer tries to revise the position by moving his device back a little, but it does not make any effect since the trainee is still inside the virtual boundary. Under such cases, the overrule behavior could be adopted to set an expected authority.

Then, the overrule authority is manually set to 1 by the trainer in phase E. It allows him guiding the slave to the right position. In phase F, the trainee gets another chance to perform the task, and, this time, he leads his device to the virtual wall. The slave enters into contact with the wall at time 50.9s. During this contact period (phase G), the trainee receives a reaction torque not only from the environment, but also the one generated by the trainer, for the reason that the trainer obtains authority

as well because the trainee exceeds the virtual boundary. Apparently, this is a useful notification delivered to the trainee for awareness of either wall contact or wrong behaviors.

Afterwards, the trainer pulls the slave to the opposite direction, to get a certain level of authority. The slave is off the wall at time 54.4s, and the trainer almost gets full control at time 54.8s. After then, the slave mainly follows the trainer. The trainee feels a bigger resistance torque, that informs him the wrong behavior. After releasing the master 2 device, he obtains full authority again. At last, he manage to lead the slave to the target position and finishes the task in phase I.

In conclusion, the AAA procedure works well within the three dual-user haptic system modes. A reaction force signal will be sent to the trainee when he/she exceeds the virtual boundary along the trajectory of the trainer. It is useful for the trainee to be aware of his gesture quality in real-time. Meanwhile, the trainer does not need to worry about the precise and frequent adjustment of control authority, he can focus on the training tasks. And last but not least, the trainer can still manually take the control over the slave anytime, thanks to the overrule function.

4.5.3 Contact Torque Tracking Under AAA

It is worth to explore the torque details during wall contact cases. The force (torque) tracking can be used to indicate whether the user feels the environment properly. In our architecture, both trainer and trainee experienced a weighted torque (due to shared control of α) compared with the one generated by the wall ($-T_e$, negative sign is for direction). Suppose the contact torque is much greater than the free motion hand torque (supposed to be 0), which is negligible in order to maintain a velocity and due to the presence of frictions.

With reference to the force tracking equations given in Eq. 3.5 and Eq. 3.31, the following relationship between human hand reaction torques and environment torque is always defined as,

$$\alpha T_{h_1} + (1 - \alpha) T_{h_2} = T_e \tag{4.7}$$

When there is contact between the tool and its environment ($T_e \neq 0$), the stiffness of the wall stops the slave robot going as deeper as the user's device. Accordingly, there are four different cases , as following:

- **Case I:** $T_{h_1} = 0,\ T_{h_2} \neq 0,\ T_e = (1-\alpha)T_{h_2}\ (\alpha < 1)$

  This case means that only the trainee leads the device onto the wall. The trainer just evaluates the trainee's behavior without injecting torque into the system. So that the position of the trainer's device is only affected by the feedback from the environment, without positioning by him/her. There will be position differences among the three devices, i.e. $\theta_{m_2} \neq \theta_{m_1},\ \theta_{m_2} \neq \theta_s,\ \theta_{m_1} \approx \theta_s$.

- **Case II:** $T_{h_1} \neq 0,\ T_{h_2} = 0,\ T_e = \alpha T_{h_1}\ (\alpha > 0)$

  This case is opposite to Case I; only the trainer leads the device onto the wall. The trainee does not import torque into the system. The position of his/her device is only affected by the feedback from the environment without positioning. Accordingly, the positions are given as: $\theta_{m_1} \neq \theta_{m_2},\ \theta_{m_1} \neq \theta_s,\ \theta_{m_2} \approx \theta_s$.

- **Case III:** $T_{h_1} \neq 0,\ T_{h_2} \neq 0,\ T_{h_1} \neq T_{h_2},\ T_e = \alpha T_{h_1} + (1-\alpha)T_{h_2}$

  In this case, both the users lead their devices onto the wall. But their own position is, each one, different from the wall position (beyond it because of the compliance of the haptic interfaces) and different to the other user, as each user injects a different torque: $\theta_{m_1} \neq \theta_{m_2} \neq \theta_s$. Human torques are a part of the environment torque, based on the control authority.

- **Case IV:** $T_{h_1} \neq 0,\ T_{h_2} \neq 0,\ T_{h_1} = T_{h_2},\ T_e = \alpha T_{h_1} + (1-\alpha)T_{h_2}$

  In this case, both users apply the same torque to the devices. Owing to the proposed ESC structure, both users experimence full velocity (same values) feedback from the slave regardless the values of α. Thus, it is possible to conclude that both users lead their device to the same position (inside the wall). i.e., $\theta_{m_1} = \theta_{m_2} \neq \theta_s$. Consequently, they import the same hand torque into the system, which is equal to the environment torque by $T_{h_1} = T_{h_2} = T_e$.

Considering the above cases, in order for the user who has no authority (the follower) to be aware of the contact force, it is necessary to provide him with a visual feedback featuring the level of force feedback felt by the user who is manipulating (the leader). Indeed, the haptic interface of the follower follows the slave position but when in contact, the stiffness of the wall and the compliance of the haptic interface of the leader make that the leader position goes beyond the slave position. Hence the follower position does not follow any more the leader one, and, without complementary information, the follower could think that the leader just stopped his motion. By providing the follower, a visual information about the leader position the slave interaction force, it permits to him to push his own device until he reaches the same values.

In order to figure out the torque tracking performance during contact with an wall, we implemented another experiment, shown in Figure 4-6. The setup was the same as in previous experiments, with the same parameters. The experiment can be divided into three phases A, B and C.

- During phase A, the trainee guides the slave to the virtual wall, and gets into contact with it at time $2.9s$.

- Then in phase B, the trainee continues his motion in depth until 0.6 rad. In the figure, one can observe that the trainee experiences a torque feedback based on the control authority, while the trainer does not perceive any torque, which corresponds to previous experiment case I. After that, when the trainer notices the wall contact, he leads his device to the same position as the trainee. Hence, the trainer receives a torque feedback from the environment, which corresponds to cases III and IV. Notice that the slave goes deeper "inside" the wall (which features a rather soft stiffness) due to the trainer's motion, and the torque perceived by the trainee is updated as well.

- Then the trainer releases his device by achieving case I. Finally, the trainee guides the slave off the wall and back to the initial position in phase C.

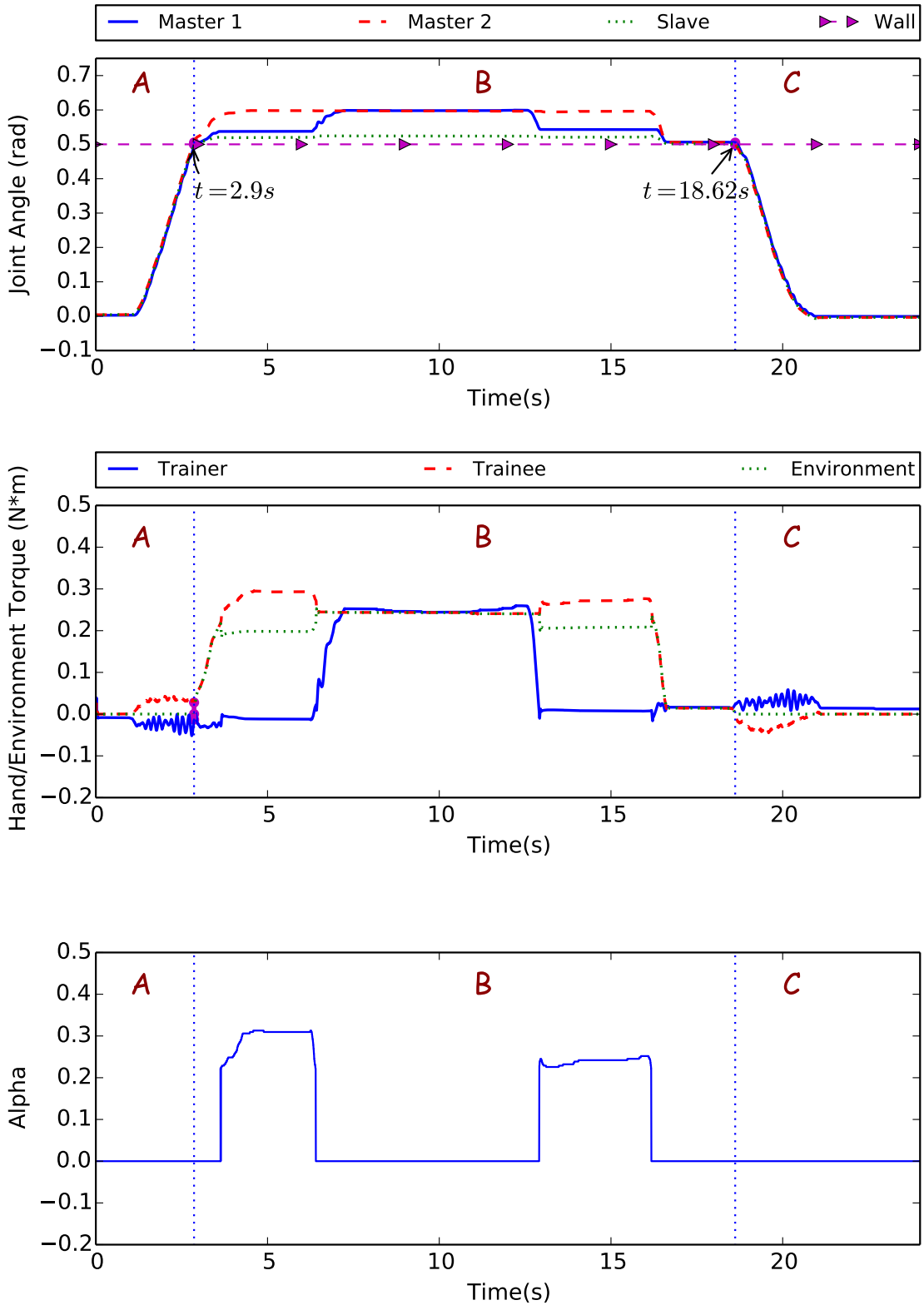

Figure 4-6: Positions and torques tracking with wall contact

4.6 Conclusions

In this chapter, we introduced an Adaptive Authority Adjusting (AAA) mechanisme, based on the concept of Guidance Virtual Fixtures (GVFs) initially developed in bilateral teleoperation. It adapts the control authority on-line according to the expertise of the trainee. It is worth to mention that the passivity of this closed-loop system could be preserved in presence of the AAA mechanism.

To evaluate its performances in practice, some experiments were carried out on a one degree of freedom system. The results demonstrate that AAA would be useful both to the trainee, in terms of undesired gestures notification, and to the trainer who may react without having to adapt manually the authority. Further experiments should be carried out in order to validate the mechanism with a multiple degrees of freedom system and on a real application with several real trainees.

Chapter 5

Comparative Study of Dual-user Architecture

5.1 Introduction

During the past decades, a wide spectrum of bilateral control teleoperation architectures has been developed. It has progressively solved the various problems encountered in practice in teleoperation systems (stability issues in presence of varying delays and data packet loss, lack of transparency, position drift, ...). Since 70s, this variety of approaches and architectures has provoked the need for surveys to get a global comparative overview of this robotics field. The first proposed comparative criteria were task based completion time and execution accuracy. For example, [Mullen, 1972] found that position control was up to four times faster than rate control without force feedback. Extended results from [Wilt et al, 1977] showed that large-sized bilateral teleoperators with position and force feedback control were up to two times faster than with resolved rate control. These early experiments paved the way for further researches, mainly led by NASA Jet Propulsion Laboratory [Bejczy and Handlykken, 1981, Sorenson and Akin, 1995], but also by other researchers [Kim et al, 1987].

Since 1990s, the comparison studies over bilateral teleoperation have focused on stability and transparency oriented objectives: for instance, position/force tracking, impedance perception. Considering applications in medical fields, it is important for

the user to get the sense of remote environment (e.g., tissue or simulated material properties), i.e., the impedance/stiffness of the environment. Therefore, it requires the teleoperation systems to provide accurate sensory information (e.g, position, force, impedance) besides efficient control strategies.

In early 1990s, bilateral teleoperation with force feedback based on passivity approach obtained high-fidelity results. This inspired the researchers to investigate the comparison within/without force feedback and passivity algorithms frames. Hannaford et al, in [Hannaford et al, 1991], conducted a series of experiments showing that the performance of teleoperation improved as some capabilities were added, ranging from pure position control (without force feedback) to with force feedback control. Afterwards, in [Lawn and Hannaford, 1993], the performance test of several candidate control laws for a single-axis telemanipulation system indicated that the task completion time was as much as 50% greater for passivity based methods.

The conflict between stability and transparency was firstly explicitly introduced with a four-channel (4C) bilateral control architecture in [Lawrence, 1993]. The interpretation of the 4C architecture was extended to systems with master/slave manipulators of either the admittance or impedance type in [Hashtrudi-Zaad and Salcudean, 2001]. Moreover, the control parameters was compared among different two-channel (2C) architectures, indicating a trade-off between stability and performance. Nevertheless, the transparency could be improved within 4C architecture.

Considering the existing bilateral architectures, such as the ones based on passivity, compliance, predictive or adaptive control, etc., Arcara et al made a comparative study in [Arcara and Melchiorri, 2002] under constant time delays and evaluated their performance on stability, tracking error, stiffness, and perceived inertia. They provided some general recommendations for the selection of control parameters regarding stability and performance. Some other performance evaluation works had been conducted in [Aliaga et al, 2004, Aziminejad et al, 2008b, Botturi et al, 2004, Marcassus et al, 2006, Moschini and Fiorini, 2004]. Overall, all these research efforts proved the 4C architecture clearly better than any other. In addition to the aforementioned comparative studies, [Kim et al, 2007] and [Rodriguez-Seda et al, 2009] conducted a

complementary comparison over the frameworks involving time-varying delays and Internet based communication channel. These works addressed different defects of the system, such as data losses, environmental constraints etc. Overall, they reported a deteriorating effect in the performance (i.e., larger position errors and lower fidelity of contact information) due to delays and data losses.

To our best knowledge, there is not yet any comparative study over dual-user systems. In this chapter, we provide the results of a comparative study over the two dual-user frameworks proposed in [Khademian and Hashtrudi-Zaad, 2011], i.e., Complementary Linear Combination (CLC) and Masters Correspondence with Environment Transfer (MCET), and our ESC framework. The principal reason explaining that we chose them and not some other architectures such as the ones introduced in [Ghorbanian et al, 2013, Li et al, 2014, Razi and Hashtrudi-Zaad, 2014], is that they were the closer ones in terms of behavior and functions compared to ours. For instance, concerning the feedback and feedfoward signals (velocity/force), the desired feedback velocity to the trainer is given as $\dot{\theta}_{h_{1d}} = \alpha\dot{\theta}_s$ in [Razi and Hashtrudi-Zaad, 2014], while $\dot{\theta}_{h_{1d}} = \alpha\dot{\theta}_s + (1-\alpha)\dot{\theta}_{h_2}$ in CLC of [Khademian and Hashtrudi-Zaad, 2011]. It can be easily noticed when $\alpha = 0$, that there will be no velocity feedback to the trainer with Razi's framework, while there will be a full desired feedback from the trainee in Khademian's framework.

In this chapter, we detail a comparative study based on motion tracking criteria proposed in the following section. We focus on the analysis of the structure of these systems in absence of time-delays. Also, in order to compare each system in its best configuration, we provide the tuning guidelines to get optimized behaviors for each of them.

5.2 Position Tracking Performance Criteria

The main purpose of a teleoperation system is to perform a desired task remotely. To evaluate the performance of a robotic system according to a given task, physically accessible quantities have to be used. In the case of a dual-user training system, it

is worth to explore the performance of the human/environment power port variables (position, force/torque), i.e., $(T_{h_1}, \dot{\theta}_{m_1})$, $(T_{h_2}, \dot{\theta}_{m_2}), (-T_e, \dot{\theta}_e)$. The position tracking errors between the users and the slave have been chosen to evaluate the different architectures. As it is a haptic system, force tracking can also be a good metrics but the architectures tested in this study do not share the same policy in terms of force feedback (for instance, for CLC, $T_{h_1} \rightarrow \alpha T_e + (1-\alpha)T_{h_2}$, $T_{h_2} \rightarrow (1-\alpha)T_e + \alpha T_{h_1}$ while in MCET, T_{h_1} and $T_{h_2} \rightarrow T_e/2$ and, in ESC, as indicated by Eq. (4.7) in the above section). An end-user study would be necessary to compare the effectiveness of all these systems in practice. This is why we limited this comparative study to motion tracking.

In free motion, the performance is evaluated through the tracking errors between the actual positions and the referenced ones, given by;

$$\begin{aligned} \Phi_i &= \left(\frac{1}{n} \sum_{k=1}^{n} \|\varepsilon_i(k)\|^2 \right)^{\frac{1}{2}} \\ \Delta_i &= \left(\frac{1}{n} \sum_{k=1}^{n} \|\varepsilon_i(k) - \bar{\varepsilon}_i\|^2 \right)^{\frac{1}{2}} \end{aligned} \tag{5.1}$$

where $\|\cdot\|$ is the Euclidean norm of $\mathbb{R}^2$. $\varepsilon_i(k) = |\theta_i(k) - \theta_{i_r}(k)| \,/\, |\max(\theta_{i_r}) - \min(\theta_{i_r})|$, $i \in \{m_1, m_2, s\}$ represents the relative error of the masters' and the slave's position (θ_i) with the amplitude of the reference trajectory (θ_{i_r}). $\bar{\varepsilon}_i$ indicates the mean value of relative position errors and n is the total number of samples of free motion positions. Φ_i reveals the position tracking preciseness, and Δ_i shows the standard deviation of position tracking errors. In case of perfect transparency, $\Phi_i = 0$ and $\Delta_i = 0$. Hence, a higher value indicates an undesirable performance.

5.3 Simulation Setup

In haptic systems, users plays an important role as their dynamics and capabilities may vary in time. The human can be modeled as a one-port system, which exchanges force and velocity through the power channel. The energy exchanged between the

system and the human is limited. The damper-spring model [Lee and Spong, 2006] provides robust behaviors and the ability to also include nonlinear robot dynamics in the context of teleoperation. We reuse this representation to build the virtual trainer/trainee.

The simulation model, which is employed in this comparative study, is shown in Fig. 5-1. It consists of one d.o.f. joint mass robots as master and slave devices. Both the trainer and the trainee are modeled as damper-spring position-tracker systems. Through this way, a same virtual human perception and reaction mechanism is guaranteed for every tested dual-user architecture. In addition, the stiffness of a virtual wall is represented by using a parallel connection of a spring and a damper . The simulation is conducted with Mathworks® MATLAB/Simulink.

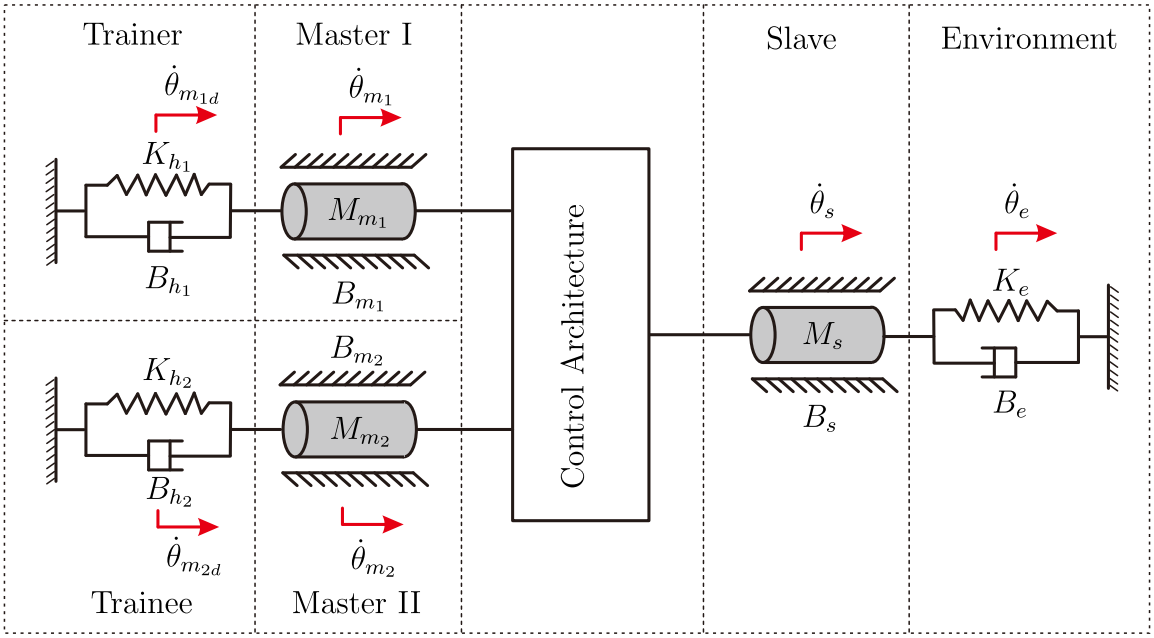

Figure 5-1: Simulation setup of comparative study over different architectures.

5.4 Trajectory Tracking Tasks

To compare the three architectures on the same basis, we set the trajectory tracking task for each one. Since we focus on the study over position tracking, the simulation is only set in free motion (i.e., no contact force from the environment). The virtual

trainer and trainee are simulated to move the master robots by following a desired trajectory.

Regarding different control authority values, the task is defined as follows:

1. when $\alpha = 1$, the trainer is the leader, and the trainee is the follower (i.e. training mode). They are modeled by

$$\begin{aligned} T_{h_1} &= K_{h_1} \cdot (\theta_{m_{1d}} - \theta_{m_1}) - B_{h_1} \cdot \dot{\theta}_{m_1} \\ T_{h_2} &= 0 \end{aligned} \tag{5.2}$$

   where $\theta_{m_{1d}}$ represents the position desired by the trainer[1]. In this case, the reference trajectories (defined in Eq. (5.1)) of both masters and the slave are given by:

$$\theta_{m_{1r}} = \theta_{m_{1d}}, \quad \theta_{m_{2r}} = \theta_{m_1}, \quad \theta_{m_{sr}} = \theta_{m_1} \tag{5.3}$$

   which means that the trainer tries to move the master 1 according to his desired trajectory while master 2 and the slave try to track the real motion of the trainer.

2. When $\alpha = 0$, the trainee is the leader, while the trainer is the follower (i.e. evaluation mode). Their models become

$$\begin{aligned} T_{h_1} &= 0 \\ T_{h_2} &= K_{h_2} \cdot (\theta_{m_{2d}} - \theta_{m_2}) - B_{h_2} \cdot \dot{\theta}_{m_2} \end{aligned} \tag{5.4}$$

   In this case, the reference trajectories of both masters and the slave are given by:

$$\theta_{m_{1r}} = \theta_{m_2}, \quad \theta_{m_{2r}} = \theta_{m_{2d}}, \quad \theta_{m_{sr}} = \theta_{m_2} \tag{5.5}$$

3. When $0 < \alpha < 1$, the trainer and the trainee are in shared control (i.e. guidance

[1]The next two cases follow the same sign convention.

mode). Their models become then

$$\begin{aligned} T_{h_1} &= K_{h_1} \cdot (\theta_{m_{1d}} - \theta_{m_1}) - B_{h_1} \cdot \dot{\theta}_{m_1} \\ T_{h_2} &= K_{h_2} \cdot (\theta_{m_{2d}} - \theta_{m_2}) - B_{h_2} \cdot \dot{\theta}_{m_2} \end{aligned} \tag{5.6}$$

In this case, the reference trajectories of both masters and the slave are given by:

$$\theta_{m_{1r}} = \theta_{m_{1d}}, \quad \theta_{m_{2r}} = \theta_{m_{2d}}, \quad \theta_{m_{sr}} = \alpha\theta_{m_1} + (1-\alpha)\theta_{m_2} \tag{5.7}$$

which shows that the slave tries to track the resulting shared motion of the two users, while the master 1 and master 2 try to track their respective desired trajectories.

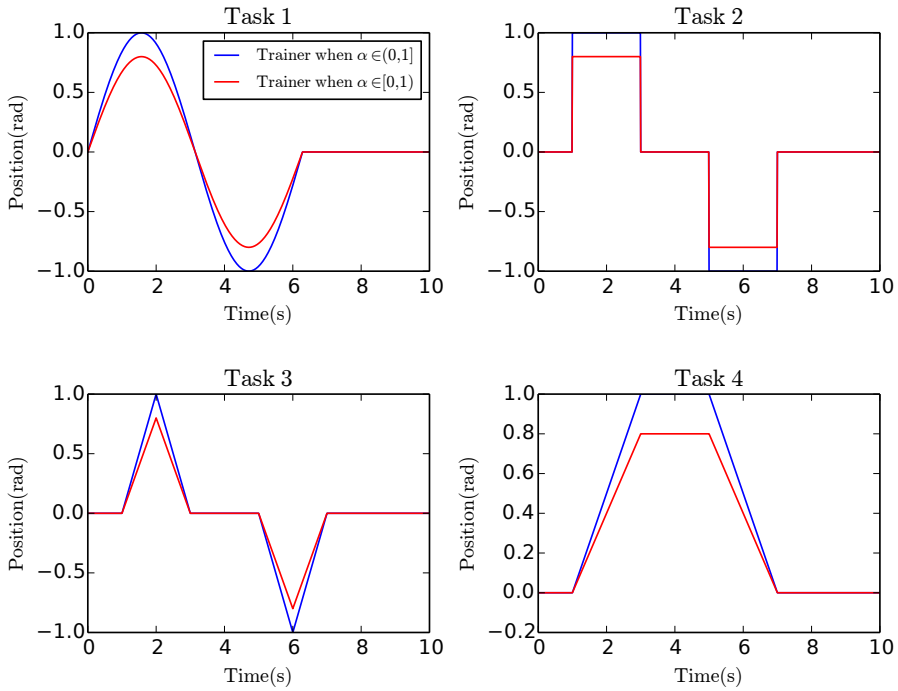

Figure 5-2: Desired trajectories of tracking tasks.

We set four different trajectories for tracking tasks as shown in Fig. 5-2. The plotted curves are in different control authority cases, i.e. trainer when $\alpha \in (0, 1]$, trainee when $\alpha \in [0, 1)$.

Notice that the differences between them are their amplitude and the situations when they are applied (α values). For example, there is no need to define the desired trajectory for master 1 when $\alpha = 0$ when the trainer is the follower.

5.5 Tuning the Controller

In the traditional bilateral teleoperation, stability and transparency are two conflicting control objectives. For example, higher gains of the controller may achieve faster convergence and smaller tracking errors, so a better transparency, but it may also decrease the stability of the system, or increase the stiffness perceived by the operator [Hirche and Buss, 2007]. In order to compare the CLC, MCET and ESC architectures in the best situation, we have set their own parameters to guarantee their stability at first. Then, under the same excitation and parameters (same human force input signal, same control authority, etc.), we tuned the parameters of each controller to get their best position tracking performances. These parameters were then used in Matlab/Simulink®, in order to reproduce exactly the same stimuli for each scheme.

In Section 3.7, we've already introduced the method for tuning of IPC controller in ESC architecture. Concerning the CLC and MCET architectures, the four-channel controller of bilateral teleoperation is employed. Adopting the notation for ESC scheme in Fig. 3-3, the four-channel controller (see [Lawrence, 1993]) is given as:

$$\begin{aligned} F_i &= -C_i\dot{\theta}_i - C_{4_j}\dot{\theta}_i^d + C_{6_j}T_{h_j} - C_{2_j}T_{h_j}^d \\ F_s &= -C_s\dot{\theta}_s + C_{1_s}\dot{\theta}_s^d - C_{5_s}T_e + C_{3_s}T_e^d \end{aligned} \tag{5.8}$$

where $i = m_1, m_2$ and $j = 1, 2$ denote for master 1 and master 2 respectively. The desired position and force commands (indicated by superscript d, see [Khademian

and Hashtrudi-Zaad, 2011]) for each robot is given as:

$$
\begin{aligned}
\text{CLC}: &\begin{cases}
\dot{\theta}_{m_1}^d = \alpha\dot{\theta}_s + (1-\alpha)\,\dot{\theta}_{m_2} \\
\dot{\theta}_{m_2}^d = (1-\alpha)\,\dot{\theta}_s + \alpha\dot{\theta}_{m_1} \\
\dot{\theta}_s^d = \alpha\dot{\theta}_{m_1} + (1-\alpha)\,\dot{\theta}_{m_2} \\
T_{h_1}^d = \alpha T_e + (1-\alpha)\,T_{h_1} \\
T_{h_2}^d = (1-\alpha)\,T_e + \alpha T_{h_1} \\
T_e^d = \alpha T_{h_1} + (1-\alpha)\,T_{h_2}
\end{cases} \\
\text{MCET}: &\begin{cases}
\dot{\theta}_{m_1}^d = \dot{\theta}_{m_2} \\
\dot{\theta}_{m_2}^d = \dot{\theta}_{m_1} \\
\dot{\theta}_s^d = \alpha\dot{\theta}_{m_1} + (1-\alpha)\,\dot{\theta}_{m_2} \\
T_{h_1}^d = \dfrac{T_e}{2} \\
T_{h_2}^d = \dfrac{T_e}{2} \\
T_e^d = \alpha T_{h_1} + (1-\alpha)\,T_{h_2}
\end{cases}
\end{aligned}
\tag{5.9}
$$

The following relationship of parameters are given as (see Tavakoli [2008]):

$$
\begin{aligned}
C_{1_s} &= Z_s + C_s & C_{2_j} &= 1 + C_{6_i} \\
C_{3_s} &= 1 + C_{5_s} & C_{4_j} &= -\left(Z_i + C_i\right) \\
Z_i &= M_i s + B_i & Z_s &= M_s s + B_s \\
C_i &= D_i + \frac{K_i}{2} & C_s &= D_s + \frac{K_s}{2}
\end{aligned}
\tag{5.10}
$$

Therefore, we could tune the parameters for each controller to achieve similar responses. The tuning procedure is:

- **Step 1**: Define a step response shape trajectory for tracking, and set the $\alpha = 1$ (leave the trainee in free motion, treat the dual-user system as bilateral teleoperation).

- **Step 2**: Assign an initial set of parameters to the controllers, which guarantee

stable behaviors.

- **Step 3**: Tune the parameters based on the performance of each controller, i.e., overshoot, rise time and settling time, in order to produce similar motions.

- **Step 4**: Determine the control parameters and reuse them for the tasks.

This tuning procedure provides similar initial conditions for the tracking errors for each architecture. Controller parameters are provided in Table 5.1.

Table 5.1: Parameters for each control architecture

Scheme	**Parameters**	**Unit**	**Value**
Human Dynamics ($i = h_1, h_2$)	B_i	$\mathrm{N \cdot m \cdot s/rad}$	10
	K_i	$\mathrm{N \cdot m/rad}$	500
Robot Dynamics ($i = m_1, m_2, s$)	B_i	$\mathrm{N \cdot m \cdot s/rad}$	10
	M_i	$\mathrm{kg \cdot m^2}$	0.1
CLC[a] ($i = m_1, m_2, s; j = 1, 2$)	D_i	$\mathrm{N \cdot m \cdot s/rad}$	1
	K_i	$\mathrm{N \cdot m/rad}$	50
	C_{5_s}	-	0.2
	C_{6_j}	-	0.2
MCET[b] ($i = m_1, m_2, s; j = 1, 2$)	D_i	$\mathrm{N \cdot m \cdot s/rad}$	1
	K_i	$\mathrm{N \cdot m/rad}$	50
	C_{5_s}	-	0.2
	C_{6_j}	-	0.2
ESC[c] ($i = m_1, m_2$)	$K_{c,i}$	$\mathrm{N \cdot m/rad}$	200
	$K_{r,i}$	$\mathrm{N \cdot m/rad}$	200
	$K_{c,s}$	$\mathrm{N \cdot m/rad}$	100
	$M_{c,i}$	$\mathrm{kg \cdot m^2}$	0.0001
	$M_{c,s}$	$\mathrm{kg \cdot m^2}$	0.01
	$B_{c,i}$	$\mathrm{N \cdot m \cdot s/rad}$	0.8
	$B_{c,s}$	$\mathrm{N \cdot m \cdot s/rad}$	0.2

[a,b]Notation as in Eq. 5.8. [c]Notation as in Section 3.7.

5.6 Comparison Over Different Control Authority Values

We conducted a comparative study with different values of α over Task 1. The position tracking errors (Φ_i, Δ_i) of each control framework are illustrated in Figure 5-3.

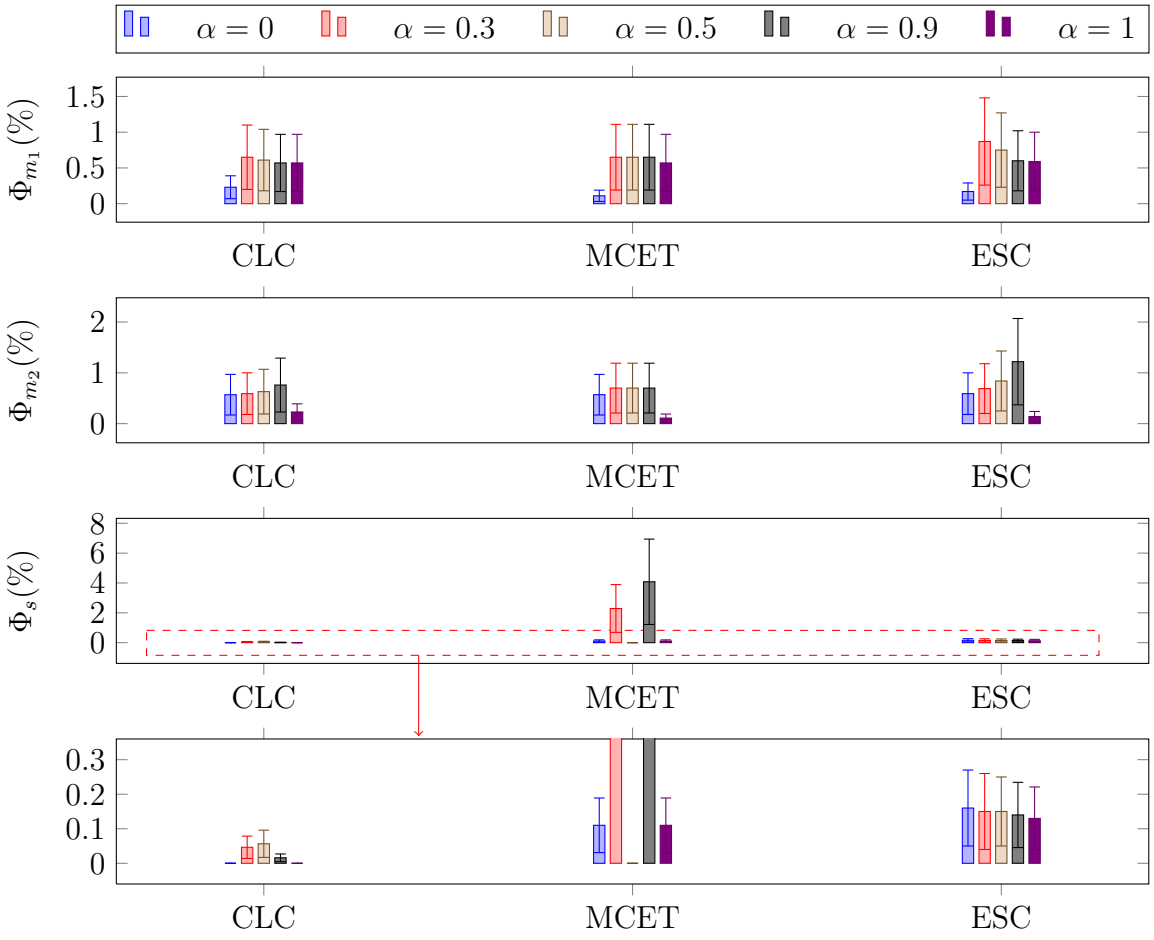

Figure 5-3: Position tracking errors for different values of α.

For master 1 (trainer), we could conclude that the position tracking error is roughly the same with CLC, MCET and ESC for the same values of α. More precisely, ESC presents a little higher error than the other two frameworks when $\alpha \in \{0.3; 0.5; 0.9\}$, but when $\alpha \in \{0; 1\}$, ESC gives slightly better results (for example, $\Phi_{m_1} = 0.17\%$ for ESC and 0.23% for CLC when $\alpha = 0$).

Notice that all the three architectures lead to better behaviors in the evaluation/training modes ($\alpha \in \{0; 1\}$) than in the guidance mode ($0 < \alpha < 1$). For instance, the average error is 3 times bigger when $\alpha = 0.3$ (i.e. $\Phi_{m_1} = 0.65\%$) than when $\alpha = 0$ (i.e. $\Phi_{m_1} = 0.23\%$) of CLC scheme. This is mainly because during the guidance mode, both users control the system in a shared way, which introduced more undesired errors than the full control modes (with only one user controlling the system). Furthermore, it shows that the tracking performance for master 1 is better acting as follower than acting as leader. The reason is that the trainer does not provide any control forces to the system except following motion for evaluation. It is worth to mention that the tracking error is globally inversely proportional to α when $0 < \alpha < 1$ in CLC and our schemes. It reveals that best performance is obtained by the user possessing most of the control authority, which is coherent with the general rule of this system. Similar results could be obtained for master 2 (trainee) due to the symmetry property of the system.

Considering the slave, good tracking performances are attained under CLC and our ESC framework despite the variations of control authority. This can be observed in Fig. 5-3 where the error bars indicate standard deviation errors ($\Delta_i, i = m_1, m_2, s$). Notice that subfigure 4 is the enlarged version of subfigure 3. It is worth to mention that the tracking error is significantly smaller when $\alpha \in \{0, 1\}$ than when $0 < \alpha < 1$ for CLC framework (e.g., $\Phi_{m_1} \approx 0$ when $\alpha = 0, 1$). This reveals that the leader-follower mode (training/evaluation) outcomes better performance. The errors are almost the same within different authorities in our ESC architecture, yet good enough for tracking purpose with the error less than 0.2%. Concerning the MCET framework, the best tracking performance is achieved when $\alpha = 0.5$. It discloses that the MCET scheme is competitive only when $\alpha \in \{0; 0.5; 1\}$.

5.7 Comparison Over Different Desired Trajectories

The performance of the frameworks under different desired trajectories is another subject for comparison. At this point, we set $\alpha = 0.5$ for study, in which case the

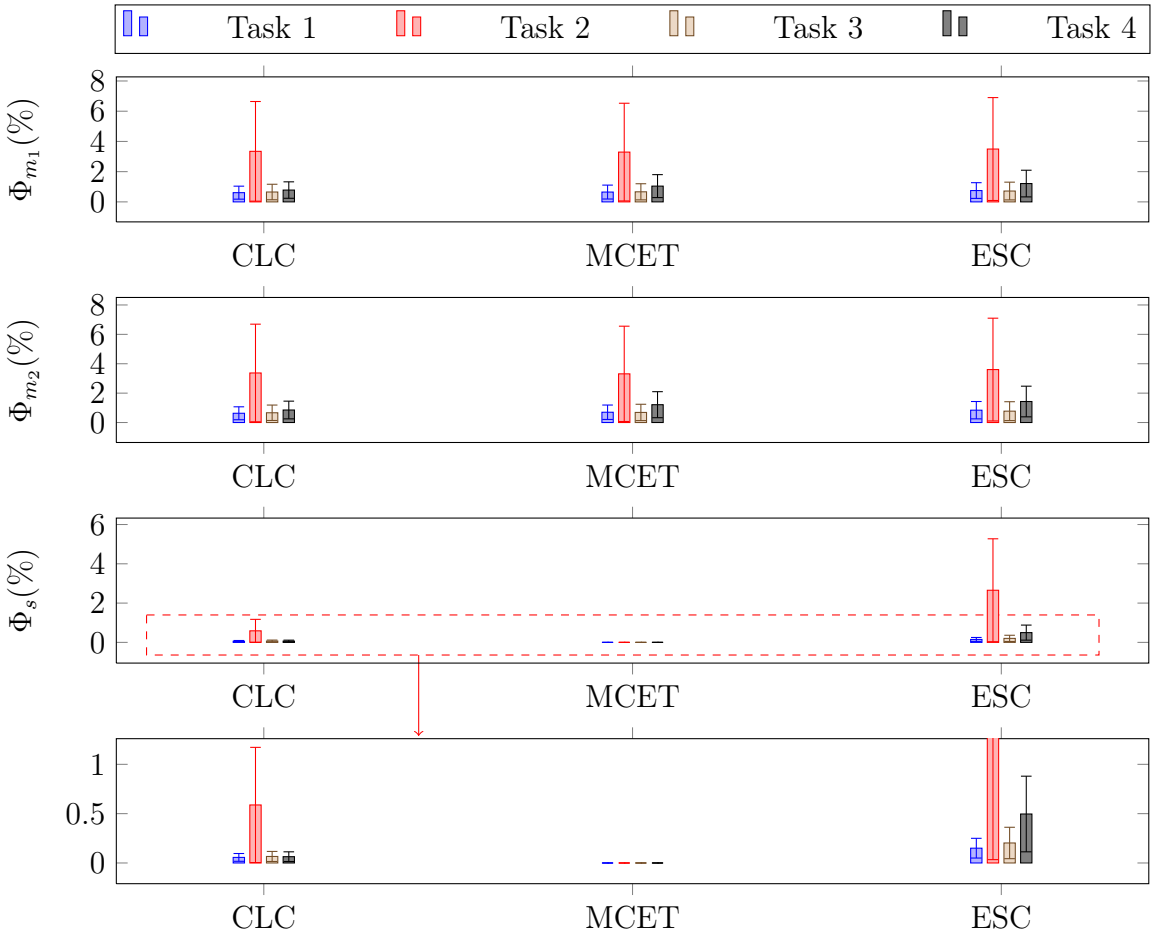

Figure 5-4: Position tracking errors under different desired trajectories.

average errors are similar between different schemes. Figure 5-4 depicts the position errors (Φ_i) under different desired trajectories (i.e., different tasks). Notice that subfigure 4 is the enlarged version of subfigure 3.

Concerning master 1 (trainer), generally Task 2 introduces bigger position errors than other tasks. For instance, Task 2 generates an error of $\Phi_{m_1} = 3.34\%$, while $\Phi_{m_1} = 0.61\%$ for Task 1, $\Phi_{m_1} = 0.65\%$ for Task 3, and $\Phi_{m_1} = 0.78\%$ for Task 4 of CLC framework. There is no significant difference in tracking errors among Task 1, 3 and 4 over CLC, MCET, and ESC. Task 1 outputs the smallest error among four tasks, and Task 2 introduces biggest error. It is worth mentioning that Task 2 yields bad tracking performance, basically due to the shape of the desired trajectory. Since Task 2 requires a rectangular pulse signal, the response time and overshoot are longer and larger than the other tasks. Moreover, task 2 also generates larger variations in position errors as indicated by the vertical lines on the figures, which represent standard deviations (Δ_i) from the mean values.

Likewise, it can be found similar results (almost the same) for master 2, with same control authority ($\alpha = 0.5$) and same shapes of desired trajectories except their amplitude.

With respect to the slave, it can be concluded from these results that the MCET generates negligible small errors (almost 0) for all tasks, while Tasks 2 produces bigger errors over the other two frameworks (i.e., CLC, ESC). It shows MCET scheme is a good choice regarding slave tracking performance when both the trainer and the trainee hold equivalent shared authority, i.e. $\alpha = 0.5$. Overall, the slave tracking error is smaller than master 1 and master 2. For example, averagely, the position error of master 1/master 2 is $5 \sim 10$ times bigger compared with the slave.

5.8 Conclusions

In this comparative study, three different dual-user architectures were compared. Overall, it is difficult to determine which framework provides the best tracking performance, since the results greatly varied according to the control authority and the

desired trajectories (tasks). Nevertheless, here is what we can conclude from these results:

- **Stability**: All the architectures are considered in no-delay cases. They are experimentally stable by choosing proper parameters. A controller tuning procedure is given for consistency of initial conditions over different frameworks. However, there is no need for stability analysis of ESC framework since it is passively controlled, even under unknown robot dynamics and models cases. While for the other two schemes, the asymptotic stability condition has to be satisfied. Moreover, ESC scheme enables stable behaviors with mode switching mechanism.

- **Control Authority**: The control authority has an effect on the system performance, especially for the slave tracking in the MCET scheme, where a perfect result is obtained for $\alpha = 0.5$. This can be explained through Eq. 5.9, where only a half of the environment force is directly fedback to each master, which is also the case for CLC when $\alpha = 0.5$.

- **Desired Trajectories**: The desired tracking trajectories also introduce uncertainties into the system. It is highly dependant on the shape of the trajectories, which will directly effect the performance, i.e., response time and overshoot error. An interesting result showed that MCET architecture performs good slave tracking even in presence of sharp trajectories when $\alpha = 0.5$. This gives an alternative option when the other frameworks are not fit with the requirements, for instance, high precision operation during medical training or surgery when the two users are working simultaneously.

As a conclusion, this comparative study demonstrated that our ESC architecture displays almost equal performances compared with CLC and MCET schemes, in common use cases (training/guidance/evaluation modes). The essential differences between these architectures are the shared control structures. These results are explained by the fact that only a portion of slave position signal is fed back to the

users in CLC scheme enriched by a part formed from the other user, while in MCET scheme, there is no direct slave position signal feedback to either of the users (see Khademian and Hashtrudi-Zaad [2011]). This means that this study situates globally the ESC framework at the same level as CLC and MCET schemes in terms of position tracking. What positively differentiates ESC from these two architectures is the possibility to get more transparence (full slave velocity and force feedback to both users) in training and evaluation modes. It also doesn't require stability analysis, even in presence of non-linear system models and unknown robot dynamics.

Chapter 6

A Preliminary Study of ESC Architecture with Constant Time Delays

6.1 Introduction

In bilateral teleoperation system, the human and the environment are connected by a communication channel, which plays an important role as exchanging power signals (force/velocity) between master and slave. Time delays, inherent to them, affect both the stability and transparency. Even a small delay may destabilize the system. In order to provide better performance, many research efforts have been provided.

The first work concerning time delays in bilateral teleoperation is found in [Sheridan and Ferrell, 1963], with an open-loop control. Some other strategies have been proposed after then, such as *move and wait* [Ferrell, 1965] or supervisory and shared control [Ferrell and Sheridan, 1967]. Until 1989, the first work using passivity theorem was developed in [Anderson and Spong, 1989b]. It revealed the characteristics of the time delays from an energy based point of view, which make a communication channel non-passive. The method proposed to solve this problem was based on the scattering theory, which was later reformulated into *Wave Variable Transformation*

(WVT) approach [Niemeyer and Slotine, 1991]. This WVT contains some drawbacks:

- the passivity cannot be guaranteed with time-varying delays,
- position drift may occur without direct position tracking, and
- wave reflections can cause larger signal variations.

Based on this conventional WVT approach, many works have been carried out to overcome the aforementioned drawbacks. For instance, wave prediction derived from a modified Smith predictor along with a Kalman estimator and an energy regulator is used to enhance the teleoperation performance in the presence of a constant delay in [Munir and Book, 2001, 2002]. Other methods with extra biased compensation terms to reduce tracking errors are introduced in [Li and Kawashima, 2014, Ye and Liu, 2009]. A new method has been presented in [Bate et al, 2011] to reduce the wave reflections when operating in unknown environments. The WVT (initially designed in two-channel cases) has been incorporated into a four-channel architecture in [Aziminejad et al, 2008a]; it is capable of achieving ideal transparency in presence of time delays. A review of various wave variable methods has been conducted in [Sun et al, 2014].

More generally, the time-domain passivity approach (TDPA) has been proposed to fight time delays effects in [Ryu et al, 2004], and then extended by [Artigas et al, 2010b] to deal with time-varying delays. Although stability can be guaranteed, the transparency can be easily disturbed even under small delays. Other techniques combined with TDPA to solve the position drift problems are achieved in [Artigas et al, 2010a, Chawda et al, 2014].

In this Chapter, we introduce a preliminary study over constant time delays, by applying the Augmented WVT (AWVT) to our ESC shared control communication channel. The AWVT method is retrieved from [Li and Kawashima, 2014]. Both the position drift and wave reflection problems are eliminated though compensation signals. The tracking performance is improved with guaranteed stable position and force tracking.

6.2 Wave Variable Transformation

Since in a teleoperation system, the slave has to track the motion of the master and the master gets feedback from the slave in interaction with the environment, a first approach concerning the communication strategy consists in transferring the velocity and force information directly through the communication channel. For example, the master transfers a velocity to the slave while the slave transmits back to the master an effort. However, this simple strategy has been proved (amongst others, see [Secchi et al, 2007]) to lead to a non passive communication channel. Indeed, it has been proved that the communication delays inject some artificial energy into the transmission block. One out of the different strategies available in the scientific literature is the use of the Wave Variable Transformation (WVT) which we detail further on.

6.2.1 Conventional WVT (CWVT)

Using an energetic modeling of the transmission block, each (terminal) power port plays a role of exchange of the energy between the system connected to the transmission block (the master on one side and the slave on the other side) which can be divided into two parts:

- an incoming power flow representing the energy supplied to the transmission block,
- an outgoing power flow representing the power extracted from the transmission block.

The conventional wave variable Transformation (CWVT) framework shown in Figure 6-1 has been introduced by Spong et al in [Anderson and Spong, 1989a]. The aforementioned power variables can be transformed into two wave variables ((u_i, v_i) and (u_j, v_j)) which represent two different power waves circulating in opposite directions. This way, the transmission line transfers power directly and not power

variables, which preserves passivity independently of transmission delays, as shown further on.

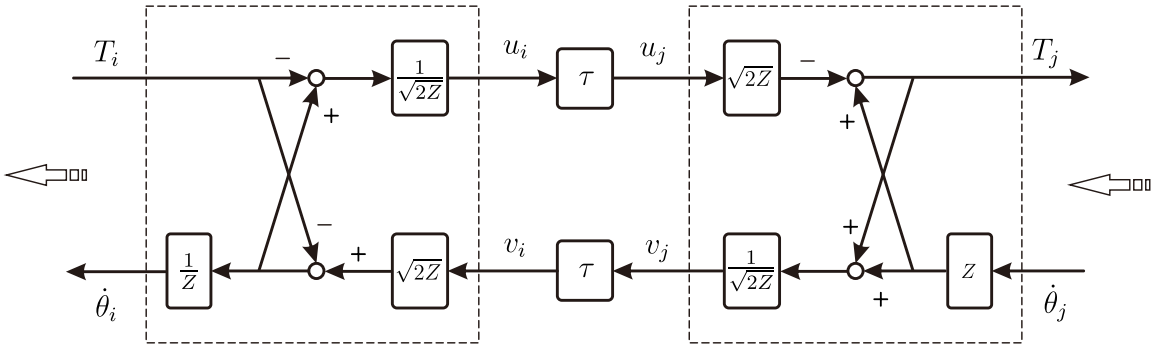

Figure 6-1: Conventional WVT (CWVT) framework

The wave variables are expressed as:

$$\begin{aligned} u_i(t) &= \frac{-T_i(t) + Z\dot{\theta}_i(t)}{\sqrt{2Z}} \\ v_j(t) &= \frac{T_j(t) + Z\dot{\theta}_j(t)}{\sqrt{2Z}} \end{aligned} \tag{6.1}$$

where Z is the is a positive semi-definite matrix defining the characteristic impedance of the wave transformation. It represents the stiffness sense of propagation of the power. The transmitted wave variables in the communication channel are given as:

$$u_j(t) = u_i(t-\tau) \qquad\qquad v_i(t) = v_j(t-\tau) \tag{6.2}$$

The following relations can be derived from the above equations:

$$\begin{cases} T_i(t) = \sqrt{\dfrac{Z}{2}}(v_i(t) - u_i(t)) \\ \dot{\theta}_i(t) = \dfrac{v_i(t) + u_i(t)}{\sqrt{2Z}} \end{cases} \qquad \begin{cases} T_j(t) = \sqrt{\dfrac{Z}{2}}(v_j(t) - u_j(t)) \\ \dot{\theta}_j(t) = \dfrac{v_j(t) + u_j(t)}{\sqrt{2Z}} \end{cases} \tag{6.3}$$

The position and force tracking at master and slave side can be written as

$$\begin{aligned} \dot{\theta}_i(t) &= \dot{\theta}_j(t-\tau) + \frac{1}{Z}\left(T_j(t-\tau) - T_i(t)\right) \\ T_j(t) &= T_i(t-\tau) + Z(\dot{\theta}_j(t) - \dot{\theta}_i(t-\tau)) \end{aligned} \tag{6.4}$$

It can be noticed that both tracking equations introduce the biased terms (besides the identical one with time delay, i.e., $\frac{1}{Z}(T_j(t-\tau) - T_i(t))$ and $Z(\dot{\theta}_j(t) - \dot{\theta}_i(t-\tau))$), which can greatly influence the tracking performance. For instance, a position drift may occur during contact phases because of the difference of the values of $T_j(t-\tau)$ and $T_i(t)$.

Define $E_{cwvt}(t)$ as the energy flowing into the communication channel (regrading the positive direction of power flows indicated by white arrows), with a zero initial condition. The passivity of CWVT can be verified:

$$\begin{aligned} E_{cwvt}(t) &= \int_0^t \left[T_j^T(s)\dot{\theta}_j(s) - T_i^T(s)\dot{\theta}_i(s)\right] \mathrm{ds} \\ &= \frac{1}{2}\int_0^t \left[v_j^T(s)v_j(s) - u_j^T(s)u_j(s) - v_i^T(s)v_i(s) + u_i^T(s)u_i(s)\right] \mathrm{ds} \\ &= \frac{1}{2}\int_{t-\tau}^t v_j^T(s)v_j(s)\mathrm{ds} + \frac{1}{2}\int_{t-\tau}^t u_i^T(s)u_i(s)\mathrm{ds} \geq 0 \end{aligned} \tag{6.5}$$

Therefore, the communication system is passive independently of time delay τ. Yet, it presents the counterpart of a *wave refection* phenomenon: the power waves get reflected at terminal points, where the impedance of the wave carrier changes [Niemeyer and Slotine, 1991]. To avoid this reflection, an enhancement to the previous WVT transformation has been proposed by Niemeyer et al, by introducing impedance matching terms, as in Fig. 6-2 in following section.

6.2.2 Augmented WVT (AWVT)

Aiming at improving the performance of conventional WVT, the augmented WVT (AWVT) framework with 2-channel power port, shown in Fig. 6-2, has been introduced in [Li and Kawashima, 2014].

The new outgoing and incoming wave compensation terms are used to eliminate the velocity and force offset visible in Eq. 6.4, which improves the tracking performance. In this scheme, the impedance matching parts as in [Niemeyer and Slotine, 1991] are located inside the gray-filled blocks.

The compensation terms are inserted into both the forward and backward wave

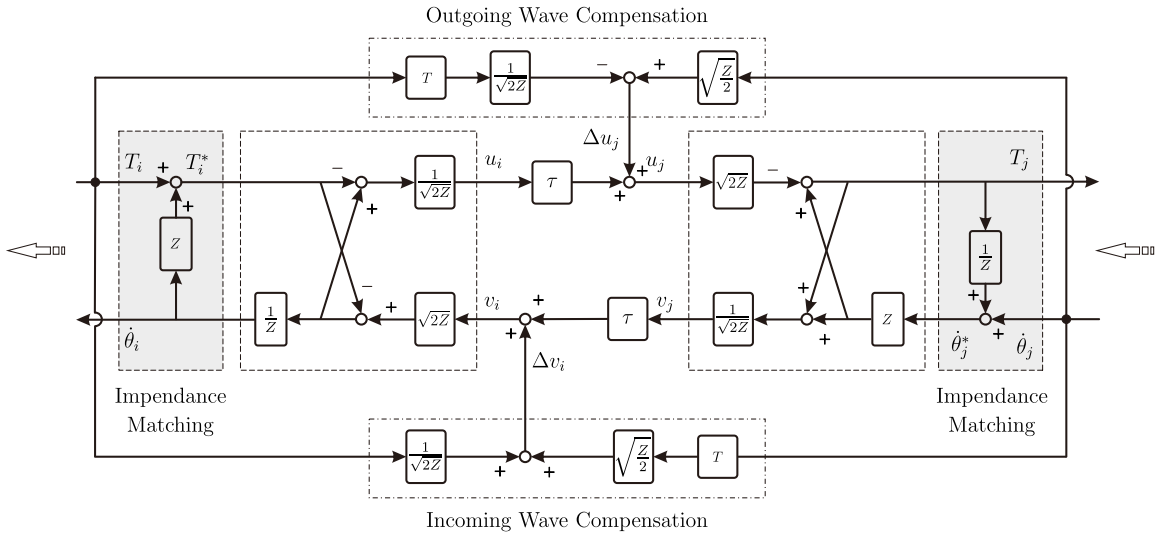

Figure 6-2: Augmented WVT (AWVT)

path at slave and master sides, named by $\Delta u_j, \Delta v_i$. They are expressed as:

$$\begin{aligned} \Delta u_j(t) &= \sqrt{\frac{Z}{2}}\dot{\theta}_j(t) - \frac{1}{\sqrt{2Z}}T_i(t-\tau) \\ \Delta v_i(t) &= \frac{T_i(t)}{\sqrt{2Z}} + \sqrt{\frac{Z}{2}}\dot{\theta}_j(t-\tau) \end{aligned} \tag{6.6}$$

The wave variables are expressed as:

$$\begin{aligned} u_i(t) &= \frac{-T_i(t)}{\sqrt{2Z}} \\ v_j(t) &= \sqrt{\frac{Z}{2}}\dot{\theta}_j(t) \end{aligned} \tag{6.7}$$

Thus, the following relations can be derived from the AWVT:

$$\begin{cases} T_i(t) = -\sqrt{2Z}u_i(t) \\ \dot{\theta}_i(t) = \dfrac{u_i(t) + v_i(t)}{\sqrt{2Z}} \end{cases} \qquad \begin{cases} T_j(t) = \sqrt{\dfrac{Z}{2}}(v_j(t) - u_j(t)) \\ \dot{\theta}_j(t) = \sqrt{\dfrac{2}{Z}}v_j(t) \end{cases} \tag{6.8}$$

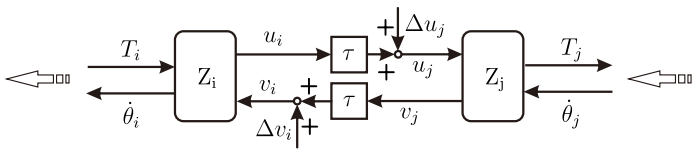

Figure 6-3: Integrated graphical representation of AWVT

where

$$\begin{aligned} u_j(t) &= u_i(t-\tau) + \Delta u_j(t) \\ v_i(t) &= v_j(t-\tau) + \Delta v_i(t) \end{aligned} \tag{6.9}$$

As a result, combining this with Eq. 6.6 and 6.7, the position and force trackings become:

$$\begin{aligned} T_j(t) &= T_i(t-\tau) \\ \dot{\theta}_i(t) &= \dot{\theta}_i(t-\tau) \end{aligned} \tag{6.10}$$

Transparency is improved since the force and position at both sides are identical (without position drift anymore). There remains only a natural time shift between the signals.

For an integrated graphical representation which will be used in the following sections, the AWVT is provided in Fig. 6-3. Note that compensation terms keep the same definitions as in Eq. 6.6, and the impedance matching parts are included in the blocks Z_i, Z_j.

In terms of the AWVT in Eq. 6.8, the energy flowing into the communication channel $E_{awvt}(t)$ with zero initial condition is:

$$\begin{aligned} E_{awvt}(t) &= E_{left}(t) + E_{right}(t) \\ &= \int_0^t -T_i^T(s)\dot{\theta}_i(s)\mathrm{dt} + \int_0^t T_j^T(s)\dot{\theta}_j(s)\mathrm{dt} \\ &= \int_0^t \left[-T_i^T(s)\dot{\theta}_i(s) + T_j^T(s)\dot{\theta}_j(s)\right]\mathrm{dt} \\ &= \frac{1}{2}\int_0^t \left[u_i^T(s)u_i(s) + u_i^T(s)v_i(s) + v_j^T(s)v_j(s) - u_j^T(s)v_j(s)\right]\mathrm{dt} \end{aligned} \tag{6.11}$$

It can be seen $E_{awvt}(t)$ cannot be guaranteed to be non-negative for all t. Therefore, it indicates that the AWVT may violate the passivity condition due to both impedance matching and compensation terms. For this reason, we propose to ensure the passivity in the following sections.

6.3 ESC Dual-user System with Constant Delays

In order to deal with time delays, we adopt the AWVT (see Sect. 6.2.2) to build a stable communication channel within the framework of ESC dual-user system.

Fig. 6-4 shows our designed ESC dual-user system under constant time delays. Four AWVTs are inserted inside the shared-control structure encapsulating the four communication paths. Then, based on position and force tracking defined in Eq. (6.10), we obtain:

$$\begin{aligned} T_i^*(t) &= T_i(t-\tau) \\ \dot{\theta}_i(t) &= \dot{\theta}_i^*(t-\tau) \end{aligned} \tag{6.12}$$

where $i = s_1, s_2, sf_1, sf_2$. As a result, the position and force signals exchanged will not introduce any perturbation or distortion besides the unavoidable time shift due to the data transportation delay. Accordingly, the ESC structure is shaped with delays,

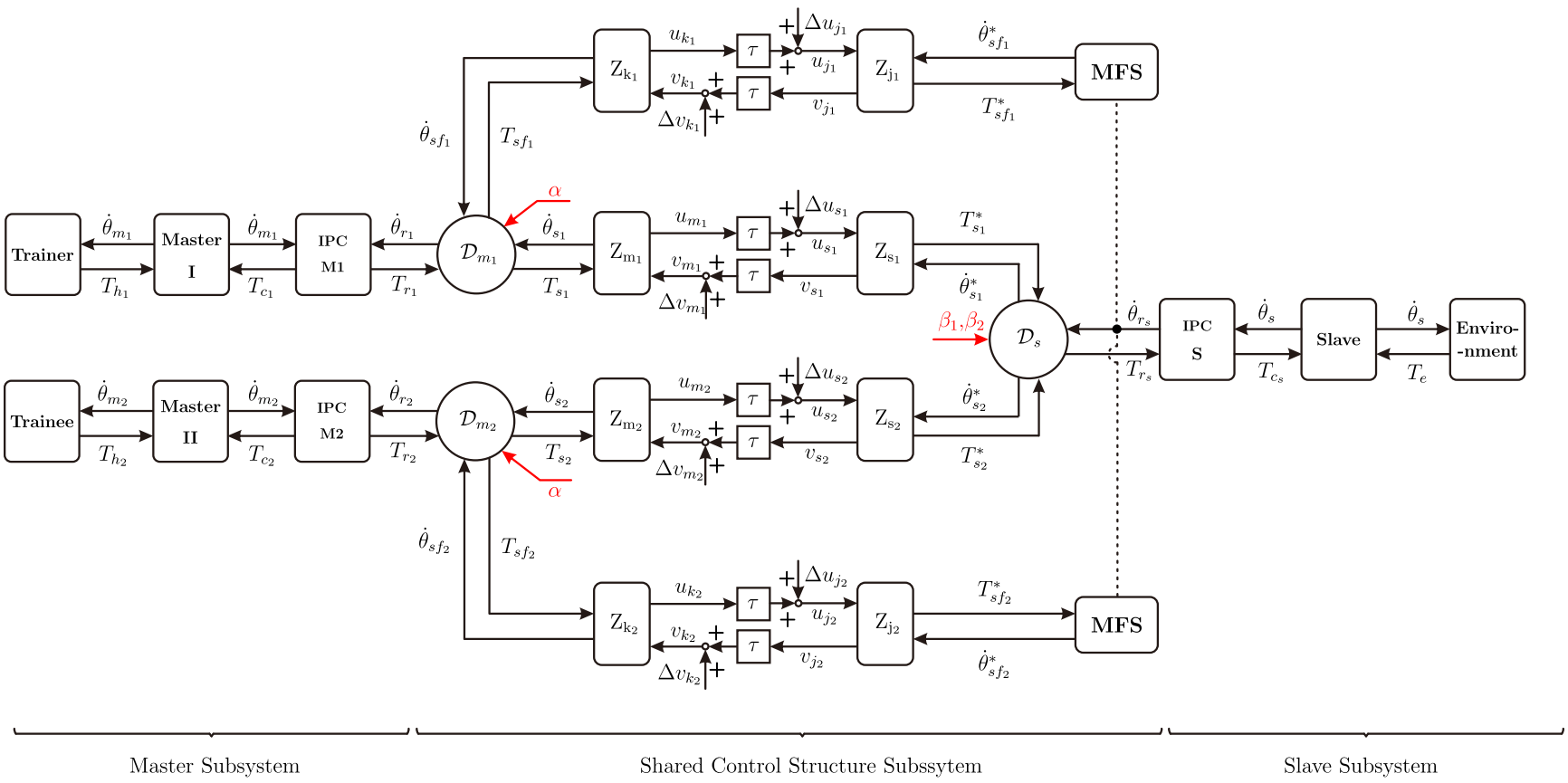

Figure 6-4: ESC dual-user system incorporating AWVT under constant time delays.

represented by input-output matrices as follows:

$$
\begin{aligned}
\mathcal{D}_{m_1}: \begin{pmatrix} \dot{\theta}_{r_1}(t) \\ T_{s_1}(t) \\ T_{sf_1}(t) \end{pmatrix} &= \begin{pmatrix} 0 & \alpha & 1-\alpha \\ -\alpha & 0 & 0 \\ \alpha-1 & 0 & 0 \end{pmatrix} \begin{pmatrix} T_{r_1}(t) \\ \dot{\theta}^*_{s_1}(t-\tau) \\ \dot{\theta}^*_{sf_1}(t-\tau) \end{pmatrix} + \begin{pmatrix} \gamma_{m_1} & \gamma_{k_1} \\ 0 & 0 \\ 0 & 0 \end{pmatrix} \begin{pmatrix} T_{s_1}(t) \\ T_{sf_1}(t) \end{pmatrix} \\
\mathcal{D}_{m_2}: \begin{pmatrix} \dot{\theta}_{r_2}(t) \\ T_{s_2}(t) \\ T_{sf_2}(t) \end{pmatrix} &= \begin{pmatrix} 0 & 1-\alpha & \alpha \\ \alpha-1 & 0 & 0 \\ -\alpha & 0 & 0 \end{pmatrix} \begin{pmatrix} T_{r_2}(t) \\ \dot{\theta}^*_{s_2}(t-\tau) \\ \dot{\theta}^*_{sf_2}(t-\tau) \end{pmatrix} + \begin{pmatrix} \gamma_{m_2} & \gamma_{k_2} \\ 0 & 0 \\ 0 & 0 \end{pmatrix} \begin{pmatrix} T_{s_2}(t) \\ T_{sf_2}(t) \end{pmatrix} \\
\mathcal{D}_{s}: \begin{pmatrix} \dot{\theta}^*_{s_1}(t) \\ \dot{\theta}^*_{s_2}(t) \\ T_{r_s}(t) \end{pmatrix} &= \begin{pmatrix} 0 & 0 & \beta_1 \\ 0 & 0 & 1-\beta_2 \\ \beta_1 & 1-\beta_2 & 0 \end{pmatrix} \begin{pmatrix} T_{s_1}(t-\tau) \\ T_{s_2}(t-\tau) \\ \dot{\theta}_{r_s}(t) \end{pmatrix} + \begin{pmatrix} 0 & 0 \\ 0 & 0 \\ \gamma_{s_1} & \gamma_{s_2} \end{pmatrix} \begin{pmatrix} \dot{\theta}^*_{s_1}(t) \\ \dot{\theta}^*_{s_2}(t) \end{pmatrix}
\end{aligned}
\tag{6.13}
$$

The dominance factors α and β_1, β_2 represent the ESC strategy, same as specified in Eq. 3.3, and $\gamma_i, i \in \{m_1, k_1, m_2, k_2, s_1, s_2\}$ [1] are diagonal matrices in multiple degree of freedom cases (with no coupling between each degree), while α and β_1, β_2 are one dimensional number values. Actually α, β_1, β_2 could be adjusted using AAA method or pre-configured, and γ_i are parameters going to be tuned according to passivity. Note that the modulated flow sources (MFS) provide signals such as:

$$
\dot{\theta}^*_{sf_1}(t) = \dot{\theta}^*_{sf_2}(t) = \dot{\theta}_{r_s}(t) \tag{6.14}
$$

[1] The notations for α, β_1, β_2, and γ_i with time-varying $*(t)$ are abridged for simplification.

Hence, the position feedbacks to the masters become:

$$\begin{aligned}
\dot{\theta}_{r_1}(t) &= \alpha\dot{\theta}^*_{s_1}(t-\tau) + (1-\alpha)\dot{\theta}^*_{sf_1}(t-\tau) + \gamma_{m_1}T_{s_1}(t) + \gamma_{k_1}T_{sf_1}(t) \\
&= \alpha\dot{\theta}_{r_s}(t-\tau) + (1-\alpha)\dot{\theta}_{r_s}(t-\tau) + \gamma_{m_1}T_{s_1}(t) + \gamma_{k_1}T_{sf_1}(t) \\
&= \dot{\theta}_{r_s}(t-\tau) + \gamma_{m_1}T_{s_1}(t) + \gamma_{k_1}T_{sf_1}(t) \\
\dot{\theta}_{r_2}(t) &= (1-\alpha)\dot{\theta}_{s_2}(t-\tau) + \alpha\dot{\theta}^*_{sf_2}(t-\tau) + \gamma_{m_2}T_{s_2}(t) + \gamma_{k_2}T_{sf_2}(t) \\
&= (1-\alpha)\,\dot{\theta}_{r_s}(t-\tau) + \alpha\dot{\theta}_{r_s}(t-\tau) + \gamma_{m_2}T_{s_2}(t) + \gamma_{k_2}T_{sf_2}(t) \\
&= \dot{\theta}_{r_s}(t-\tau) + \gamma_{m_2}T_{s_2}(t) + \gamma_{k_2}T_{sf_2}(t)
\end{aligned} \tag{6.15}$$

where both masters receive a full position feedback with a position shift under constant time delay T, including passivity compensation terms. The force feedforward to the slave side is,

$$\begin{aligned}
T_{r_s}(t) &= \beta_1 T_{s_1}(t-\tau) + (1-\beta_2)T_{s_2}(t-\tau) + \gamma_{s_1}\dot{\theta}^*_{s_1}(t) + \gamma_{s_2}\dot{\theta}^*_{s_2}(t) \\
&= -\alpha T_{r_1}(t-\tau) - (1-\alpha)T_{r_2}(t-\tau) + \gamma_{s_1}\dot{\theta}^*_{s_1}(t) + \gamma_{s_2}\dot{\theta}^*_{s_2}(t)
\end{aligned} \tag{6.16}$$

where the slave experiences shared control signals, including passivity compensation terms. It reveals that the shared control concept is well realized with ideal force and position tracking in presence of constant delays. The authority adjustment methods (i.e., AAA) could be maintained as well.

6.4 Modeling

This modelling is performed for constant delays. As there was no change in the structure of the shared control when we introduced the AWVT, we reused the port-Hamiltonian framework employed in Sect. 3.5.

As shown in Fig. 6-4, it can be seen that the coupled subsystem of master/slave robots and the IPC controllers hold the same port-Hamiltonian model as depicted in Eq. 3.14. Thus, we only need to rewrite the interconnection of authority sharing

mechanism compared to Eq. 3.17. The interaction power variables become:

$$
\begin{aligned}
u^2_{c,m_1}(t) &= y^2_{c,s}(t-\tau) + \left[\alpha\gamma_{m_1} + (1-\alpha)\gamma_{k_1}\right] y^2_{c,m_1}(t) \\
u^2_{c,m_2}(t) &= y^2_{c,s}(t-\tau) + \left[(1-\alpha)\gamma_{m_2} + \alpha\gamma_{k_1}\right] y^2_{c,m_2}(t) \\
u^2_{c,s}(t) &= -\alpha y^2_{c,m_1}(t-\tau) - (1-\alpha) y^2_{c,m_2}(t-\tau) + \left[\beta_1\gamma_{s_1} + (1-\beta_2)\gamma_{s_2}\right] y^2_{c,s}(t)
\end{aligned}
\tag{6.17}
$$

where the superscripts 1 and 2 represent the number of input/output signal.

Combining this equation with the masters/slave robot-controller subsystem in Eq. 3.14, the closed-loop system now takes the following form[2]:

$$
\begin{aligned}
[J_g]_t &= \begin{bmatrix} [J_{rc,m_1}]_t & 0 & 0 \\ 0 & [J_{rc,m_2}]_t & 0 \\ 0 & 0 & [J_{rc,s}]_t \end{bmatrix} \quad [R_g]_t = \begin{bmatrix} [R_{rc,m_1}]_t & 0 & 0 \\ 0 & [R_{rc,m_2}]_t & 0 \\ 0 & 0 & [R_{rc,s}]_t \end{bmatrix} \\
Q_g &= \begin{bmatrix} h_{rc,m_1}\left(\alpha\gamma_{m_1} + (1-\alpha)\gamma_{k_1}\right) h^T_{rc,m_1} & 0 & 0 \\ 0 & h_{rc,m_2}\left((1-\alpha)\gamma_{m_2} + \alpha\gamma_{k_1}\right) h^T_{rc,m_2} & 0 \\ 0 & 0 & h_{rc,s}\left(\beta_1\gamma_{m_1} + (1-\beta_2)\gamma_{m_2}\right) h^T_{rc,s} \end{bmatrix} \\
M_g &= \begin{bmatrix} 0 & 0 & h_{rc,m_1} h^T_{rc,s} \\ 0 & 0 & h_{rc,m_2} h^T_{rc,s} \\ -\alpha h_{rc,s} h^T_{rc,m1} & -(1-\alpha) h_{rc,s} h^T_{rc,m_2} & 0 \end{bmatrix} \\
G_g &= \begin{bmatrix} g_{rc,m_1} & 0 & 0 \\ 0 & g_{rc,m_2} & 0 \\ 0 & 0 & g_{rc,s} \end{bmatrix} \quad u_g = \begin{bmatrix} T_{h_1} \\ T_{h_2} \\ T_e \end{bmatrix} \quad y_g = \begin{bmatrix} \dot{\theta}_{m_1} \\ \dot{\theta}_{m_2} \\ \dot{\theta}_s \end{bmatrix}
\end{aligned}
\tag{6.18}
$$

where the system can be expressed as

$$
\begin{cases}
\dot{x}_g(t) = [J_g - R_g + Q_g]_t [\nabla_{x_g} H_g]_t + M_g [\nabla_{x_g} H_g]_{t-\tau} + G_g u_g(t) \\
y_g(t) = G^T_g [\nabla_{x_g} H_g]_t
\end{cases}
\tag{6.19}
$$

The state variables are $x_g := [x^T_{rc,m_1} \;\; x^T_{rc,m_2} \;\; x^T_{rc,s}]^T$, and the Hamiltonian becomes:

[2]The functions or matrices which are themselves functions of time, are denoted by the symbol enclosed by a pair of square bracket with a subindex t or other time frame. For example, $[J_g]_t$ denotes the function of time $J_g(x_g(t))$

$$H_g(x_g) = H_{rc,m_1} + H_{rc,m_s} + H_{rc,s} \tag{6.20}$$

6.5 Passivity

6.5.1 Passivity Based on Closed-loop System

The above delayed closed-loop ESC dual-user system, no longer preserves the classical port-Hamiltonian framework. Considering the power port (u_g, y_g), the energy balance equation takes the form of

$$\begin{aligned}[\dot{H}_g]_t = &-[\nabla^T_{x_g} H_g]_t [R_g]_t [\nabla_{x_g} H_g]_t + [\nabla^T_{x_g} H_g]_t Q_g [\nabla_{x_g} H_g]_t \\ &+ [\nabla^T_{x_g} H_g]_t M_g [\nabla_{x_g} H_g]_{t-\tau} + y_g^T(t) u_g(t)\end{aligned} \tag{6.21}$$

Since the second term in the right hand side may not be negative-semidefinite, the passivity can not always be preserved. It is needed to find a solution to guarantee stability. This balance equation can be derived as

$$\begin{aligned}&H_g(x_g(t)) - H_g(x_g(0)) \\ &= \int_0^t y_g^T(s) u_g(s) \mathrm{d}s + \int_0^t [\nabla^T_{x_g} H_g]_s Q_g [\nabla_{x_g} H_g]_s + [\nabla^T_{x_g} H_g]_s M_g [\nabla_{x_g} H_g]_{s-\tau} \mathrm{d}s - D(t)\end{aligned} \tag{6.22}$$

where $D(t)$ is a non-negative function which represents the dissipated energy through the robot-controllers.

From the point of vie of the human/environment global power port (u_g, y_g), the passivity condition can be written as

$$H_g(x_g(t)) - H_g(x_g(0)) \leq \int_0^t y_g^T(s) u_g(s) \mathrm{d}s \tag{6.23}$$

Then, the following equation must always be satisfied to meet passivity,

$$\int_0^t [\nabla_{x_g}^T H_g]_s Q_g [\nabla_{x_g} H_g]_s + [\nabla_{x_g}^T H_g]_s M_g [\nabla_{x_g} H_g]_{s-\tau} \mathrm{d}s - D(t) \leq 0 \tag{6.24}$$

Thus, the introduction of passivity tuning parameters $\gamma_i, i \in \{m_1, k_1, m_2, k_2, s_1, s_2\}$ and the delayed shared control structure embedding AWVTs adds (to the structure depicted in Fig. 3-3) an energy term:

$$E_{dsc}(t) = \int_0^t [\nabla_{x_g}^T H_g]_s Q_g [\nabla_{x_g} H_g]_s + [\nabla_{x_g}^T H_g]_s M_g [\nabla_{x_g} H_g]_{s-\tau} \mathrm{d}s \tag{6.25}$$

We conclude that the passivity condition is:

$$E_{dsc}(t) \leq D(t) \tag{6.26}$$

Since the dynamics of the robots are sometimes unknown, it is hard to get the precise form of H_g and, and M_g. Thus, the passivity related parameters γ_i in Q_g are not able to be obtained. Under such cases, one possible solution is to exclude the robot parts, i.e., just to consider the controllers and the shared control structure instead, as the robots are passive with IPC controllers. This way, the coupled system still follows the same framework architecture, just by replacing the input/output/state variables.

In next section, we devote to seek for another method from the subsystem point of view to preserve passivity.

6.5.2 Passivity Based on AWVT

As for the analysis performed in Section 3.6.2, it is possible for us to study passivity by dividing the closed-loop system into several parts. Since the masters and the slave subsystems shown in Fig. 6-4 are passive (written within port-Hamiltonian framework), we just need to exploit the passivity of the shared control structure embedding the AWVT.

In order to insure passivity, the energy transmitted into the shared control struc-

ture should satisfy the following equation with a zero initial condition:

$$\int_0^t \left(T_{r_1}^T(s)\dot{\theta}_{r_1}(s) + T_{r_2}^T(s)\dot{\theta}_{r_2}(s) + T_{r_s}^T(s)\dot{\theta}_{r_s}(s) \right) \mathrm{d}s \geq 0, \ \forall t \geq 0 \tag{6.27}$$

For this passivity condition, we can substitute Eq. 6.13 and the value of α to obtain

$$\begin{aligned}\int_0^t \Big[& -T_{s_1}^T(s)\dot{\theta}_{s_1}(s) - T_{sf_1}^T(s)\dot{\theta}_{sf_1}(s) - T_{s_1}^T(s)\Gamma_{m_1}(s)T_{s_1}(s) - T_{sf_1}^T(s)\Gamma_{k_1}(s)T_{sf_1}(s) \\ & -T_{s_2}^T(s)\dot{\theta}_{s_2}(s) - T_{sf_2}^T(s)\dot{\theta}_{sf_2}(s) - T_{s_2}^T(s)\Gamma_{m_2}(s)T_{s_2}(s) - T_{sf_1}^T(s)\Gamma_{k_2}(s)T_{sf_2}(s) \\ & +T_{s_1}^{*T}(s)\dot{\theta}_{s_1}^*(s) + T_{s_2}^{*T}(s)\dot{\theta}_{s_2}^*(s) + \dot{\theta}_{s_1}^{*T}(s)\Gamma_{s_1}(s)\dot{\theta}_{s_1}^*(s) + \dot{\theta}_{s_2}^{*T}(s)\Gamma_{s_2}(s)\dot{\theta}_{s_2}^*(s) \Big] \mathrm{d}s \geq 0, \ \forall t \geq 0\end{aligned} \tag{6.28}$$

where the parameters $\Gamma_i(t), i \in \{m_1, k_1, m_2, k_2, s_1, s_2\}$ are as

$$\begin{aligned}\Gamma_{m_1}(t) &= \begin{cases} 0, & \alpha = 0 \\ \dfrac{\gamma_{m_1}}{\alpha}, & 0 < \alpha \leq 1 \end{cases} \qquad \Gamma_{m_2}(t) = \begin{cases} 0, & \alpha = 1 \\ \dfrac{\gamma_{m_2}}{1-\alpha}, & 0 \leq \alpha < 1 \end{cases} \\ \Gamma_{s_1}(t) &= \begin{cases} 0, & \alpha = 0 \\ \dfrac{\gamma_{s_1}}{\beta_1}, & 0 < \alpha \leq 1 \end{cases} \qquad \Gamma_{s_2}(t) = \begin{cases} 0, & \alpha = 1 \\ \dfrac{\gamma_{s_2}}{1-\beta_2}, & 0 \leq \alpha < 1 \end{cases} \\ \Gamma_{k_1}(t) &= \begin{cases} 0, & \alpha = 1 \\ \dfrac{\gamma_{k_1}}{1-\alpha}, & 0 \leq \alpha < 1 \end{cases} \qquad \Gamma_{k_2}(t) = \begin{cases} 0, & \alpha = 0 \\ \dfrac{\gamma_{k_2}}{\alpha}, & 0 < \alpha \leq 1 \end{cases}\end{aligned} \tag{6.29}$$

Then, substituting the AWVT transformation equations given in Eq. 6.8, we define the power flow transfered into every AWVT as,

$$\begin{aligned}P_i(t) &= -T_k^T(t)\dot{\theta}_k(t) = u_i^T(t)u_i(t) + u_i^T(s)v_i(t) \\ P_j(t) &= T_k^{*T}(t)\dot{\theta}_k^*(t) = v_j^T(t)v_j(t) - u_j^T(t)v_j(t)\end{aligned} \tag{6.30}$$

and similarly, we denote

$$\begin{aligned}\Pi_i(t) &= -T_k^T(t)\Gamma_i(t)T_k(t) = \left[\sqrt{2Z_i}u_i(t)\right]^T \Gamma_i(t) \left[\sqrt{2Z_i}u_i(t)\right] \\ \Pi_j(t) &= \dot{\theta}_k^{*T}(t)\Gamma_j(t)\dot{\theta}_k^*(t) = \left[\sqrt{2Z_j^{-1}}v_j(t)\right]^T \Gamma_j(t) \left[\sqrt{2Z_j^{-1}}v_j(t)\right]\end{aligned} \tag{6.31}$$

where $i \in \{m_1, m_2, k_1, k_2\}$, $j \in \{s_1, s_2, j_1, j_2\}$, $k \in \{s_1, s_2, sf_1, sf_2\}$ represent each AWVT variables (forces/velocities/power variables) respectively, i.e, $i = m_1, j = s_1, k = s_1$ are the ones formed by Z_{m_1} and Z_{s_1}; and $i = m_2, j = s_2, k = s_2$ are the ones formed by Z_{m_2} and Z_{s_2}, and $i = k_1, j = j_1, k = sf_1$ is the ones formed by Z_{k_1} and Z_{j_1}; and $i = k_2, j = j_2, k = sf_2$ are the ones formed by Z_{k_2} and Z_{j_2}, as shown in Fig. 6-4.

Then, the passivity condition in Eq. 6.28 can be rewritten:

$$\begin{aligned}\int_0^t &[P_{m_1}(s) + P_{m_2}(s) + P_{k_1}(s) + P_{k_2}(s) + P_{s_1}(s) + P_{s_2}(s) \\ &+\Pi_{m_1}(s) + \Pi_{m_2}(s) + \Pi_{k_1}(s) + \Pi_{k_2}(s) + \Pi_{s_1}(s) + \Pi_{s_2}(s)]\ \mathrm{d}s \geq 0,\ \forall t \geq 0\end{aligned} \tag{6.32}$$

Actually, the AWVT consists of two modifications compared with the CWVT: impedance matching and biased compensation terms. Both of them may violate the passivity condition. Since some delay is present inside the communication channel, the global system could be divided into the master and the slave sides respectively, by denoting power flows as $P_m(t)$ and $P_s(t)$. Therefore, we redefine the above energy

equation as:

$$
\begin{aligned}
P_m(t) &= P_{m_1}(t) + P_{m_2}(t) + P_{k_1}(t) + P_{k_2}(t) + \Pi_{m_1}(t) + \Pi_{m_2}(t) + \Pi_{k_1}(t) + \Pi_{k_2}(t) \\
&= \sum_{i=m_1,m_2,k_1,k_2} u_i^T(t)u_i(t) + u_i^T(t)v_i(t) + \left[\sqrt{2Z_i}u_i(t)\right]^T \Gamma_i(t) \left[\sqrt{2Z_i}u_i(t)\right] \\
\\
P_s(t) &= P_{s_1}(t) + P_{s_2}(t) + \Pi_{s_1}(t) + \Pi_{s_2}(t) \\
&= \sum_{j=s_1,s_2} v_j^T(t)v_j(t) - u_j^T(t)v_j(t) + \left[\sqrt{2Z_j^{-1}}v_j(t)\right]^T \Gamma_j(t) \left[\sqrt{2Z_j^{-1}}v_j(t)\right]
\end{aligned}
\tag{6.33}
$$

which leads to the passivity condition of Eq. 6.32 into the form:

$$
E_p(t) = \int_0^t P_m(s) + P_s(s)\ \mathrm{d}s \geq 0,\ \forall t \geq 0 \tag{6.34}
$$

where $E_p(t)$ represents the total energy transmitted into the shared control structure at time t. This condition should always be satisfied through choosing proper parameters of $\gamma_i, i \in \{m_1, k_1, m_2, k_2, s_1, s_2\}$.

In practice, the energy function at the masters side (trainer and trainee together, by supposing no delay between each other) and slave side cannot be simultaneously obtained on one site. The benefit of splitting the energy function into each sides in Eq. 6.33 is that it becomes possible to check each side individually rather than requiring both sides available at the same time. Thus, a more conservative condition is given as:

$$
\begin{aligned}
E_m(t) &= \int_0^t P_m(s)\ \mathrm{d}s \geq 0,\ \forall t \geq 0 \\
E_s(t) &= \int_0^t P_m(s)\ \mathrm{d}s \geq 0,\ \forall t \geq 0
\end{aligned}
\tag{6.35}
$$

where $E_m(t)$ and $E_s(t)$ indicate the energy transfered into the shared control structure by the masters side and the the slave side, respectively.

6.5.3 Transparency Based Parameters Configuration

The parameters $\gamma_i, i \in \{m_1, k_1, m_2, k_2, s_1, s_2\}$ should be designed to satisfy the above condition in real-time. Many strategies are possible for choosing these parameters. In this section, we give an example based on a transparency objective.

Transparency Characterization

Substuting Eq. 6.8 into Eq. 6.15 and Eq. 6.16, the feedback and feed-forward reference position/force for the master and slave side are:

$$\begin{aligned}
\dot{\theta}_{r_1}(t) &= \dot{\theta}_{r_s}(t-\tau) - \left[r_{m_1}(t)\sqrt{2Z_{m_1}}u_{m_1}(t) + r_{k_1}(t)\sqrt{2Z_{k_1}}u_{k_1}(t)\right] \\
\dot{\theta}_{r_2}(t) &= \dot{\theta}_{r_s}(t-\tau) - \left[r_{m_2}(t)\sqrt{2Z_{m_2}}u_{m_2}(t) + r_{k_2}(t)\sqrt{2Z_{k_2}}u_{k_2}(t)\right] \\
T_{r_s}(t) &= -\alpha T_{r_1}(t-\tau) - (1-\alpha)T_{r_2}(t-\tau) \\
&\quad + \left[r_{s_1}(t)\sqrt{2Z_{s_1}^{-1}}v_{s_1}(t) + r_{s_2}(t)\sqrt{2Z_{s_2}^{-1}}v_{s_2}(t)\right]
\end{aligned} \tag{6.36}$$

It can be seen when all $\gamma_i = 0$, the ideal transparency (defined as fidelity of feedback and feed-forward position/force) for reference signal is achieved. That is,

$$\begin{aligned}
\dot{\theta}_{r_1}(t) &= \dot{\theta}_{r_s}(t-\tau) \\
\dot{\theta}_{r_2}(t) &= \dot{\theta}_{r_s}(t-\tau) \\
T_{r_s}(t) &= -\alpha T_{r_1}(t-\tau) - (1-\alpha)T_{r_2}(t-\tau)
\end{aligned} \tag{6.37}$$

which is same as the desired case in Eq. 3.5, except for a time shift of delays. Thus γ_i could be configured to achieve the trade-off balance between passivity and transparency for both masters and the slave. The ideal reference position/force should be obtained as far as possible.

In consideration of Eq. 6.33, γ_i is only related with the terms Π_i, $i \in \{m_1, k_1, m_2, k_2, s_1, s_2\}$, which represent a part of power flow transfered into the shared control structure. They can be viewed as the power flow for passivity tuning. When all $\Pi_i = 0$, ideal situations could be obtained. That is, good transparency is considered without any passivity tunning.

Energy Functions Definition

The energy functions of $E_m(t)$ and $E_s(t)$ of Eq. 6.35 and Eq. 6.33 can be rewritten in discrete time form. The one for master side is given as:

$$\begin{aligned} E_m(n) &= \Delta t \sum_{i=1}^{n} \left[\sum_{j=m_1,k_1} P_j(i) + \sum_{j=m_2,k_2} P_j(i) + \sum_{j=m_1,k_1} \Pi_j(i) + \sum_{j=m_2,k_2} \Pi_j(i) \right] + \epsilon_m(n) \\ &= \Delta t \sum_{i=1}^{n} \left[P_m(i) + \sum_{j=m_1,k_1} \Pi_j(i) + \sum_{j=m_2,k_2} \Pi_j(i) \right] + \epsilon_m(n) \\ &= \Delta E_m(n) + \Delta \Pi_m(n-1) + \Delta t\, \Pi_m(n) \\ &= \bar{E}_m(n) + \bar{\Pi}_m(n) \end{aligned} \tag{6.38}$$

where

$$P_m(n) = \sum_{j=m_1,k_1,m_2,k_2} \left[u_j^T(n) u_j(n) + u_j^T(n) v_j(n) \right]$$

$$\widetilde{P}_m(n) = \begin{cases} P_m(n), & \text{if } P_m(n) - P_m(n-1) \geq 0 \\ P_m(n) + \left[P_m(n) - P_m(n-1) \right], & \text{if } P_m(n) - P_m(n-1) < 0 \end{cases}$$

$$\epsilon_m(n) = \Delta t \sum_{i=1}^{n} \left[\widetilde{P}_m(i) - P_m(i) \right]$$

$$\Delta E_m(n) = \Delta t \sum_{i=1}^{n} \widetilde{P}_m(i)$$

$$\Pi_m(n) = \sum_{j=m_1,k_1,m_2,k_2} \Pi_j(n) = \sum_{j=m_1,k_1,m_2,k_2} \left[\sqrt{2Z_j} u_j(n) \right]^T \Gamma_j(n) \left[\sqrt{2Z_j} u_j(n) \right]$$

$$\Delta \Pi_m(n-1) = \Delta t \sum_{i=1}^{n-1} \Pi_m(i)$$

$$\bar{E}_m(n) = \Delta E_m(n) + \Delta \Pi_m(n-1)$$

$$\bar{\Pi}_m(n) = \Delta t\, \Pi_m(n)$$

and the one for the slave side is given as:

$$\begin{aligned} E_s(n) &= \Delta t \sum_{i=1}^{n} \left[P_{s_1}(i) + P_{s_2}(i) + \Pi_{s_1}(i) + \Pi_{s_2}(i) \right] + \epsilon_s(n) \\ &= \Delta t \sum_{i=1}^{n} \left[P_s(i) + \Pi_{s_1}(i) + \Pi_{s_2}(i) \right] + \epsilon_s(n) \\ &= \Delta E_s(n) + \Delta \Pi_s(n-1) + \Delta t \ \Pi_s(n) \\ &= \bar{E}_s(n) + \bar{\Pi}_s(n) \end{aligned} \tag{6.39}$$

where

$$P_s(n) = \sum_{k=s_1,s_2} \left[v_k^T(n) v_k(n) - u_k^T(n) v_k(n) \right]$$

$$\widetilde{P}_s(n) = \begin{cases} P_s(n), & \text{if } P_s(n) - P_s(n-1) \geq 0 \\ P_s(n) + \left[P_s(n) - P_s(n-1) \right], & \text{if } P_s(n) - P_s(n-1) < 0 \end{cases}$$

$$\epsilon_s(n) = \Delta t \sum_{i=1}^{n} \left[\widetilde{P}_s(i) - P_s(i) \right]$$

$$\Delta E_s(n) = \Delta t \sum_{i=1}^{n} \widetilde{P}_s(i)$$

$$\Pi_s(n) = \sum_{k=s_1,s_2} \Pi_k(n) = \sum_{k=s_1,s_2} \left[\sqrt{2Z_k^{-1}} v_k(t) \right]^T \Gamma_k(t) \left[\sqrt{2Z_k^{-1}} v_k(t) \right]$$

$$\Delta \Pi_s(n-1) = \Delta t \ \sum_{i=1}^{n-1} \Pi_s(i)$$

$$\bar{E}_s(n) = \Delta E_s(n) + \Delta \Pi_s(n-1)$$

$$\bar{\Pi}_s(n) = \Delta t \ \Pi_s(n)$$

In the above equations, Δt is the time step, $P_j(n), \Pi_j(n)$, $P_k(n), \Pi_k(n)$, $j = m_1, k_1, m_2, k_2$ and $k = s_1, s_2$ follow the conventions in Eq. 6.33 representing the power flow at discrete time step n. $\Delta E_m(n), \Delta E_s(n)$ indicate the total energy transfered into the shared control structure from both masters side and the slave side before passivity tuning (with good transparency by providing full reference energy), respectively. $\Delta \Pi_m(n-1), \Delta \Pi_s(n-1)$ is the total energy already tuned (for passivity)

at time step $n-1$, and $\bar{\Pi}_m(n), \bar{\Pi}_s(n)$ are the energy to be tuned (for passivity) at time step n from the masters side and the slave side respectively. $\bar{E}_m(n), \bar{E}_s(n)$ indicate summation of $\Delta E_m(n), \Delta E_s(n)$ and $\Delta\Pi_m(n-1), \Delta\Pi_s(n-1)$.

It is worth noting that an error is introduced in the energy function $E_m(n)$ and $E_s(n)$, respectively. This error is caused by discretization (Euler's first order method) of the above equations, and may cause $E_i(n) \geq 0, i = m, s$ even if the passivity is not satisfied. For this reason, we defined a less conservative value of the transfered power flow (to make it less than the continues one) as $\widetilde{P}_i(n)$ for $\bar{P}_i(n)$, $i = m, s$ at each time step n, and the errors are estimated accordingly.

Parameters Tuning Guideline

In regard of the trade-off between passivity and transparency, we would like $\Pi_i(n)$, $i \in \{m_1, k_1, m_2, k_2, s_1, s_2\}$ to be as small as possible (ideal when equal to 0 without any passivity tunning). The following parameters tuning guideline at the time step n is specified:

- when $0 \leq \alpha \leq 0.5$,

  for the masters side: the trainee is main operator (more authority), while the trainer is minor operator (less authority). In this case, we want the trainee to experience good transparency without concerning passivity. Thus, we could set $\Pi_i(n) = 0, i = m_2, k_2$ (do nothing for tuning). The only need is to tune $\Pi_i(n), i = m_1, k_1$ to ensure passivity. Notice that, when $\alpha = 0$, there is no velocity transfered to trainer side through the channel of Z_{m_1}-Z_{s_1} (see Eq. 6.13). $\Pi_{m_1}(n) = 0$ is given for the reason that tuning takes no effect by multiplying a zero signal (as indicated in Eq. 6.29). In this case, we could only tune $\Pi_{k_1}(n)$ to ensure passivity.

  for the slave side: The power flow $\Pi_{s_1}(n)$ and $\Pi_{s_2}(n)$ should be tuned regarding their energy transfered into the shared control structure respectively (according to control authority). Notice that, when $\alpha = 0$, there is no velocity transfered to trainer side through the channel of Z_{m_1}-Z_{s_1}. $\Pi_{s_1}(n) = 0$ is given

(as indicated in Eq. 6.29). In this case, we could only tune $\Pi_{s_2}(n)$ to ensure passivity.

- when $0.5 < \alpha \leq 1$,

  for the masters side: the trainer is main operator (more authority), while the trainee is minor operator (less authority). In this case, we want the trainer to experience good transparency without concerning passivity. Thus, we could set $\Pi_i(n) = 0, i = m_1, k_1$ (do nothing for tuning). The only need is to tune $\Pi_i(n), i = m_2, k_2$ to ensure passivity. Notice that, when $\alpha = 1$, there is no velocity transfered to trainee side through the channel of Z_{m_2}-Z_{s_2} (see Eq. 6.13). $\Pi_{m_2}(n) = 0$ is given (as indicated in Eq. 6.29). In this case, we could only tune $\Pi_{k_2}(n)$ to ensure passivity.

  for the slave side: The power flow $\Pi_{s_1}(n)$ and $\Pi_{s_2}(n)$ should be tuned regarding their energy transfered into the shared control structure respectively (according to control authority). Notice that, when $\alpha = 1$, there is no velocity transfered to trainee side through the channel of Z_{m_2}-Z_{s_2}. $\Pi_{s_2}(n) = 0$ is given (as indicated in Eq. 6.29). In this case, we could only tune $\Pi_{s_1}(n)$ to ensure passivity.

In consideration of the shared control structure given in Eq. 6.13 and Eq. 6.29, and to fulfill the transparency guideline above, we assume an example of following parameter relations are existed (other choices are possible):

- when $0 \leq \alpha \leq 0.5$,

$$\begin{aligned} \gamma_{m_2} &= 0 \\ \gamma_{k_2} &= 0 \\ (1-\alpha)\gamma_{m_1} &= \alpha\gamma_{k_1} \\ (1-\alpha)\gamma_{s_1} &= \alpha\gamma_{s_2} \end{aligned} \tag{6.40}$$

- when $0.5 < \alpha \leq 1$,

$$\begin{aligned} \gamma_{m_1} &= 0 \\ \gamma_{k_1} &= 0 \\ \alpha\gamma_{m_2} &= (1-\alpha)\gamma_{k_2} \\ (1-\alpha)\gamma_{s_1} &= \alpha\gamma_{s_2} \end{aligned} \tag{6.41}$$

Passivity Controller

In order to fit the passivity requirements in Eq. 6.35, we need Eq. 6.38 and 6.39 to satisfy:

$$\begin{aligned} E_m(n) &\geq 0 \\ E_s(n) &\geq 0 \end{aligned} \tag{6.42}$$

then, we could adopt the following control law:

$$\begin{aligned} \bar{\Pi}_m(n) &= E_{tm}(n) \\ \bar{\Pi}_s(n) &= E_{ts}(n) \end{aligned} \tag{6.43}$$

where

$$\begin{aligned} E_{tm}(n) &= \begin{cases} 0, & \text{if } \bar{E}_m(n) \geq 0 \\ -\bar{E}_m(n), & \text{if } \bar{E}_m(n) < 0 \end{cases} \\ E_{ts}(n) &= \begin{cases} 0, & \text{if } \bar{E}_s(n) \geq 0 \\ -\bar{E}_s(n), & \text{if } \bar{E}_s(n) < 0 \end{cases} \end{aligned} \tag{6.44}$$

Here we give a solution for the parameters in consideration of 1-DoFs case. By calculation using Eq., 6.38, 6.39 and 6.43, the parameters are obtained in Table 6.1.

Table 6.1: An example for parameters $\gamma_i, i \in \{m_1, k_1, m_2, k_2, s_1, s_2\}$

Case	$0 \leq \alpha \leq 0.5$	$0.5 < \alpha \leq 1$
$\gamma_{m_1}(n)$	$\frac{\alpha E_{tm}(n)}{\Delta t\left[2\alpha Z_{m_1} u_{m_1}^2(n)+2(1-\alpha)Z_{k_1} u_{k_1}^2(n)\right]}$	0
$\gamma_{k_1}(n)$	$\frac{(1-\alpha) E_{tm}(n)}{\Delta t\left[2\alpha Z_{m_1} u_{m_1}^2(n)+2(1-\alpha)Z_{k_1} u_{k_1}^2(n)\right]}$	0
$\gamma_{m_2}(n)$	0	$\frac{(1-\alpha) E_{tm}(n)}{\Delta t\left[2(1-\alpha)Z_{m_2} u_{m_2}^2(n)+2\alpha Z_{k_2} u_{k_2}^2(n)\right]}$
$\gamma_{k_2}(n)$	0	$\frac{\alpha E_{tm}(n)}{\Delta t\left[2(1-\alpha)Z_{m_2} u_{m_2}^2(n)+2\alpha Z_{k_2} u_{k_2}^2(n)\right]}$
$\gamma_{s_1}(n)$	$\frac{\alpha E_{ts}(n)}{\Delta t\left[2\alpha Z_{s_1}^{-1} v_{s_1}^2(n)+2(1-\alpha)Z_{s_2}^{-1} v_{s_2}^2(n)\right]}$	
$\gamma_{s_2}(n)$	$\frac{(1-\alpha) E_{ts}(n)}{\Delta t\left[2\alpha Z_{s_1}^{-1} v_{s_1}^2(n)+2(1-\alpha)Z_{s_2}^{-1} v_{s_2}^2(n)\right]}$	

Remark. It can been seen all the denominators are non-negative values. $\gamma_i(n)$ is set to 0 when the corresponding denominator equals to zero. This happens during the wave variables, i.e., $u_j(n)$ or $v_j(n)$, are zeros, which indicate no power is generated at time step n. As a result, passivity is preserved.

6.6 Real-time Experiments

6.6.1 Experiment Setup

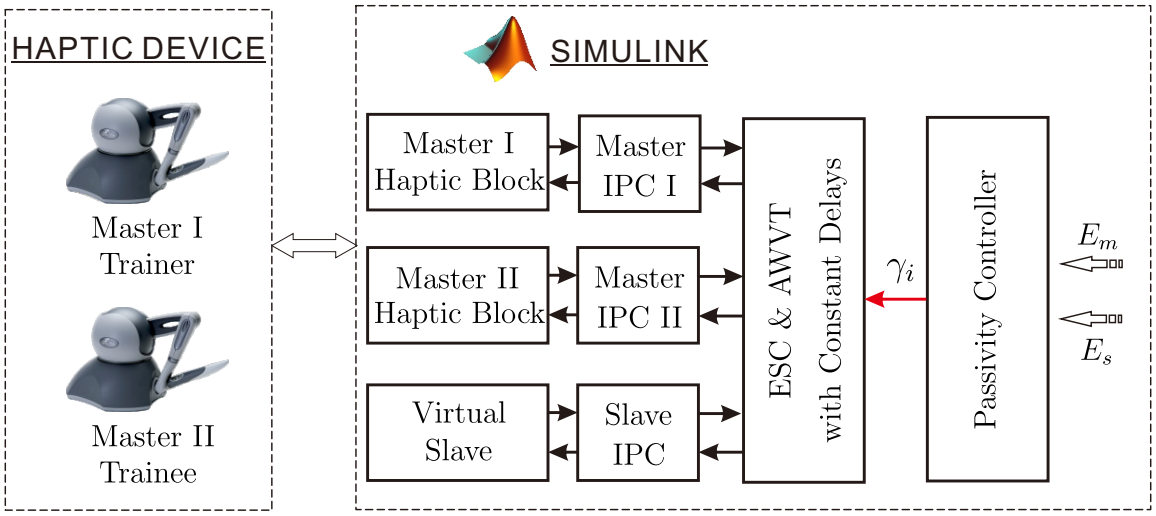

Figure 6-5: Experiment setup with constant time delays

The efficiency of the proposed scheme in presence of constant time delays is verified through the experimental set up shown in Fig. 6-5, where two Sensable® PHANTOM Omni are used for masters devices. The slave is built virtually inside Simulink®. The master haptic blocks and the IPC controllers adopt the same configuration as described for the no delay case in Section 3.8.1. The proposed ESC shared control structure embedding AWVT with constant time delays can be found in Fig. 6-4. The passivity controller is realized in real-time through calculation of energy functions, i.e., E_m and E_s (see Eq. 6.38, 6.39). Parameters are displayed in Table 6.2. Time delays are $\tau \in \{1\text{ms}, 10\text{ms}, 100\text{ms}\}$.

6.6.2 Experimental Results

In these experiments, both the trainer and trainee were asked to follow a given sinusoidal trajectory from time 10s to 100s, defined as:

$$\theta_i = 0.5 sin\left(\frac{\pi}{15}t - \frac{10\pi}{15}\right), \qquad i \in \{m_1, m_2\} \tag{6.45}$$

Table 6.2: Real-time experiment parameters of ESC structure under constant time delays

Items	**Parameters**	**Unit**	**Value**
Slave Robot Dynamics	B_s	$\mathrm{N \cdot m \cdot s/rad}$	0.5
	M_s	$\mathrm{kg \cdot m^2}$	0.1
IPC Controller $i \in \{m_1, m_2, s\}$	$K_{c,i}$	$\mathrm{N \cdot m/rad}$	10
	$K_{r,i}$	$\mathrm{N \cdot m/rad}$	10
	$M_{c,i}$	$\mathrm{kg \cdot m^2}$	0.01
	$B_{c,i}$	$\mathrm{N \cdot m \cdot s/rad}$	1
AWVT $i \in \{m_1, m_2, k_1, k_2, s_2, s_2, j_1, j_2\}$	Z_i	-	5
Discretization Step	Δt	s	0.001

The energy functions from masters side E_m and slave side E_s are recorded to check passivity, respectively. They represent the total energy entered into the ESC shared control structure from each side after passivity tuning. The energy transmitted before the passivity tuning controller takes effect (i.e., removing the total tuned energy) from each side, is also calculated: $\Delta E_m(n), \Delta E_s(n)$ in Eq. (6.38) and (6.39). It is used to see the energy changes before and after passivity tuning.

We select $\alpha \in \{0, 0.5, 1\}$ as a representative for training mode, guidance mode, and evaluation mode.

Free Motion Case

The first part is conducted in free motion. Three groups of experiments were conducted with different time delays. Two groups are shown in Fig. 6-6, Fig. 6-7 and Fig. 6-8, when the time delay is set at $\tau = 1$ms and $\tau = 100$ms. The other group is provided in Appendix B.1.

From the figures, we could observe that:

1. The three training modes could be well performed under specified time delays. Stable dual-user teleoperated simulation is achieved. The energy functions plotted at both the masters side and the slave side, demonstrate that the proposed controller effectively ensures passivity. This is indicated by the non-negative

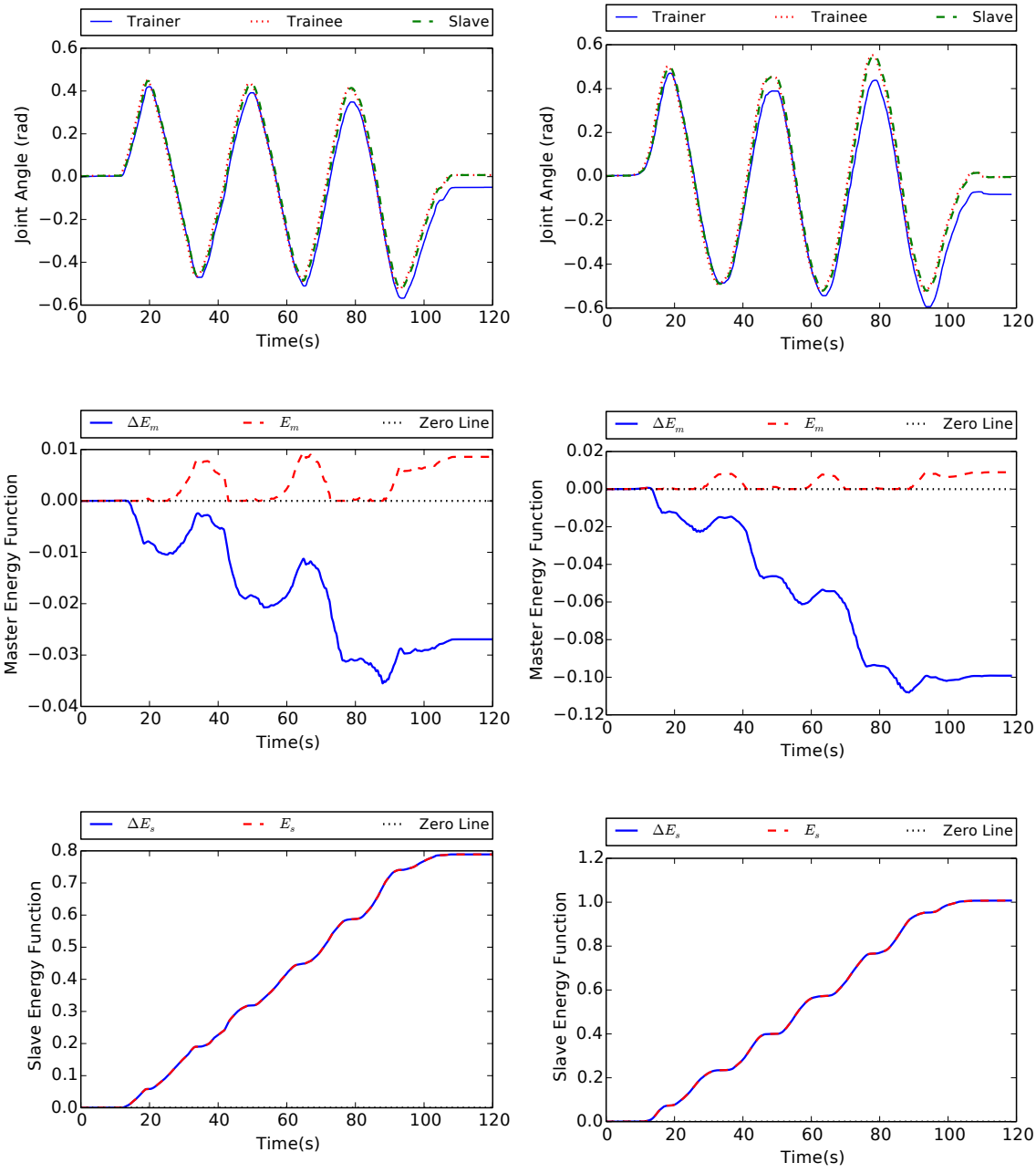

Figure 6-6: Free motion case: positions tracking, masters and slave side energy functions when $\alpha = 0$ (Left: $\tau = 1$ms, Right: $\tau = 100$ms).

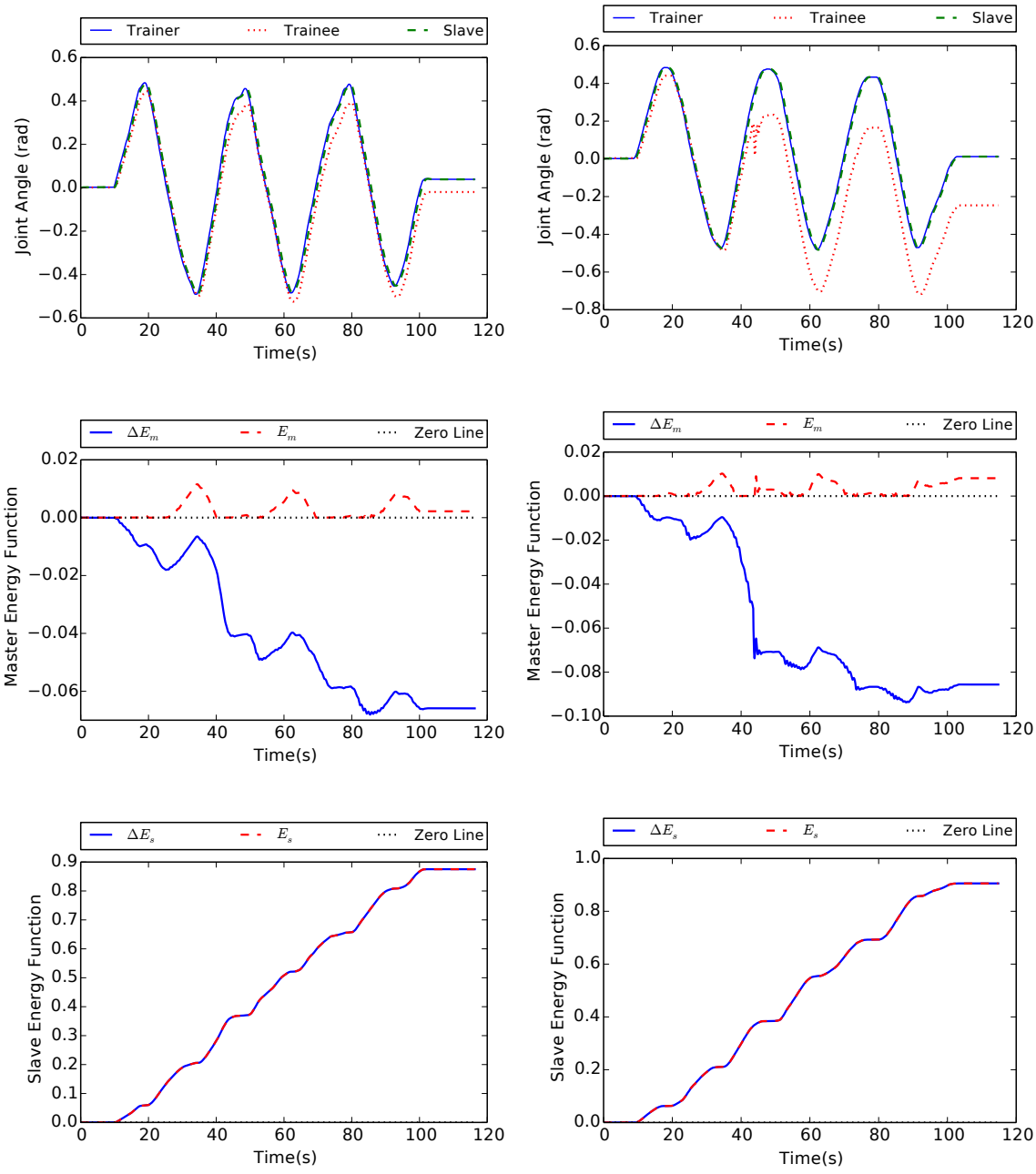

Figure 6-7: Free motion case: positions tracking, masters and slave side energy functions when $\alpha = 1$ (Left: $\tau = 1$ms, Right: $\tau = 100$ms).

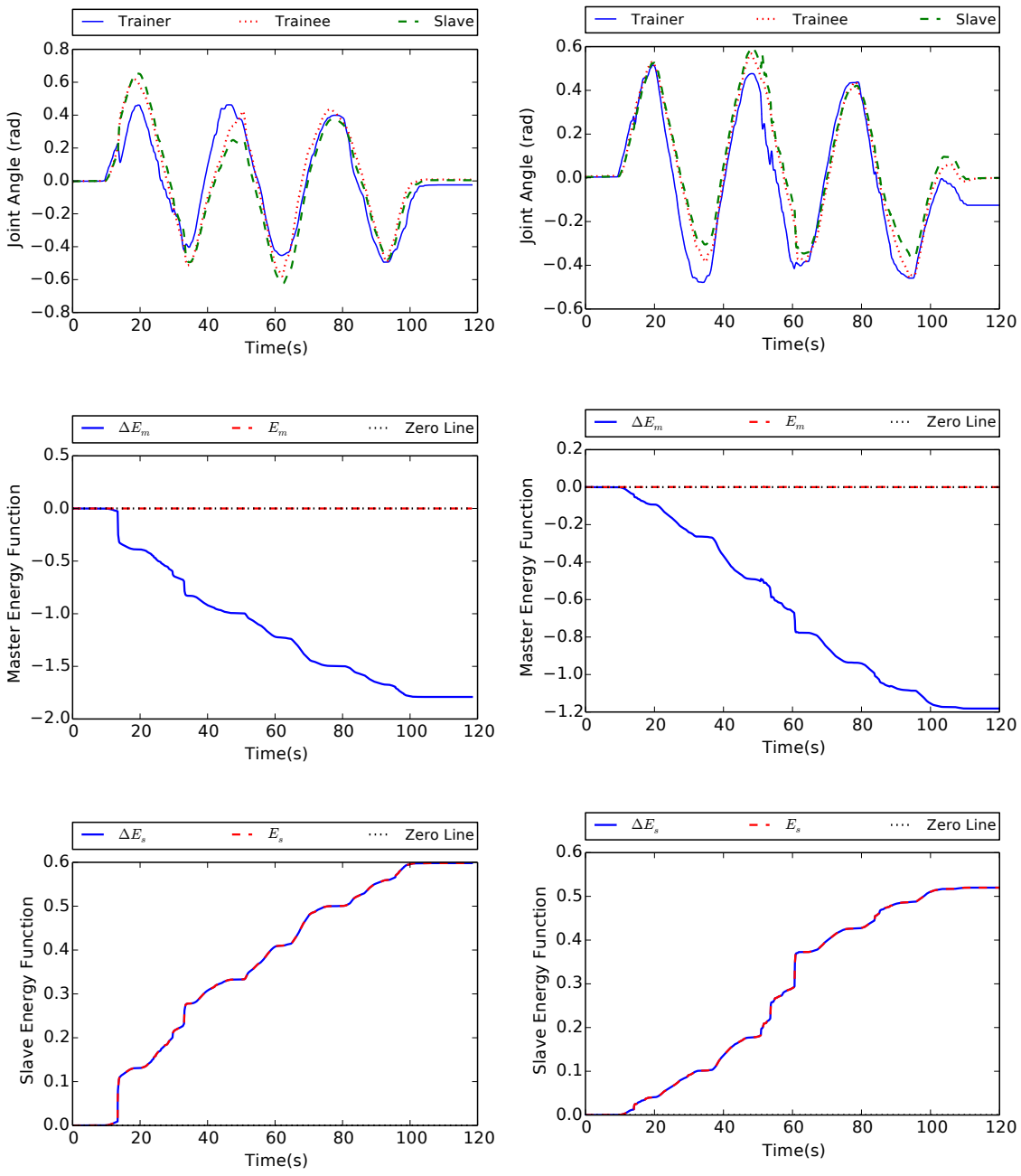

Figure 6-8: Free motion case: positions tracking, masters and slave side energy functions when $\alpha = 0.5$ (Left: $\tau = 1$ms, Right: $\tau = 100$ms).

values of E_m and E_s tuned in real-time. Actually, only the masters side energy function shows negative values before tuning, which means that more energy comes out than the one going into the ESC shared control structure. The slave side injects more energy from IPC controller than it extracts some, which results in a positive value all the time. Thus, in practice, the passivity tuning mechanism did not trigger at slave side. It is worth mentioning that during the periods when E_m is positive, the passivity tuning mechanism did not trigger at the master side as well. When $\alpha = 0$ and $\alpha = 1$, similar passivity tuning situations are obtained. However, passivity tuning of the masters side was always triggering (i.e., $E_m = 0$, $\Delta E_m < 0$) when $\alpha = 0.5$. In this case, both the trainer and the trainee control the slave in a shared way. The reason could be attributed to the uncoordinated actions between them. It is different from the case when one of the users holds full control authority acting as the leader, while the other one is the follower. Similar situations could be expected for $\alpha \in (0, 1)$.

2. A position drift appears (visible in position tracking figures), although the system is stable. For the purpose of position synchronization, the controller ideally should be acting on the errors between the positions of masters and slave. Since our system exchanges power variables (force/velocity), this is velocity signal which is transmitted over the communication channels. As shown in the system architecture in Fig. 6-4, the reference velocity $\dot{\theta}_s$ at slave side is fed back through the AWVT to the masters side: $\dot{\theta}_{r_1}$ and $\dot{\theta}_{r_2}$. The IPC controllers located at both masters sides take these velocities as inputs (admittance causality). As a matter of fact $\dot{\theta}_{r_1}$ and $\dot{\theta}_{r_2}$ are modified according to passivity tuning, see Eq. 6.36. It is straightforward to conclude that the position drift may occur due to the accumulative nature of the integral terms. This in turn has an effect on performance.

3. The position drift varies with respect to different control authorities. This could be observed in the parameters tuning guideline in Section 6.5.3.

- When $0 \leq \alpha \leq 0.5$, the trainee (main operator) could experience full velocity feedback. The passivity tuning is only concerned at the trainer side. Consequently, only the trainer is victim of position drifts (see Fig. 6-6 and 6-8). The slave follows the movement of the trainee. It is worth noting that during $\alpha = 0.5$, the position drift occurs all the time at the masters side, for the reason that passivity tuning was always triggering.
- When $0.5 < \alpha \leq 1$, the trainer (main operator) could experience full velocity feedback. The passivity tuning is only concerned at the trainee side. Consequently, only the trainee gets position drifts (see Fig. 6-7). The slave follows the movement of the trainer.

4. The position drift varies in terms of time delays. It can be seen in the figures: the position drift tends to raise as the time delay increases, for all values of α. In fact, it is possible that more energy is produced from the ESC shared control structure when the time delay is increasing. This is consistent with the common results obtained in literature for bilateral system (such as [Lee and Spong, 2006]).

Wall Contact Case

The second part of these experiments considers the presence of a virtual wall, in order to evaluate the system's contact behavior. The model of virtual wall takes the form defined in Eq. 6.46 as,

$$-T_e = \begin{cases} 0, & \theta_s < 0.3 \text{ rad} \\ -k_e(\theta_s - 0.3), & \theta_s \geq 0.3 \text{ rad} \end{cases} \tag{6.46}$$

where $k_e = 10$ N $\cdot$ m/rad is the wall stiffness and θ_s is the slave robot's joint angle.

Three groups of experiments are conducted with different time delays. Two groups are shown in Fig. 6-9, Fig. 6-10 and Fig. 6-11, when the time delay is set to $\tau = 1$ms and $\tau = 100$ms. The other group is given in Appendix B.2. It is interesting to plot also the human reaction torques for checking the tracking performance of force

feedback. The human hand torques are estimated using the Nicosia observer provided in [Nicosia and Tomei, 1990].

The dual-user teleoperated simulator is tested for the three different training modes, i.e., $\alpha = 0, 1, 0.5$. The passivity controllers are here to ensure stable interaction with the virtual wall. From the figures, we could observe similar position tracking results as the cases in free motion. For instance, the passivity tuning mechanisms at masters side only triggered when $E_m = 0$ and $\Delta E_m < 0$, while the one at slave side did not trigger, i.e., $E_s > 0$. The position drifts also accumulated. They were affected by both the control authority (by way of parameters tuning guideline) and the time delays. Thus, we only detail here the force tracking performance.

In Eq. 4.7, the desired torque tracking is defined under no delay ESC structure. Based on it, we provided an ideal torque tracking definition during contact motions, in presence of time delay as:

$$\alpha T_{h_1}(t) + (1 - \alpha) T_{h_2}(t) = T_e(t - \tau) \tag{6.47}$$

1. The leader (trainee $\alpha = 0$, and trainer when $\alpha = 1$) is able to experience full environment force feedback. It could be checked by the correspondence between the hand torque and the environment in the figures. Meanwhile in free motion, the leader applies a torque to drive the movement of the system. Likewise, the follower feels driving torque (quite smaller and in opposite direction compared to the one of the leader) due to the motions of his/her device, which could be ignored. The main information obtained by the follower is position.

2. When $\alpha = 0.5$, the accuracy of the torque tracking is significantly affected, see Fig. 6-11. The aforementioned ideal torque tracking performance cannot be guaranteed all the time (during contact periods). It is mainly visible at trainer side. Sometimes an opposite direction of torque (compared to the environment torque) is perceived by the trainer. This leads to a misinterpretation of the environment by the trainer. The reason for this originates from the parameter tuning guideline applied at masters side. The passivity tuning mechanism only

triggers at trainer side. Accordingly, the modified reference velocity yields a disorientating reference torque transmitted to the trainer IPC controller.

3. Similar force tracking performances could be expected for $\alpha \in (0, 1)$. Practically, this was impossible for users to get precise awareness of the environment. Under such cases, only the position information is useful to confirm the operating conditions.

Discussion

These experimental results indicate that both stable position and force tracking are achieved for the proposed ESC shared control structure in presence of constant time delays. It appears that the embedded passivity controller suffers from a position drift issue. This is a common phenomenon of passivity-based schemes, since the position and force are not power (velocity-force instead) correlated. Modifications in feedback velocity to the masters side are accumulated over time, resulting to position drifts. In addition, the force tracking performance cannot be guaranteed when both users share the control of the system, i.e., $\alpha \in (0, 1)$. The reason is derived from the disorientating reference torques generated at the master IPC controllers. Therefore, further approaches for increasing the transparency of dual-user system should be developed.

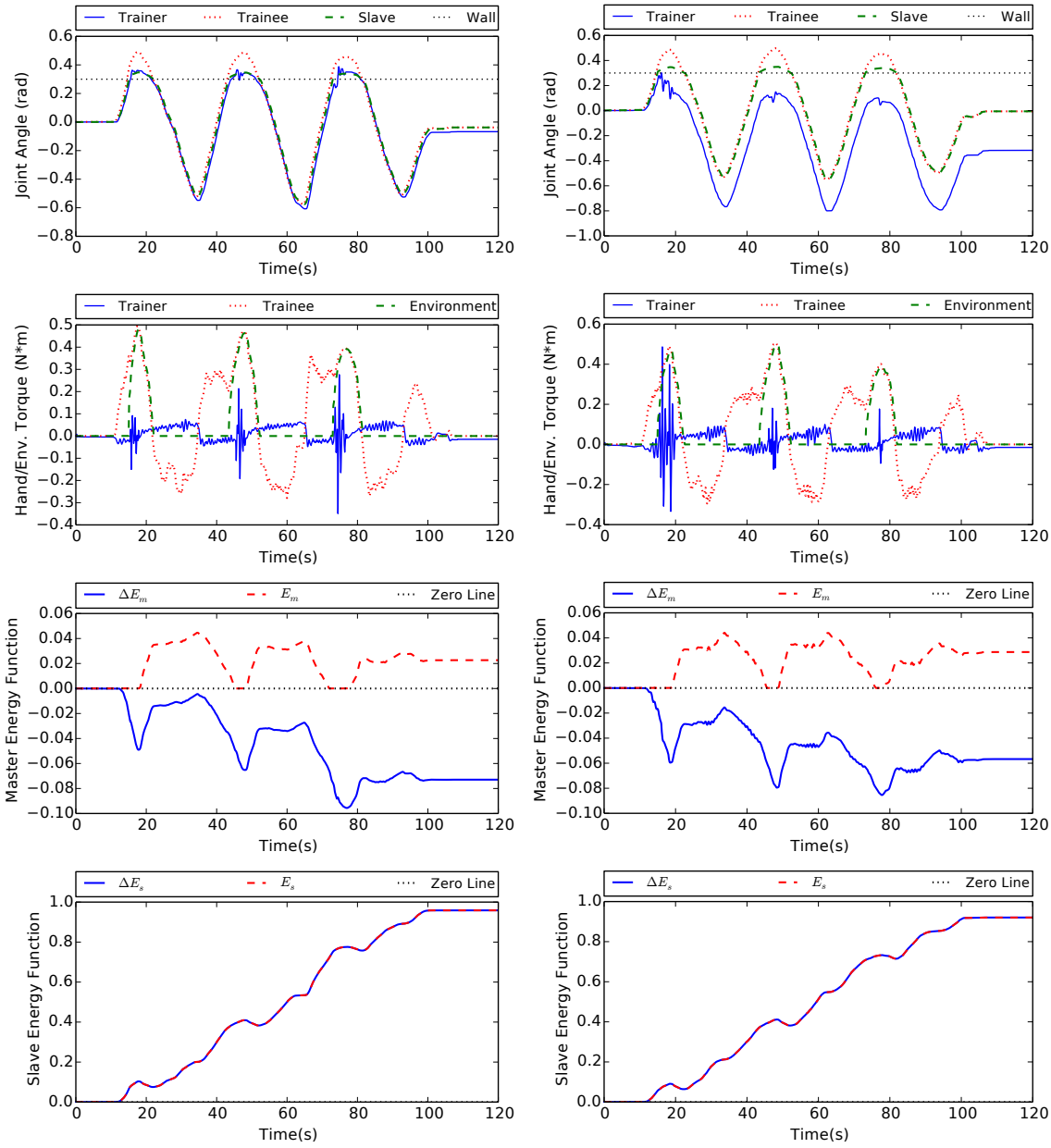

Figure 6-9: Wall contact case: position tracking, force tracking, masters and slave side energy functions when $\alpha = 0$ (Left: $\tau = 1$ms, Right: $\tau = 100$ms).

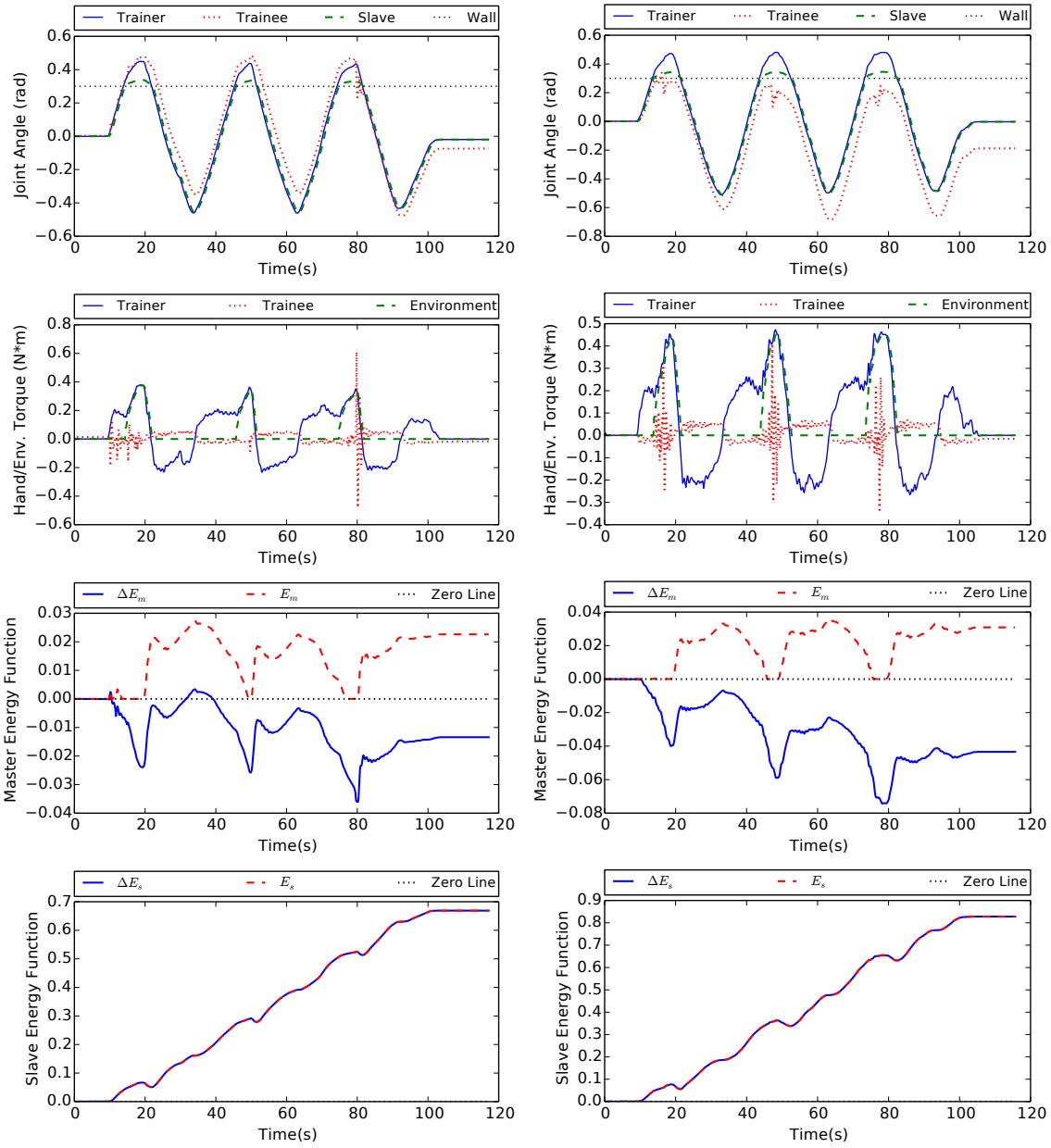

Figure 6-10: Wall contact case: position tracking, force tracking, masters and slave side energy functions when $\alpha = 1$ (Left: $\tau = 1$ms, Right: $\tau = 100$ms).

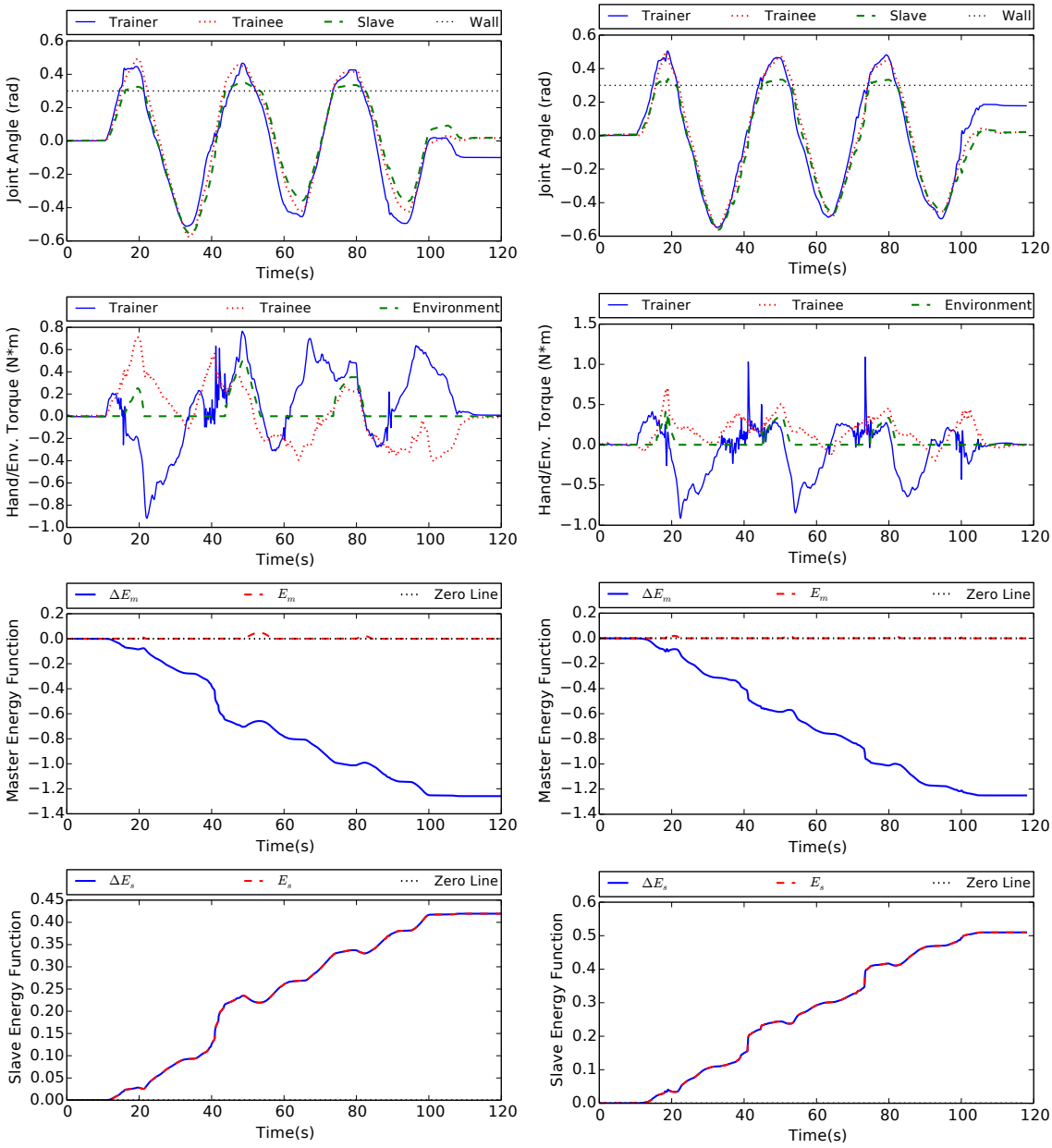

Figure 6-11: Wall contact case: position tracking, force tracking, masters and slave side energy functions when $\alpha = 0.5$ (Left: $\tau = 1$ms, Right: $\tau = 100$ms).

6.7 Conclusion

In this Chapter, we conducted a preliminary study of dual-user haptic system with constant time delays. By introducing the Augmented Wave Variable Transformation (AWVT), we enhanced the shared control authority mechanism. It could demonstrate that the passivity of this new system could be checked through a closed-loop model with port-Hamiltonian formulation. Since the dynamic model of the robot is not always available, another approach for passivity checking is based on the AWVT communication channel. The passivity condition is formed into a less conservative condition, by relating the energy transfered into the shared control structure with the wave variables, at both the master sides and the slave side. As long as the parameters are set properly, the passivity is guaranteed. Finally, an example is provided as a guideline for parameters configuration. Real-time experiments were conducted to validate the proposed scheme. Both the free motion and the wall contact cases were studied. Further efforts should be provided to solve the position drift issue revealed in the experimental results. Moreover, the impact of variable communication delays the proposed architecture should be considered.

Chapter 7

Conclusion and Future Directions

Simulation for hands-on training has appeared two decades ago but it starts to democratize only nowadays. It fulfills requirements for less training time which cause dangerous situations, notably in medical fields where residents end up their curricula by practicing on real patients. It is also a technological response to a lack of realism of classical hardware simulators (cadavers, pigs, latex manikins, ... to remain in the medical field) which are qualified as low fidelity simulators. However, even though it helps trainees to autonomously acquire gesture skills, actual simulators do not offer a satisfactory way to transpose a fellowship training (or supervised training) where trainer and trainee tightly collaborate. Indeed, the trainer generally has access to some information about the simulation of this trainee through a monitor but only one person has access to the (haptic) interface at any moment. Therefore, the trainer cannot show, apply corrections, accompany, ... the trainee making gestures, particularly in complex and/or unforeseen situations not managed by the simulator itself. Consequently, we addressed this issue by establishing at first a requirement specification of the expected behavior of this kind of simulator which led us to consider these four questions:

- **Q1**: How to enable both the trainer and trainee to simultaneously perform gestures with same tools in a common task ?
- **Q2**: How, by way of a controller, to guarantee the stability of the system?

- **Q3**: What are the performances of the designed system?
- **Q4**: What happens if both users and the slave are away from each other ?

We then conducted a survey concerning the haptic systems (Chapter 2). Depending on the number of users, one finds bilateral systems and multilateral systems (and more particularly dual-user systems). The latter ones correspond to our needs. We analyzed their design and properties to check more precisely the compliance to our requirements. At first, As for bilateral teleoperation systems, theses systems design has to establish a trade-off between *stability* and *transparency*. Also, most of dual-user systems use a concept of **shared control**, by introducing a dominance factor α which represents the authority of each user over the tool. We could conclude that no existing dual-user system matched all of our haptic training simulator requirements. So we reused and adapted the interesting concepts of existing ones for the design of our system.

The first contribution was introduced in Chapter 3. A new dual-user haptic system architecture based on a novel Energy Shared Controller (ESC) is introduced. The whole design approach is modular, by proposing authority sharing mechanism, adding compliance and providing full feedback to both users, for a one-degree-of-freedom system. The port-Hamiltonian approach is employed to model the global closed-loop system. To study the passivity of the system (to ensure stability), two different aspects are considered, i.e., from both the closed-loop system and subsystems point of view. As a conclusion, the designed architecture fulfills our training system requirements and answers to questions **Q1** and **Q2**, for a local use (no communication delay between the trainee, trainer and slave robot).

Chapter 4 was dedicated to authority management: an Adaptive Authority Adjusting (AAA) mechanism is introduced. It is based on the concept of Guidance Virtual Fixtures (GVFs) yet developed in bilateral teleoperation. The introduction of the AAA mechanism does not violate the passivity of the closed-loop system. Real-time experiments conclude that this mechanism benefits to both the trainee and the trainer: the trainer can notify to the trainee about undesired gestures and he may

react quickly without having to manually acquire the authority over the slave. To conclude, the AAA mechanism is a complementary answer to the questions **Q1** and **Q2**.

In order to show the interest of this new architecture compared to existing ones, we performed a comparative study, detailed in Chapter 5. We compared it with two dual-user architectures: CLC and MCET both introduced in [Khademian and Hashtrudi-Zaad, 2011]. A position tracking study was carried out and shows that our scheme is competitive compared to the two other ones. Various control authorities and desired trajectories were tested. It reveals that the performances of the ESC scheme is competitive with the other ones in terms of position tracking. In addition, ESC enables full force feedback for both users, which is not possible with the two other ones. There is no need for stability analysis since the system is passively controlled, as well the cases in presence of non-linear system models and unknown robot dynamics. Hence, this study answers question **Q3**.

Concerning the teleoperated case of the system, where users are away from each other, time delays may appear inside the communication channel, which potentially would degrade the transparency and even destabilize the system. A preliminary study of an enhancement of the ESC architecture to cope constant time delays is conducted in Chapter 6. In this study, we covered the stability issue (using passivity analysis), but also we tried to take into account the transparency. As a solution, we proposed to embed the Augmented Wave Variable Transformation (AWVT) into the system, accompanied with an enhanced passivity controller to ensure the system passivity. An example of configuration was proposed to obtain a good trade-off between passivity and transparency. The proposals have been validated through real-time experiments, in consideration of free motion and wall contact cases, under constant delays. We could conclude that the system behaves as predicted except for a position drift which occurs between users and slave. As a conclusion, this chapter provides an architecture to answer question **Q4**, when constant time delays are present.

To sum up, these contributions have brought a solid and extensible start of solution to fulfill the haptic dual-user training system. To go further, several tracks will have

to be deepened:

Multiple degree of freedom (dof): the model will have to be extended to multiple dof of haptic interfaces. For instance, this scheme could be duplicated for each new degree of freedom as long as there is no coupling between them. A low level control law with nonlinear decoupling could be used to help in this approach. A cartesian space based controller should also be studied to deal with haptic interfaces and slave robot with different kinematics.

Time varying delays: In Chapter 6, the considered time delays were constant. As time varying delays are present on Internet connections, this aspect will have to be studied. Also, the transparency will have to be enhanced by avoiding the position drifts.

Transparency analysis: Transparency is not explicitly defined in this thesis. We assess it implicitly through the fidelity feedback and feed-forward of power variables (i.e., position and force, see Eq. 6.15 and Eq. 6.16). Thus, other transparency definitions could be also studied, such as the ones reviewed in Section 2.4.5.

End-user study: The validating experimental and comparative studies only study the position and force tracking performances. Yet, they does not prove that this system is more efficient for training than others. An end-user experimental study should be performed to analyze this kind of performance and to conclude on the real interest of this system.

Appendix A

Appendix A: Fundamental Concepts and Tools

A.1 Physical Modeling and Bond Graph

The bond graph theory of modeling physical system was invented by Paynter in [Paynter, 1961]. The fundamental idea of a bond graph is that a large class of physical system could be modeled by a set of interconnected components, which characterized by energetic behaviors. The power is transmitted between the *power port* (see Definition A.1) through two variables called *power conjugated variables*, by means of a inner product operation. They are generically named *efforts* and *flows*. The energy signals in mechanical domain are described in Table A.1.

Table A.1: Energy signals in different energy domains

Signal	**Mechanical System**	
	Translation	Rotation
Effort e	Force (N)	Torque ($\mathrm{N} \cdot \mathrm{m}$)
Flow f	Linear Velocity (m/s)	Angular Velocity (rad/s)
Generalized Momentum $p = \int e\mathrm{dt}$	Momentum ($\mathrm{kg} \cdot \mathrm{m/s}$)	Angular Momentum ($\mathrm{kg} \cdot \mathrm{m}^2/\mathrm{s}$)
Generalized Displacement $q = \int f\mathrm{dt}$	Position (m)	Angle (rad)

Definition A.1 (**Power Port**, see e.g., [Macchelli, 2003])**.** *Let $\mathcal{F}$ and $\mathcal{E}$ be the flow and effort vector. A power port is defined as $\mathcal{P} = \mathcal{F} \times \mathcal{E}$. Given $f \in \mathcal{F}$ and $e \in \mathcal{E}$, the product $\langle e, f \rangle$ is called the power, where $\langle , \rangle$ is the inner product operation in mathematics.*

Figure A-1: Example of a mass-spring system (left), and the bond graph representation (right).

As an example illustrated in Fig. A-1, we consider the mass-spring system, where the mass is given by m and interconnected with a spring of stiffness k. Suppose x denotes the spring deformation and p is the mass momentum (state variables), then the two elements can be modeled by the following dynamical systems:

$$\Sigma_m : \begin{cases} \dot{p} = F \\ y = \dfrac{p}{m} = v \end{cases} \qquad \Sigma_s : \begin{cases} \dot{x} = v \\ y = -kx = F \end{cases} \tag{A.1}$$

where Σ_m is the mass model and Σ_s is the spring model, and F represents the force (*effort*) applied to the mass , v is the velocity (*flow*) of the mass. Thus the power port of it can be given as (F, v), by leading the *power* as:

$$P = F \cdot v \tag{A.2}$$

Consequently, the power is exchanged through the interaction port formed by the two subsystems, i.e., mass and spring [Macchelli, 2003].

Remark. The following points in Fig. A-1 should be noted [Macchelli, 2003]:

- Both an *effort* and a *flow* form a *bond* that represents a power interconnection.
- The half-arrow gives the positive direction of power. It doesn't indicate the positive direction of neither the effort nor the flow. If $P > 0$, it means the

power is transmitted from the mass to the spring. If $P > 0$, the power from the spring to the mass is present.

- The red vertical line in Fig. A-1 denotes causality, i.e., the direction of the *effort* is specified. Accordingly, the direction of the *flow* is the opposite one.

Generally speaking, physical system interconnections could be modeled in view of energetic approach. It is possible to track the energy flows and power variables explicitly, which could be used for passivity analysis in the following sections.

A.2 Passive System and Passivity

A.2.1 Passive of Nonlinear System

Consider an input-output affine nonlinear system given by:

$$\begin{cases} \dot{x} = f(x) + g(x)u \\ y = h(x) \\ f(x_0) = 0, x_0 = 0 \end{cases} \tag{A.3}$$

where $x \in \mathbb{R}^n$ is the state space, $u \in \mathbb{R}^m$ is the input space and $y \in \mathbb{R}^m$ is the output space. Moreover, f, g and h are *smooth* mappings, with initial condition: $f(x_0) = 0, x_0 = 0$.

Definition A.2 (**Supply rate**, [Willems, 1972]). *The function $w : u \times y \to \mathbb{R}$, for all $t_0, t_1 \in \mathbb{R}$ satisfied*

$$\int_{t_0}^{t_1} |w(u(t), y(t))| \mathrm{dt} < \infty \tag{A.4}$$

is defined as supply rate.

Definition A.3 (**Dissipative system**, see e.g., [Willems, 1972]). *System A.3 is said to be dissipative if there is a nonnegative function $V : x \to \mathbb{R}^+$, called storage function*

and a supply rate $w : u \times y \to \mathbb{R}$*, such that, for all* u *and* $t \geq 0$

$$V(x(t)) - V(x_0) \leq \int_0^t w(u, y)\mathrm{dt}. \tag{A.5}$$

where $x(t)$ is a solution of Eq. A.3. When a specific supply rate is chosen, the passive system can be defined as:

Definition A.4 (**Passive system**, see e.g., [Byrnes et al, 1991])**.** *System A.3 is passive if it is dissipative with the supply rate* $w(u, y) = \langle u, y \rangle = y^T u$ *and if the storage function satisfies* $V(0) = 0$*.*

If the storage function $V(x(t))$ is differentiable, we can write as,

$$\dot{V}(x(t) \leq u^T y \tag{A.6}$$

Passivity, thus, is the property that the rate of increase of storage (energy) is not higher than the scalar product between the input and the output (power, as given in Section A.1). In other words, a passive system respects that the energy supplied is either stored or dissipated. There is no production of extra power inside it.

Remark. The system A.3 is said to be **lossless** if the equality in Eq. A.6 is true.

Many researches on the stability analysis of the passive systems have been carried out. For instance, in [Byrnes et al, 1991], the *Kalman-Yakubovitch-Popov* (KYP) lemma is introduced to analyze the stability.

Definition A.5 (**KYP property**, see e.g., [Byrnes et al, 1991])**.** *A non linear system represented by Eq. A.3 has the Kalman-Yakubovitch-Popov (KYP) property if there exists a non negative function* $V(x) \to \mathbb{R}^+$*, with* $V(0) = 0$ *such that:*

$$\begin{aligned} L_f V(x) &\leq 0 \\ L_g V(x) &= h^T(x) \end{aligned} \tag{A.7}$$

for each $x \in \mathbb{R}^n$*.*

Theorem A.1 (see e.g., [Byrnes et al, 1991]). *A system has the KYP property is passive. Conversely, if a system is passive with a storage function, it has the KYP property.*

A.3 Port-Hamiltonian Systems

Port-Hamiltonian systems are defined on the state space of $x \in \mathbb{R}^n$, characterized by an Hamiltonian energy function $H : x \mapsto \mathbb{R}$ corresponding to the stored energy, and by a Dirac structure (one of the representation is skew-symmetric matrix, see [Maschke and van der Schaft, 1992]), representing internal energetic interconnections. These systems exchange energy through the so-called *power ports* that are represented by a pair of power variables: effort and flow, e.g. (u, y). The power exchanged through them is $y^T u$.

Definition A.6 (**Port-Hamiltonian System**, [Maschke and van der Schaft, 1992]). *The input-state-output port-Hamiltonian system model is defined as:*

$$\begin{cases} \dot{x} = [J(x) - R(x)]\dfrac{\partial H}{\partial x} + G(x)u \\ y = G^T(x)\dfrac{\partial H}{\partial x} \end{cases} \tag{A.8}$$

where $x = (x_1, x_2, ..., x_n)^T \in \mathbb{R}^n$ is the state vector, $J(x) = -J^T(x)$ is a skew-symmetric matrix representing Dirac structure, $R(x) = R^T(x) \geq 0$ specifies the energy dissipation symmetric, positive semidefinite, due to dampers, viscosity, resistors, etc.), $G(x)$ is a matrix representing the way the power is exchanged through the power ports formed by input-output pair (u, y) between the system and its environment, and H is the Hamiltonian function.

A.3.1 Passivity of port-Hamiltonian System

Proposition 2. *The port-Hamiltonian system in Eq. A.8 with dissipation and Hamiltonian function as storage function, is passive.*

By straightforward calculation, we could obtain:

$$\frac{dH}{dt} = -\underbrace{\frac{\partial^T H}{\partial x} R(x) \frac{\partial H}{\partial x}}_{P_{diss}} + y^T u \leq y^T u \tag{A.9}$$

then, by integration, it can be deduced that,

$$H(x(t)) - H(x(0)) \leq \int_0^t y(\tau)^T u(\tau) \mathrm{d}\tau \tag{A.10}$$

where $P_{diss} \geq 0$ is the energy dissipated. Regarding Eq. A.6, it could be easily concluded that port-Hamiltonian system with dissipation is passive, and Hamiltonian function is the storage function.

A.3.2 Interconnection of port-Hamiltonian System

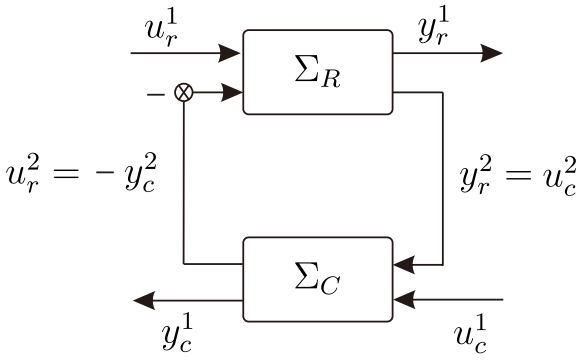

Figure A-2: Interconnection of Port-Hamiltonian System

Considering two port-Hamiltonian systems Σ_R and Σ_C, shown in Figure A-2, the power preserving interconnection (Dirac structures with skew-symmetric matrix) can be represented as:

$$\begin{pmatrix} u_c^2 \\ u_r^2 \end{pmatrix} = \begin{pmatrix} 0 & 1 \\ -1 & 0 \end{pmatrix} \begin{pmatrix} y_c^2 \\ y_r^2 \end{pmatrix} \tag{A.11}$$

where

$$\begin{cases} \dot{x_i} = (J_i - R_i)\dfrac{\partial H_i}{\partial x_i} + \begin{pmatrix} g_i^1 & g_i^2 \end{pmatrix} \begin{pmatrix} u_i^1 \\ u_i^2 \end{pmatrix} \\ \begin{pmatrix} y_i^1 \\ y_i^2 \end{pmatrix} = \begin{pmatrix} g_i^1 & g_i^2 \end{pmatrix}^T \dfrac{\partial H_i}{\partial x_i} \end{cases} \quad i = r, c \tag{A.12}$$

The interconnection of these two port-Hamiltonian systems can be proved and leads to a new global port-Hamiltonian system, as follows:

$$\begin{aligned} \dot{x} &= (J - R)\frac{\partial H}{\partial x} + gu \\ y &= g^T \frac{\partial H}{\partial x} \end{aligned} \tag{A.13}$$

where $x = (x_r, x_c)^T$, $H = H_r + H_c$ is the sum of the energies of the two systems and

$$J = \begin{pmatrix} J_r & -g_r^2(g_c^2)^T \\ g_c^2(g_r^2)^T & J_c \end{pmatrix} \qquad R = \begin{pmatrix} R_r & 0 \\ 0 & R_c \end{pmatrix} \qquad g = \begin{pmatrix} g_r^1 & 0 \\ 0 & g_c^1 \end{pmatrix} \tag{A.14}$$

It means that the interconnected system holds all the properties of the two previous port-Hamiltonian systems.

More generally, the interconnected n port-Hamiltonian systems $\Sigma_i, i = 1, 2, .., n$ yields a new formed port-Hamiltonian system with the power preserving interconnection. The global port-Hamiltonian system has $H = H_1 + H_2 + ... + H_n$, and the power preserving interconnection is determined by the structures of n port-Hamiltonian systems.

A.3.3 IPC Controller

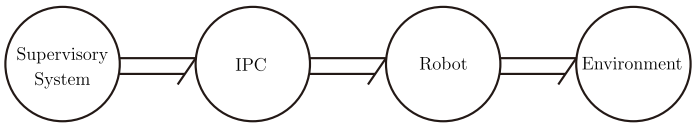

Figure A-3: General intrinsically passive control, from [Secchi et al, 2007]

Many physical systems are passive and can be modeled as port-Hamiltonian sys-

tems. Considering a passive physical system to be controlled, if we find a controller which is by itself passive, it is possible to have the controlled system passive with and without contact with any passive environment. It preserves the passivity through the power preserving interconnection of Section A.3.2. This kind of controller, entitled Intrinsically Passive Controller (IPC), has been proposed at first in [Stramigioli, 2001, 1996]. Its scheme is shown in Figure A-3. Since the IPC can only shape the dynamics of physical elements (even be modeled virtually), but cannot generate energy by itself, so it is intrinsically passive. It only affects the performance of the controlled system but **NEVER** passivity, whatever the characteristics of the system and the controller parameters be. Its parameters can be changed in real time for better performances.

The IPC controller can be built as a physical system which could be modeled with port-Hamiltonian formalism. An example of IPC proposed by Stramigioli [Stramigioli, 1996] is shown in Figure A-4. It is a one dimensional case and can be easily extended to multidimensional cases. The virtual mass m_c provides some internal kinetic energy, and the damper b_1 is the element that dissipates the energy. The energy received from the supervisory system is transmitted through the springs k_i, k_c and virtual mass m_c, to the mass robot. A damper b_1 is also connected to the controller whereas dissipation is introduced. The damped behaviors avoid overshooting and other undesirable oscillatory effects. Thus the IPC can only supply the energy stored in the virtual mass, which is limited. Unlike other types of controllers (for instance, PD-controller), they can draw from an infinite supply of energy. Therefore, passivity of the IPC controller is ensured intrinsically.

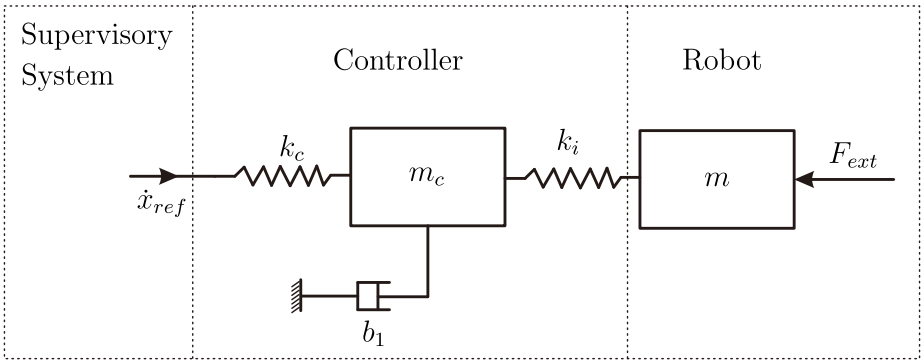

Figure A-4: IPC controller proposed in [Stramigioli, 1996]

In his studies [Secchi et al, 2007], Secchi applied the IPC into bilateral teleoperation systems. He added a damper b_2 to the Stramigioli's IPC (shown in Figure A-5) to compensate *wave reflections*. This phenomenon is caused by the use of scattering transformations used to passify the communication channel in presence of delays (see Section 6.2.1).

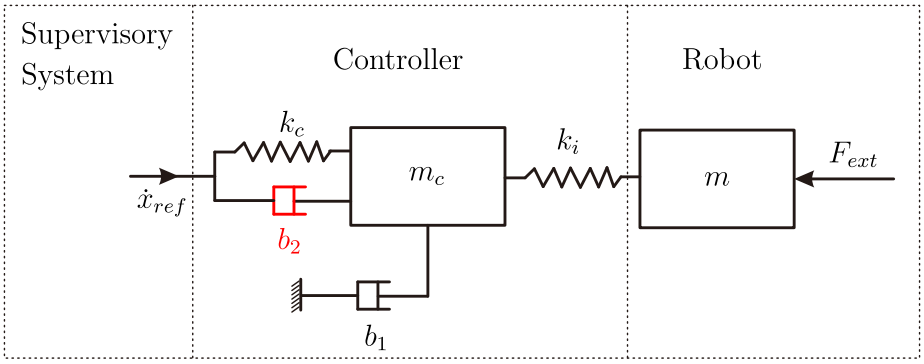

Figure A-5: IPC controller proposed in [Secchi et al, 2007]

The IPC controllers used in our ESC dual-user system in Chapter 3, is modeled in port-Hamiltonian formalism. The robot and controller here (by taking 1-DoF for example) is described in mechanical rotation domain using bond graph representation (see Section A.1) as following:

Master IPC

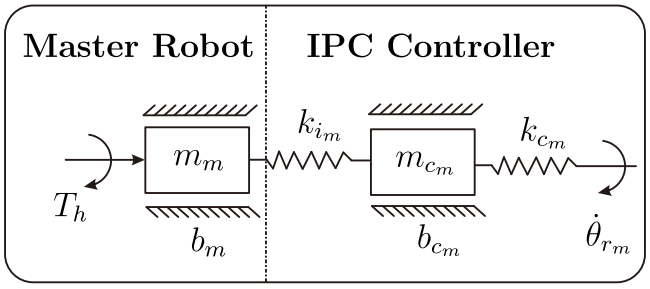

Figure A-6: Master IPC controller described in rotation case.

Fig. A-6 shows the IPC controller proposed by Stramigioli redrawed with a rotation model. The bond graph representation of master robot and IPC controller are given in Fig. A-7. Through it, the models of the robot and IPC controller in

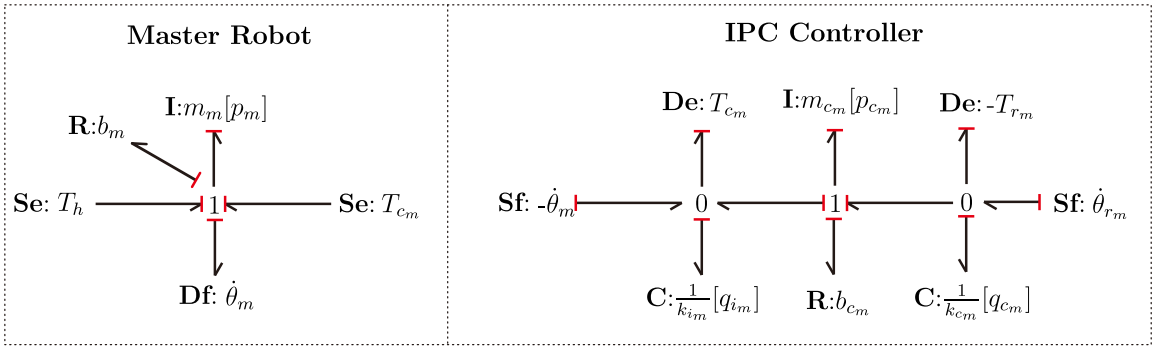

Figure A-7: Bond graph representation of master robot and IPC controller

port-Hamiltonian framework are:

$$\text{Master Robot}: \begin{pmatrix} \dot{\theta}_m \\ \dot{p}_m \end{pmatrix} = \begin{pmatrix} 0 & 1 \\ -1 & b_m \end{pmatrix} \begin{pmatrix} 0 \\ \frac{p_m}{m_m} \end{pmatrix} + \begin{pmatrix} 0 & 0 \\ 1 & 1 \end{pmatrix} \begin{pmatrix} T_h \\ T_{c_m} \end{pmatrix} \\ \begin{pmatrix} \dot{\theta}_m \\ \dot{\theta}_m \end{pmatrix} = \begin{pmatrix} 0 & 1 \\ 0 & 1 \end{pmatrix} \begin{pmatrix} 0 \\ \frac{p_m}{m_m} \end{pmatrix} \tag{A.15}$$

$$\text{Controller}: \begin{pmatrix} \dot{q}_{c_m} \\ \dot{p}_{c_m} \\ \dot{q}_{i_m} \end{pmatrix} = \begin{pmatrix} 0 & -1 & 0 \\ 1 & -b_{c_m} & -1 \\ 0 & 1 & 0 \end{pmatrix} \begin{pmatrix} k_{c_m} q_{c_m} \\ \frac{p_{c_m}}{m_{c_m}} \\ k_{i_m} q_{i_m} \end{pmatrix} + \begin{pmatrix} 0 & 1 \\ 0 & 0 \\ 1 & 0 \end{pmatrix} \begin{pmatrix} -\dot{\theta}_m \\ \dot{\theta}_{r_m} \end{pmatrix} \\ \begin{pmatrix} T_{c_m} \\ -T_{r_m} \end{pmatrix} = \begin{pmatrix} 0 & 0 & 1 \\ 1 & 0 & 0 \end{pmatrix} \begin{pmatrix} k_{c_m} q_{c_m} \\ \frac{p_{c_m}}{m_{c_m}} \\ k_{i_m} q_{i_m} \end{pmatrix} \tag{A.16}$$

where θ_m, p_m are the joint position and moment of mass robot; p_{c_m} is moment of mass m_{c_m}; q_{c_m}, q_{i_m} are the rotated displacement of spring with stiffness k_{c_m}, k_{i_m}; b_m, b_{c_m} are the damping elements; T_h, T_{c_m}, T_{r_m} are the human torque, control torque and reference reaction torque, respectively; and $\dot{\theta}_{r_m}$ is the reference position from the slave side.

Slave IPC

The slave controller of ESC structure (see Fig. 3-3) leads to a different causality than the one of master. That is, the slave controller inputs torque and outputs velocity, while the master controller inputs velocity and outputs torque. In order to fit the causality requirement, we gives a different model for slave IPC controller, as shown in Fig. A-8, and a bond graph representation in Fig. A-9.

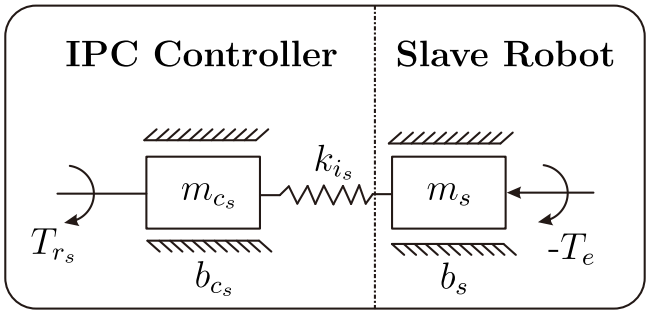

Figure A-8: Slave IPC controller described in rotation case.

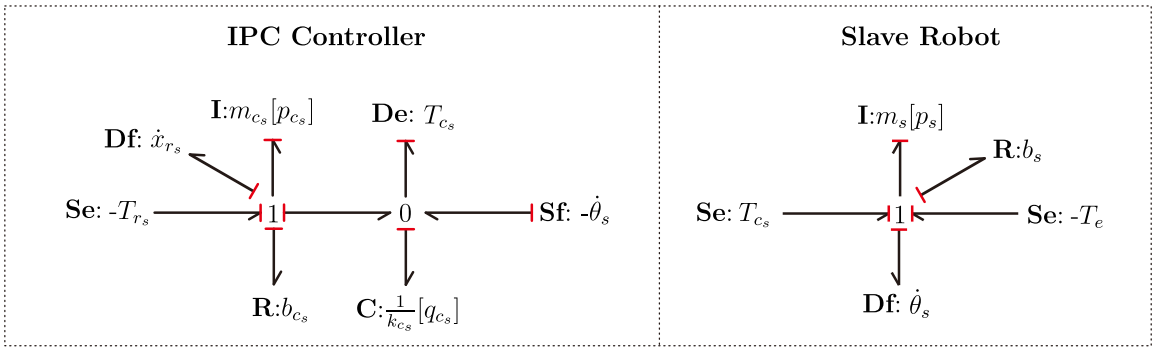

Figure A-9: Bond graph representation of master robot and IPC controller

The model of the slave robot and IPC controller in port-Hamiltonian framework is given as:

$$\text{Slave Robot}: \begin{pmatrix} \dot{\theta}_s \\ \dot{p}_s \end{pmatrix} = \begin{pmatrix} 0 & 1 \\ -1 & b_s \end{pmatrix} \begin{pmatrix} 0 \\ \frac{p_s}{m_s} \end{pmatrix} + \begin{pmatrix} 0 & 0 \\ 1 & 1 \end{pmatrix} \begin{pmatrix} -T_e \\ T_{c_s} \end{pmatrix} \tag{A.17}$$
$$\begin{pmatrix} \dot{\theta}_s \\ \dot{\theta}_s \end{pmatrix} = \begin{pmatrix} 0 & 1 \\ 0 & 1 \end{pmatrix} \begin{pmatrix} 0 \\ \frac{p_s}{m_s} \end{pmatrix}$$

$$\text{Controller}: \begin{pmatrix} \dot{p}_{c_s} \\ \dot{q}_{i_s} \end{pmatrix} = \begin{pmatrix} -b_{c_s} & -1 \\ 1 & 0 \end{pmatrix} \begin{pmatrix} \frac{p_{c_s}}{m_{c_s}} \\ k_{i_s} q_{i_s} \end{pmatrix} + \begin{pmatrix} 0 & 1 \\ 1 & 0 \end{pmatrix} \begin{pmatrix} -\dot{\theta}_s \\ -T_{r_s} \end{pmatrix} \quad (A.18)$$
$$\begin{pmatrix} T_{c_s} \\ \dot{\theta}_{r_s} \end{pmatrix} = \begin{pmatrix} 0 & 1 \\ 1 & 0 \end{pmatrix} \begin{pmatrix} \frac{p_{c_s}}{m_{c_s}} \\ k_{i_s} q_{i_s} \end{pmatrix}$$

where θ_s, p_s are the joint position and moment of mass robot; p_{c_s} is moment of mass m_{c_s}; q_{i_s} is the rotated displacement of spring with stiffness k_{i_s}; b_s, b_{c_s} are the damping elements; T_e, T_{c_s}, T_{r_s} are the environment torque, slave control torque and reference reaction torque, respectively; and $\dot{\theta}_{r_s}$ is the reference position from the master side.

A.4 Port-Hamiltonian Representation of ESC Dual-User System

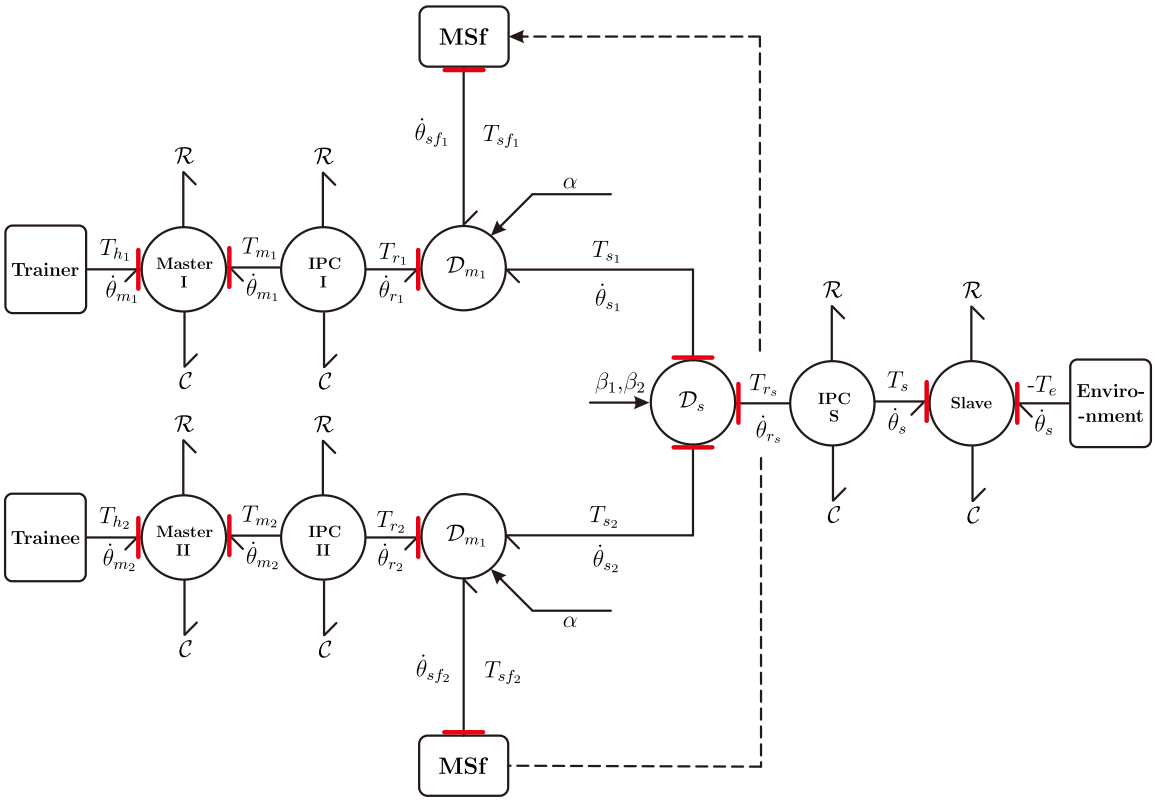

Figure A-10: Port-Hamiltonian representation of ESC dual-user system using bond graphs

The ESC dual-user system is shown in Fig. A-10 in a port-Hamiltonian representation (using bond graphs). The trainer and trainee interact with the system via the power ports of the master haptic interfaces which are formed by $(T_{h_1}, \dot{\theta}_{m_1})$ and $(T_{h_2}, \dot{\theta}_{m_2})$. On the other side, the slave haptic interface interacts with the environment through the power port formed by $(-T_e, \dot{\theta}_s)$. Both the masters and the slave are locally controlled by IPC (see above sections). The masters, the slave, and the IPC controllers have energy dissipating elements $\mathcal{R}$ and energy storing elements $\mathcal{C}$. The model of this system can be found in Section 3.5.

Appendix B

Appendix B: Experiment Results

B.1 Free Motion Case in Section 6.6.2: $\tau = 10$ms

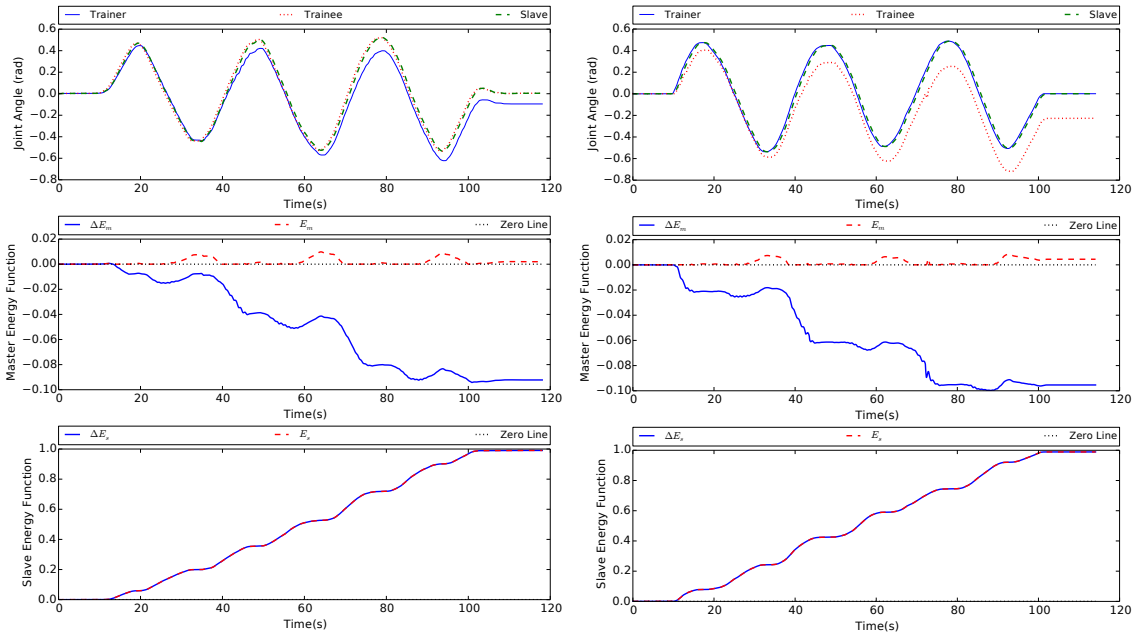

Figure B-1: Free motion case: position tracking, masters and slave side energy functions when $\tau = 10$ms (Left: $\alpha = 0$, Right: $\alpha = 1$).

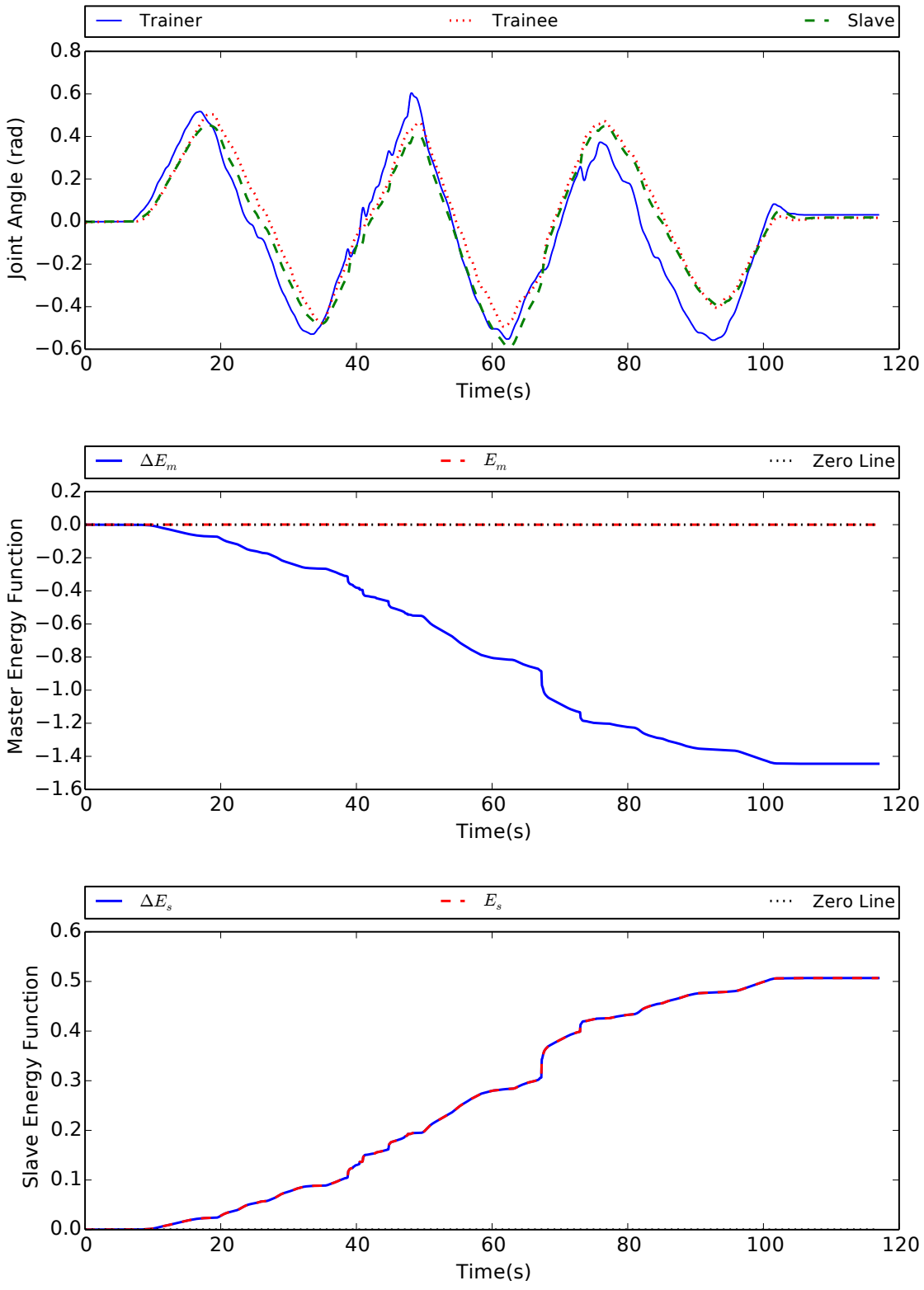

Figure B-2: Free motion case: position tracking, masters and slave side energy functions when $\alpha = 0.5$, $\tau = 10$ms.

B.2 Wall Contact Case in Section 6.6.2: $\tau = 10$ms

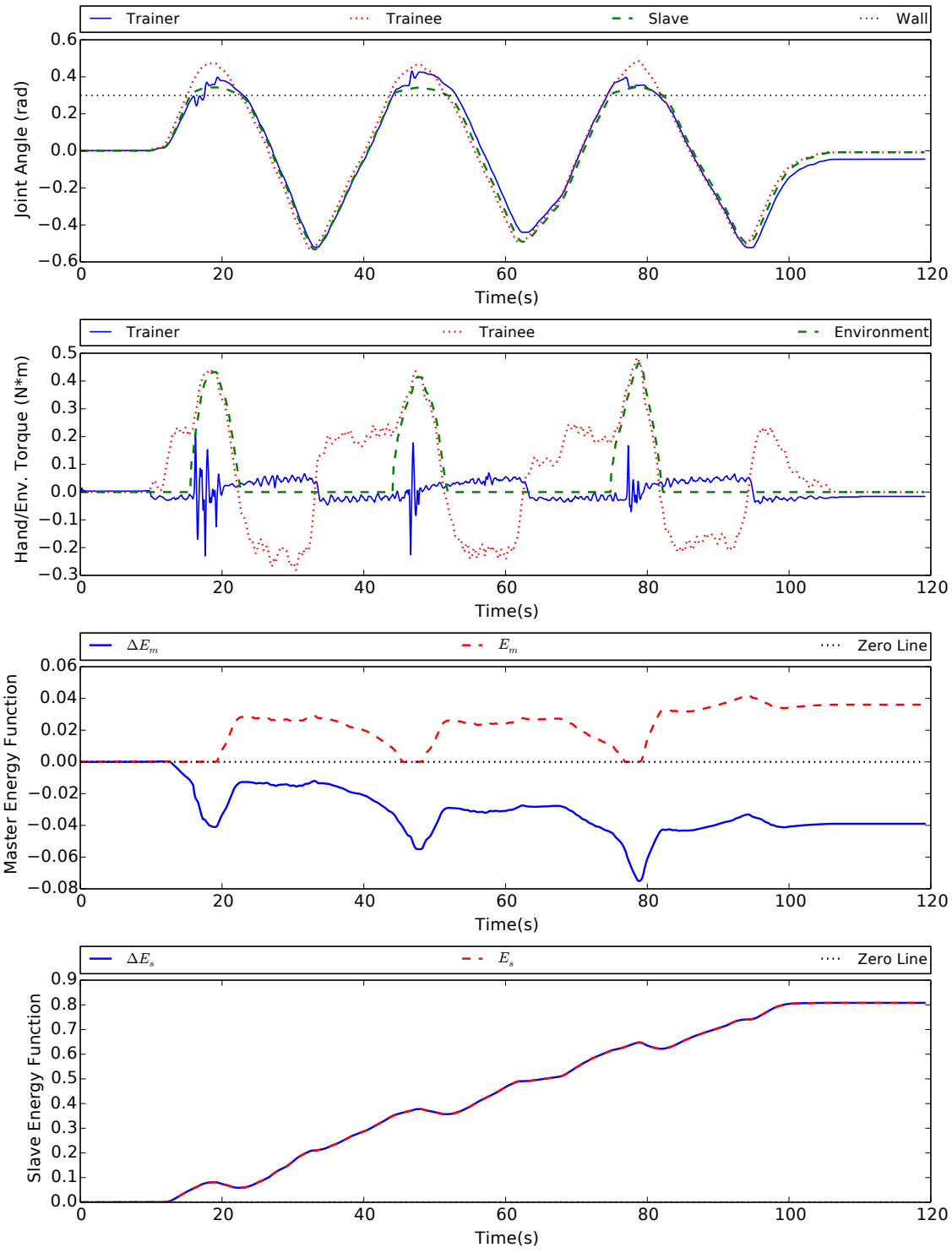

Figure B-3: Wall contact case: position tracking, force tracking, masters and slave side energy functions when $\alpha = 0$, $\tau = 10$ms.

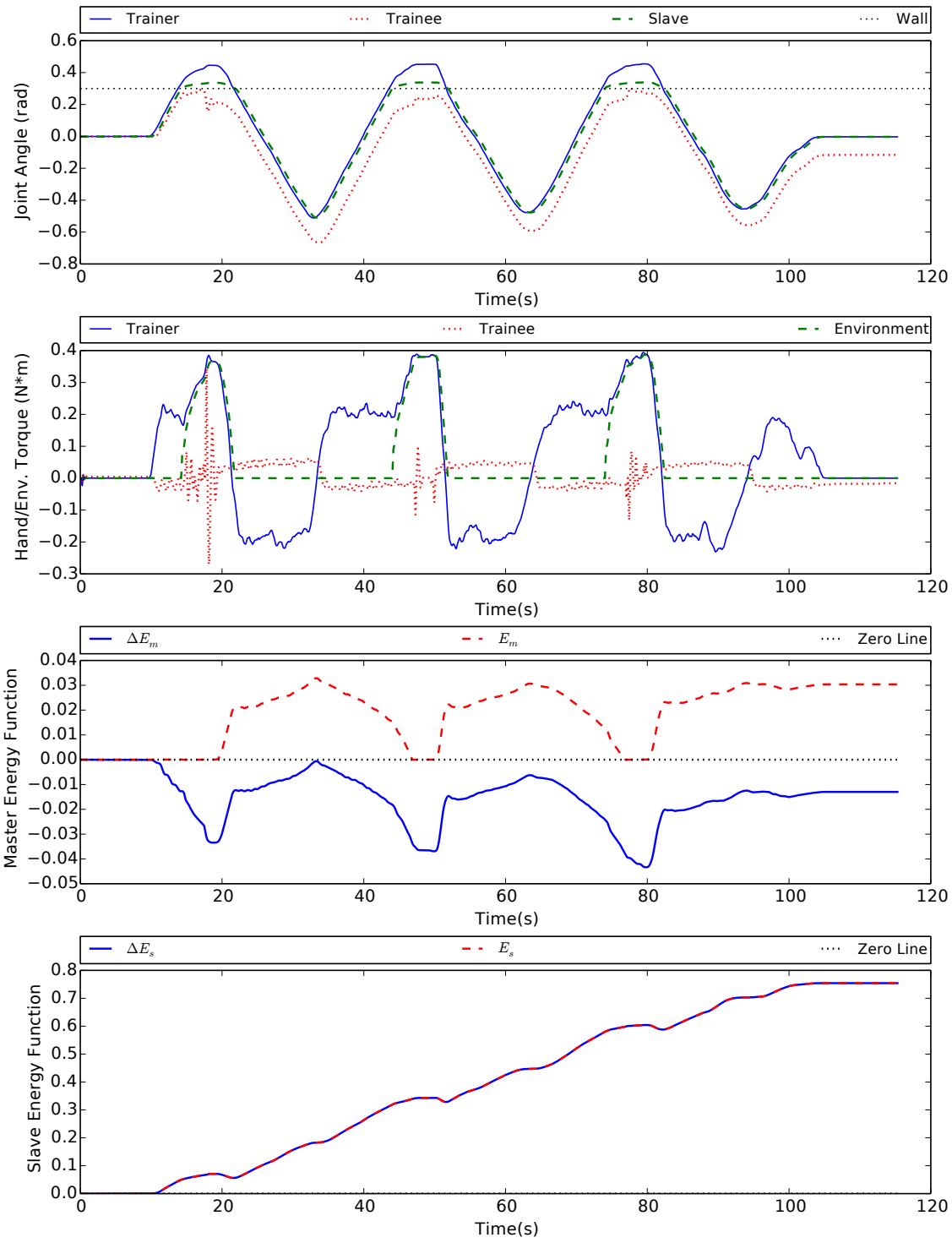

Figure B-4: Wall contact case: position tracking, force tracking, masters and slave side energy functions when $\alpha = 1$, $\tau = 10$ms.

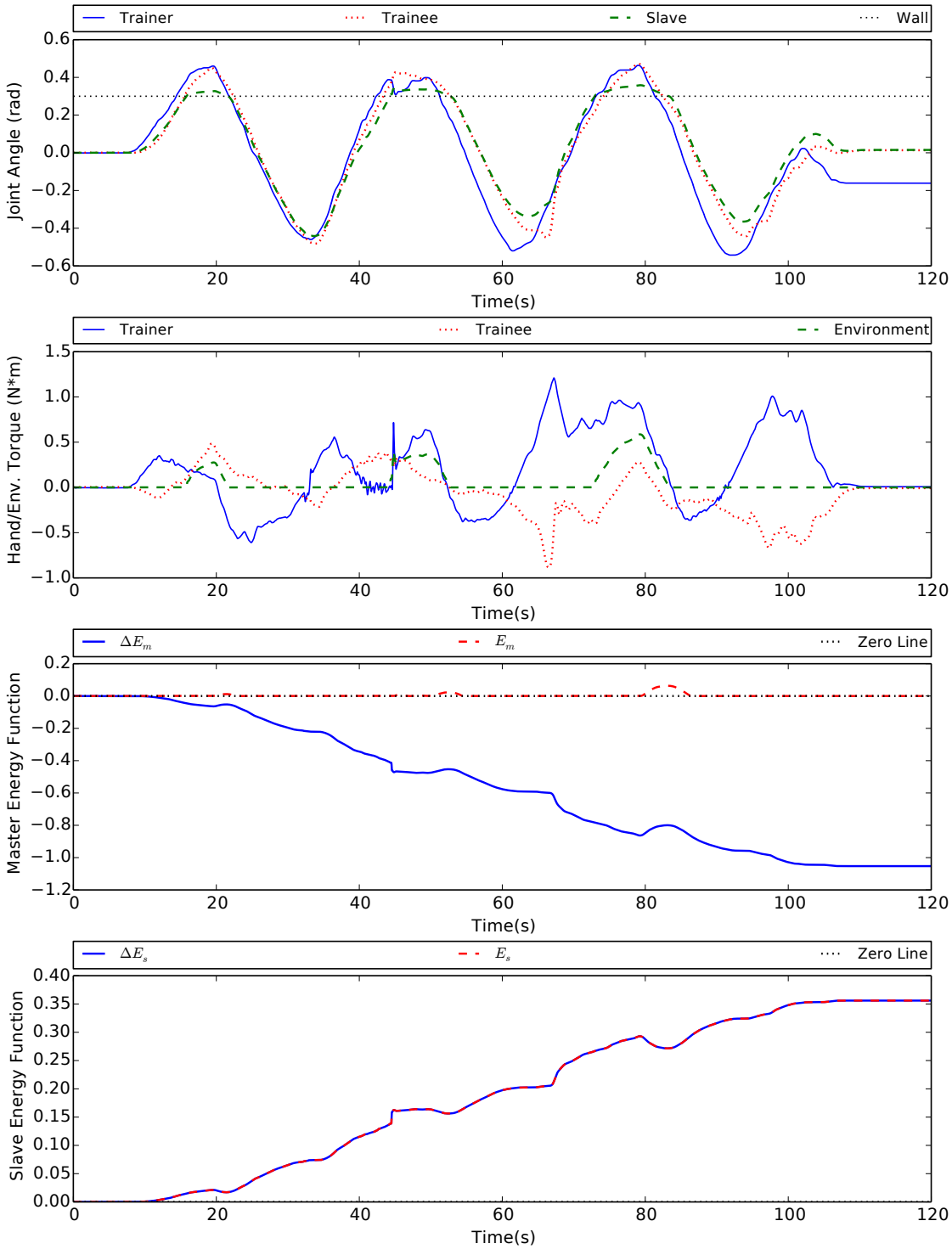

Figure B-5: Wall contact case: position tracking, force tracking, masters and slave side energy functions when $\alpha = 0.5$, $\tau = 10$ms.

Publications

1. **F. Liu**, A. Lelevé, D. Eberard, T. Redarce. An energy based approach for passive dual-user haptic training systems. In: *2016 IEEE/RSJ International Conference on Intelligent Robots and Systems*, Oct. 2016. (Accepted)

2. **F. Liu**, A. Lelevé, D. Eberard, T. Redarce. A dual-user teleoperation system with online authority adjustment for haptic training. In: *2015 37th Annual International Conference of the IEEE Engineering in Medicine and Biology Society (EMBC)*, Aug. 2015, p. 1168-1171

3. **F. Liu**, A. Lelevé, D. Eberard, T. Redarce. A dual-User teleoperation system with adaptive authority adjustment for haptic training. In: *New Trends in Medical and Service Robots: Human Centered Analysis, Control and Design*, Aug. 2016, p. 165-177
   (presented in *4th International Workshop on Medical and Service Robots, MESROB 2015*)

Bibliography

[Abbott et al 2007] Abbott, Jake J. ; Marayong, Panadda ; Okamura, Allison M.: *Robotics Research: Results of the 12th International Symposium ISRR*. Chap. Haptic Virtual Fixtures for Robot-Assisted Manipulation, p. 49–64. Berlin, Heidelberg : Springer Berlin Heidelberg, 2007

[Adams and Hannaford 1999] Adams, R. J. ; Hannaford, B.: Stable haptic interaction with virtual environments. In: *IEEE Transactions on Robotics and Automation* 15 (1999), Jun, No. 3, p. 465–474. – ISSN 1042-296X

[Aldana et al 2014] Aldana, Carlos I. ; no, Emmanuel N. ; nez, Luis B. ; Romero, Eduardo: Operational space consensus of multiple heterogeneous robots without velocity measurements. In: *Journal of the Franklin Institute* 351 (2014), No. 3, p. 1517–1539

[Aliaga et al 2004] Aliaga, I. ; Rubio, A. ; Sanchez, E.: Experimental quantitative comparison of different control architectures for master-slave teleoperation. In: *IEEE Transactions on Control Systems Technology* 12 (2004), Jan, No. 1, p. 2–11

[Anderson and Spong 1989a] Anderson, R. ; Spong, M.W.: Bilateral control of teleoperators with time delay. In: *Automatic Control, IEEE Transactions on* 34 (1989), May, No. 5, p. 494–501

[Anderson and Spong 1989b] Anderson, R. J. ; Spong, M. W.: Bilateral control of teleoperators with time delay. In: *IEEE Transactions on Automatic Control* 34 (1989), May, No. 5, p. 494–501

[Arcara and Melchiorri 2002] Arcara, Paolo ; Melchiorri, Claudio: Control schemes for teleoperation with time delay: A comparative study. In: *Robotics and Autonomous Systems* 38 (2002), No. 1, p. 49–64

[Artigas et al 2010a] Artigas, J. ; Ryu, J. H. ; Preusche, C.: Position drift compensation in time domain passivity based teleoperation. In: *Intelligent Robots and Systems (IROS), 2010 IEEE/RSJ International Conference on*, Oct 2010, p. 4250–4256. – ISSN 2153-0858

[Artigas et al 2010b] Artigas, J. ; Ryu, J. H. ; Preusche, C.: Time Domain Passivity Control for Position-Position Teleoperation Architectures. In: *Presence* 19 (2010), Oct, No. 5, p. 482–497. – ISSN 1054-7460

[Aziminejad et al 2008a] Aziminejad, A. ; Tavakoli, M. ; Patel, R. V. ; Moallem, M.: Transparent Time-Delayed Bilateral Teleoperation Using Wave Variables. In: *IEEE Transactions on Control Systems Technology* 16 (2008), May, No. 3, p. 548–555. – ISSN 1063-6536

[Aziminejad et al 2008b] Aziminejad, A. ; Tavakoli, M. ; Patel, R.V. ; Moallem, M.: Stability and performance in delayed bilateral teleoperation: Theory and experiments. In: *Control Engineering Practice* 16 (2008), No. 11, p. 1329 – 1343

[Baser et al 2012] Baser, O. ; Konukseven, E. i. ; Gurocak, H.: Stability and transparency improvement in haptic device employing both MR-brake and active actuator. In: *2012 IEEE RO-MAN: The 21st IEEE International Symposium on Robot and Human Interactive Communication*, Sept 2012, p. 12–18. – ISSN 1944-9445

[Bate et al 2011] Bate, L. ; Cook, C. D. ; Li, Z.: Reducing Wave-Based Teleoperator Reflections for Unknown Environments. In: *IEEE Transactions on Industrial Electronics* 58 (2011), Feb, No. 2, p. 392–397. – ISSN 0278-0046

[Bejczy and Handlykken 1981] Bejczy, A. K. ; Handlykken, M.: Experimental results with a six-degree-of-freedom force-reflecting hand controller. In: *17th Ann. Conf. on Manual Control*, Oct. 1981, p. 465–477

[Bemporad 1998] Bemporad, A.: Predictive control of teleoperated constrained systems with unbounded communication delays. In: *Decision and Control, 1998. Proceedings of the 37th IEEE Conference on* Volume 2, Dec 1998, p. 2133–2138

[Berkelman and Hollis 2000] Berkelman, Peter ; Hollis, Ralph: Lorentz Magnetic Levitation for Haptic Interaction: Device Design, Performance, and Integration with Physical Simulations. In: *The International Journal of Robotics Research* 19 (2000), July, No. 7, p. 644–667

[Botturi et al 2004] Botturi, D. ; Castellani, A. ; Moschini, D. ; Fiorini, P.: Performance evaluation of task control in teleoperation. In: *Robotics and Automation, 2004. Proceedings. ICRA '04. 2004 IEEE International Conference on* Volume 4, April 2004, p. 3690–3695

[Buerger and Hogan 2010] Buerger, Stephen P. ; Hogan, Neville: *Novel Actuation Methods for High Force Haptics.* In: *Advances in Haptics*, 2010

[Buss et al 2009] Buss, M ; Peer, A ; Schauss, T ; Stefanov, N ; Unterhinninghofen, U ; Behrendt, S ; Leupold, J ; Durkovic, M ; Sarkis, M: Development of a Multi-modal Multi-user Telepresence and Teleaction System. In: *The International Journal of Robotics Research* (2009)

[Buttolo et al 1994] Buttolo, Pietro ; Braathen, Petter ; Hannaford, Blake: Sliding Control of Force Reflecting Teleoperation: Preliminary Studies. In: *PRESENCE* 3 (1994), p. 158–172

[Byrnes et al 1991] Byrnes, C. ; Isidori, A. ; Willems, J.: Passivity, feedback equivalence and the global stabilization of minimum phase nonlinear systems. In: *IEEE Transactions on Automatic Control* 31 (1991), No. 11, p. 1228–1240

[Cavusoglu et al 2001] Cavusoglu, M. C. ; Sherman, A. ; Tendick, F.: Bilateral controller design for telemanipulation in soft environments. In: *Robotics and Automation, 2001. Proceedings 2001 ICRA. IEEE International Conference on* Volume 1, 2001, p. 1045–1052 vol.1. – ISSN 1050-4729

[Chawda and O'Malley 2015] Chawda, V. ; O'Malley, M. K.: Position Synchronization in Bilateral Teleoperation Under Time-Varying Communication Delays. In: *IEEE/ASME Transactions on Mechatronics* 20 (2015), Feb, No. 1, p. 245–253. – ISSN 1083-4435

[Chawda et al 2014] Chawda, V. ; Quang, Ha V. ; O'Malley, M. K. ; Ryu, J. H.: Compensating position drift in Time Domain Passivity Approach based teleoperation. In: *2014 IEEE Haptics Symposium (HAPTICS)*, Feb 2014, p. 195–202. – ISSN 2324-7347

[Coles et al 2011] Coles, T.R. ; Meglan, D. ; N.W., John: The Role of Haptics in Medical Training Simulators: A Survey of the State of the Art. In: *IEEE Transactions on Haptics* 4 (2011), Jan, No. 1, p. 51–66

[Daly and Wang 2014] Daly, J. M. ; Wang, D. W. L.: Time-Delayed Output Feedback Bilateral Teleoperation With Force Estimation for n-DOF Nonlinear Manipulators. In: *IEEE Transactions on Control Systems Technology* 22 (2014), Jan, No. 1, p. 299–306. – ISSN 1063-6536

[Delorme et al 2012] Delorme, S. ; Laroche, D. ; DiRaddo, R. ; F. Del Maestro, R.: NeuroTouch: A physics-based virtual simulator for cranial microneurosurgery training. In: *Neurosurgery* 71 (2012), Sep., p. 32–42

[Deng et al 2014] Deng, Shujie ; Chang, Jian ; Zhang, Jian J.: *A Survey of Haptics in Serious Gaming*. p. 130–144. In: *Games and Learning Alliance: Second International Conference, GALA 2013*. Cham : Springer International Publishing, 2014

[Dietz-Uhler and Hurn 2013] Dietz-Uhler, Beth ; Hurn, Janet E.: Using Learning Analytics to Predict (and Improve) Student Success: A Faculty Perspective. In: *Journal of Interactive Online Learning* 12 (2013), No. 1, p. 17–26. – ISSN 1541-4914

[Fairhurst and Strickland 2011] Fairhurst, K. ; Strickland, A.: Simulation Speak. In: *Journal of Surgical Education* 68 (2011), No. 5, p. 382–386

[Ferraguti et al 2015] Ferraguti, F. ; Preda, N. ; BonfÃĺ, M. ; Secchi, C.: Bilateral teleoperation of a dual arms surgical robot with passive virtual fixtures generation. In: *Intelligent Robots and Systems (IROS), 2015 IEEE/RSJ International Conference on*, Sept 2015, p. 4223–4228

[Ferrell 1965] Ferrell, W. R.: Remote manipulation with transmission delay. In: *IEEE Transactions on Human Factors in Electronics* HFE-6 (1965), Sept, No. 1, p. 24–32. – ISSN 0096-249X

[Ferrell and Sheridan 1967] Ferrell, W. R. ; Sheridan, T. B.: Supervisory control of remote manipulation. In: *IEEE Spectrum* 4 (1967), Oct, No. 10, p. 81–88. – ISSN 0018-9235

[Fichtinger et al 2008] Fichtinger, G. ; Kazanzides, P. ; Okamura, A. M. ; Hager, G. D. ; Whitcomb, L. L. ; Taylor, R. H.: Surgical and interventional robotics: Part II. In: *IEEE Robotics Automation Magazine* 15 (2008), September, No. 3, p. 94–102. – ISSN 1070-9932

[Fite et al 1999] Fite, K.B. ; Speich, J.E. ; Goldfarb, M.: Transparency and Stability Robustness in Two-Channel Bilateral Telemanipulation. In: *Journal of Dynamic Systems, Measurement, and Control* 123 (1999), No. 3, p. 400–407

[Franken et al 2011] Franken, M. ; Willaert, B. ; Misra, S. ; Stramigioli, S.: Bilateral telemanipulation: Improving the complementarity of the frequency- and time-domain passivity approaches. In: *Robotics and Automation (ICRA), 2011 IEEE International Conference on*, May 2011, p. 2104–2110. – ISSN 1050-4729

[Gazebo 2016] Gazebo: *Gazebo*. `http://gazebosim.org/`. 2016

[Ghorbanian et al 2013] Ghorbanian, A. ; Rezaei, S.M. ; Khoogar, A.R. ; Zareinejad, M. ; Baghestan, K.: A novel control framework for nonlinear time-delayed Dual-master/Single-slave teleoperation. In: *ISA Transactions* 52 (2013), Mar., No. 2, p. 268–277

[Guthart and Salisbury 2000] Guthart, G. S. ; Salisbury, J. K.: The IntuitiveTM telesurgery system: overview and application. In: *Robotics and Automation, 2000. Proceedings. ICRA '00. IEEE International Conference on* Volume 1, 2000, p. 618–621

[Hannaford 1989a] Hannaford, B.: A design framework for teleoperators with kinesthetic feedback. In: *IEEE Transactions on Robotics and Automation* 5 (1989), Aug, No. 4, p. 426–434

[Hannaford 1989b] Hannaford, B.: Stability and performance tradeoffs in bilateral telemanipulation. In: *Robotics and Automation, 1989. Proceedings., 1989 IEEE International Conference on* Volume 3, May 1989, p. 1764–1767

[Hannaford and Ryu 2002] Hannaford, B. ; Ryu, Jee-Hwan: Time-domain passivity control of haptic interfaces. In: *IEEE Transactions on Robotics and Automation* 18 (2002), Feb, No. 1, p. 1–10

[Hannaford et al 1991] Hannaford, B. ; Wood, L. ; McAffee, D. A. ; Zak, H.: Performance evaluation of a six-axis generalized force-reflecting teleoperator.

In: *IEEE Transactions on Systems, Man, and Cybernetics* 21 (1991), May, No. 3, p. 620–633

[Hashtrudi-Zaad and Salcudean 2002] Hashtrudi-Zaad, K. ; Salcudean, S. E.: Transparency in time-delayed systems and the effect of local force feedback for transparent teleoperation. In: *IEEE Transactions on Robotics and Automation* 18 (2002), Feb, No. 1, p. 108–114. – ISSN 1042-296X

[Hashtrudi-Zaad and Salcudean 2001] Hashtrudi-Zaad, Keyvan ; Salcudean, Septimiu E.: Analysis of Control Architectures for Teleoperation Systems with Impedance/Admittance Master and Slave Manipulators. In: *The International Journal of Robotics Research* 20 (2001), No. 6, p. 419–445

[Hayward and Astley 1996] Hayward, Vincent ; Astley, Oliver R.: *Performance Measures for Haptic Interfaces*. p. 195–206. In: Giralt, Georges (Editor) ; Hirzinger, Gerhard (Editor): *Robotics Research: The Seventh International Symposium*. London : Springer London, 1996

[Hayward et al 2004] Hayward, Vincent ; Astley, Oliver R. ; Cruz-Hernandez, Manuel ; Grant, Danny ; Torre, Gabriel R. de-la: Haptic interfaces and devices. In: *Sensor Review* 24 (2004), No. 1, p. 16–29

[Herzig et al 2015] Herzig, N. ; Moreau, R. ; Redarce, T. ; Abry, F. ; Brun, X.: Non linear position and closed loop stiffness control for a pneumatic actuated haptic interface: the BirthSIM. In: *Intelligent Robots and Systems (IROS), 2015 IEEE/RSJ International Conference on*, Sept 2015, p. 1612–1618

[Hirche and Buss 2007] Hirche, S. ; Buss, M.: Human Perceived Transparency with Time Delay. In: *Advances in Telerobotics* Volume 31. Springer Berlin Heidelberg, 2007, p. 191–209

[Hokayem and Spong 2006] Hokayem, Peter F. ; Spong, Mark W.: Bilateral teleoperation: An historical survey. In: *Automatica* 42 (2006), No. 12, p. 2035–2057

[Islam et al 2015] Islam, Shafiqul ; Liu, Peter X. ; Saddik, Abdulmotaleb E. ; Dias, J. ; Seneviratne, Lakmal: Bilateral shared autonomous systems with passive and nonpassive input forces under time varying delay. In: *ISA Transactions* 54 (2015), No. 1, p. 218–228

[Jazayeri and Tavakoli 2011] Jazayeri, A. ; Tavakoli, M.: A passivity criterion for sampled-data bilateral teleoperation systems. In: *World Haptics Conference (WHC), 2011 IEEE*, June 2011, p. 487–492

[Jazayeri and Tavakoli 2015] Jazayeri, Ali ; Tavakoli, Mahdi: Bilateral teleoperation system stability with non-passive and strictly passive operator or environment. In: *Control Engineering Practice* 40 (2015), No. 1, p. 45–60

[Kaufmann and Liu 2001] Kaufmann, Christoph ; Liu, Alan: *Trauma Training: Virtual Reality Applications*. Volume 81. p. 236–241. In: *Medicine Meets Virtual Reality* Volume 81, 2001

[Kawada and Namerikawa 2008] Kawada, Hisanosuke ; Namerikawa, Toru: Bilateral control of nonlinear teleoperation with time varying communication delays. In: *2008 American Control Conference*, June 2008, p. 189–194. – ISSN 0743-1619

[Khademian and Hashtrudi-Zaad 2011] Khademian, B. ; Hashtrudi-Zaad, K.: Shared control architectures for haptic training: performance and coupled stability analysis. In: *The International Journal of Robotics Research* 30 (2011), Mar., No. 13, p. 1627–1642

[Khademian and Hashtrudi-Zaad 2012] Khademian, B. ; Hashtrudi-Zaad, K.: Dual-User Teleoperation Systems: New Multilateral Shared Control Architecture and Kinesthetic Performance Measures. In: *IEEE/ASME Transactions on Mechatronics* 17 (2012), Oct, No. 5, p. 895–906. – ISSN 1083-4435

[Kim et al 2013] Kim, J. ; Chang, P. H. ; Park, H. S.: Two-Channel Transparency-Optimized Control Architectures in Bilateral Teleoperation With Time Delay. In: *IEEE Transactions on Control Systems Technology* 21 (2013), Jan, No. 1, p. 40–51. – ISSN 1063-6536

[Kim et al 2007] Kim, K. ; Cavusoglu, M. C. ; Chung, W. K.: Quantitative Comparison of Bilateral Teleoperation Systems Using μ-Synthesis. In: *IEEE Transactions on Robotics* 23 (2007), Aug, No. 4, p. 776–789

[Kim et al 1987] Kim, Won ; Tendick, F. ; Ellis, S. ; Stark, L.: A comparison of position and rate control for telemanipulations with consideration of manipulator system dynamics. In: *IEEE Journal on Robotics and Automation* 3 (1987), October, No. 5, p. 426–436

[Kron et al 2004] Kron, A. ; Schmidt, G. ; Petzold, B. ; Zah, M. I. ; Hinterseer, P. ; Steinbach, E.: Disposal of explosive ordnances by use of a bimanual haptic telepresence system. In: *Robotics and Automation, 2004. Proceedings. ICRA '04. 2004 IEEE International Conference on* Volume 2, April 2004, p. 1968–1973

[Lawn and Hannaford 1993] Lawn, C. A. ; Hannaford, B.: Performance testing of passive communication and control in teleoperation with time delay. In: *Robotics and Automation, 1993. Proceedings., 1993 IEEE International Conference on*, May 1993, p. 776–783 vol.3

[Lawrence 1993] Lawrence, D. A.: Stability and transparency in bilateral teleoperation. In: *IEEE Transactions on Robotics and Automation* 9 (1993), Oct, No. 5, p. 624–637. – ISSN 1042-296X

[Lee and Li 2003] Lee, Dongjun ; Li, P.Y.: Passive bilateral feedforward control of linear dynamically similar teleoperated manipulators. In: *Robotics and Automation, IEEE Transactions on* 19 (2003), Jun., No. 3, p. 443–456

[Lee et al 2005] Lee, Dongjun ; Martinez-Palafox, O. ; Spong, M. W.: Bilateral Teleoperation of Multiple Cooperative Robots over Delayed Communication Networks: Application. In: *Proceedings of the 2005 IEEE International Conference on Robotics and Automation*, April 2005, p. 366–371

[Lee and Spong 2005] Lee, Dongjun ; Spong, M. W.: Bilateral Teleoperation of Multiple Cooperative Robots over Delayed Communication Networks: Theory. In: *Proceedings of the 2005 IEEE International Conference on Robotics and Automation*, April 2005, p. 360–365

[Lee and Spong 2006] Lee, Dongjun ; Spong, M.W.: Passive bilateral teleoperation with constant time delay. In: *Robotics, IEEE Transactions on* 22 (2006), Apr., No. 2, p. 269–281

[Lee and Chung 1998] Lee, Hyoung-Ki ; Chung, Myung J.: Adaptive controller of a master-slave system for transparent teleoperation. In: *Journal of Robotic Systems* 15 (1998), No. 8, p. 465–475

[Leung et al 1995] Leung, G. M. H. ; Francis, B. A. ; Apkarian, J.: Bilateral controller for teleoperators with time delay via μ-synthesis. In: *IEEE Transactions on Robotics and Automation* 11 (1995), Feb, No. 1, p. 105–116

[Lewis et al 2011] Lewis, T.M. ; Aggarwal, R. ; Rajaretnam, N. ; Grantcharov, T.P. ; Darzi, A.: Training in Surgical Oncology - the Role of VR Simulation. In: *Surgical Oncology* 20 (2011), No. 3, p. 134–139

[Li and Kawashima 2014] Li, H. ; Kawashima, K.: Achieving Stable Tracking in Wave-Variable-Based Teleoperation. In: *IEEE/ASME Transactions on Mechatronics* 19 (2014), Oct, No. 5, p. 1574–1582. – ISSN 1083-4435

[Li et al 2014] Li, J. ; Tavakoli, M. ; Mendez, V. ; Huang, Q.: Passivity and Absolute Stability Analyses of Trilateral Haptic Collaborative Systems. In: *Journal of Intelligent & Robotic Systems* (2014), Apr., p. 1–18

[Li et al 2005] Li, Ming ; Kapoor, A. ; Taylor, R. H.: A constrained optimization approach to virtual fixtures. In: *2005 IEEE/RSJ International Conference on Intelligent Robots and Systems*, Aug 2005, p. 1408–1413

[Liu and Tavakoli 2011] Liu, X. ; Tavakoli, M.: Inverse dynamics-based adaptive control of nonlinear bilateral teleoperation systems. In: *Robotics and Automation (ICRA), 2011 IEEE International Conference on*, May 2011, p. 1323–1328

[Liu et al 2015] Liu, Zhengxiong ; Huang, Panfeng ; Lu, Zhenyu ; Pan, Jixiang: A compound virtual fixture for dexterous space teleoperation. In: *Ubiquitous Robots and Ambient Intelligence (URAI), 2015 12th International Conference on*, Oct 2015, p. 261–266

[Macchelli 2003] Macchelli, Alessandro: *Port Hamiltonian Systems - A unified approach for modeling and control finite and infinite dimensional physical systems*, University of Bologna, Ph.D. thesis, 2003

[Mahapatra and Zefran 2003] Mahapatra, S. ; Zefran, M.: Stable haptic interaction with switched virtual environments. In: *Proceedings of IEEE International Conference on Robotics and Automation (ICRA)*, Sep 2003, p. 1241–1246

[Malysz and Sirouspour 2009] Malysz, P. ; Sirouspour, S.: Nonlinear and Filtered Force/Position Mappings in Bilateral Teleoperation With Application to Enhanced Stiffness Discrimination. In: *IEEE Transactions on Robotics* 25 (2009), Oct, No. 5, p. 1134–1149

[Marcassus et al 2006] Marcassus, N. ; Chriette, A. ; Gautier, M.: Theoretical and experimental overview of bilateral teleoperation control laws. In: *2006 14th Mediterranean Conference on Control and Automation*, June 2006, p. 1–6

[Maschke and van der Schaft 1992] Maschke, B. ; Schaft, A.J. van der: Port controlled hamiltonian systems: modeling origins and system theoretic properties. In: *Nonlinear Control Systems (NOLCOS), Proceedings of the Third Conference on*, 1992

[Mazzone et al 2003] Mazzone, Andrea ; Zhang, Rui ; Kunz, Andreas: Novel Actuators for Haptic Displays Based on Electroactive Polymers. In: *Proceedings of the ACM Symposium on Virtual Reality Software and Technology*. New York, NY, USA : ACM, 2003, p. 196–204. – ISBN 1-58113-569-6

[Mendez and Tavakoli 2010] Mendez, V. ; Tavakoli, M.: A passivity criterion for N-port multilateral haptic systems. In: *Decision and Control (CDC), 49th IEEE Conference on*, Dec. 2010, p. 274–279

[Mohammadi et al 2011] Mohammadi, A. ; Tavakoli, M. ; Marquez, H. J.: Control of nonlinear bilateral teleoperation systems subject to disturbances. In: *2011 50th IEEE Conference on Decision and Control and European Control Conference*, Dec 2011, p. 1765–1770

[Moreau et al 2012] Moreau, R. ; Pham, M.T. ; Tavakoli, M. ; Le, M.Q. ; Redarce, T.: Sliding-mode bilateral teleoperation control design for masterâĂŞslave pneumatic servo systems. In: *Control Engineering Practice* 20 (2012), No. 6, p. 584–597. – ISSN 0967-0661

[Moschini and Fiorini 2004] Moschini, D. ; Fiorini, P.: Performance of robotic teleoperation system with flexible slave device. In: *Robotics and Automation, 2004. Proceedings. ICRA '04. 2004 IEEE International Conference on* Volume 4, April 2004, p. 3696–3701

[Mullen 1972] Mullen, D.P.: *An Evaluation of Resolved Motion Rate Control for Remote Manipulators thesis*, MIT, Master thesis, 1972

[Munir and Book 2001] Munir, S. ; Book, W. J.: Wave-based teleoperation with prediction. In: *American Control Conference, 2001. Proceedings of the 2001* Volume 6, 2001, p. 4605–4611. – ISSN 0743-1619

[Munir and Book 2002] Munir, S. ; Book, W. J.: Internet-based teleoperation using wave variables with prediction. In: *IEEE/ASME Transactions on Mechatronics* 7 (2002), Jun, No. 2, p. 124–133. – ISSN 1083-4435

[Muradore and Fiorini 2016] Muradore, Riccardo ; Fiorini, Paolo: A Review of Bilateral Teleoperation Algorithms. In: *Acta Polytechnica Hungarica* 13 (2016), No. 1, p. 191–208

[Nicosia and Tomei 1990] Nicosia, S. ; Tomei, P.: Robot control by using only joint position measurements. In: *IEEE Transactions on Automatic Control* 35 (1990), Sep., No. 9, p. 1058–1061

[Niculescu et al 2003] Niculescu, Silviu-Iulian ; Taoutaou, Damia ; Lozano, Rogelio: Bilateral teleoperation with communication delays. In: *International Journal of Robust and Nonlinear Control* 13 (2003), No. 9, p. 873–883

[Niemeyer and Slotine 1991] Niemeyer, G. ; Slotine, J. J. E.: Stable adaptive teleoperation. In: *IEEE Journal of Oceanic Engineering* 16 (1991), Jan, No. 1, p. 152–162. – ISSN 0364-9059

[Nudehi et al 2005] Nudehi, S.S. ; Mukherjee, R. ; Ghodoussi, M.: A shared-control approach to haptic interface design for minimally invasive telesurgical training. In: *Control Systems Technology, IEEE Transactions on* 13 (2005), Jul., No. 4, p. 588–592

[Nuno and Basanez 2009] Nuno, E. ; Basanez, L.: Nonlinear Bilateral Teleoperation: Stability Analysis. In: *Robotics and Automation, 2009. ICRA '09. IEEE International Conference on*, May 2009, p. 3718–3723. – ISSN 1050-4729

[Nuno et al 2011] Nuno, E. ; Basanez, L. ; R., Ortega: Passivity-based control for bilateral teleoperation: A tutorial. In: *Automatica* 47 (2011), No. 3, p. 485–495

[Nuno et al 2009] Nuno, Emmanuel ; Basanez, Luis ; Ortega, Romeo ; Spong, Mark W.: Position Tracking for Non-linear Teleoperators with Variable Time Delay. In: *The International Journal of Robotics Research* 28 (2009), No. 7, p. 895–910

[Nuno et al 2010] Nuno, Emmanuel ; Ortega, Romeo ; Basanez, Luis: An adaptive controller for nonlinear teleoperators. In: *Automatica* 46 (2010), No. 1, p. 155–159

[OpenHaptics 2016] OpenHaptics: *OpenHaptics Toolkit*. `http://www.geomagic.com/en/products/open-haptics/overview`. 2016

[Park and Lee 2011] Park, Adrian E. ; Lee, Tommy H.: *Evolution of Minimally Invasive Surgery and Its Impact on Surgical Residency Training*. p. 11–22. In: *Minimally Invasive Surgical Oncology: State-of- the-Art Cancer Management*. Berlin, Heidelberg : Springer Berlin Heidelberg, 2011

[Park and Cho 1999] Park, Jong H. ; Cho, Hyun C.: Sliding-mode controller for bilateral teleoperation with varying time delay. In: *Advanced Intelligent Mechatronics, 1999. Proceedings. 1999 IEEE/ASME International Conference on*, 1999, p. 311–316

[Paynter 1961] Paynter, H. M.: *Analysis and design of engineering systems*. Cambridge, Massachusetts. : The M.I.T. Press, 1961

[Peer 2008] Peer, Angelika: *Design and Control of Admittance-Type Telemanipulation Systems*, Technische Universitat Munchen, Ph.D. thesis, 2008

[Penin 2000] Penin, L. F.: Teleoperation with time delay - A survey and its issue in space robotics. In: *Proceedings of 6th ESA Workshop Adv. Space Technol. Robot. Autom.*, 2000, p. 1–8

[Pezzementi et al 2007] Pezzementi, Z. ; Okamura, A. M. ; Hager, G. D.: Dynamic Guidance with Pseudoadmittance Virtual Fixtures. In: *Proceedings 2007 IEEE International Conference on Robotics and Automation*, April 2007, p. 1761–1767. – ISSN 1050-4729

[Polushin et al 2013] Polushin, Ilia G. ; Dashkovskiy, Sergey N. ; Takhmar, Amir ; Patel, Rajni V.: A small gain framework for networked cooperative force-reflecting teleoperation. In: *Automatica* 49 (2013), No. 2, p. 338–348

[QUARC 2016] QUARC: *QUARC Control Software*. `http://www.quanser.com/products/omni_bundle`. 2016

[Razi and Hashtrudi-Zaad 2014] Razi, K. ; Hashtrudi-Zaad, K.: Analysis of coupled stability in multilateral dual-user teleoperation systems. In: *Robotics, IEEE Transactions on* 30 (2014), Jun., No. 3, p. 631–641

[Rodriguez-Seda et al 2009] Rodriguez-Seda, E. J. ; Lee, D. ; Spong, M. W.: Experimental Comparison Study of Control Architectures for Bilateral Teleoperators. In: *IEEE Transactions on Robotics* 25 (2009), Dec, No. 6, p. 1304–1318

[ROS 2016] ROS: *Robot Operating System (ROS)*. `http://www.ros.org/`. 2016

[Rosenberg 1993] Rosenberg, L. B.: Virtual fixtures: Perceptual tools for telerobotic manipulation. In: *Virtual Reality Annual International Symposium, 1993., 1993 IEEE*, Sep 1993, p. 76–82

[Ryu et al 2010] Ryu, Jee-Hwan ; Artigas, Jordi ; Preusche, Carsten: A passive bilateral control scheme for a teleoperator with time-varying communication delay. In: *Mechatronics* 20 (2010), No. 7, p. 812–823

[Ryu and Kwon 2001] Ryu, Jee-Hwan ; Kwon, Dong-Soo: A novel adaptive bilateral control scheme using similar closed-loop dynamic characteristics of master/slave manipulators. In: *Journal of Robotic Systems* 18 (2001), No. 9, p. 533–543

[Ryu et al 2004] Ryu, Jee-Hwan ; Kwon, Dong-Soo ; Hannaford, B.: Stable teleoperation with time-domain passivity control. In: *IEEE Transactions on Robotics and Automation* 20 (2004), April, No. 2, p. 365–373. – ISSN 1042-296X

[Saltaren et al 2007] Saltaren, R. ; Aracil, R. ; Alvarez, C. ; Yime, E. ; Sabater, J. M.: Field and service applications - Exploring deep sea by teleoperated robot - An Underwater Parallel Robot with High Navigation Capabilities. In: *IEEE Robotics Automation Magazine* 14 (2007), Sept, No. 3, p. 65–75

[Sansanayuth et al 2012] Sansanayuth, T. ; Nilkhamhang, I. ; Tungpimolrat, K.: Teleoperation with inverse dynamics control for PHANToM Omni haptic device. In: *Proceedings of SICE Annual Conference (SICE)*, Aug. 2012, p. 2121–2126

[Schaft 2000] Schaft, A. J. Van d.: *L2-Gain and Passivity Techniques in Nonlinear Control*. Springer-Verlag London, 2000

[Secchi et al 2007] Secchi, Cristian ; Stramigioli, Stefano ; Fantuzzi, Cesare: *Control of Interactive Robotic Interfaces: A Port-Hamiltonian Approach*. Springer, 2007

[Shahbazi et al 2013] Shahbazi, M. ; Atashzar, S. F. ; Patel, R. V.: A dual-user teleoperated system with Virtual Fixtures for robotic surgical training. In: *Robotics and Automation (ICRA), 2013 IEEE International Conference on*, May 2013, p. 3639–3644. – ISSN 1050-4729

[Shahbazi et al 2014] Shahbazi, M. ; Atashzar, S. F. ; Patel, R. V.: A framework for supervised robotics-assisted mirror rehabilitation therapy. In: *2014 IEEE/RSJ International Conference on Intelligent Robots and Systems*, Sept 2014, p. 3567–3572

[Shahbazi et al 2015] Shahbazi, M. ; Atashzar, S. F. ; Talebi, H. A. ; Patel, R. V.: Novel Cooperative Teleoperation Framework: Multi-Maste/Single-Slave System. In: *IEEE/ASME Transactions on Mechatronics* 20 (2015), Aug, No. 4, p. 1668–1679

[Shahbazi et al 2016] Shahbazi, M. ; Atashzar, S. F. ; Tavakoli, M. ; Patel, R. V.: Robotics-Assisted Mirror Rehabilitation Therapy: A Therapist-in-the-Loop Assist-as-Needed Architecture. In: *IEEE/ASME Transactions on Mechatronics* 21 (2016), Aug, No. 4, p. 1954–1965. – ISSN 1083-4435

[Shamaei et al 2015] Shamaei, K. ; Kim, L. H. ; Okamura, A. M.: Design and evaluation of a trilateral shared-control architecture for teleoperated training robots. In: *2015 37th Annual International Conference of the IEEE Engineering in Medicine and Biology Society (EMBC)*, Aug 2015, p. 4887–4893. – ISSN 1094-687X

[Sheridan 1989] Sheridan, T. B.: Telerobotics. In: *Automatica* 25 (1989), Jul., No. 4, p. 487–507

[Sheridan and Ferrell 1963] Sheridan, T. B. ; Ferrell, W. R.: Remote Manipulative Control with Transmission Delay. In: *IEEE Transactions on Human Factors in Electronics* HFE-4 (1963), Sept, No. 1, p. 25–29

[Sirouspour 2005] Sirouspour, S.: Modelling and control of cooperative teleoperation systems. In: *IEEE Transaction on Robotics* 21 (2005), p. 1220–1225

[Sirouspour and Setoodeh 2005] Sirouspour, S. ; Setoodeh, P.: Multi-operator/Multi-robot Teleoperation: An Adaptive Nonlinear Control Approach. In: *Proceedings of IEEE/RSJ International Conference on Intelligent Robots and Systems* (2005), p. 1576–1581

[Slater et al 2001] Slater, Mel ; Steed, Anthony ; Chrysanthou, Yiorgos: *Computer Graphics and Virtual Environments: From Realism to Real Time*. Addison-Wesley, 2001

[Sorenson and Akin 1995] Sorenson, E. A. ; Akin, D. L.: Operator interface testing of a space telerobotic system. In: *Systems, Man and Cybernetics, 1995. Intelligent Systems for the 21st Century., IEEE International Conference on* Volume 5, Oct 1995, p. 4065–4072

[Stramigioli 2001] Stramigioli, S.: Modeling and IPC Control of Interactive Mechanical Systems: A Coordinate-Free Approach. In: *Springer* (2001)

[Stramigioli 1996] Stramigioli, Stefano: Creating Artificial Damping By Means Of Damping Injection. In: *In Proceedings of the ASME Dynamic Systems and Control Division*, 1996, p. 601–606

[Sun et al 2016] Sun, D. ; Naghdy, F. ; Du, H.: Wave-Variable-Based Passivity Control of Four-Channel Nonlinear Bilateral Teleoperation System Under Time Delays. In: *IEEE/ASME Transactions on Mechatronics* 21 (2016), Feb, No. 1, p. 238–253. – ISSN 1083-4435

[Sun et al 2014] Sun, Da ; Naghdy, Fazel ; Du, Haiping: Application of wave-variable control to bilateral teleoperation systems: A survey. In: *Annual Reviews in Control* 38 (2014), No. 1, p. 12 – 31. – ISSN 1367-5788

[Surgical 2016] Surgical, Intuitive: *da Vinci Surgery: Minimally Invasive Surgery*. `http://www.davincisurgery.com/`. 2016

[SurgicalScience 2016a] SurgicalScience: *da Vinci®Si Optional Dual Console*. `http://intuitivesurgical.com/products/davinci_surgical_system/davinci_surgical_system_si/dualconsole.html`. 2016

[SurgicalScience 2016b] SurgicalScience: *LapSim: The Proven Training System.* http://www.surgical-science.com/lapsim-the-proven-training-system/. 2016

[Tavakoli 2008] Tavakoli, M.: *Haptics For Teleoperated Surgical Robotic Systems.* 1st. River Edge, NJ, USA : World Scientific Publishing Co., Inc., 2008

[Varalakshmi et al 2012] Varalakshmi, B. D. ; Thriveni, J. ; R., Venugopal K. ; Patnaik, L. M.: Haptics: State of the Art Survey. In: *International Journal of Computer Science Issues* 5 (2012), No. 3, p. 234–244

[Ware et al 2014] Ware, J. ; Cha, E. ; Peshkin, M. A. ; Colgate, J. E. ; Klatzky, R. L.: Search Efficiency for Tactile Features Rendered by Surface Haptic Displays. In: *IEEE Transactions on Haptics* 7 (2014), Oct, No. 4, p. 545–550. – ISSN 1939-1412

[Willems 1972] Willems, Jan C.: Dissipative dynamical systems part I: General theory. In: *Archive for Rational Mechanics and Analysis* 45 (1972), No. 5, p. 321–351

[Wilt et al 1977] Wilt, D. R. ; Pieper, D. L. ; Frank, A. S. ; Glenn, G. G.: An evaluation of control modes in high gain manipulator systems. In: *Mechanism and Machine Theory* 12 (1977), p. 373–386

[Yan and Salcudean 1996] Yan, J. ; Salcudean, S. E.: Teleoperation controller design using H infin;-optimization with application to motion-scaling. In: *IEEE Transactions on Control Systems Technology* 4 (1996), May, No. 3, p. 244–258

[Ye and Liu 2009] Ye, Y. ; Liu, P. X.: Improving Haptic Feedback Fidelity in Wave-Variable-Based Teleoperation Orientated to Telemedical Applications. In: *IEEE Transactions on Instrumentation and Measurement* 58 (2009), Aug, No. 8, p. 2847–2855. – ISSN 0018-9456

[Yiannakopoulou et al 2014] Yiannakopoulou, E. ; Nikiteas, N. ; Perrea, D. ; Tsigris, C.: Virtual reality simulators and training in laparoscopic surgery. In: *International Journal of Surgery* 13 (2014), Feb., No. 9, p. 60–64

[Yokokohji and Yoshikawa 1994] Yokokohji, Y. ; Yoshikawa, T.: Bilateral control of master-slave manipulators for ideal kinesthetic coupling-formulation and experiment. In: *IEEE Transactions on Robotics and Automation* 10 (1994), Oct, No. 5, p. 605–620. – ISSN 1042-296X

[Zhu and Salcudean 2000] Zhu, Wen-Hong ; Salcudean, S. E.: Stability guaranteed teleoperation: an adaptive motion/force control approach. In: *IEEE Transactions on Automatic Control* 45 (2000), Nov, No. 11, p. 1951–1969. – ISSN 0018-9286

FOLIO ADMINISTRATIF

THESE DE L'UNIVERSITE DE LYON OPEREE AU SEIN DE L'INSA LYON

NOM : LIU
(avec précision du nom de jeune fille, le cas échéant)

DATE de SOUTENANCE : 22/09/2016

Prénoms : Fei

TITRE : Dual-user Haptic Training System

NATURE : Doctorat

Numéro d'ordre : 2016LYSEI082

Ecole doctorale : Électronique, Électrotechnique, Automatique (EEA)

Spécialité : Automatique

RESUME :
Dans le secteur médical tout particulièrement, la qualité du geste est primordiale et les professionnels doivent être formés par la pratique pour acquérir un niveau de compétences compatible avec l'exercice de leur métier. Depuis une dizaine d'année, les simulateurs informatiques aident les apprenants dans de nombreux apprentissages mais ils doivent encore être associés à des travaux pratiques sur mannequins, animaux ou cadavres, qui pourtant n'offrent pas toujours suffisamment de réalisme par rapport aux vrais patients, et sont coûteux à l'usage. Aussi, leur formation s'achève généralement sur de vrais patients, ce qui présente des risques. Les simulateurs haptiques (fournissant une sensation d'effort) deviennent aujourd'hui une solution plus appropriée car ils peuvent reproduire des efforts résistant réalistes et proposer une infinité de cas d'étude pré-enregistrés. Cependant, apprendre seul sur un simulateur n'est pas toujours aussi efficace qu'un apprentissage "à quatre mains" (celles de l'instructeur et de l'apprenant manipulant les mêmes outils en coopération).

Cette étude propose donc un système haptique de formation pratique à deux utilisateurs : l'instructeur et l'apprenant, interagissant chacun à travers leur propre interface haptique. Ils collaborent ainsi, avec des outils et un environnement de travail soit réels (l'outil est manipulé par un robot) soit virtuels. Une approche énergétique, faisant appel notamment à la modélisation par port-Hamiltonien, a été utilisée pour garantir la stabilité et la robustesse du système. Une étude comparative (en simulation) avec deux autres systèmes haptiques multi utilisateurs a montré l'intérêt de ce nouveau système pour la formation pratique. Il a été développé et validé expérimentalement sur des interfaces à un seul degré de liberté. Son extension à six degrés de liberté est facilitée par les choix de modélisation. Afin de pouvoir utiliser le système quand les deux protagonistes sont éloignés, cette étude propose des pistes d'amélioration qui ne sont pas encore optimisées.

MOTS-CLÉS : Haptique, Simulateur, Apprentissage supervisé, Dual-user, Passivité, Étude comparative, Retards de transmission, Système à ports hamiltoniens

Laboratoire (s) de recherche : Laboratoire Ampère UMR CNRS 5005

Directeur de thèse : Tanneguy REDARCE
Co-directeur de thèse : Arnaud LELEVÉ

Président de jury : FRAISSE Philippe

Composition du jury :
Bernard BAYLE (Rapporteur), Mahdi TAVAKOLI (Rapporteur), Philippe FRAISSE, Cyril NOVALES, Tanneguy REDARCE, Arnaud LELEVÉ, Damien EBERARD